Functional characterisation of dyslexia-susceptibility candidate genes *KIAA0319* and *KIAA0319L*



L. G. Guidi

St John's College

University of Oxford

A thesis submitted for the degree of

Doctor of Philosophy

Hilary Term 2017

Abstract

The capacity for language is one of the key features underlying human cognition and evolution. However, little is known about the neurobiological mechanisms underlying normal or impaired linguistic ability. Developmental dyslexia refers to a specific impairment in reading performance and it is one of the most common neurodevelopmental disabilities in school-aged children. It has a well-established genetic component and *KIAA0319* is one of the prime susceptibility candidate genes associated with it, also showing some genetic overlap with other language-related disorders. Its paralogous gene, *KIAA0319L* (or *KIAA0319-Like*), is the only other member of this gene family and has also been linked to dyslexia. This thesis interrogates the function of the mouse homologs of *KIAA0319* and *KIAA0319L* at the molecular, cellular, electrophysiological and behavioural levels in order to uncover the mechanisms through which they may underlie the neural architecture of language, and susceptibility to dyslexia and related disorders.

Both KIAA0319 and KIAA0319L have been implicated in neuronal migration in the developing neocortex following *in utero* knockdown in rats using shRNA. However, our laboratories have recently shown that genetic ablation of KIAA0319 does not affect cortical migration. Given functional redundancy between paralogous genes is a well-known source of compensation in biological systems, I hypothesised that this may derive from compensation between KIAA0319 and AU040320, the mouse homolog of KIAA0319L. Using a range of anatomical methods to investigate *AU040320* and double *Kiaa0319;AU040320* KOs, I have found no evidence for a role of these proteins in cell migration in the mouse brain, in contrast to previous reports.

To interrogate other putative functions of KIAA0319 and AU040320, I performed a series of behavioural experiments on *Kiaa0319;AU040320* KO mice to examine potential deficits in their behaviour. Despite a largely normal behavioural profile, these animals displayed impaired auditory processing in a gap detection task and in auditory brainstem recordings (ABRs) due to a potential reduction in neural activity in the early central auditory pathway - with similar deficits observed in *AU040320* single KOs. These results raise the possibility these genes mediate the normal structure/function of the auditory system, in line with auditory-related deficits being one of the hallmarks of dyslexia.

Given the paucity of knowledge on the AU040320 protein, I interrogate its function at the cellular level by examining the male infertility observed in *AU040320* KO mice. Spermatozoa in these mice were found to have round heads lacking the sperm secretory organelle called acrosome, features which mimic those of globozoospermia - a rare genetic condition affecting humans. Ultrastructural analyses revealed that acrosome formation in AU040320-deficient males resulted from an impairment in the fusion of proacrosomic vesicles during the early stages. Preliminary molecular analyses revealed that the AU040320 protein may interact with AP-1, AP-2 and ASAP1, key proteins in intracellular trafficking which regulate vesicle transport and function, suggesting a pathway which could be involved in the malformations observed in *AU040320* KOs.

Acknowledgements

I am glad that acknowledgements are at the front of the thesis, despite being the last thing to write, as for me this is the most important part. It is also the best one to write as I get to look back over everything I struggled with and learned, all the people I met and the friends I made. I most certainly stood on the shoulder of giants during the DPhil, but not only for the science but for the support and encouragement I received throughout.

Firstly, Zoltán: thank you so much for sharing your enthusiasm for science, your knowledge and for the unique humility you have about it all that is so encouraging and inspiring. Thank you also for being so human and for becoming not only my supervisor but also a friend and supporter, giving me the opportunity to grow as an independent scientist and as a person.

Antonio, thank you so much for taking me under your wing during the early years of MSc, for being so patient, for looking out for me and after me almost like a father during all these almost 5 years. Thank you also for teaching me the value of stepping back and doing things right, for the moments of joy and for the heated discussions too - I would not be half the 'scientist' I am now without you.

Fernando, I had many mentors along this period but, as everyone knows, no one had an impact as big as you - and 'Fernando knows it'. I feel so privileged to have had you around, sharing your contagious passion, your wisdom, for being such an inspiration and role model, and for teaching me not only how to do science but also how to be a scientist. And, of course, for giving me my own version of the critical hat, *la gorra*. So, thank you for being a best friend, a father, mentor, teacher, buddy, clown, and so many other things all at once. Thank you for the laughs that kept me sane and for the shoulder to cry and ears to listen when things were difficult - and for the *budismo acalorado*. Having you around made this a lot more rewarding and enjoyable.

Thank you also to Isabel, who helped to shape much of the vision of this project, for showing me the ropes, for always helping to put things in perspective, for the clear advice, and for always leaving her door and mind open, even if not physically around. Thank you to Tony Monaco who allowed for all this to happen and for always bringing insight to the discussions.

Zoe, thank you, too, for sharing your knowledge and time with me, for supporting me along the way, for all the sperm talk, for the friendship and advice you offered, for putting up with me in difficult times and for the many laughs.

A huge thank you goes also to those in the Molnár and the Monaco laboratories who have shared so many exciting, difficult and fun moments together, and for putting up with me all these years. Special thanks to Wei-Zhi who offered so much help in the lab but also comfort, advice, yummy food and constant reminders to keep exercising and stay away from boozy friends! Thank you to Dianne Newbury for advice and many discussions, and to Conor, for those hyperactive afternoons in the lab and for genotyping.

My appreciation also goes to Simon Butt who was always at hand with an endless supply of coffee, laughs and good stories, but also ready to advise and inspire through his vision on neuroscience, development and the academic world. Thank you for making me part of your social team, and many thanks also to Jacqui and Cristiana for listening and unbounded support.

I am also hugely indebted to all my collaborators, especially Jane Mattley and Jennifer Linden, at the UCL Ear Institute, who have added a new dimension to my work and made so many things possible. Thank you so much for the hard work and for the unparalleled focus and enthusiasm. Thank you also to Prof Pierre Ray in the Institut Albert Bonniot in Grenoble, France, for sharing his patient DNA samples.

But there are many others who helped me along the way and whom I would like to thank: Sergi Padilla-Parra for imaging help (and many discussions about science and Brazil!); Jérome Nicod for general advice and help with ultrasonic vocalisation tests; Daniella Moralli for help with sperm experiments; Errin Johnson for fixing me up with EM; Tomaz Schneider for getting me started with behaviour, João Lima, David Bannerman and Chris Barkus, Katie Hewitt, for help with numerous questions, Keith Gull and his group for advice on cilia structure/function, and many others. Many thanks also to all the personnel in the animal house, particularly Laura, Angela and James. Many many thanks also to those I met along the way, either in Oxford or in the many conferences and workshops I have been so fortunate to attend - these meetings made for some of the most inspiring and rewarding moments of the DPhil! You know who you are.

I am also thankful to those in St John's College, especially the team in the lodge and Hall, who have looked after me so well and who have become friends. Much of this thesis was written in several cafés in Oxford so I am thankful to them too for good coffee, free internet and a place to work.

I feel an immense privilege to have had so many other enriching friendships who supported me along the way and shared many highs and lows, and for being surrounded by so many people who have become family to me.

First of all, thank you very much to my parents for laying inside me the foundation, curiosity and strength that allowed me to learn so much from life and to get here.

My gratitude goes also to Cecilia, Ursula, Richard and the rest of the Gibbons family for their eternal support and encouragement, and for always making me feel like part of the family. I would not be standing on this side now without your support through all these years,

Oh, friends. There are too many friends to mention here but some deserve special attention, so thank you (in no specific order): to friends who marked the early days but with whom I sadly lost touch (Jono, Joseph, Miles, Ellie); Alexei who became my chalice of wisdom for all things behaviour and who quickly became a best friend; Eddie whose presence in the lab was brief (and never started early) but who turned into a lifelong friend; to recent additions Emma and Katherine; Carlos for the uncomplicated friendship; Jon for countless coffees which, thankfully turned into tea; Carla, for Catan, pizza and bitching about academia; Marina for being a good friend and never passing judgement; Borja for his long-lasting presence and fraternity; the MSc Neuro crowd, Friederike, Clio, Fabian, Sana, Matt, Martin, for seeing me through the journey and for solid friendship.

Thank you also, James. Your presence along the way made it all much easier, be it through giving me space to share some of my feelings and anger without judging, through sharing a vision of the future, and for swimming in Port Meadow at 6 in the morning. Hannah, my neighbour turned best friend turned role model, thank you for your limitless wisdom and for sharing your joy for life; being your friend makes me a better person. Henry, you saw through me and went from 'daddy' to brother, and helped to get the grump out of me; thank you for that, and for the never-ending positivity, for being a mentor in life, for always checking and never failing to be free when I needed help, distraction, food, or a bed for the night. And thank you, Jacob, for wearing that pink wig when we met and for the incessant fraternity, for showing me how to see the big picture in the world through your probabilistic brain, for looking out for me and after me.

To all of you and those I missed, thank you!

Statement of Authorship

The work presented in this thesis is my own with the exceptions and collaborations listed below. No work or part thereof has been submitted for consideration for another degree.

Chapters 3 and 4 have been combined into a research article and published as; Guidi L, Mattley J, Martinez-Garay I, Monaco AP, Linden JF, Velayos-Baeza A, Molnár Z. 2017. *Knockout mice for dyslexia susceptibility gene homologs KIAA0319 and KIAA0319L have unaffected neuronal migration but display abnormal auditory processing.* Cerebral Cortex. 27:5831-5845.

Chapter 5 has been submitted as a research article entitled *AU040320 is a novel protein required for acrosome biogenesis* and it is currently under review.

Section 3.2.1: The generation of the *AU040320* transgenic mouse lines was conducted together with Dr Antonio Velayos-Baeza.

Section 3.2.6: Micro-injections of modified embryonic stem cells for generation of *AU040320* transgenic mouse line (Table 3.1) was performed by the Transgenics Core of the Wellcome Trust Centre for Human Genetics.

Section 4.2.8: Auditory brainstem response recordings, data analyses and graphs were conducted in collaboration with Jane Mattley and Prof Jennifer Linden at University College London, on animals bred and genotyped at Oxford.

Section 5.2.1 and 5.2.2: Western blot and quantification of sperm number was performed by Dr Zoe Holloway (Fig. 5.4). Collection of testes weight data and H & E stainings were performed in collaboration with Dr Zoe Holloway (Fig. 5.4).

Section 5.2.3: Sample collection, immunostaining and analyses of meiotic profile of spermatocytes were conducted by Dr Daniella Moralli (Fig. 5.5).

Section 5.2.6: Collection of epididymal cells and seminiferous tubules was conducted in collaboration with Dr Zoe Holloway and samples were processed for electron microscopy by Errin Johnson at the Dunn School of Pathology (Fig. 5.6, 5.8).

Section 5.2.9: Co-immunoprecipitation assay between KIAA0319L and AP-1 was conducted by Dr Clotilde Levecque 5.12.

Contents

Abstract iii

Acknowledgements v

Statement of Authorship ix

List of Figures xiii

List of Tables xv

List of Abbreviations xvii

1 Introduction 1

1.1 Developmental dyslexia . . . 3
1.1.1 Neuropsychology of reading and dyslexia . . . 4
1.1.2 Neurobiology of reading and dyslexia . . . 8
1.1.2.1 The neural architecture of reading . . . 8
1.1.2.2 Human neuropathology . . . 8
1.1.2.3 Functional and structural neuroimaging studies . . . 10
1.2 Genetics of dyslexia . . . 12
1.2.1 Classic linkage and association studies . . . 13
1.2.2 Genome-wide studies of dyslexia . . . 19
1.3 *KIAA0319* and *KIAA0319L* as dyslexia susceptibility candidate genes 21
1.3.1 *KIAA0319*: a prime candidate gene . . . 21
1.3.2 *KIAA0319L* . . . 24
1.3.3 Functional relevance of risk alleles . . . 25
1.4 The KIAA0319 and KIAA0319L proteins . . . 26
1.4.1 KIAA0319 . . . 26
1.4.2 KIAA0319L . . . 28
1.4.3 Homology, conservation and evolution . . . 32
1.4.4 Gene expression studies . . . 32
1.5 Functional studies of *KIAA0319* and *KIAA0319L* . . . 35
1.5.1 Rodent neuronal migration . . . 35

1.5.2 Behavioural effects of *Kiaa0319* knockdown 40
1.6 The neocortex 43
1.6.1 Development of the neocortex 46
1.6.2 Cortical neurogenesis 46
1.6.3 Radial cortical migration 49
1.6.4 Tangential cortical migration 51
1.6.5 Disorders of neuronal migration 51
1.7 Aims of this thesis 53

2 Methods **57**
2.1 General methods 57
2.1.1 Experimental animals 57
2.1.2 Genotyping and PCRs 58
2.1.3 Sanger sequencing 58
2.1.4 Western blot 59
2.1.5 LacZ staining 60
2.2 Chapter 3 methods 61
2.2.1 Immunohistochemistry 61
2.2.2 Nissl-staining 61
2.2.3 *In utero* electroporation 62
2.2.4 Antibodies 63
2.2.5 Image acquisition and statistical analyses 63
2.3 Chapter 4 methods 65
2.3.1 Behavioural testing 65
2.3.1.1 Locomotor activity 65
2.3.1.2 Light/dark box 66
2.3.1.3 Accelerating rotarod 66
2.3.1.4 Olfactory preference task 66
2.3.1.5 Y-maze spatial novelty 67
2.3.1.6 Spontaneous alternations in T-maze 67
2.3.1.7 Startle reflex and prepulse inhibition of acoustic startle 68
2.3.1.8 Silent gap detection 68
2.3.2 Auditory brainstem responses 69
2.3.3 Quantification of synapse number by immunohistochemistry 70
2.4 Chapter 5 methods 72
2.4.1 Hematoxylin & eosin staining 72
2.4.2 Giemsa staining 72
2.4.3 Epididymal sperm count 72

2.4.4 Meiotic profile analysis of spermatocytes . . . 72
2.4.5 Immunohistochemistry & Immunofluorescence . . . 73
2.4.6 Antibodies . . . 74
2.4.7 Scanning electron microscopy . . . 74
2.4.8 Transmission electron microscopy . . . 75
2.4.9 GST pulldowns/*in vitro* binding assay . . . 75
2.4.10 Mutation screening in human cases of globozoospermia . . . 76

3 Chapter 3 **77**
3.1 Introduction . . . 78
3.2 Results . . . 79
3.2.1 Generation of *AU040320* conditional KO mouse lines . . . 79
3.2.2 Generation of *Kiaa0319;AU040320* double KO mice . . . 88
3.2.3 Normal cortical neurogenesis in *AU040320* and double KOs 89
3.2.4 Absence of *AU040320* does not affect cortical lamination . . 94
3.2.5 Normal cortical lamination in double KOs . . . 96
3.2.6 Acute knockdown of *Kiaa0319* and *AU040320* does not affect radial migration . . . 100
3.2.7 No changes in position of cortical interneurons following double *Kiaa0319;AU040320* KO . . . 103
3.2.8 Unaltered lamination of hippocampus and cerebellum in the absence of *AU040320* alone and in conjunction with KIAA0319 104
3.3 Discussion . . . 109
3.3.1 Discrepancy with shRNA experiments . . . 109
3.3.2 The neuronal migration hypothesis of dyslexia susceptibility 114
3.4 Conclusion . . . 119

4 Chapter 4 **121**
4.1 Introduction . . . 122
4.2 Results . . . 123
4.2.1 Locomotor activity in a novel environment . . . 123
4.2.2 Accelerating rotarod . . . 124
4.2.3 Spatial memory tests . . . 125
4.2.4 Anxiety-like behaviour in the light-dark box . . . 126
4.2.5 Olfactory response . . . 129
4.2.6 Startle response, PPI and rapid auditory processing in dKO mice . . . 130

4.2.7 Startle response, PPI and rapid auditory processing in single *Kiaa0319* and *AU040320* KOs . . . 133
4.2.8 Impaired auditory brainstem responses in *AU040320* and double KO mice . . . 136
4.2.8.1 ABR thresholds . . . 137
4.2.8.2 Reduced wave amplitudes indicate altered auditory processing in *AU040320* and dKO mice . . . 138
4.2.8.3 ABR deficits in *AU040320* and double KOs in response to sounds in noise suggest impaired temporal processing . . . 144
4.2.9 Expression of *Kiaa0319* and *AU040320* in the lower auditory pathway . . . 148
4.2.10 Synapse number in the auditory pathway of dKO mice . . . 151
4.3 Discussion . . . 155
4.4 Conclusion . . . 164

5 Chapter 5 **165**
5.1 Introduction . . . 166
5.1.1 Introduction to spermatogenesis . . . 166
5.1.2 Spermiogenesis: acrosome development . . . 169
5.1.3 Disorders of acrosome formation: globozoospermia . . . 170
5.2 Results . . . 172
5.2.1 Expression of AU040320 in the reproductive system . . . 172
5.2.2 *AU040320* KO leads to male infertility . . . 173
5.2.3 Normal meiotic progression of spermatocytes is unaffected following *AU040320* KOs . . . 173
5.2.4 Absence of *AU040320* leads to abnormal sperm morphology with globozoospermia-like features . . . 175
5.2.5 Impaired acrosome biogenesis in *AU040320* KO mice . . . 178
5.2.6 Failure in vesicle transport and fusion in *AU040320*-deficient spermatids . . . 180
5.2.7 Normal Sertoli cells & manchette in *AU040320* KOs . . . 182
5.2.8 AU040320 localises to the trans-Golgi network . . . 184
5.2.9 Interaction with proteins involved in acrosome development and intracellular trafficking . . . 186
5.2.10 Mutation screening in human globozoospermia . . . 189
5.3 Discussion . . . 191
5.4 Conclusion . . . 197

6 General Discussion **199**
6.1 Introduction 200
6.2 Summary of findings & final considerations 200
6.2.1 The role of KIAA0319 & KIAA0319L proteins in neuronal migration 200
6.2.2 The role of KIAA0319 & AU040320 in mouse behaviour and auditory processing 202
6.2.3 Subcellular function of AU040320 and a new hypothesis . . . 204
6.3 Unresolved questions and future work 207
6.4 Final conclusion 212

Appendices

A Appendix 1 **217**
A.1 List of primers 217
A.2 Sequence of the AU040320-KO1 allele and flanking regions 220
A.3 Primary cilia in double KO cortical neurons 229

B Appendix 2 **231**
B.1 ABR comparisons by gender for each cohort 232
B.2 ABR comparisons by age for each cohort 234
B.3 Tables with statistical values for each experimental condition tested 236

References **247**

List of Figures

1.1 Neurobiology of reading 5
1.2 Cortical migration abnormalities in human dyslexia histopathology 10
1.3 Dyslexia susceptibility *loci* 14
1.4 The *DYX2* locus. 23
1.5 The *KIAA0319* gene and its encoded protein 27
1.6 The *KIAA0319L* gene 29
1.7 Alignment of human KIAA0319 and KIAA0319L proteins. 30
1.8 Alignment of mouse KIAA0319 and AU040320 proteins. 31
1.9 Expression of *KIAA0319* and *KIAA0319L*/*AU040320* in developing and adult brain 34
1.10 Knockdown of *Kiaa0319* with shRNA via *in utero* electroporation in rats impairs neuronal migration 36
1.11 shRNA-mediated knockdown of *Kiaa0319-Like* impairs neuronal migration in rats 39
1.12 Rats treated with *Kiaa0319*-shRNA show impaired rapid auditory processing 41
1.13 The structure of the neocortex and brain development 45
1.14 The development of the neocortex 48

3.1 Generation of AU040320 mouse lines: *AU040320 locus* 81
3.2 Generation of AU040320 mouse lines: Western blot and PCRs . . . 83
3.3 Schematic representation of PCR approach for analysis of *AU040320* trasgenic alleles. 84
3.4 Western blot of multiple mouse tissues to detect AU040320 protein. 86
3.5 Generation of AU040320 mouse lines: Nissl stainings 88
3.6 Normal cell division profiles in *AU040320* and double KOs 91
3.7 Radial glial and intermediate progenitors are unaffected in *AU040320* KO 92
3.8 Normal progenitor pool in the developing cortex of dKO mice . . . 93
3.9 Normal cortical lamination in *AU040320* KOs throughout development 95
3.10 Double KOs exhibit normal overall brain anatomy and no cortical ectopias 97

3.11 Double KO mice exhibit unaltered cortical lamination 99
3.12 Normal subplate in absence of Kiaa0319 and AU040320 100
3.13 Acute KO of *Kiaa0319* and *AU040320* does not affect neuronal migration 102
3.14 Normal distribution of interneurons in the dKO neocortex 104
3.15 Normal hippocampal morphology in *AU040320* KO mice 106
3.16 Hippocampus of P10 dKOs exhibit normal lamination pattern . . . 107
3.17 Normal cerebellar anatomy in *AU040320* and double KOs 108

4.1 Double KOs exhibit normal locomotor activity in a novel environment 124
4.2 Motor coordination and learning in accelerating rotarod is unaffected in dKOs 125
4.3 Normal spatial memory and exploration in dKOs 127
4.4 Double KOs display a mild increase in anxiety-levels in the light-dark box 128
4.5 No change in olfactory preference test in Double KOs 130
4.6 Double KOs have normal startle reflex and prepulse inhibition but impaired silent gap detection 132
4.7 Normal startle reflex and PPI in *Kiaa0319* and *AU040320* single KOs. 134
4.8 Normal silent gap detection in single *Kiaa0319* and *AU040320* KO mice 135
4.9 Auditory brainstem responses 137
4.10 Click ABR thresholds 138
4.11 Peak amplitudes and latencies for dKO and wildtype controls in click ABRs 140
4.12 Peak amplitudes and latencies for wildtype, *Kiaa0319* and *AU040320* KO mice in click ABRs 141
4.13 Peak amplitudes and latencies for wildtype, *Kiaa0319* and *AU040320* KO mice in click ABRs at a slow click rate 143
4.14 Comparisons of responses to sound clicks following noise with responses to clicks following silence in wildtypes *Kiaa0319* and *AU040320* 145
4.15 Double KO mice show impaired wave III in responses to clicks 20 and 50 ms after noise 147
4.16 Flow-chart of experimental progression of double and single cohorts in ABR experiments. 148
4.17 Expression of *Kiaa0319* and *AU040320* in the adult lower auditory pathway by X-gal staining. 150

4.18 Absence of KIAA0319 and AU040320 does not affect the number of synaptic puncta in the ventral cochlear nucleus, inferior colliculus and medial geniculate body. 154

5.1 The male reproductive system and spermatogenesis in mammals . . 168
5.2 Schematic representation of rodent spermiogenesis 170
5.3 Human globozoospermia and proteins involved in globozoospermia in mice 171
5.4 Absence of AU040320 leads to male infertility 174
5.5 Normal meiotic progression of spermatocytes is unaffected following *AU040320* KO 175
5.6 AU040320-deficient spermatozoa exhibit globozoospermia-like features 177
5.7 Developmental course of the acrosome is disrupted in AU040320-deficient mice 179
5.8 Ultrastructure of developing acrosomes shows impaired vesicle fusion in *AU040320* mutants 181
5.9 Pseudoacrosomal structures in *AU040320* -/- mice 182
5.10 Cytoskeletal arrangement of Sertoli cells and developing manchette appears unaltered 183
5.11 Immunohistochemistry of AU040320 and its subcellular localisation. 185
5.12 The C-terminal domain of human KIAA0319L protein is pulled-down with intracellular trafficking proteins AP-1, AP-2 and ASAP1 . . . 187
5.13 Co-localisation of AU040320 with other mouse globozoospermia-associated proteins 189

A.1 Cilia morphology unaffected by absence of KIAA0319 and AU040320 229

B.1 Click-evoked ABR wave amplitudes and latencies by gender. 233
B.2 Click-evoked ABR wave amplitudes and latencies by age 235

List of Tables

1.1 Table of linkage studies for each dyslexia susceptibility *locus*. 17
1.2 List of association reported for the main dyslexia susceptibility candidate genes. 18

2.1 List of antibodies used in Chapter 3 for immunofluorescence or Western blotting. 63
2.2 List of antibodies used in Chapter 5 for all experiments 74

3.1 ES cells injections and chimeras obtained per ES cell clone 81
3.2 Genotype analysis of progeny from crosses of *AU040320* +/- mice. . 87
3.3 Weight of AU040320 mutants during early development. 87

A.1 List of primers for genomic AU040320 and transgenic gene trapping cassette. 218
A.2 List of primers for genomic KIAA0319L. 219

List of Abbreviations

ISH . . . . . *In situ* hybridisation

SNARE . . . . Soluble NSF Attachment protein Receptor

SNP . . . . . Single nucleotide polymorphism

DCDC2 . . . . Doublecortin domain-containing protein 2

DYX1C1 . . . Dyslexia susceptibility 1 candidate 1

AP-1 . . . . . Adaptor protein 1

AP-2 . . . . . Adaptor protein 2

NgR . . . . . Nogo receptor

AAV . . . . . Adeno-associated virus

GWAS . . . . . Genome-wide association study

PKD . . . . . Polycystic kidney disease

MANEC . . . (motif at N terminus with eight cysteines

CAS . . . . . Childhood apraxia of speech

BA . . . . . Broadmann area

ASD . . . . . Autism spectrum disorder

DNA . . . . . Deoxyribonucleic acid

bp . . . . . base pair

VZ . . . . . Ventricular zone

KO1 . . . . . Knockout-first

dKO . . . . . Double knockout

E . . . . . Embryonic day

P . . . . . Postnatal day

KO . . . . . Knockout

CNV . . . . . Copy number variation

ADHD . . . . Attention-deficit hyperactivity disorder

SLI . . . . . Specific language impairment

Ctip2 . . . . . COUP-TF interacting protein 2

DAPI . . . . . 4',6'-diamidino-2-phenylindole

EDTA . . . . . Ethylene diamine tetra-acetic acid

GFP . . . . . Green fluorescent protein

EGFP . . . . . Enhanced green fluorescent protein

GABA . . . . . Gamma amino butyric acid

HCl . . . . . Hydrochloric acid

Ig . . . . . Immunoglobulin

TGN . . . . . *Trans*-Golgi network

C-terminus . . Carboxyl-terminus

N-terminus . . Amino-terminus

IRES . . . . . Internal ribosome entry sites

CP . . . . . Cortical plate

lcp . . . . . Lower cortical plate

MZ . . . . . Marginal zone

WM . . . . . White matter

ucp . . . . . Upper cortical plate

IZ . . . . . Intermediate zone

SVZ . . . . . Sub-ventricular zone

VZ . . . . . Ventricular zone

LGE . . . . . Lateral ganglionic eminence

CGE . . . . . Caudal ganglionic eminence

MGE . . . . . Medial ganglionic eminence

Pax6 . . . . . Paired box 6 gene

Tbr2 . . . . . T-box brain related gene 2

PCR . . . . . Polymerase chain reaction

ph3 . . . . . Phospho-histone H3

qPCR . . . . . Quantitative polymerase chain reaction

RNA . . . . . Ribonucleic acid

rpm . . . . . Revolutions per minute

shRNA . . . . short hairpin ribonucleic acid

RIPA . . . . . Radio-Immunoprecipitation Assay buffer

PBS . . . . . Phosphate buffered saline

PFA . . . . . Paraformaldehyde

ABR . . . . . Auditory brainstem responses

PPI . . . . . Prepulse inhibition

AU AU040320

KA Kiaa0319

MGB . . . . . Medial geniculate body

A1 . . . . . Primary auditory cortex

IC . . . . . Inferior colliculus

VCN . . . . . Ventral cochlear nucleus

DCN . . . . . Dorsal cochlear nucleus

SOC . . . . . Superior olivary complex

β-gal . . . . . β-galactosidase

RNAi . . . . . RNA-interference

mRNA . . . . messenger RNA

LMA . . . . . Locomotor activity

2-MA . . . . . 2-methylbutiric acid

1 Introduction

Contents

1.1 Developmental dyslexia 3
1.1.1 Neuropsychology of reading and dyslexia 4
1.1.2 Neurobiology of reading and dyslexia 8
1.2 Genetics of dyslexia 12
1.2.1 Classic linkage and association studies 13
1.2.2 Genome-wide studies of dyslexia 19
1.3 *KIAA0319* and *KIAA0319L* as dyslexia susceptibility candidate genes 21
1.3.1 *KIAA0319*: a prime candidate gene 21
1.3.2 *KIAA0319L* 24
1.3.3 Functional relevance of risk alleles 25
1.4 The KIAA0319 and KIAA0319L proteins 26
1.4.1 KIAA0319 26
1.4.2 KIAA0319L 28
1.4.3 Homology, conservation and evolution 32
1.4.4 Gene expression studies 32
1.5 Functional studies of *KIAA0319* and *KIAA0319L* . . 35
1.5.1 Rodent neuronal migration 35
1.5.2 Behavioural effects of *Kiaa0319* knockdown 40
1.6 The neocortex 43
1.6.1 Development of the neocortex 46
1.6.2 Cortical neurogenesis 46
1.6.3 Radial cortical migration 49
1.6.4 Tangential cortical migration 51
1.6.5 Disorders of neuronal migration 51
1.7 Aims of this thesis 53

The capacity for language is a key innovation underlying the complexity of human cognition and evolution, and it is likely to have been involved in the vast cognitive and cultural advances of our species – the 'great leap forward' (Diamond 1997). Whilst spoken and/or gestural language may have emerged over a long period through biological as well as cultural evolution (Pinker & Bloom 1990; Hauser et al. 2002; Pinker & Jackendoff 2005; Fitch 2010; Christiansen & Chater 2008; Dediu & Levinson 2013; de Boer 2016; Friederici 2016), written language is a very recent event in evolutionary history. Dating back to around 5,000 years ago, it is likely to have emerged through cultural innovations only (Lawler 2001; Dehaene 2009). Language in its written form is considered secondary to spoken language, as Leonard Bloomfield put it:

> *"Writing is not language, but merely a way of recording [spoken] language by visible marks"*
>
> (Bloomfield 1933, p. 21).

As such, our ability to read and write is shaped by neural circuits that are not specialised for the task but which became exapted (or 'recycled') into reading – nonetheless, learning to read can also shape brain function and structure (Gould 1991; Dehaene et al. 2005; Dehaene 2010). Understanding the biology of language and reading can give us insights into how these traits function, interact and influence cognition as well as shed light onto how they may have evolved. Research into the neurobiology of language from the perspective of neuropsychology and cognitive neuroscience has been a very productive field over the past few decades and revealed a great deal of the neurobiology of underlying language and reading. However, little is known about the molecular and cellular basis of these systems. With the advent of molecular genetics, it became possible to identify genes that correlate with impaired (and normal) linguistic ability and thus offering a way to interrogate the underlying neural architecture of language – providing a 'molecular window' into the neurobiology of language (Fisher 2007).

1.1 Developmental dyslexia

From this perspective, several language-related disorders have been subjected to investigation in the past couple of decades: verbal dyspraxia, developmental dyslexia, specific language impairment (SLI), stuttering, and speech-sound disorder, as well as more general neurodevelopmental disorders where language ability is affected such as autism spectrum disorder (ASD), Williams syndrome, Rett syndrome and so forth (reviewed in Fisher 2007; Newbury et al. 2010; Kang & Drayna 2011; Szalontai & Csiszar 2013; Kere 2014; Graham & Fisher 2015). Developmental dyslexia is one of the most studied amongst these disabilities and it refers to a neurological condition manifested by impaired reading ability despite normal intelligence, adequate instruction and socio-cultural opportunity, and intact general sensory abilities (Lyon et al. 2003; World Health Organisation 2008). Developmental dyslexia (henceforth, dyslexia) is a congenital neurodevelopmental disorder and it contrasts with acquired dyslexia, where reading impairment typically results from brain damage. The Fifth Edition of the Diagnostic and Statistical Manual of Mental Disorders (DSM 5) of the American Psychiatric Association defines dyslexia as a 'specific learning disorder' where reading is below the expectations for an individual's age category (American Psychiatric Association 2013). Dyslexia can have grave consequences for affected individuals as they generally attain a lower educational level, have higher rates of stress and unemployment and it can cause an estimated cost of £80,000 to an individual's lifetime earnings (The Government Office for Science 2008)

Dyslexia is one of the most common learning disabilities and it is estimated to occur in 5-17% of school-aged children (Shaywitz et al. 1990; Katusic et al. 2001; Zhang et al. 1996; Shaywitz & Shaywitz 2005; Chan et al. 2007; Schumacher et al. 2007). These estimates can vary, however, depending on several factors such as categorisation thresholds, reading tests used to diagnose, whether IQ is taken into account, and so on – there is also some evidence suggesting cross-linguistic

differences in incidence (Farrag et al. 1988; Ziegler & Goswami 2005). Some reports also indicate a higher prevalence of dyslexia in males, possibly 3-6 times more common than in females, although this difference may result from boys being more commonly referred than girls (Rutter et al. 2004; Flannery et al. 2000). Dyslexia commonly co-occurs with other neurodevelopmental disorders and it has a high co-morbidity rate with SLI at around 50% (Snowling et al. 2000; Bishop & Snowling 2004; Newbury et al. 2011), attention deficit hyperactivity disorder (ADHD) at 15-40% rate (Gilger 1992; Willcutt & Pennington 2000; Germanò et al. 2010), mathematical disability, approximately 50% (Landerl & Moll 2010; Ritchie & Bates 2013; Davis et al. 2014), speech sound disorder (Pennington & Bishop 2009; Nittrouer & Pennington 2010; Eicher et al. 2015), verbal dyspraxia (Richardson & Ross 2000), amongst others. As Gilger & Kaplan (2001, p. 465) put it, comorbidity is "the rule rather than the exception".

1.1.1 Neuropsychology of reading and dyslexia

Whilst a child acquires their native language virtually effortlessly, learning to read requires explicit instruction and effort and it culminates in the acquisition of a complex interplay of linguistic, sensory and attentional processes. Reading involves mapping written symbols (i.e. graphemes) onto their corresponding phonological representations in the lexicon, the mental dictionary. For example, in the English word 'ball' the letter 'b' is mapped onto the phoneme /b/ (Fig. 1.1A). Thus, the reading task involves the perception and recognition of the visual input which is then mapped onto an orthographic lexicon interacting with the corresponding phonological, semantic and structural representations (Carreiras et al. 2014). Psycholinguistic models of visual word recognition indicate this is typically achieved through a dual route of processing: one which operates at the single unit level, decoding individual graphemes into phonemes, and another which recognises whole word patterns and shapes directly (Coltheart et al. 2001; Coltheart 2006; Norris 2013).

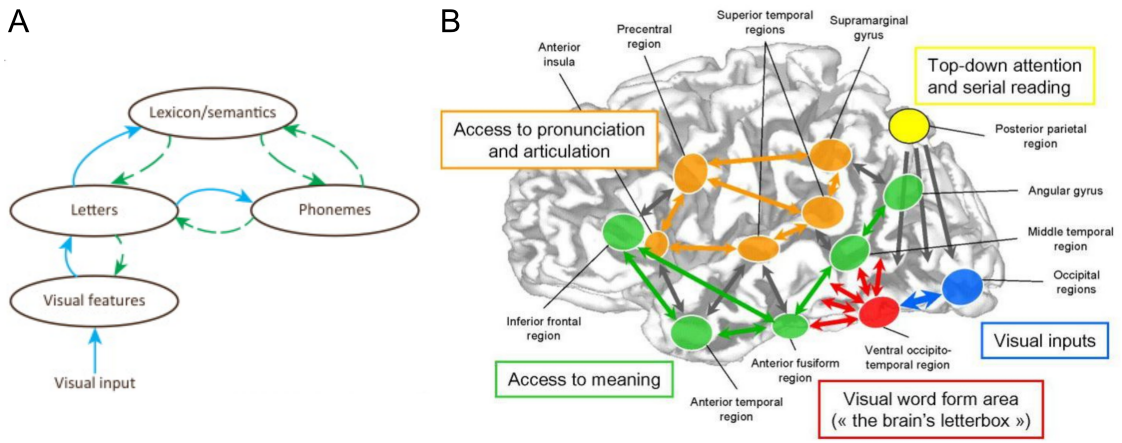


Figure 1.1: Neurobiology of reading. (A) Basic model of visual word recognition in reading where visual input is processed by combining letter recognition in interaction with the phonological and lexico-semantic system; adapted from Carreiras et al. 2014. (B) Cortical network for reading indicating main areas implicated and the flow of information from early visual areas (blue) to the visual word form area in the left fusiform gyrus (red). The information then proceeds via a ventral (green) or dorsal pathway (orange), with attentional systems exerting top-down control from the posterior parietal cortex (yellow); adapted from Dehaene 2009.

Neuropsychological studies of dyslexic individuals have identified the main types of tasks in which their performance is impaired: (a) phonological awareness, which tests the ability to manipulate phonemes (e.g. say the word 'ball' without the /b/); (b) rapid automatised naming, where the speed of naming a familiar stimulus is measured (e.g. the latency to name repeated presentations of letters, objects, etc); (c) reading fluency, where the speed and accuracy of reading is determined by reading a word list aloud; (d) reading of non-words, which involves reading possible but non-existent words and dyslexics perform worse than when compared to reading existing words (Shaywitz & Shaywitz 2005; Norton et al. 2015). Although the neuropsychology of dyslexia has been the focus of extensive research efforts over the years, there is no general consensus on the underlying nature of the problems leading to dyslexia. Several proposals have been ranging from deficits which specifically affect linguistic systems, particularly phonology, to more general

but subtle impairments in sensory perception or attention (Habib 2000; Shaywitz & Shaywitz 2008; Ramus & Ahissar 2012; Goswami 2014).

Initial observations over a hundred years ago described dyslexia as 'congenital word blindness', with visual aspects of reading being the centre of attention for most of the 20th century (Morgan 1896; Hinshelwood 1911; Orton 1925; Hallgren 1950; Dunlop 1972; Ramus & Ahissar 2012). Although visual impairment is still debated as a potential causative factor in dyslexia, early work in cognitive psychology shifted the attention from visual impairment to possible underlying linguistic processes, particularly phonological processing (Liberman 1973). This work formed the basis of what has now become the most widely accepted theory for the underlying cause of dyslexia given that dyslexics typically exhibit poor performance on phonological awareness tasks – according to this view, reading impairment is caused by a specific impairment in the representation, access or storage of phonemes which later on lead to impaired sound-to-symbol mapping (Snowling 1981; Wagner & Torgesen 1987; Goswami 2000; Snowling et al. 2000; Ramus & Ahissar 2012; Boets et al. 2013).

The phonological processing theory of dyslexia is challenged by evidence showing that dyslexics suffer from subtle problems in sensory perception, particularly in the auditory domain. Several studies have demonstrated that dyslexics suffer from impaired auditory processing of rapidly changing stimuli such as frequency/amplitude modulation, gap detection, rapid auditory naming, and so forth (Shaywitz & Shaywitz 2005; Ramus & Ahissar 2012; Goswami 2014). As such, it has been proposed that dyslexia emerges due to difficulties in detecting short and rapid transitions between sounds which affect sampling of the acoustic signal, eventually leading to impaired phonology (Tallal 1980; Tallal 2004).

Building on the early work on vision, visual perception deficits have also been argued as a causative mechanism for dyslexia based on evidence of impairment in the visual magnocellular pathway, particularly in thalamic magnocells which control visual parsing in detection of motion, low spatial frequencies and high-frequency temporal input (Lovegrove et al. 1980; Livingstone et al. 1991; Stein & Walsh 1997;

Stein 2001). The visual domain is also implicated in a widely reported deficit in attentional processes seen in dyslexics, in line with its co-morbidity with ADHD: according to this proposal, dyslexia results from impaired ability to selectively attend to relevant information when reading (Geiger et al. 1994; Facoetti et al. 2000; Vidyasagar & Pammer 2010; Franceschini et al. 2012).

Causative neuropsychological theories of dyslexia also implicate the motor system as it has been shown that dyslexics perform poorly in certain fine motor tasks which may result from impaired function of cerebellum (Nicolson et al. 2001; Ramus & Ahissar 2012; Goswami 2014). A related proposal, the magnocellular theory, combines this with evidence of abnormal function of magnocellular pathways more generally, extending it beyond vision, to suggest the dyslexia phenotype emerges due to general sensorimotor problems (Stein & Walsh 1997; Stein 2001; Ramus & Ahissar 2012; Gori et al. 2015). Given the involvement of the motor system in speech perception (Liberman & Mattingly 1985; Hickok & Poeppel 2007), a motor/cerebellar deficit may account for the attested phonological/auditory deficit whilst also establishing a link with proposals that impaired language ability results from abnormal procedural learning (Ullman & Pierpont 2005; Nicolson et al. 2010; Lum et al. 2013).

Although the phonological deficit theory is the most widely accepted account, lack of consensus is the norm in this debate – proposals typically only cover a subset of the observed deficits and fail to explain the whole range of symptoms (Ramus et al. 2003; Shaywitz & Shaywitz 2005; Ramus & Ahissar 2012; Goswami 2014) This is further complicated by the several divergent diagnostic criteria employed by researchers to define dyslexic cohorts as well as the highly heterogeneous nature of the disorder (Bakker 1992; Castles & Coltheart 1993; Menghini et al. 2010; Heim et al. 2008; Newbury et al. 2014; Bishop 2015). In addition, the brains of dyslexics have reduced reading experience and do not undergo the same sensory and attentional learning processes as non-dyslexic ones, thus making it difficult to disentangle observed differences as cause or consequences (Goswami 2014).

1.1.2 Neurobiology of reading and dyslexia

1.1.2.1 The neural architecture of reading

Neuroimaging studies over the past decades or so have uncovered the underlying neural architecture that supports reading. Like language more generally, reading depends on the combination of sensorimotor systems (particularly early visual pathways in reading), alongside the core processing 'language network', a left-lateralised system involving temporo-parietal areas connected to the inferior frontal cortex via the arcuate fasciculus (Fig. 1.1B; (Dehaene 2009; Price 2012; Hagoort 2014; Friederici & Gierhan 2013; Carreiras et al. 2014). A key element of this circuit is the visual word form area in the left fusiform gyrus which is responsible for word recognition, possibly due to specialisation for recognition of objects more generally (Logothetis & Sheinberg 1996; Cohen et al. 2002; Dehaene 2005; Dehaene 2009). The reading network consists of two major pathways: a dorsal circuit involving the occipital, supramarginal and angular gyri which connect to the premotor cortex and pars opercularis around Broca's area in the inferior frontal cortex; and a ventral pathway which connects the left fusiform gyrus and the middle/anterior temporal gyrus with the pars triangularis in the frontal cortex (Dehaene 2009; Price 2012; Carreiras et al. 2014).

1.1.2.2 Human neuropathology

Some of the earliest investigations into the neurobiological basis of dyslexia come from a series of *postmortem* neuropathological examinations of human brains diagnosed with dyslexia that were conducted around the 1980s by a team at the Harvard Medical School led by Albert Galaburda. These studies involved anatomical analyses of serial sections of 8 brains which identified two main features in their specimens: (a) an altered degree of asymmetry in the planum temporale, a region lying immediately posterior to the primary auditory cortex which typically contains more gray matter in the left hemisphere than in the right (Geschwind & Levitsky 1968; Geschwind & Galaburda 1985); and (b) a high incidence of small

malformations in the neocortex typically appearing as layer I neuronal ectopias, with some laminar dysplasia and focal microgyria (Fig. 1.2A) (Galaburda & Kemper 1979; Galaburda et al. 1985; Humphreys et al. 1990). These cortical malformations somewhat resembled those found in two other separate cases reported by different groups (Drake 1968; Levine et al. 1981; Cohen et al. 1989). The authors report that in some cases the number of the observed cortical anomalies amounted to 30 to 140 per brain and they tended to cluster around the left peri-sylvian region, in the superior temporal gyrus and Heschl's gyrus (Brodmann areas 22, 41, 42), key regions in the language network (Fig. 1.2B; Poeppel et al. 2012; Friederici & Gierhan 2013; Hagoort 2014; Carreiras et al. 2014). A separate later study examined similar cortical dysgenesis in non-dyslexic specimens but found that, although such micro-abnormalities were also present, they appeared in much smaller numbers, 1-2 per brain in only 3 out of 10 samples (Kaufmann & Galaburda 1989). Given focal ectopias and microgyria are characteristics of abnormal neuronal migration during the development of the neocortex, these observations led to suggestions that impaired neuronal migration may underlie dyslexia (Galaburda et al. 1985; Galaburda 1989; Galaburda & Livingstone 1993). Additional reports later on also identified abnormal organisation of thalamic magnocells in the same human dyslexic specimens (Livingstone et al. 1991; Galaburda et al. 1994). Around the same time, studies of mice with autoimmune disorders exhibiting similar cortical ectopias were found to suffer from auditory deficits similar to those found in dyslexics which, combined with reports of higher incidence of immune deficiencies in the dyslexic population, provided some added support for the neuronal migration hypothesis (Sherman et al. 1985; Sherman et al. 1987; Galaburda & Livingstone 1993).

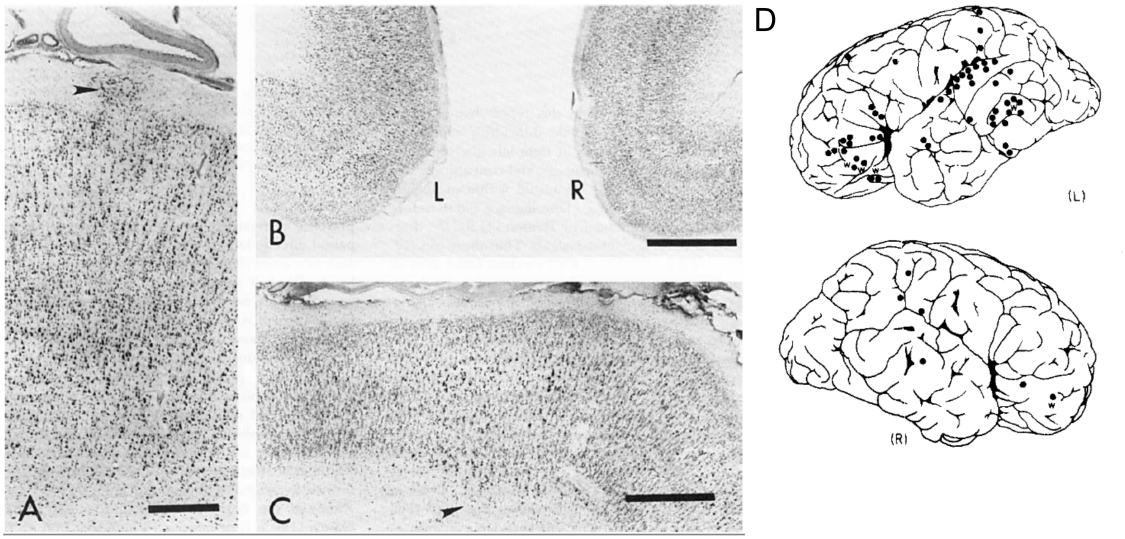


Figure 1.2: Cortical migration abnormalities in human dyslexia histopathology. (A-C) Specimens from the case study in Galaburda & Kemper (1979) showing an example of layer I ectopia found in the cortex (A), dyslamination of the left cingulate gyrus when compared to the right (B), dysplasia of cortical neurons which appear in white matter in the occipital cortex (C). Scale bars: 1 mm (A), 2mm (B, C). (D) Topographical distribution of cortical ectopias and dysplasias (indicated by solid circles) and brain warts (w) between left and right hemisphere in a dyslexic case investigated in Galaburda et al. (1985). Adapted from Galaburda & Kemper 1979 and Galaburda et al. 1985.

1.1.2.3 Functional and structural neuroimaging studies

Further evidence in support of cortical migration deficits did not emerge until years later with two neuroimaging studies where individuals displaying a type of cortical migration disorder, periventricular nodular heterotopias, were tested on their reading ability and intelligence (Chang et al. 2005; Chang et al. 2007). These studies revealed that the majority of subjects with periventricular nodular heterotopias performed poorly on reading tasks, with their performance comparable to the dyslexia group; in addition, poorer performance was observed in subjects exhibiting more widespread heterotopias. Although there has been no further attempts to confirm this, some studies have reported an enrichment of polymicrogyria, another type of cortical migration abnormality, in SLI populations – but this has not been consistently replicated (Guerreiro et al. 2002; Hage et al. 2005; Oliveira et al. 2008; Webster et al. 2008; Leventer et al. 2010; Jansen et al. 2016).

Beyond cortical migration, a vast number of other neuroimaging studies have been conducted over the past couple of decades and identified several features that are commonly observed in cohorts with reading impairment. At the structural level, neuroimaging studies using MRI have attempted to validate the original findings of Galaburda and colleagues on the altered degree of asymmetry of the planum temporale in dyslexics; although some reports confirm the reduced asymmetry, several others, including some meta-analyses, have failed to validate it (Larsen et al. 1990; Eckert 2004; Bloom et al. 2013; Altarelli et al. 2014; Norton et al. 2015). However, there is evidence indicating that altered asymmmetry of this region is modulated by sex differences between males and females (Guadalupe et al. 2015). Other putative signatures of morphological changes in dyslexia include abnormal white matter integrity along the left arcuate fasciculus (Klingberg et al. 2000; Beaulieu et al. 2005; Hoeft et al. 2007; Vandermosten et al. 2012; Zhao et al. 2016) and altered cortical thickness in the visual wordform area (Frye et al. 2010; Richardson et al. 2011; Monzalvo et al. 2012; Altarelli et al. 2013; Norton et al. 2015). In some cases, differences between males and females have also been reported (Evans et al. 2014; Altarelli et al. 2013). Functionally, hypoactivation of the left occipitotemporal region is one of the most consistent findings, particularly in the visual word-form area (Maisog et al. 2008; Richlan et al. 2011; Richlan 2012). Other cortical regions have also been shown to have altered activation as the temporo-parietal and inferior frontal cortex, and sub-cortical areas (Schlaggar & McCandliss 2007; Pugh et al. 2013). Studies using fMRI and auditory brainstem responses have also reported dysfunction in non-cortical areas such as the auditory thalamus and the brainstem (Díaz et al. 2012; Hornickel & Kraus 2013).

It is important to note that the majority of these findings are somewhat inconsistent and not reliably replicated. This is likely to result from the methodological issues which have been strongly debated in psychology and cognitive neuroscience in recent years. Studies typically have low sample sizes and divergent study designs that hinder reproducibility in the field (e.g. Open Science Collaboration 2015).

This inconsistency may also originate from issues specific to dyslexia as mentioned above (diagnostic criteria, heterogeneity, differences in adult-child profiles, and so forth; see e.g. Goswami 2014).

1.2 Genetics of dyslexia

Early studies from over a hundred years ago had already pointed towards a familial basis for dyslexia (e.g. Thomas 1905; Fisher 1905; Stephenson 1907; Hinshelwood 1911) and later studies with twins and family groups have confirmed a genetic component of the disorder (Hallgren 1950; DeFries et al. 1978; DeFries et al. 1987; DeFries & Alarcón 1996; Pennington et al. 1991; Fisher & DeFries 2002). These behavioural genetics studies have shown dyslexia is a highly heritable disorder, with some concordance rates reaching 68% for monozygotic twins and 38% for dizygotic ones – estimates of heritability vary between 40-70% (DeFries & Alarcón 1996; Schumacher et al. 2007). The early studies had already made clear that dyslexia does not follow a classic Mendelian or monogenic line of transmission and that, like most other common traits, dyslexia is a complex, multifactorial disorder (Lewitter et al. 1980; Pennington et al. 1991; Gilger et al. 1994). As such, multiple genetic and environmental risk factors play a role in susceptibility to dyslexia. At the environmental level, evidence is still very scarce and somewhat circumstantial but it is likely to include factors such as preliteracy environments, socio-economic status and parental education (Grigorenko et al. 2001). With respect to its genetic architecture, dyslexia susceptibility parallels other complex disorders and it involves a number of genes combined in different types of risk variants: common or rare, with high or low penetrance (see e.g. Plomin et al. 2009; Mitchell 2012). The next section outlines the development and current knowledge on the genes and variants involved in dyslexia susceptibility.

1.2.1 Classic linkage and association studies

Investigation into genetic *loci* associated with susceptibility to dyslexia (and other complex disorders) started with the use of linkage analysis and early studies had limited success in identifying reliable signals of genomic regions conferring risk (Smith et al. 1983; Bisgaard et al. 1987; Froster et al. 1993; Rabin et al. 1993; reviewed in Fisher & DeFries 2002). However, methodological advances such as the incorporation of quantitative designs alongside the typical case-control cohorts led to the identification of several susceptibility regions over the years, with nine of them being established as dyslexia susceptibility *loci* (*DYX1-9*) (Fig. 1.3; Cardon et al. 1994; Grigorenko et al. 1997; Schulte-Körne et al. 1998; Fisher et al. 1999; Fisher & DeFries 2002; Kaplan et al. 2002; Fagerheim et al. 1999; Kaminen et al. 2003; Francks et al. 2002; Nopola-Hemmi et al. 2001; Petryshen et al. 2001; Petryshen et al. 2002; Schumacher et al. 2006; Grigorenko et al. 2001; Tzenova et al. 2004; de Kovel et al. 2008). Once established, these *loci* later became the focus of targeted studies attempting to uncover the specific candidate genes underlying the identified susceptibility.

The first susceptibility candidate gene was identified using positional cloning in cases of rare chromosomal translocations and revealed *DYX1C1* (Dyslexia susceptibility candidate 1) in *DYX1* as a candidate gene (Taipale et al. 2003; Bates et al. 2010). Cloning also permitted identification of another gene later on, *ROBO1* in *DYX5* (Hannula-Jouppi et al. 2005). Alongside this, fine-mapping association studies using single nucleotide polymorphisms (SNPs) have revealed two genes associated with dyslexia in *DYX2*, *DCDC2* (Doublecortin domain-containing protein 2) and *KIAA0319* (Meng et al. 2005b; Schumacher et al. 2006; Francks et al. 2004; Cope et al. 2005b), as well as *C2Orf3* and *MRPL19* in *DYX3* (Fagerheim et al. 1999; Anthoni et al. 2007; Scerri et al. 2012). Other *loci* have also had specific genes associated with them such as *MC5R, DYM, MYO5B* and *NEDD4L* in *DYX6* (Fisher & DeFries 2002; Scerri & Schulte-Körne 2010; Poelmans et al.

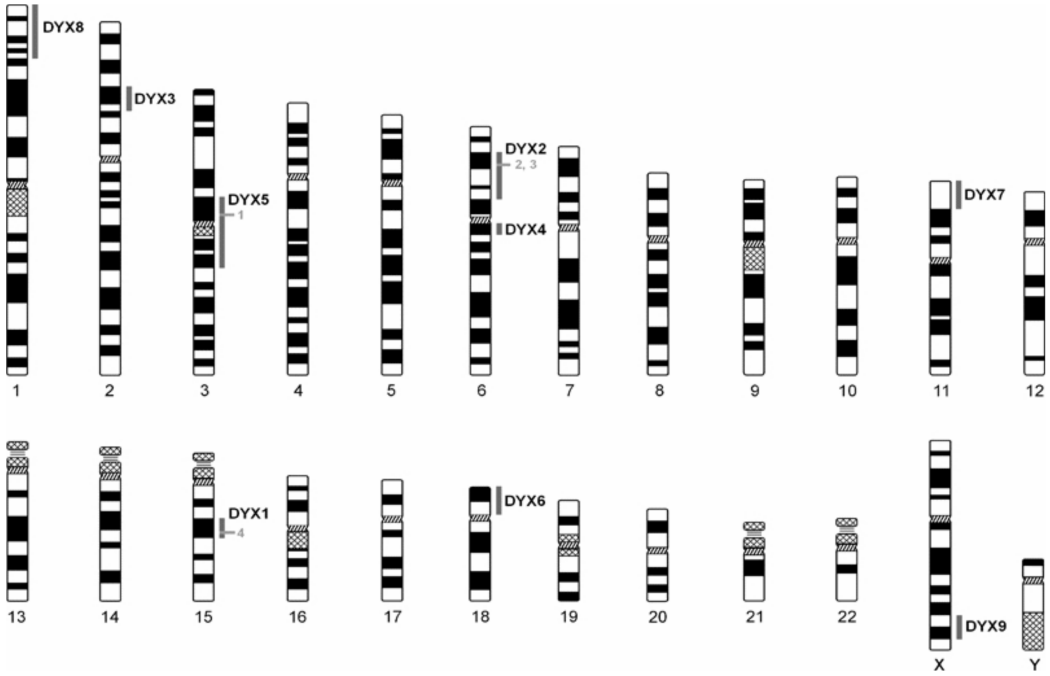


Figure 1.3: Dyslexia susceptibility *loci* identified by linkage analyses. Linkage regions are indicated with the associated *locus* name and wider regions with a bar. Recent advances in genetics have revealed association of a range of new genomic regions. 1, *ROBO1*; 2, *DCDC2*; 3, *KIAA0319*; 4, *DYX1C1*. Adapted from Schulte-Körne et al. 2007.

2011; Müller et al. 2016), *DRD4* in *DYX7* (Fisher & DeFries 2002; Hsiung et al. 2004), *KIAA0319L* in *DYX8* (Grigorenko et al. 2001; Tzenova et al. 2004; Couto et al. 2008), alongside *CYP19A1* as an additional candidate in *DYX1* (Anthoni et al. 2012). These initial studies focusing on linkage regions were later followed by an explosion of reports with association of variants in other regions implicating several other genes such as *DGKI, GRIN2B, CDK5, ZNF804A, FAM65B, CMAHP* (Matsson et al. 2011; Ludwig et al. 2010; Mueller et al. 2014; Burkhardt et al. 2012; Becker et al. 2012; Huc-Chabrolle et al. 2013; Eicher & Gruen 2014).

Genes previously implicated in other language-related disorders have also been linked to susceptibility to dyslexia. For example, SNPs in two candidate genes for SLI, *CMIP* and *CNTNAP2*, have been reported to correlate with reading ability (Newbury et al. 2009; Peter et al. 2011; Scerri et al. 2012; Veerappa et al. 2013b; Rodenas-Cuadrado et al. 2014). In addition, neuroimaging genetics studies have also reported associations between a SNP in the gene *FOXP2*, the first gene linked

to language disorder in cases of verbal dyspraxia (Lai et al. 2001; Fisher & Scharff 2009), and altered brain activation in dyslexics in regions involved in language processing (Wilcke et al. 2012; Pinel et al. 2012). Given the known comorbidity between dyslexia and other language-related disorders, these findings are indicative of shared biological pathways in the aetiology of language-related deficits.

It is important to point out that the candidate genes identified so far vary widely with respect to the robustness and amount of support they receive as dyslexia risk factors. There are several reports of negative association and failed replication for some candidates, and some of them have only been observed in a specific cohort or family, whilst other studies report very low association scores. Genetic studies suffer from similar population sampling problems as the imaging studies mentioned above, particularly in the case of low sample size which hinders statistical power (see e.g. Newbury et al. 2014). Nonetheless, amongst these candidates, *DYX1C1, DCDC2, KIAA0319* and, to some extent, *ROBO1* have received significant and consistent support in the literature due to replication in different population samples. A detailed list of linkage studies is shown in Table 1.1, and a similar list is shown in Table 1.2 for the main susceptibility candidate genes *DYX1C1, DCDC2, KIAA0319* and *ROBO1.* These studies have been conducted using a number of different datasets from different countries (Britain, US, Canada, Finland, India, China, and so on) and typically implicate a number of different markers for the same gene. For example, most reported association with *DYX1C1* are based on rs3743205 (3G>A), rs57809907 (1249G>T) and the haplotype rs3743205:rs57809907. Nonetheless, as it is seen with other candidate genes, these same SNPs are also subject of negative association – whilst Bates et al. 2010 reports strong association with rs3743205 (3G>A) and rs57809907 (1249G>T), this not replicated using a Chinese sample in Zou et al. 2012, nor in a meta-analysis by Tran et al. 2013. In other cases, a SNP may receive stasticically significant association in one study, such as rs4504469 in *KIAA0319* in Luciano et al. 2007, but only nominally associate in another as in Müller et al. 2016. But perhaps the most important point comes from the fact that

no marker in these genes (or any other) hold as significant in larger scale studies such as meta-analyses across multiple datasets (Becker et al. 2014), or in genome-wide association studies (see next section). Overall, classical genetic approaches have revealed *DYX1C1*, *DCDC2* and *KIAA0319*, with *ROBO1* as a more peripheral candidate, as the key dyslexia susceptibility candidate genes, with *KIAA0319* and *DCDC2* as the strongest candidates (Fisher & Marcus 2006; Paracchini et al. 2007; Scerri & Schulte-Körne 2010; Raskind et al. 2013; Carrion-Castillo et al. 2013; Becker et al. 2014; Kere 2014; Graham & Fisher 2015).

DYX#	Chr	Positive studies	Negative studies	Candidate genes
DYX1	15q21	Chapman et al. 2004; Fulker et al. 1991; Grigorenko et al. 1997; Marino et al. 2004; Morris et al. 2000; Nöthen et al. 1999; Schulte-Körne et al. 1998; Schumacher et al. 2008; Smith et al. 1991	Bisgaard et al. 1987; de Kovel et al. 2004; Fagerheim et al. 1999; Fisher et al. 2002; Kaminen et al. 2003; Marlow et al. 2003; Nopola-Hemmi et al. 2001; Rabin et al. 1993	*DYX1C1*
DYX2	6p22.3-p21.3	Cardon et al. 1994; Cardon et al. 1995; Fisher et al. 2002; Fisher et al. 1999; Gayán et al. 1999; Grigorenko et al. 2003; Grigorenko et al. 1997; Grigorenko et al. 2000; Kaplan et al. 2002; Marlow et al. 2003; Smith et al. 1991; Turic et al. 2003	Chapman et al. 2004; de Kovel et al. 2004; Fagerheim et al. 1999; Fagerheim et al. 2000; Field et al. 1998; Igo et al. 2006; Kaminen et al. 2003; Nopola-Hemmi et al. 2001; Norton et al. 2000; Nöthen et al. 1999; Petryshen et al. 2000; Raskind et al. 2005; Schulte-Körne et al. 1998; Sawyer et al. 1998	*DCDC2 and KIAA0319*
DYX3	2p16-p15	Fagerheim et al. 2000; Fagerheim et al. 1999; Fagerheim et al. 2002; Fisher et al. 2002; Francks et al. 2002; Marlow et al. 2003; Petryshen et al. 2002 (Peyrard-Janvid et al. 2004)	Chapman et al. 2004; de Kovel et al. 2004; Igo et al. 2006; Nopola-Hemmi et al. 2001; Norton et al. 2000; Raskind et al. 2005	*MRPL19 and C2ORF3*
DYX4	6q11.2-q12	Petryshen et al. 2000	de Kovel et al. 2004; Fagerheim et al. 1999; Fisher et al. 2002; Igo et al. 2006; Kaminen et al. 2003; Marlow et al. 2003; Nopola-Hemmi et al. 2001; Norton et al. 2000; Raskind et al. 2005	–
DYX5	3p12-q13	Fisher et al. 2002; Hannula-Jouppi et al. 2005; Nopola-Hemmi et al. 2001 (Fisher et al. 2002; Marlow et al. 2003)	de Kovel et al. 2004; Fagerheim et al. 1999; Igo et al. 2006; Kaminen et al. 2003; Norton et al. 2000; Raskind et al. 2005	*ROBO1*
DYX6	18p11.2	Fisher et al. 2002; Marlow et al. 2003	Chapman et al. 2004; de Kovel et al. 2004; Fagerheim et al. 1999; Igo et al. 2006; Kaminen et al. 2003; Nopola-Hemmi et al. 2001; Norton et al. 2000; Raskind et al. 2005; Schumacher et al. 2006	–
DYX7	11p15.5	Hsiung et al. 2004 (Marlow et al. 2003)	de Kovel et al. 2004; Fagerheim et al. 1999; Fisher et al. 2002; Igo et al. 2006; Kaminen et al. 2003; Marlow et al. 2003; Nopola-Hemmi et al. 2001; Norton et al. 2000	–
DYX8	1p36-p34	Grigorenko et al. 2001; Rabin et al. 1993; Tzenova et al. 2004	de Kovel et al. 2004; Fagerheim et al. 2000; Fagerheim et al. 1999; Fagerheim et al. 2002; Igo et al. 2006; Kaminen et al. 2003; Marlow et al. 2003; Nopola-Hemmi et al. 2001; Norton et al. 2000; Raskind et al. 2005; Sawyer et al. 1998	*KIAA0319L*
DYX9	Xq27.2-q28	de Kovel et al. 2004; Fisher et al. 2002	Kaminen et al. 2003; Nopola-Hemmi et al. 2001; Norton et al. 2000	–

Table 1.1: Table of linkage studies for each dyslexia susceptibility *locus*.

	Positive association	**Negative association**
DYX1C1	Taipale et al. 2003; Scerri et al. 2004; Wigg et al. 2004; Marino et al. 2005; Marino et al. 2007; Bellini et al. 2005; Brkanac et al. 2007; Dahdouh et al. 2009; Wigg et al. 2005; Wigg et al. 2008; Bates et al. 2010; Venkatesh et al. 2014; Zhang 2012; Lim et al. 2011; Paracchini et al. 2011	Cope et al. 2005a; Meng et al. 2005a; Ylisaukko-oja et al. 2004; Zou et al. 2012; Tran et al. 2013
DCDC2	Kaplan et al. 2002; Meng et al. 2005b; Deffenbacher et al. 2004; Francks et al. 2004; Schumacher et al. 2006; Ludwig et al. 2008; Brkanac et al. 2007; Couto et al. 2009; Chen et al. 2017; Zhang et al. 2016; Matsson et al. 2015; Zuo et al. 2012; Zhong et al. 2013; Scerri et al. 2012; Lind et al. 2010; Newbury et al. 2011	Cope et al. 2005b; Luciano et al. 2007; Müller et al. 2016; Sun et al. 2014; Svidnicki et al. 2013; Venkatesh et al. 2013a; Venkatesh et al. 2013a
KIAA0319	Deffenbacher et al. 2004; Francks et al. 2004; Harold et al. 2006; Dennis et al. 2009; Cope et al. 2005b; Paracchini et al. 2006; Luciano et al. 2007; Rice et al. 2009; Scerri et al. 2011; Newbury et al. 2011; Kirsten & Other 2012; Venkatesh et al. 2013a; Lim et al. 2014; D'Souza et al. 2016	Kaplan et al. 2002; Schumacher et al. 2006; Brkanac et al. 2007; Couto et al. 2009; Bates et al. 2007; de Kovel et al. 2008; Ludwig et al. 2008; Venkatesh et al. 2011; Paracchini et al. 2011; Svidnicki et al. 2013; Kong et al. 2016
ROBO1	Bates et al. 2011; Platko et al. 2008; Tran et al. 2014; Mascheretti et al. 2014	Newbury et al. 2011; Venkatesh et al. 2013b

Table 1.2: List of association reported for the main dyslexia susceptibility candidate genes.

1.2.2 Genome-wide studies of dyslexia

With advances in genetic technology and the development of high-throughput genotyping and sequencing platforms, the identification of genetic variants conferring risk to complex diseases shifted from linkage-based analyses to studies interrogating the contribution of variants across the whole genome in a largely unbiased way (Visscher et al. 2012). The first genome-wide association study (GWAS) examining reading ability was conducted by Meaburn et al. (2008) and subsequent analyses often incorporated SLI cohorts so as to increase statistical power – nonetheless, studies conducted thus far have not identified genetic variants meeting the stringent genome-wide significance threshold required for reliable associations due to multiple testing (1×10^8; Luciano et al. 2013; Eicher et al. 2013; Field et al. 2013; Gialluisi et al. 2014). These studies have reported nominal association for SNPs in several genes such as *RBFOX2, ABCC13, ZNF385D, COL4A2* and *FGF18*, although none of them have been replicated in different samples, including in a recent study specifically targeting previously identified variants (Carrion-Castillo et al. 2016). GWAS targeting language ability more generally or in SLI cohorts have revealed similarly weak association results to date (Harlaar et al. 2014; St Pourcain et al. 2014; Nudel et al. 2014).

Genome-wide approaches have also questioned the contribution to dyslexia brought by structural variants known as copy number variations (CNVs), typically deletions or insertions that are larger than 1kb. CNVs have been shown to contribute to increased susceptibility to more severe neurodevelopmental and neuropsychiatric disorders such as ASD, schizophrenia and intellectual disability and, thus, may also be important in dyslexia (Mitchell 2015; Malhotra & Sebat 2012). Studies targeting CNVs in dyslexia populations have so far focused on specific families where the disorder aggregates and have led to the identification of variants affecting several *loci* which include genes such as *PCNT2, DIP2A, S100B, PRMT2, PCDH11X, GABARAP, NEGR1, ACCN1, DCDC5, CNTNAP2*

(Poelmans et al. 2009; Veerappa et al. 2013a; Veerappa et al. 2013c), whilst a larger population study has found disruptions in other genes such as *IMMP2L* and *AUTS2* (Girirajan et al. 2011). Variants in *CNTNAP5* and *DOCK4* have also been identified in individuals showing additional deficits alongside dyslexia, such as intellectual disability and ASD (Pagnamenta et al. 2010; Hofmeister et al. 2015). In addition, a recent large study interrogated whether CNVs are enriched in dyslexia and language-impaired populations but found no evidence for increased CNV burden in these cohorts (Gialluisi et al. 2016).

De novo point mutations are added components in the genetic architecture of complex diseases with variants that are often (ultra-)rare but can affect protein coding and lead to high phenotypic penetrance (Bras et al. 2012; Ku et al. 2013). Such rare variants, alongside gene x gene interactions, are likely to contribute to uncovering part of the 'missing heritability' problem – common variants cannot explain most of the observed heritability of common disorders (Manolio et al. 2009; Graham & Fisher 2015; Mascheretti et al. 2015). It is possible that certain complex disorders emerge through the combination of common and rare variants - the 'double-hit' hypothesis (Girirajan et al. 2010; Leblond et al. 2012). Next generation sequencing technologies such as exome sequencing have allowed for comprehensive screening of such variants, although only one study so far has been conducted in dyslexia cohorts. Einarsdottir et al. (2015) have identified a two-base pair mutation leading to a coding change in a highly conserved region of the gene *CEP63* that is seen only in dyslexic members of a Swedish family. This gene encodes a protein that localises to the centrosome, a microtubule-organising center and an important regulator of cell division and proliferation (Kumar & Purohit 2012). In the brain, mutations in this gene is known to cause Seckel syndrome, a type of microcephaly (Sir et al. 2011) . However, the challenge for these approaches lies in the ability to demonstrate these identified mutations have a causal relationship with the disease, particularly as potentially deleterious coding mutations are also found in normal, healthy individuals (MacArthur et al. 2014; Newbury et al. 2014).

As sequencing becomes more accessible, it is expected that new variants will start to emerge reporting other new candidate genes in dyslexia, as it has already been the case for SLI and childhood apraxia of speech (Worthey et al. 2013; Villanueva et al. 2015; Kornilov et al. 2016).

Although research into the genetic basis of dyslexia to date has provided a great deal of insight into the genomic architecture that underlies it, work on language-related disorders lags somewhat behind when compared to other neurodevelopmental and psychiatric disorders such as ASD and schizophrenia. For these, the move from classical genetic approaches to genome-wide studies took place much earlier and with more powerful and larger studies, with recent advances revealing a good picture of the heterogeneous nature of the variants that underlie them (Bourgeron 2015; Rees et al. 2015; Gratten et al. 2014). Given genetic studies are likely to identify only those variants which confer a relatively strong contribution to risk, it is imperative that dyslexia genetics research overcomes issues such as diagnostic criteria across clinics, standardisation of cut-off points for categorisation into case-control groups (e.g. is dyslexia the tail end of normal distribution or do dyslexics differ qualitatively?), increase the size of the population investigated to increase the statistical power, and so on (Newbury et al. 2014; Bishop 2015). Co-morbidity must also be taken into account given the ample overlap of such neurodevelopmental disorders.

1.3 *KIAA0319* and *KIAA0319L* as dyslexia susceptibility candidate genes

1.3.1 *KIAA0319*: a prime candidate gene

Amongst the dyslexia susceptibility genes identified so far, *KIAA0319* emerges as a prime candidate gene based on several replications using independent samples. *KIAA0319* lies in the *DYX2 locus* on chromosome 6 in 6p21.3-23 (Fig. 1.4), the region with best support so far given it is where most consistent linkage and associations have been observed (see e.g. Carrion-Castillo et al. 2013). Following its first identification in a quantitative trait *loci* study by Cardon et al. (1994), a

number of other reports that followed showed strong linkage to *DYX2* (Grigorenko et al. 1997; Fisher et al. 1999; Gayán et al. 1999; Grigorenko et al. 2000; Fisher & DeFries 2002; Kaplan et al. 2002; Grigorenko et al. 2003) before the identification of two candidate genes by fine-mapping association studies: *DCDC2* and *KIAA0319* (Fig. 1.4; Meng et al. 2005b; Francks et al. 2004; Cope et al. 2005b; Paracchini et al. 2006). Further investigation confirmed the association with *KIAA0319* in several other sample sets, including performance variation in reading tasks in the normal population or in relation to specific reading-related endophenotypes (Harold et al. 2006; Luciano et al. 2007; Paracchini et al. 2008; Rice et al. 2009; Dennis et al. 2009; Scerri et al. 2011; Kirsten & Other 2012; Venkatesh et al. 2013a; Lim et al. 2014; Müller et al. 2016; D'Souza et al. 2016; Carrion-Castillo et al. 2017). It is important to note that these replications vary in robustness as some reports link different alleles of the same SNP or have the opposite direction of effect (conferring risk to dyslexia in some cases but 'protection' in others). As it is the case with all other candidates, there are also several reports of negative association of the differing SNPs (Bates et al. 2007; de Kovel et al. 2008; Brkanac et al. 2007; Ludwig et al. 2008; Venkatesh et al. 2011; Paracchini et al. 2011).

Nonetheless, recent reports have continued to link variation in *KIAA0319* as a risk factor underlying susceptibility to dyslexia, although with different degrees of robustness. In many cases, the reported association is only nominal, as it does not hold for the multiple statistical comparisons required (Sun et al. 2014; Zhao et al. 2016; Müller et al. 2016; Carrion-Castillo et al. 2017). *KIAA0319* also receives nominal association in a meta-analysis in a German sample (Müller et al. 2016), whilst a meta-analysis study focusing on one particular *KIAA031* SNP (rs4504469) reported significant association (Zou et al. 2012). On the other hand, a separate meta-analysis study did not replicate this finding using data from 12 different studies (Shao et al. 2016). Interestingly, this study found that interrogationo across different populations revealed that one allele in rs4504469 had a protective effect in Europeans but conferred increased risk in Asian populations (Shao et al. 2016).

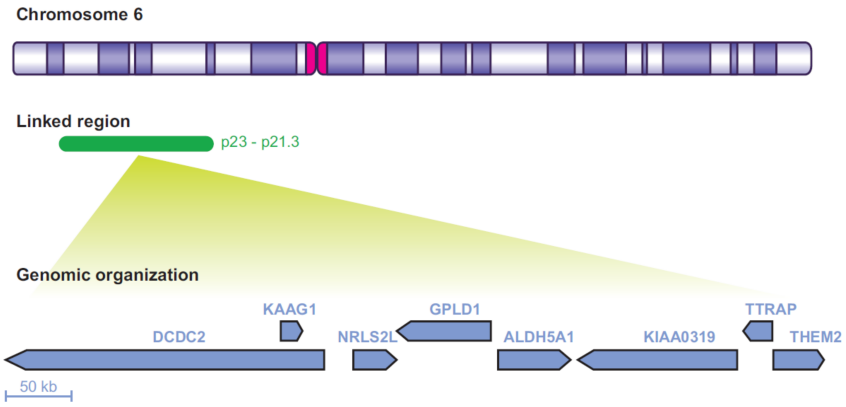


Figure 1.4: Schematic representation of the *DYX2* locus in chromosome 6. Several studies have identified a consensus region in 6p23-p21.3 which encompasses around 8 genes. Amongst these, *KIAA0319* and *DCDC2* have been singled out as susceptibility candidate genes and have been consistently replicated in a number of studies. Adapted from Paracchini et al. 2007.

More recent studies also include reports of negative association (Svidnicki et al. 2013; Matsson et al. 2015; Kong et al. 2016).

In addition, as mentioned above, larger scale studies using multiple cohorts such as NeuroDys, which includes samples from eight countries, did not reveal association with any marker in*KIAA0319* and dyslexia using either case-control or quantitative measures designs (Becker et al. 2014). Furthermore, no association has been found between *KIAA0319* and dyslexia in genome-wide studies (see above, Luciano et al. 2013; Eicher et al. 2013; Field et al. 2013; Gialluisi et al. 2014), although one study has reported nominal association of a marker in *KIAA0319* when interrogating quantitative measures of reading and language impairment more generally (Eicher et al. 2013).

On the other hand, evidence from several other studies suggests that *KIAA0319* may play a wider role in the proper development of linguistic ability and cognition more generally as *KIAA0319* variants exhibit some genetic overlap with other neurodevelopmental disorders. Association of SNPs in *KIAA0319* have been reported to contribute to risk to ADHD (Couto et al. 2009), SLI (Rice et al. 2009;

Newbury et al. 2011), IQ (Eicher et al. 2014) and mathematical ability (Mascheretti et al. 2014). Moreover, reports are not limited only to SNP associations as other types of variants have been found in similar cohorts: for example, Holt et al. (2012) reports a CNV disrupting *KIAA0319* in ASD cases whilst an exome sequencing screening in individuals diagnosed with verbal dyspraxia has found 3 out of 10 individuals shared the same potentially deleterious mutation in *KIAA0319* (Worthey et al. 2013). A putative contribution of *KIAA0319* to general cognition is also supported by a study examining semantic ability in schizophrenia patients, although the population sampled is relatively small (Nicodemus et al. 2014). Furthermore, imaging genetics studies have reported that SNP markers in *KIAA0319* correlate with altered cortical thickness and white matter integrity in the general population (Darki et al. 2012; Eicher et al. 2016; Paternicó et al. 2016), as well as abnormal activation of language-related brain regions in reading tasks in normal and dyslexic individuals (Pinel et al. 2012; Cope et al. 2012; Jamadar et al. 2013).

1.3.2 *KIAA0319L*

Chromosome 1 was first linked to dyslexia in an early study with a small family presenting severe reading and writing difficulties which led to the identification of a translocation in 1p22 (Rabin et al. 1993). Later analyses pointed towards a different region, 1p34-36, as a locus of dyslexia susceptibility based on quantitative and qualitative measures (Grigorenko et al. 2001; Tzenova et al. 2004; de Kovel et al. 2008), with a another study using an SLI cohort also reporting linkage to the 1p36 locus (Rice et al. 2009). Interestingly, the linkage region in *DYX8* encompasses *KIAA0319L*, a gene homologous to *KIAA0319* and the only other member of this gene family. Based on this, markers in *KIAA0319L* were interrogated for association to dyslexia as a categorical trait as well as in quantitative measures of word reading and rapid naming, with results revealing a weak association signal with one particular SNP within this gene (Couto et al. 2008). Whilst this association would not survive correction for multiple testing and provided only circumstantial evidence, a more

recent study has added some further weight to a role of *KIAA0319L* as a dyslexia susceptibility candidate gene by reporting association of a different SNP in a Chinese cohort of dyslexics (Shao et al. 2016). Other studies have linked *KIAA0319L* to neurodevelopmental disorders through nominal associations in ASD populations. Using a case-control design, Wang et al. (2013) found that rare *KIAA0319L* variants correlate with IQ, and a separate investigation has revealed SNPs in *KIAA0319L* are associated with language ability in cases of ASD (Eicher & Gruen 2014). Combined with the shared homology with *KIAA0319*, these studies suggest *KIAA0319L* may play a role in the aetiology of dyslexia and in neurodevelopment more generally.

1.3.3 Functional relevance of risk alleles

Aside from the few studies identifying CNVs or coding mutations, the bulk of the evidence linking the majority of susceptibility genes in dyslexia and neurodevelopmental disorders comes from different SNPs with no obvious consequences or relationship to function. However, *KIAA0319* is somewhat of an exception as risk variants in the gene have been shown to significantly influence levels of gene expression.

Firstly, several markers within *KIAA0319* which associate with dyslexia susceptibility lie within the promoter region, suggesting a putative role in transcriptional regulation (Francks et al. 2004; Cope et al. 2005b; Harold et al. 2006). Two functional studies interrogated directly whether these variants can affect levels of *KIAA0319* expression and found that presence of the risk haplotype or the risk allele of one of the main associated SNPs (rs9461045) in human cell lines can lead to reduction in the levels of *KIAA0319* RNA of around 40% (Paracchini et al. 2006; Dennis et al. 2009). In addition, it has been shown that the risk allele of the aforementioned SNP creates a new binding site for the transcriptional silencer OCT-1 which can regulate the expression of the *KIAA0319* risk allele (Dennis et al. 2009).

Further evidence linking transcriptional regulation of *KIAA0319* and dyslexia susceptibility comes from other associated SNPs within this *locus* that lie in a region near the variant studied in Dennis et al. (2009). Using chromatin

immunoprecipitation in human and mouse cell lines, this region was found to contain signals of open chromatin as indicated by H3K9ac histone acetylation sites, indicating further regulatory sites within *KIAA0319* (Couto et al. 2010; Elbert et al. 2011; Powers et al. 2013). A more recent report further suggests this region interacts with a nearby regulatory element controlled by transcription factor *ETV6* (Powers et al. 2016).

Although similar analyses have not been conducted for *KIAA0319L*, one of the two variants linked to susceptibility to dyslexia (rs7523017, reported in Couto et al. 2008) falls immediately downstream of the untranslated exon 1 in a region containing strong H3K27Ac signal in the UCSC Genome Browser (Kent et al. 2002). However, no direct functional evidence has been obtained for this.

1.4 The KIAA0319 and KIAA0319L proteins

1.4.1 KIAA0319

The main isoform encoded by the *KIAA0319* gene is a highly-glycosylated type I (single pass) transmembrane protein that, when overexpressed, localises primarily to the plasma membrane and can form dimers (Fig. 1.5A, B; Velayos-Baeza et al. 2007; Velayos-Baeza et al. 2008). It contains a large extracellular region with a MANEC motif at the N-terminus, five polycystic kidney disease (PKD) domains and a cysteine-rich region adjacent to the transmembrane domain (Fig. 1.5C; Velayos-Baeza et al. 2007). PKD domains have an immunoglobulin-like (Ig-like) fold, are often found in extracellular regions, and have been shown to mediate protein interactions as well as cell adhesion (Hughes et al. 1995; Ibraghimov-Beskrovnaya et al. 2000). Two other minor variants have been detected in human fetal brain which are predicted to encode soluble proteins lacking the transmembrane domain and which could be secreted isoforms (Velayos-Baeza et al. 2008).

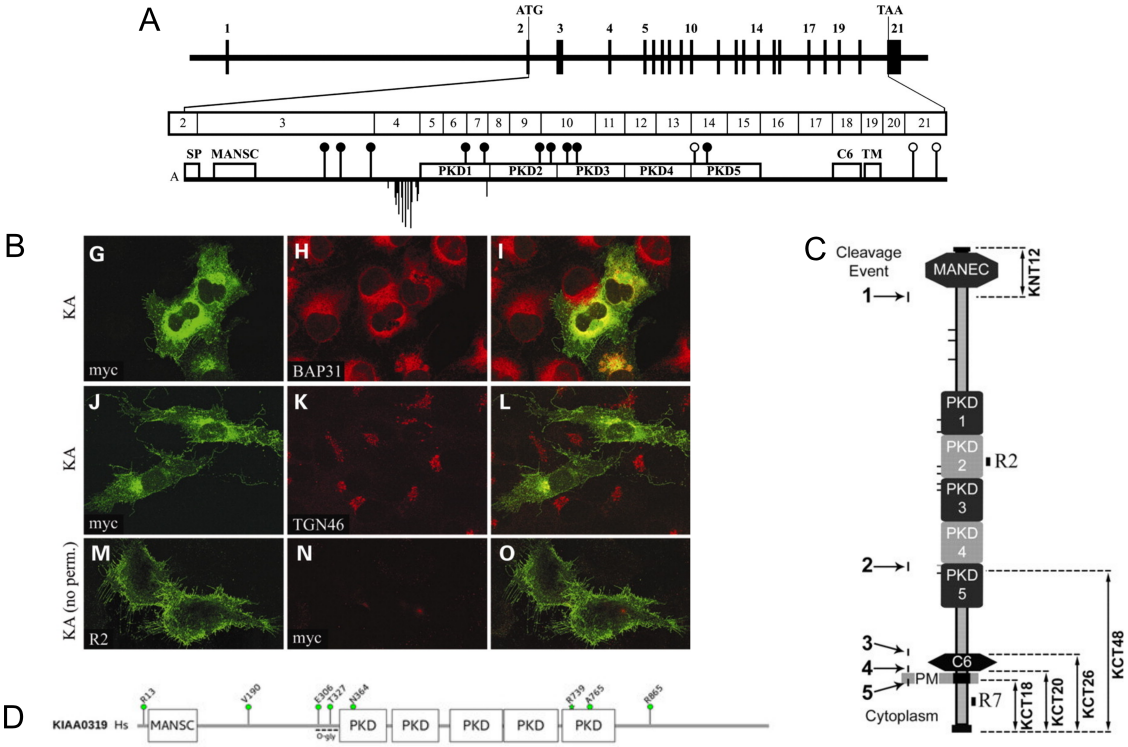


Figure 1.5: The *KIAA0319* gene and its encoded protein. (A) The *KIAA0319* gene (genomic DNA with exons represented by black vertical bars, top; cDNA, middle) and the full-length protein with its functional regions: SP, signal peptide; MANEC domain (previously called MANSC), PKD domains (1-5), cysteine-rich domain C6 and TM, transmembrane domain. Predicted N-glycosylation sites are indicated with circles and O-glycosylation ones with vertical lines. Adapted from Velayos-Baeza et al. (2008). (B) KIAA0319 localises to the plasma membrane, ER and TGN following overexpression in MRC5 cells. A custom made anti-KIAA0319 antibody recognising one of the PKD domains (R2 indicated in C) in the full-length protein (KA, green) was found to co-localise with ER and TGN markers (BAP31, TGN46, red; G-L). Full-length KIAA0319 also show plasma membrane localisation in non-permeabilising conditions as detection with C-terminal myc-tag does not give the same pattern given antibodies cannot enter the cell (M-O). Adapted from Velayos-Baeza et al. 2008. (C) Representation of KIAA0319 proteolytic processing. Cleavage locations detected are indicated by numbers (1-5). Diagram also shows epitope recognised by R2 and R7 antibodies used for protein labelling. The detected cleaved fragments are indicated with dotted lines and arrows on the right, with CT, C-terminal; NT, N-terminal; numbers indicate molecular weight in kDa. Adapted from Velayos-Baeza et al. 2010. (D) Sites in human KIAA0319 exhibiting sites of positive selection in the human lineage as labelled by light green circles. Dark green circle indicate positively selected site in the gorilla lineage. Adapted from Mozzi et al. 2016

As well as in the plasma membrane, the KIAA0319 protein can also be detected in vesicles and in the *trans*-Golgi network (TGN; Fig. 1.5B; Velayos-Baeza et al. 2008), and it has been shown to be internalised into early endosomes via interaction with adaptor protein 2 (AP-2), following the clathrin-mediated endocytosis pathway (Levecque et al. 2009). Several cleavage events have been detected which can involve ectodomain shedding, which releases the N-terminal region into the extracellular medium, and also regulated intramembrane proteolysis where the C-terminal cytoplasmic domain would be cleaved. This domain, when overexpressed, has been shown to translocate into the nucleus (Velayos-Baeza et al. 2010). This is likely to be triggered by a nuclear localisation signal predicted to be at aminoacid position 986 (Brameier et al. 2007; Velayos-Baeza et al. 2008). These features, combined with secretion of minor isoforms, suggest a potential role for KIAA0319 in cell adhesion as well as in signalling pathways (Paracchini et al. 2006; Velayos-Baeza et al. 2008; Velayos-Baeza et al. 2010).

1.4.2 KIAA0319L

The *KIAA0319L* gene in chromosome 1p34 (Fig. 1.6A) encodes a protein that has not been extensively characterised but it is highly homologous to KIAA0319, with 61% sequence similarity and 45% identity, and it shares most of KIAA0319 features such as localisation in the plasma membrane, endosomes and TGN, identical functional domains, high glycosylation and so on (Poon et al. 2011a; Pillay et al. 2016; also unpublished data from the Monaco laboratory). The alignment of the human KIAA0319 and KIAA0319L proteins are shown in Fig. 1.7, and mouse homologs in 1.8 .

KIAA0319L was recently found to be an essential receptor for adeno-associated virus (AAV) entry into cells and it mediates the rapid endocytosis of AAV particles from the plasma membrane to the TGN – the KIAA0319L protein is now also known as AAV receptor, AAVR (Fig. 1.6B; Pillay et al. 2016). Unpublished work from the Monaco laboratory has also revealed that, similarly to KIAA0319, endocytosis

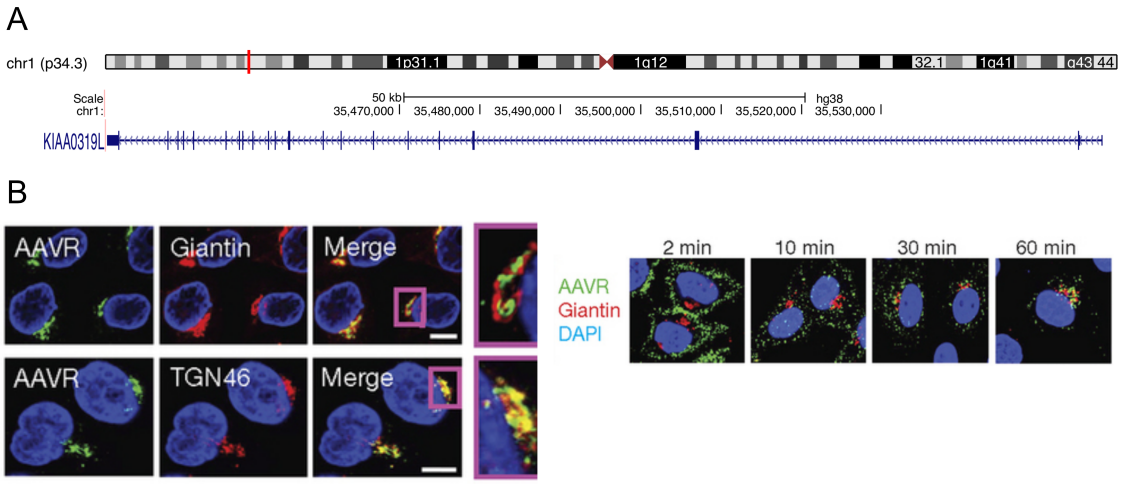


Figure 1.6: *KIAA0319L* gene and protein. (A) The human *KIAA0319L* locus at 1p34.3. Schematic representation of the 21 exons (blue bars) of the *KIAA0319L* gene. Adapted from UCSC Genome Browser; (B) Sub-cellular localisation of endogenous KIAA0319L (or AAVR, green) in HeLa cells indicate presence in the Golgi network as it shows association with cis-medial Golgi marker Giantin (red, top panel) and co-localisation with trans-Golgi network marker TGN46 (red, middle panel). KIAA0319L/AAVR is also found to localise to the plasma membrane in non-permeabilising conditions but it is found to be rapidly endocytosed as shown by staged fixation sequence over the course of 1 h. Adapted from Pillay et al. 2016.

of KIAA0319L takes place via interaction with AP-2 in the clathrin-endocytic pathway and that the C-terminal fragment can translocate to the cell nucleus. In addition, KIAA0319L has been reported to interact with axon guidance receptor Nogo receptor (*NgR*, also called Reticulon 4 receptor, RTN4R) in yeast-two-hybrid and co-immunoprecipitation assays (Poon et al. 2011b).

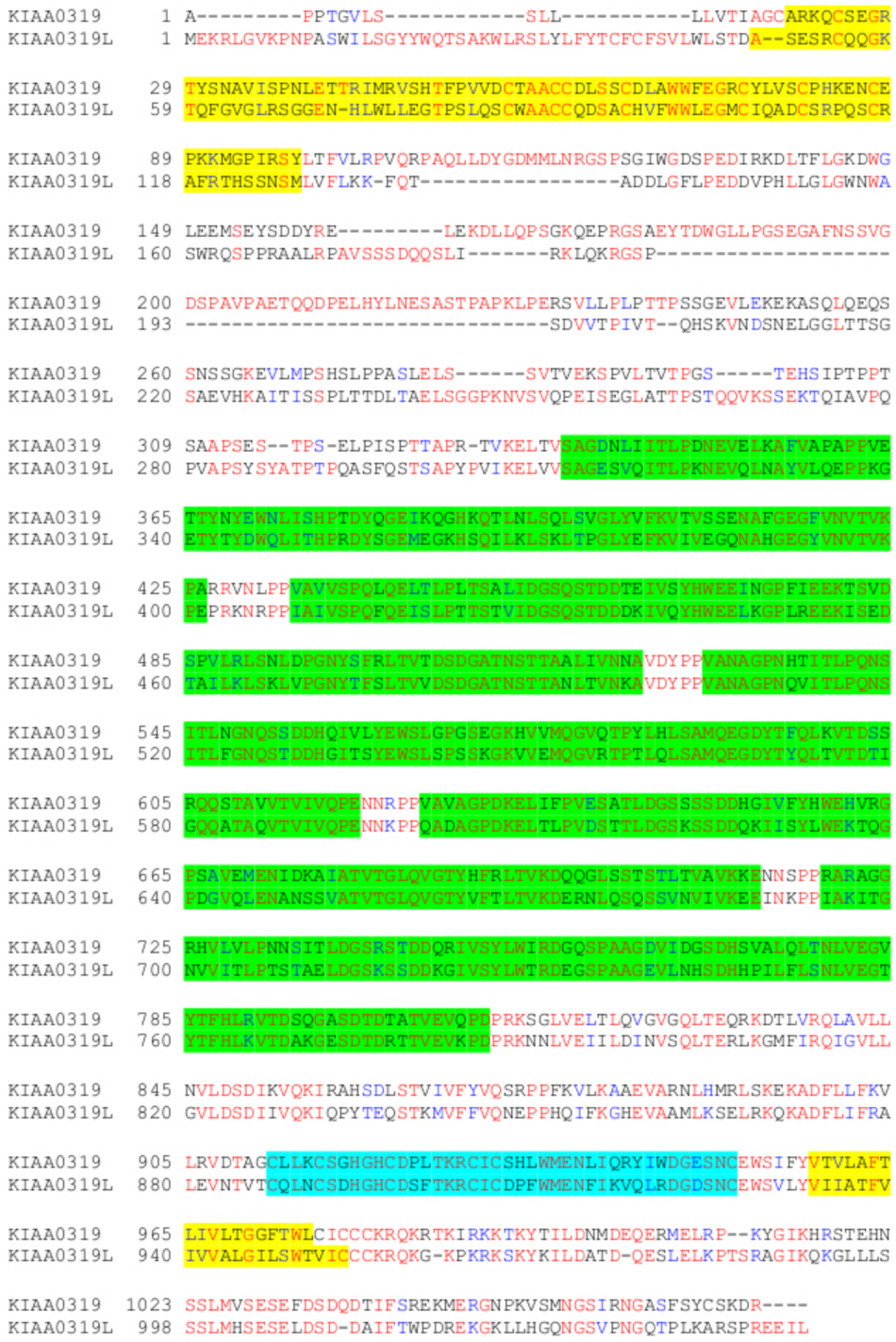


Figure 1.7: Alignment of human KIAA0319 and KIAA0319L proteins. Highlighted regions indicate MANEC domain (orange), the five PKD domains (green), the cystein-rich domain C6 (blue) and the transmembrane region (yellow). Identical aminoacids are indicated in red and similar ones in blue.



Figure 1.8: Alignment of mouse KIAA0319 and AU040320 proteins. Highlighted regions indicate MANEC domain (orange), the five PKD domains (green), the cystein-rich domain C6 (blue) and the transmembrane region (yellow). Identical aminoacids are indicated in red and similar ones in blue.

1.4.3 Homology, conservation and evolution

The *KIAA0319* and *KIAA0319L* genes have orthologs in almost all vertebrate species including fish, aves and mammals. However, *Drosophila melanogaster* and *Xenopus tropicalis* have only one homologous gene, suggesting the duplication event giving rise to the two paralogs might have taken place at some point in the early stages of vertebrate evolution. There is no ortholog present in the genome of *Caenorhabditis elegans*. In certain species lineages, gene loss or gain appears to have occurred also as they present only one ortholog or three (e.g. some bats, squirrels and certain fish). With respect to specific evolutionary changes in the protein within the primate lineage, 7 sites within KIAA0319 have been found to exhibit signatures of positive selection in the human lineage (Fig. 1.5 Mozzi et al. 2016). These aminoacid changes cluster in the extracellular region of the protein and two of them, within the PKD domains, are shared with Neanderthals and Denisovans. Comparisons of the human and mouse KIAA0319 and KIAA0319L proteins show they have a high degree of homology (over 75%), with all functional domains conserved (see Fig. 1.7).

1.4.4 Gene expression studies

Expression of *KIAA0319* in adults is mostly restricted to the brain (Nagase et al. 1997) and *in situ* hybridisation experiments revealed it is present in the developing neocortex in rodent and human brains, both in progenitor cells and postmitotic neurons (for more details on cortical development, see section 1.6.1), as well as more widespread expression in other areas during development such as the developing ganglionic eminences, thalamus, olfactory bulb, hippocampus, midbrain and cerebellum (Fig. 1.9A; Paracchini et al. 2006; Peschansky et al. 2010). *KIAA0319* expression is seen predominantly in the brain (Nagase et al. 1997), with low expression also detected in the spinal cord, lungs, and at residual levels in the testis (EBI Gene expression atlas: `https://www.ebi.ac.uk/gxa`).

KIAA0319L displays a more widespread distribution across different body tissues (Nagase et al. 2001) and is present in many body parts such as lung, liver,

spleen, heart, testis, pancreas, and so on (Nagase et al. 2001). A Western blot showing expression of the mouse KIAA0319L protein (also known as AU040320) is shown in Chapter 3 (Fig. 3.4; see also EBI Gene expression atlas). In the brain, *AU040320* shares a similar expression pattern to *Kiaa0319* (*D130043K22Rik*) in the developing brain, including in the germinative regions of the pallium and in postmitotic neurons (Fig. 1.9B Diez-Roux et al. 2011). More specifically in the developing neocortex, publicly available microarray data indicate that expression levels in mice for both *Kiaa0319* and *Kiaa0319-Like* remain constant over early postnatal stages, with *Kiaa0319* at slightly higher levels in lower cortical layers and *Kiaa0319-Like* more widely distributed across layers (Fertuzinhos et al. 2014; Molyneaux et al. 2015). To complement this dataset, our laboratory has performed qPCR expression analysis over different developmental stages in 9 regions of the mouse brain and these show a gradual increase in expression of *Kiaa0319* after birth and more general expression of *Kiaa0319-Like* at slightly higher and stable levels during development (Fig. 1.9C, D; Bailey, unpublished).

In adulthood, mouse *Kiaa0319* and *Kiaa0319-Like* displayed enriched expression in cortical layers V-VI as well as layers II/III (Belgard et al. 2011). Beyond the neocortex, both genes exhibit expression throughout the brain at relatively similar levels in the neocortex, cerebellum, hippocampus, midbrain, amygdala, striatum and olfactory bulb based on evidence from Western and Northern Blot of human and rodent brains (Velayos-Baeza et al. 2007; Poon et al. 2011a), as well as *in situ* hybridisation from the Allen Brain Institute for mice (Fig. 1.9E, F; www.brain-map.org). Western blot data also reveals that levels of KIAA0319L in the mouse olfactory bulb to be particularly enriched, at a similarly high level to that seen in the cortex (Poon et al. 2011a).

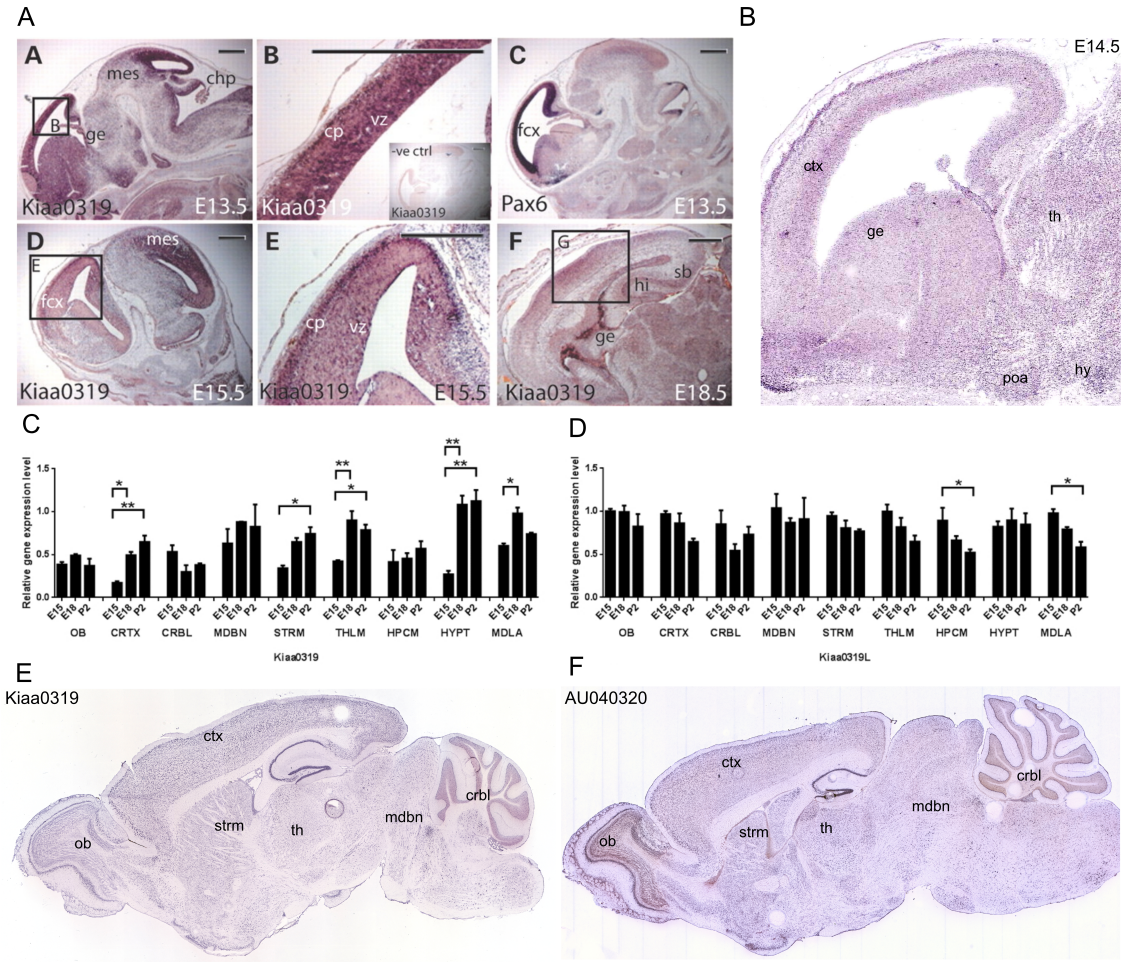


Figure 1.9: Expression of *KIAA0319* and *KIAA0319L/AU040320* in developing and adult brain. (A) *Kiaa0319 in situ* hybridisation (ISH) of mouse brain at E13.5 (A, B), E15.5 (D, E) and E18.5 (F), showing strong expression in the cortical plate (CP) and ventricular zone (VZ) throughout development. *Pax6* is used as a positive control (C) and *Kiaa0319* sense-strand as negative (B, inset). Signal also seen in ganglionic eminences, mesencephalon, hippocampus; adapted from Paracchini et al. 2006.(B) *AU040320* ISH in E14.5 embryo shows expression in the neocortex (VZ, CP) and widespread expression overall, including the preoptic area, hypothalamus, ganglionic eminences; from Diez-Roux et al. 2011 (http://www.eurexpress.org/).(C-D) Developmental qPCR of *Kiaa0319* and *AU040320*. Expression of *Kiaa0319* is moderate at late gestation but it is upregulated towards the end of embryonic and early postnatal period in several regions (C). *AU040320* has a higher baseline expression level which tends to decrease in the early stages of postnatal development. Expression levels in relation to housekeeping gene *Trfc*; * $p<0.05$; ** $p<0.005$; Melissa Bailey, unpublished.(E-F) P56 sagital sections of ISH of *Kiaa0319* (*D13004322Rik*) and *AU040320* from the Allen Brain Institute. Ge, ganglionic eminences; mes, mesencephalon; chp, choroid plexus; cp, cortical plate; vz, ventricular zone; fcx, frontal cortex; hi/hpcm, hippocampus; sb, subiculum; th/thlm, thalamus; poa, pre-optic area; hy/hypt, hypothalamus; Ob, olfactory bulb; Crtx, cortex; Crbl, cerebellum; strm, striatum; mdla, medulla.

1.5 Functional studies of *KIAA0319* and *KIAA0319L*

1.5.1 Rodent neuronal migration

Based on its expression pattern in the developing brain, the presence of the putatively adhesive PKD domains in the extracellular region of the protein and on the early findings in human *postmortem* histopathological studies by Galaburda and his team, Paracchini et al. (2006) hypothesised that KIAA0319 may play an important role in the development of the neocortex, particularly in neuronal migration. To investigate this possibility, knockdown experiments were performed in rat embryos using *in utero* electroporation of shRNA constructs targeting *Kiaa0319* in the developing neocortex. It was found that knockdown of *Kiaa0319* at embryonic day (E) 15 led to strong defects in neuronal migration as many targeted neurons migrated shorter distances than those electroporated with control constructs (which expressed only green fluorescent protein, GFP) and targeted neurons failed to enter the cortical plate (Fig. 1.10A Paracchini et al. 2006). Three other studies using the same approach have reported similar findings (Peschansky et al. 2010; Szalkowski et al. 2012; Adler et al. 2013). The failure of neurons to migrate often led to white matter heterotopias and hippocampal dysplasias (Fig. 1.10B) and ectopic neurons were often cells destined to the upper cortical layers as demonstrated by their expression of transcription factor Cux1 (Fig. 1.10C).

These ectopic cells included non-electroporated neurons derived from the dorsal cortex as well as GABAergic interneurons derived from the subpallium (Fig. 1.10C, D), suggesting the deficit induced by reduction of KIAA0319 levels is due to cell autonomous and non-cell autonomous mechanisms (Peschansky et al. 2010). Lamination of interneurons has been suggested previously to be under the control of projection neurons (Lodato et al. 2011) and this displacement following *Kiaa0319* knockdown may be another example of it.

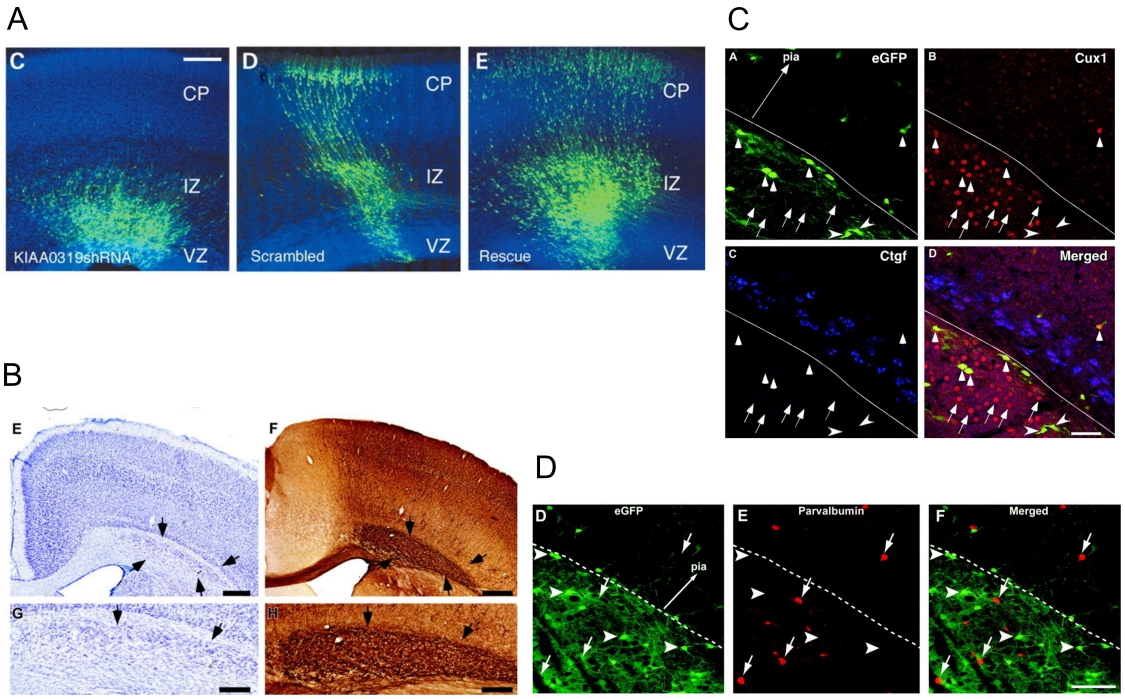


Figure 1.10: Knockdown of *Kiaa0319* with shRNA via *in utero* electroporation at E15.5 in rats impairs neuronal migration.(A) Neurons transfected with GFP and *Kiaa0319*-shRNA fail to enter the cortical plate (CP) whilst neurons in the control condition (Scrambled) appear across the length of the cortical wall (CP, IZ, VZ). Co-transfection of *Kiaa0319*-shRNA and KIAA0319 overexpression in the Rescue condition enables migration of a subset of neurons as they appear in the CP. (B) Example of a periventricular heterotopia following *Kiaa0319* knockdown. Nissl-stained section (left panels) demonstrates the accumulation of neurons in the white matter band adjacent to the lateral ventricle and below the subplate layer (arrows). Immunohistochemistry with anti-GFP antibody (right panels) shows that transfected neurons comprise the majority of neurons in the heterotopic accumulation. Scale bar: 125 μm. (C) Section of a cortex showing cells transfected with *Kiaa0319*-shRNA and GFP (green) and immunolabelled with upper-layer marker Cux1 (red) and subplate marker Ctgf (blue) to delineate white-matter region. The ectopic cluster contains GFP+ cells which are co-labelled by Cux1 (straight-sided arrowheads) and others which are not (concave-sided arrowheads). Several other Cux1+ cells are not positive for GFP, suggesting a non-cell autonomous mechanism in the emergence of the heterotopia. Scale bar: 100 um. (D) GABAergic interneurons (Parvalbumin+, red, arrows) are also present in the periventricular heterotopias resulting from transfection of cells with *Kiaa0319*-shRNA and GFP (green, arrowheads). White dotted line delineates division between white matter and subplate. CP, cortical plate; IZ, intermediate zone; VZ, ventricular zone. Adapted from Paracchini et al. 2006 (A) and Peschansky et al. 2010 (B-D).

These knockdown experiments were conducted primarily at E15 but similar effects have been found when electroporations were performed at E14 and E16 to target other neuronal populations (Adler et al. 2013). In addition, overexpression of human KIAA0319 protein alongside knockdown vectors was found to rescue the migration phenotype given that cortical lamination appeared normal and there were no observed ectopias (Fig. 1.10A Paracchini et al. 2006; Peschansky et al. 2010). It has also been reported that *Kiaa0319* knockdown in the neocortex can lead to hypertrophy of apical dendrites as well as reduced volume of the corpus callosum (Peschansky et al. 2010; Szalkowski et al. 2013).

The neuronal migration defects found after *Kiaa0319* knockdown parallel findings with a vast number of other genes, including the two other main dyslexia susceptibility candidate genes, *DCDC2* and *DYX1C1*, where similar *in utero* electroporation experiments targeting the rat homologs in the developing neocortex have been shown to cause abnormalities in cortical migration (Meng et al. 2005b; Wang et al. 2006; Rosen et al. 2007; Burbridge et al. 2008; Currier et al. 2011; Adler et al. 2013). In these experiments, knockdown of either *Dcdc2* or *Dyx1c1* led to neurons migrating past their expected position in the cortical plate, with *Dyx1c1* knockdown also leading to periventricular white matter heterotopias (Burbridge et al. 2008; Rosen et al. 2007). Another gene linked to dyslexia and which has been more extensively studied, *ROBO1*, has been shown to be important for axon growth and regulation of neuronal migration (Yuan et al. 1999; Nopola-Hemmi et al. 2001; Hannula-Jouppi et al. 2005; Gonda et al. 2013).

These functional genetics results mirrored somewhat the findings from the early *postmortem* studies of dyslexic brains by Galaburda and his team (Galaburda et al. 1985; Humphreys et al. 1990). The combination of these findings added support to original suggestions and led to the hypothesis that dyslexia is a neuronal migration disorder (Galaburda et al. 2006; Fisher & Marcus 2006; Paracchini et al. 2007; Gabel et al. 2010; Scerri & Schulte-Körne 2010; Giraud & Poeppel 2012;

Raskind et al. 2013; Adler et al. 2013; Kere 2014; Peterson & Pennington 2015). As put by Galaburda et al. (2006):

> *"Variant function in any of a number of genes involved in cortical development [. . .] can be responsible for subtle cortical malformations involving neuronal migration and axon growth, which in turn leads to abnormal cortico-cortical and cortico-thalamic circuits that affect sensorimotor, perceptual and cognitive processes critical for learning."*
>
> (Galaburda et al. 2006, p. 1216)

The view for a specific role for the neocortex in susceptibility to dyslexia is in line with evidence from human neuroimaging and neurophysiological studies with dyslexics outlined in section 1.1.2.3 where the neocortex is the key structure implicated.

Recently, based on homology to *KIAA0319* and its expression pattern in the developing neocortex mentioned above, similar knockdown experiments were performed with the rat homolog of the candidate gene *KIAA0319L* (Platt et al. 2013). After targeting *KIAA0319-Like* with shRNA constructs in the rat neocortex at E15.5, the authors reported an impairment in neuronal migration given that there were large periventricular nodular heterotopias formed, although cortical lamination remained largely normal (Fig. 1.11A, B; Platt et al. (2013)). As seen with *Kiaa0319* and *Dyx1c1*, the resulting heterotopias contained both transfected and non-transfected neurons, including interneurons, suggesting *Kiaa0319-Like* could play a role in non-cell autonomous process by signalling (Platt et al. 2013).

These results added *KIAA0319L* to the list of dyslexia susceptibility candidate genes implicated in cortical migration and provided further support to the neuronal migration hypothesis of dyslexia. Nonetheless, this is likely not the only function of this protein given that, at least in mice, the homologous AU040320 is expressed almost ubiquitously and also at post-natal stages.

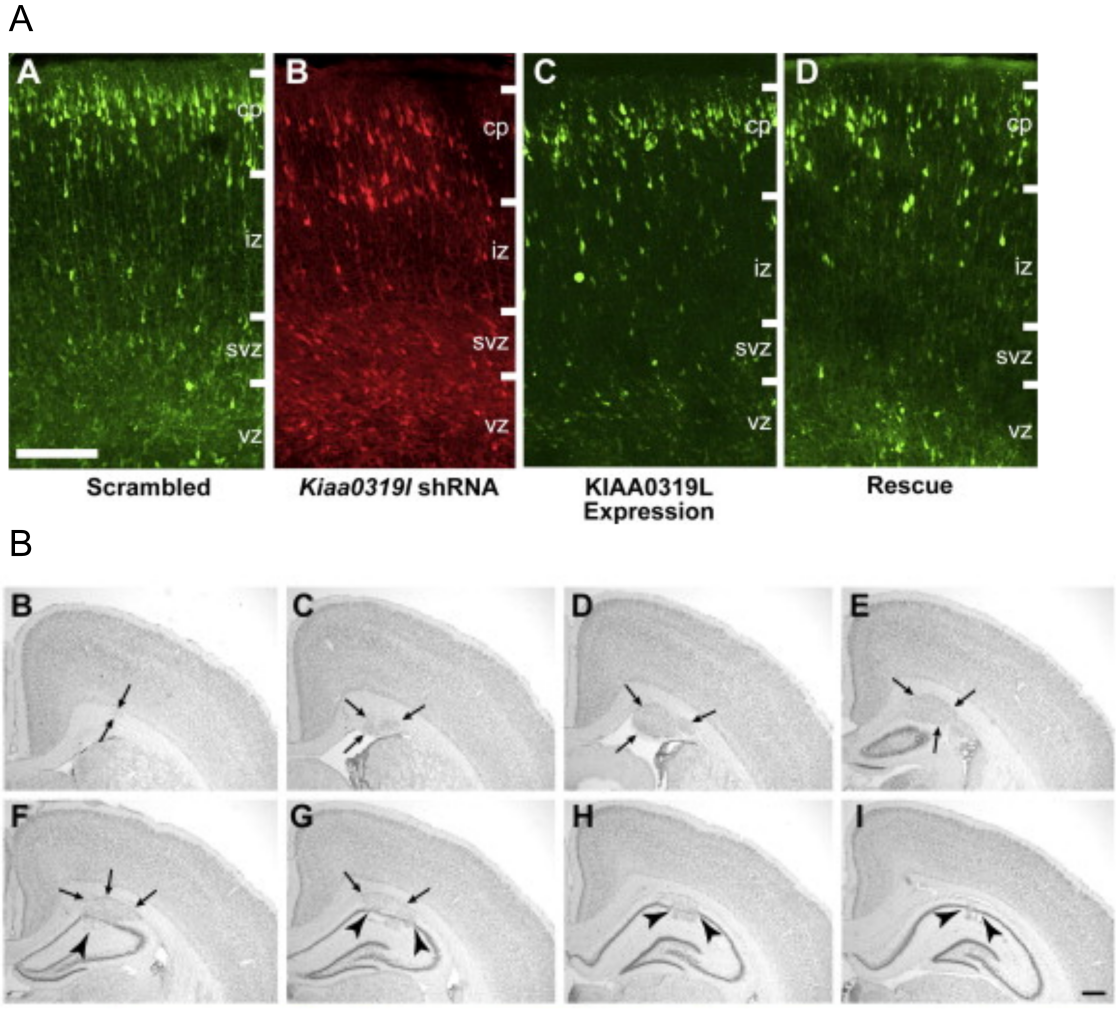


Figure 1.11: shRNA-mediated knockdown of *Kiaa0319-Like* impairs neuronal migration in rats. (A) Cortices of brains electroporated at E15.5 in each experimental condition shows cortical lamination is largely unaffected after *Kiaa0319-Like* knockdown. Neurons transfected with scrambled shRNA (green, A) appear mostly in the cortical plate (cp) and similarly for *Kiaa0319-Like* shRNA (red, B). No differences are seen between the two conditions in the number of transfected neurons across the different compartments of the cortical wall (graph not shown). Overexpression of KIAA0319L protein (green, C) produces similar results with neurons distributed along the cortical wall and similarly for co-transfection of *Kiaa0319-Like* shRNA and overexpression constructs (green, D). Scale bar: 50 μm. (B) Periventricular nodular heterotopia resulting from knockdown of *Kiaa0319-Like*. Nissl stained sections of P21 brains electroporated at E15.5 with *Kiaa0319-Like* shRNA show a large nodule of ectopic neurons adjacent to the lateral ventricle disrupting the white matter. Arrows indicate heterotopia and arrowheads indicate hippocampal malformation. Scale bar: 200 μm. Adapted from Platt et al. 2013.

1.5.2 Behavioural effects of *Kiaa0319* knockdown

The shRNA knockdown studies conducted in rats also prompted investigations into putative roles of *Kiaa0319* in mediating rodent behaviours that parallel language and reading-related endophenotypes, as well as other cognitive or sensorimotor abilities. These behavioural studies tested rats subjected to knockdown of *Kiaa0319* in the developing cortex, as well as control ones, and have revealed that altered levels of KIAA0319 protein can lead to deficits in spatial learning and in the temporal processing of complex auditory stimuli (Szalkowski et al. 2012; Centanni et al. 2014a; Centanni et al. 2014b).

More specifically, Szalkowski et al. (2012) found that rats treated with shRNA against *Kiaa0319* in the developing neocortex exhibited impaired learning ability in the Morris Water maze task, a classic test of spatial memory, as they took longer to find the platform and travelled longer paths than controls. However, this deficit was only found in animals presenting hippocampal dysplasias, while those exhibiting malformations only in the dorsal neocortex. With respect to auditory processing, animals were tested in the silent gap detection task, a modified prepulse inhibition paradigm used in rodents to parallel rapid auditory processing tests in human dyslexia and central auditory processing disorders (Fig. 1.12A Fitch et al. 2008). Results revealed a marginal difference in performance between shRNA-treated rats and control ones, although differences did not reach statistical significance thresholds and were only found in juvenile rats - a second cohort tested in adulthood performed similarly to the control group (Fig. 1.12B). On the other hand, *Kiaa0319*-shRNA treated rats exhibited difficulties in discriminating certain frequency modulation sweeps that vary at very short intervals (125 ms) but not in longer ones (175-225 ms), a significantly more complex stimulus than silent gaps (Fig. 1.12C Szalkowski et al. 2012). Combined, the authors concluded that altered KIAA0319 levels interfere with temporal auditory processing in rats in a way that mimics the rapid auditory deficits found in human dyslexics (Tallal 1980; Tallal 2004; Szalkowski et al. 2012).

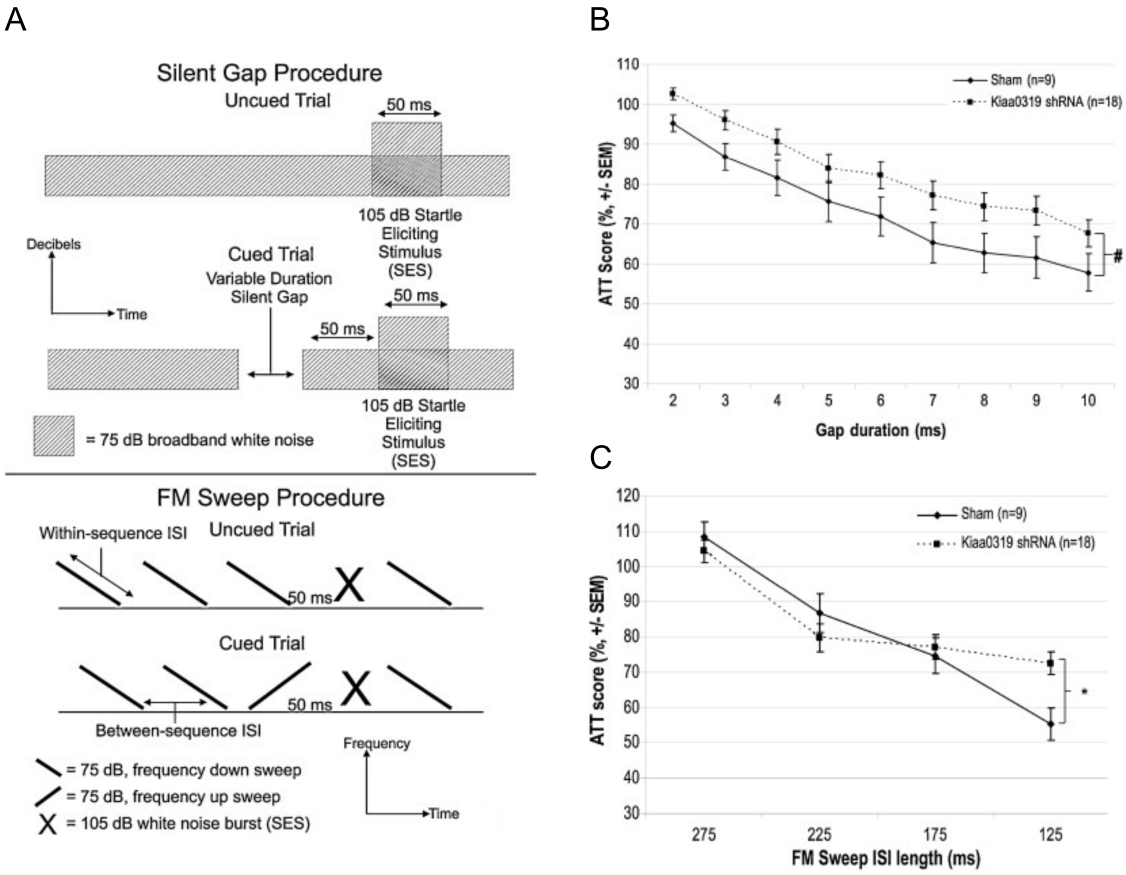


Figure 1.12: Rats treated with *Kiaa0319*-shRNA in the developing neocortex show impaired rapid auditory processing. (A) Diagram with design of modified PPI silent gap detection paradigm showing cues as variable gaps of silence preceding startle-eliciting stimulus. Frequency modulating sweep procedure also depicted. (B) Attenuation (ATT) scores of Sham and KIAA0319 shRNA groups showing marginal difference between the two groups across the different gap stimuli (# denotes p=0.07). (C) ATT scores for the frequency modulation sweep task shows no differences between the two groups for longer within-sequence interstimuli intervals but a significant difference at an ISI of 125 ms (* denotes p<0.05). Adapted from Szalkowski et al. 2012.

Building on this, Centanni et al. (2014a) performed electrophysiological experiments and recorded local field potentials from the auditory cortex of such *Kiaa0319*-shRNA treated rats during the presentation of speech-like sounds (e.g. /ba/, /da/) in awake and anaesthetised animals. These recordings revealed that reduced KIAA0319 expression led to a delay in neural responses, an increase in trial-by-trial variability and reduced firing. Moreover, intracellular recordings indicated

these effects to be due to alterations in temporal rates of neural responses to these stimuli that derived from changes in the intrinsic properties of electroporated neurons – higher excitability and increased input resistance (Centanni et al. 2014a). In a follow-up study, such speech discrimination deficit was shown to be ameliorated following intense training (Centanni et al. 2014b).

Behavioural studies have also been conducted in relation to the other two main dyslexia candidate genes, *DCDC2* and *DYX1C1*, both in rats and mice. For *DYX1C1*, shRNA-mediated knockdown in rat embryonic neocortex was also found to affect processing complex auditory stimuli, in a similar way to those found with *Kiaa0319* knockdown - DYX1C1-deficient rats exhibited poorer ability to discriminate rapidly changing auditory cues in frequency modulation sweep tasks as well as in an oddball paradigm (Threlkeld et al. 2007; Szalkowski et al. 2013). Altered levels of *Dyx1c1* were also found to affect working memory ability as measured in the 4/8 radial arm water maze and those exhibiting hippocampal malformations also performed poorly on the Morris Water maze (Szalkowski et al. 2011). More recent experiments using targeted genetic deletion of *Dyx1c1* in mice specifically in the forebrain using a *Dyx1c1-flox;Emx1-Cre* line provided further evidence for a relationship between neural circuits involved in learning and memory: *Dyx1c1* conditional knockout (KO) mice exhibited poor performance in the same radial arm water maze task, although no deficit of rapid auditory processing using PPI modified paradigms was detected (Rendall et al. 2015).

In the case of *Dcdc2*, there are no reports of behavioural studies on rats following *Dcdc2* knockdown with RNA interference methods. On the other hand, testing of *Dcdc2* KO mice revealed that absence of functional copies of the gene affects the animal's ability to discriminate rapidly changing auditory cues in an embedded tone paradigm of startle reduction – this task is similar to the silent gap test but it uses changes in tone frequency as cues instead of gaps of silence (Truong et al. 2014). In addition, *Dcdc2* KOs exhibited deficits in working and reference

memory in the radial arm water maze but not in the Hebb Williams maze (Wang et al. 2011b; Truong et al. 2014).

In summary, behavioural studies interrogating the relationship between dyslexia candidate genes and rodent behaviours have revealed a putative relationship with learning and memory as well as rapid auditory processing.

1.6 The neocortex

Given the putative roles of *KIAA0319* and *KIAA0319L* in neuronal migration in the developing cortex, understanding of cortical development and neuronal migration is fundamental for attempting to understand the function of these two genes. Thus, I will briefly introduce the neocortex and its development, along with associated disorders of neuronal migration that will shed light onto the processes where *KIAA0319* and *KIAA0319L* may be important.

The human brain contains an average of 86 billion neurons and a similar number of non-neuronal cells, with the cerebral cortex housing around 80% of the total brain mass despite only containing a fifth of the total number of neurons (Azevedo et al. 2009). The cerebral cortex is the seat of high cognitive function of the brain and the centre for neural computations upon which language is dependent (Friederici & Gierhan 2013; Poeppel 2014), and the main region implicated in structural and functional studies of dyslexia in humans (see section 1.1.2.3).

The mature neocortex is organised into distinct regions comprised of groups of vertical columns of distinct cytoarchitectonic features to perform a specific role within the brain (Fig. 1.13A, B Brodmann 1909; Kaas 2012). The neocortex is subdivided into 6-7 horizontal layers containing a variety of cell types that differ in their function, transcriptome, cell density and so forth and each cortical layer performs a particular function within the neocortex and the brain based on their afferent and efferent connections (Ramón y Cajal 1899; Gilbert & Kelly 1975; Mountcastle 1997; Molyneaux et al. 2007; Douglas & Martin 2004). The thalamus provides the major input into the cortex through projection of thalamocortical fibres

into layer IV and the incoming signal is then relayed throughout the cortex to other layers and brain regions (Jones 1985; Sherman & Guillery 2002; Sherman & Guillery 2006). Layers II/III are generally responsible for columnar/areal communication as well as for inter-hemispheric connections via the corpus callosum, whilst layers V and VI serve primarily as output layers: layer V pyramidal neurons project to the thalamus and to sub-cerebral targets such as the midbrain and spinal cord, whilst layer VI neurons target mainly the thalamus. Alongside these main cell populations, a thin layer termed VIb (or sometimes layer VII) is also contained within the cortex and is derived from remnants of the cortical subplate (Hoerder-Suabedissen & Molnár 2015).

Cortical circuits contain two main types of neurons: (a) excitatory, glutamatergic cells which comprise 70-80% of cortical neurons to form local and long-range connections within a column, a cortical area or outside the cortex (Parnavelas 2000); (b) inhibitory GABAergic interneurons that typically form local connections within a cortical column or layer (Hendry et al. 1989; Sahara et al. 2012; Markram et al. 2004).

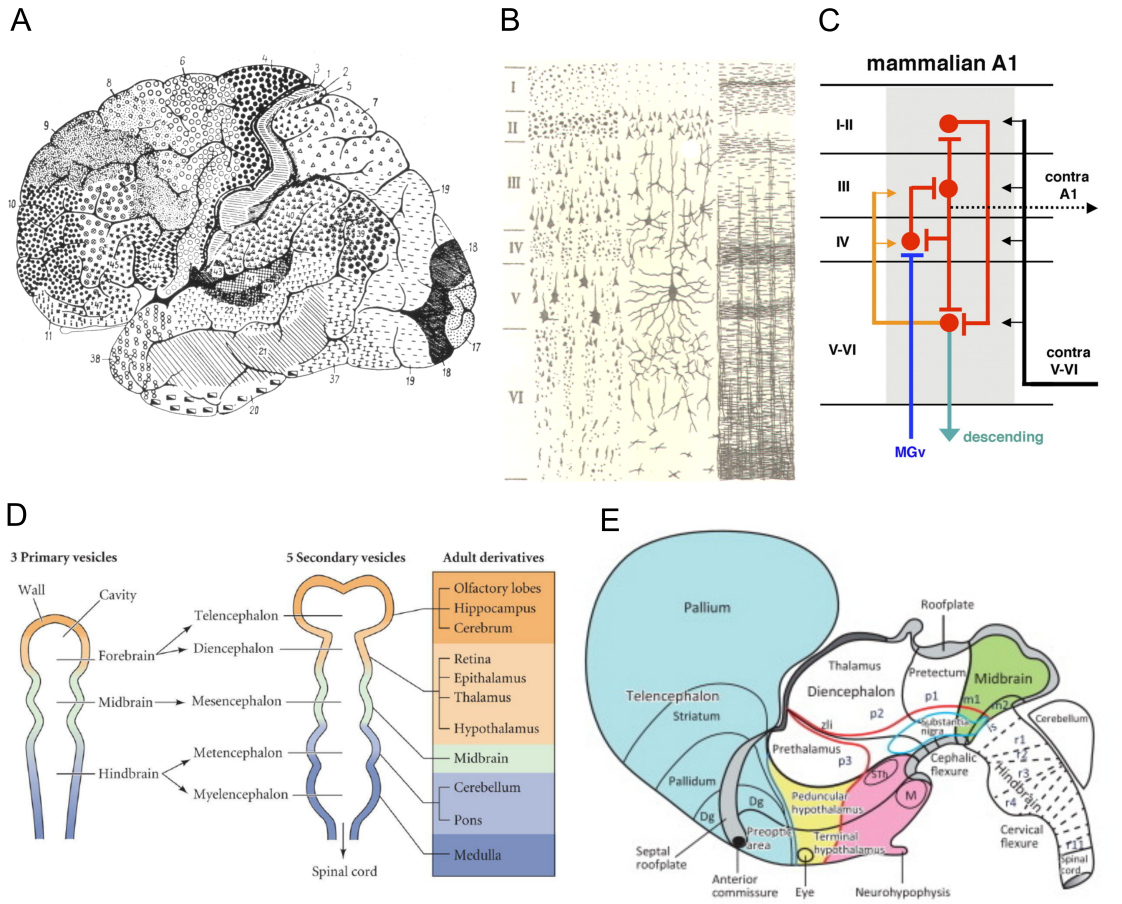


Figure 1.13: The structure of the neocortex and brain development: (A-C) cortical structure, (D, E) brain development. (A) Drawing of cortical regions identified by Brodmann 1909. (B) Drawings by Ramón y Cajal (1899) showing columnar and laminar organisation of the neocortex. (C) Schematic representation of cortical circuit with the auditory cortex as an example. Blue indicates thalamic input, red indicates intrinsic connections, green indicates descending projections, orange represents recurrent projections from deep to superficial layers, black lines indicate contralateral projections. Gray indicates functional column. Adapted from Wang et al. 2010. (D) Diagram showing development of the neural tube at the point of emergence of telencephalon, from where the neocortex develops. Adapted from Gilbert 2010. (E) Ontology of the developing brain according to the prosomeric model (Puelles et al. 2013) showing the telencephalon with the division of pallium and subpallium (striatum, pallidum, preoptic area). Adapted from Puelles et al. 2013.

1.6.1 Development of the neocortex

The developmental origin of the cells that come to comprise the cerebral cortex are dependent on the orchestration of numerous signalling molecule gradients and transcription factors over the course of the development of the central nervous system. The neocortex emerges during development within the forebrain and telencephalon (Fig. 1.13D) through signalling from the roof plate, cortical hem and anterior neural ridge to define a dorso-ventral and a medio-lateral axis, and draw hemispheric boundaries around the lateral ventricles. The dorso-lateral part of the telencephalon is defined as the pallium and it will give rise to the neocortex, hippocampus and olfactory cortex (as well as part of the claustro-amygdaloid complex), whilst the ventral region is termed the subpallium, from which the striatum, pallidum and preoptic nuclei will form (Fig. 1.13E). These two regions contain an epithelial germinative area at the margin of the lateral ventricles with the inner-most termed the ventricular zone (VZ) and the adjacent segment called subventricular zone (SVZ, Fig. 1.14 Rakic 1982; Lui et al. 2011). These germinative domains contain a variety of precursor cells subtypes which will give rise to the distinct neuronal populations that will come to occupy the neocortex.

1.6.2 Cortical neurogenesis

The VZ contains multipotent neuronal precursor cells that undergo a complex cell division program influenced by several factors such as morphology, anatomical location, expression of growth factors and molecular signalling (Lui et al. 2011; Florio & Huttner 2014). The primary type of progenitor and the first one to be identified are radial glial cells (also called apical radial glia) and they typically exhibit an apico-basal polarity with processes extending to the ventricular and pial surfaces that serve as a guiding scaffold for the migration of generated neurons (Fig. 1.14A Rakic 1971; Rakic 1972; Noctor et al. 2001; Miyata et al. 2001). Radial glial cells can undergo different types of cell division: asymmetric division to generate a post-mitotic neuron and a new progenitor (Fig. 1.14A at E11.5), or divide

symmetrically either to self-renewal and amplify their pool (Fig 1.14A at E10.5), or by giving rise to a distinct class of progenitors called intermediate progenitor cells (Miyata et al. 2001; Noctor et al. 2001; Noctor et al. 2004; Miyata et al. 2004; Haubensak et al. 2004, Fig. 1.14A at E12.5). Later in development, radial glial cells are responsible for generating a portion of astrocytes and oligodendrocytes (Malatesta et al. 2000). The majority of divisions giving rise to neurons comes from symmetric divisions of intermediate progenitors, either directly or through a further step of self-renewal to amplify the neuronal pool (Miyata et al. 2004; Noctor et al. 2004; Hansen et al. 2010; Kowalczyk et al. 2009). Several characteristics differentiate radial glial cells from intermediate progenitors aside from their mitotic pattern: morphologically, intermediate progenitors are multipolar with short processes, they typically occupy the SVZ and are characterised by expression of Tbr2 (T-box brain protein 2, also called Eomes) – radial glial cells on the other hand typically occupy the VZ and express Pax6 (paired box protein 6) (Miyata et al. 2004; Noctor et al. 2004; Englund et al. 2005).

The SVZ contains another cell population that resembles radial glial cells for their expression of Pax6 but are distinct in their lack of apical process attached to the lateral ventricle. Initially identified in humans and ferrets in a separate neurogenic region in the SVZ termed the outer SVZ (Smart et al. 2002), these 'outer radial glial cells' were later identified in several other lissencephalic species too, including rodents (Fietz et al. 2010; Hansen et al. 2010; Wang et al. 2011a; Kelava et al. 2012; García-Moreno et al. 2012). Other types of neuronal progenitors have also been described such as short neural precursor cells in the VZ, a subtype of radial glial cells called neuroepithelial progenitors, and so on (Betizeau et al. 2013; Lui et al. 2011; Florio & Huttner 2014).

On the other hand, inhibitory GABAergic cortical interneurons are generated in a different region of the brain, within a set of germinative regions in the subpallium: the

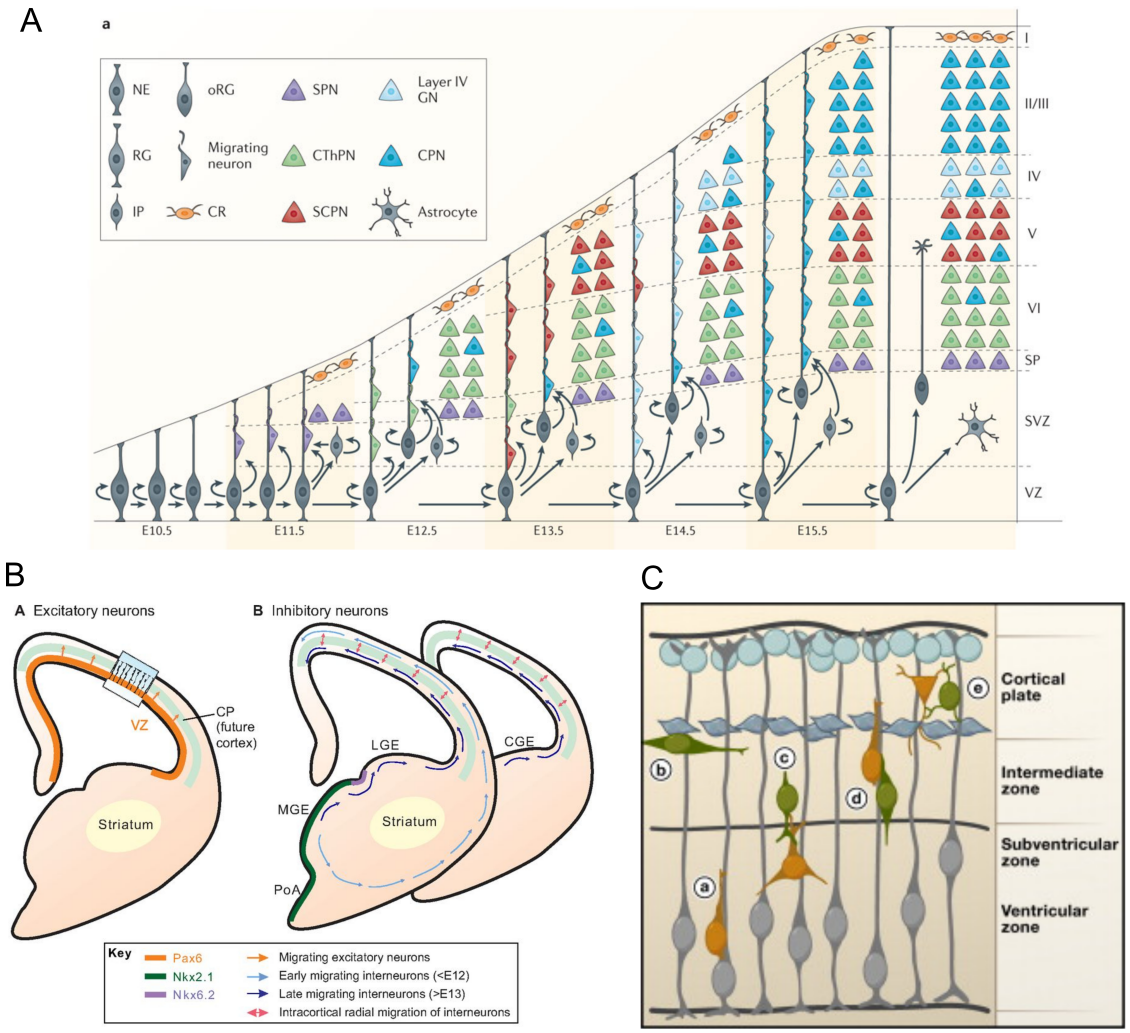


Figure 1.14: The development of the neocortex. (A) Representation of spatio-temporal pattern of cortical neurogenesis under the traditional view. Radial glial progenitors (RG) in the VZ divide to self-renew or produce different subtypes of projection neurons, intermediate progenitors (IPs), outer radial glia (oRG). Inside-out formation of cortical layers also represented. CR, Cajal-Retzius cells; SP, subplate; CThPN, corticothalamic projection neurons; SCPN, sub-cerebral projection neurons; GN, granular neurons; CPN, callosal projection neurons. Adapted from Greig et al. 2013. (B) Migration routes in cortical development. (A) Pax6+ progenitors migrate radially from the pallial VZ (orange); interneurons originating from the medial/caudal ganglionic eminences (MGE, CGE, respectively) and the preoptic area (POA) before migrating tangentially towards the cortex. Adapted from Guo & Anton 2014. (C) Schematic representation of migrating neurons in the CP. Migrating projection neurons (orange) exhibit bipolar morphology (a) as they climb towards the CP via locomotion migration mode. Interneurons (green) enter the CP via tangential migration in the IZ (b) before descending to the SVZ (c). Both projection neurons and interneurons cross into the IZ (d) and enter the CP to occupy their final position by somal translocation. Cells with shared birthdate occupy the same laminar fate. Adapted from Ayala et al. 2007.

majority of interneurons originate from the medial and caudal ganglionic eminences (MGE and CGE, respectively) whilst a small subset of them are derived from the preoptic area (Fig. 1.14; Lavdas et al. 1999; Anastasiades & Butt 2011; Marín 2013; Marín & Müller 2014). Interneurons are a very diverse cell population which is reflected by their different developmental lineages. Progenitor cells in the MGE give rise primarily to parvalbumin or somatostatin-positive fast-spiking cells (PV+ and SST+, respectively); interneuronal precursors in the CGE typically generate bipolar calretinin-positive (CR+) or multipolar vasointestinal peptide-expressing (VIP+) neurons; on the other hand, the preoptic area is the source of a wider combination of cell types such as some PV+ or SST+ cells, Reelin-positive interneurons as well as neuropeptide Y-positive ones. These germinative areas are also organised into distinct VZ and SVZ domains with a similar mitotic profile to those in the dorsal pallium but differ in some crucial aspects such as in the expression of different transcription factors for cell fate specification such as Dlx1-2/5-6, Nkx2.1/6.2 and CoupTF1/2 (Anastasiades & Butt 2011; Marín 2013; Marín & Müller 2014).

1.6.3 Radial cortical migration

As neuronal progenitors divide in the germinative VZ and SVZ to generate post-mitotic neurons, the newly-born cells have to initiate their migration towards the position they are destined to occupy in the primitive neocortex, the cortical plate (CP) - this process is called radial migration. Migrating neuroblasts typically guide their movement by exploiting cell adhesive mechanisms to contact the fibres of radial glial cells (Rakic 1990; Misson et al. 1991; Kriegstein & Noctor 2004). After their final mitosis in the VZ, neurons alter their morphology to become bipolar and start migrating by extension of their leading process and nucleokinesis along glial fibres through the intermediate zone (IZ) – the 'locomotion' mode of migration (Fig. 1.14C (a) Rakic 1972; Nadarajah et al. 2001). As they advance, a complex sequence of cell morphological and polarity changes take place to allow for the constant shortening of the leading process to pull the cell body towards the CP. When the

leading process reaches the upper-most region of the developing cortex, the marginal zone (MZ), neurons switch from locomotion to 'somal translocation' (1.14C) where they rapidly move the cell body to assume their final position in the cortical layer they are specified to occupy and fully differentiate (Fig. 1.14D (d, e) Nadarajah et al. 2001; Sekine et al. 2011). The different modes of neuronal migration have been shown to be regulated by the combination of a number of molecular signals and involve complex interactions of cellular processes such as growth cone extension, nucleokinesis, remodelling of the cytoskeleton and interaction of cell adhesion signals and guidance molecules (see e.g. Ayala et al. 2007, for a review).

The position newly-born neurons come to occupy in the developing neocortex is dependent predominantly on their birthdate – cortical layers are sequentially added in an inside-out fashion, with each layer migrating through the previously generated one (Fig. 1.14A; Rakic 1972). The earliest born neurons migrate out of the VZ to form the preplate, the primitive CP, which later splits into MZ and subplate. Subsequent waves of migrating neurons start occupying their positions between the MZ and subplate (Marin-Padilla 1971; Luskin & Shatz 1985; Del Río et al. 2000). Over the course of development, neurons born between E11-13 arrive first to settle and form cortical layer VI, followed by layer V; later born neurons from E13.5 onwards then form the upper layers (Angevine & Sidman 1961; Berry & Rogers 1965; Luskin & Shatz 1985; Tan & Shi 2013). Later on during postnatal development, neurons in the subplate eventually undergo programmed cell death and the remaining cells come to form layer VIb (Price et al. 1997; Hoerder-Suabedissen & Molnár 2015). However, recent evidence has challenged this strictly sequential developmental course of neocortical projection neurons as several 'quiescent' progenitors have been identified. Such fate-restricted cells typically remain in the ventricular zone longer than previously expected, only leaving it after several migration waves - e.g. cells born at E12 and traditionally expected to occupy lower cortical layers initiate their migration at E15/16 to occupy layers II-III (Franco et al. 2012; Guo et al. 2013; García-Moreno & Molnár 2015).

1.6.4 Tangential cortical migration

In comparison, cortical interneurons are born at significantly more distant areas from their final position and, as such, must migrate a long distance from the subpallium to invade the neocortex – called tangential migration. This involves dynamic branching modifications to determine the direction of the migrating cell via a combination of guidance molecules and chemotactic signals, with the primary cilium being a key regulator (Nóbrega-Pereira & Marín 2009; Martini et al. 2009; Baudoin et al. 2012). Interneurons derived from different progenitor areas follow somewhat distinct migratory routes but their migration is initiated by the expression of chemorepulsive signals in the subpallial VZ/SVZ. These cells typically start migrating ventrally before switching to a tangential mode and circumvent the developing striatum before crossing the pallial-subpallial boundary and enter the dorsal pallium. The first interneurons begin to arrive at the neocortex around E12 and exploit different migratory corridors (marginal zone, subplate and SVZ) to invade the cortical wall before switching to radial migration and settle into their final position (Faux et al. 2012; Marín 2013; Marín & Müller 2014; Guo & Anton 2014). Tangential migration is also important for the arrival of certain glutamatergic cell populations that occupy the mature neocortex such as a subset of subplate neurons born in the rostro-medial telencephalic wall that migrates through the medial pallium (Pedraza et al. 2014), and Cajal-Retzius cells which originate in the septum, the pallial-subpallial boundary and the caudo-medial telencephalic wall (Bielle et al. 2005; García-Moreno et al. 2008a).

1.6.5 Disorders of neuronal migration

The complexity of neuronal migration and its diverse cellular processes and molecular signals makes it highly susceptible to disruption that can lead to malfunction and eventually disease. The consequences of disruptions in neuronal migration are strongly dependent on the point in which development is disturbed but defects in migration typically cause abnormal structure-function resulting in cognitive

impairments from mild disturbances to severe mental retardation and epilepsy (Gleeson & Walsh 2000; Guerrini & Parrini 2010). Human cortical migration disorders divide broadly into two subtypes: (a) diffuse ones causing severe impairment, exemplified by lissencephaly where mutations in the gene *LIS1* lead to the lack of the characteristic gyrified structure accompanied by thickening of the cortex and laminar dysplasia; and (b) mild to severe focal disruptions such as periventricular nodular heterotopias resulting from mutations in the *FLNA* gene that lead to the formation of nodules of gray matter adjacent to the lateral ventricle, disrupting white matter and laminar organisation (Guerrini & Parrini 2010). Recently, impaired migration of interneurons more specifically have also been implicated in disease, particularly neuropsychiatric disorders such as schizophrenia or 22q11.2 deletion syndromes (Marín 2012; Meechan et al. 2012).

The best characterised neuronal migration disorder is found in a mouse mutant, reeler, with a spontaneous mutation that leads to dramatic consequences in cortical organisation: the inside-out development of the cortex is bypassed to give rise to an inverted lamination pattern, with neurons destined to the subplate and deep layers lying closer to the pial surface whilst those which typically occupy the upper layers lie adjacent to the white matter (Caviness & Sidman 1973). With advances in molecular genetics and genetic engineering techniques in animal models, several genes have been found to play a role in neuronal migration disorders and identified molecules have been found to operate in distinct stages of migration identified in Fig. 1.14C: transition out of the VZ/locomotion, early migration into the IZ, entry into the CP, switch to somal translocation, and so on (Gleeson & Walsh 2000).

1.7 Aims of this thesis

The key research question of the project this thesis explores is:

> *'What are the roles of KIAA0319 and KIAA0319L in brain structure and/or function?'*

The important position of *KIAA0319* within the classical picture of dyslexia susceptibility genes and its homology/relationships with *KIAA0139L* indicates that advancing our knowledge of the role of the encoded proteins may provide important insights into the nature of the language-ready brain as well as how these genes may contribute to susceptibility to dyslexia and other language-related disorders.

There are several levels of 'granularity' in which the influence of a particular gene can be understood in relation to the brain, from specific molecular conformations and cellular roles to their modulation of particular behaviours. This thesis attempts to tackle the problem of gene function with a multi-level approach spanning through these different dimensions to shed light on the function of KIAA0319/KIAA0319L with regards to brain development and formation of early circuits, behavioural outputs, and cellular and molecular functions. Each of the three experimental chapters interrogates the roles of KIAA0319 and KIAA0319L at one of these levels.

Aims of Chapter 3

The introduction above reviewed the current evidence pointing towards a role for KIAA0319 and KIAA0319L in neuronal migration during cortical development based on experiments performed in rats with shRNA. Combined with other functional genetics data and with the neuropathological studies on human dyslexic brains, they formed the cornerstone of the hypothesis of dyslexia as a disorder of neuronal migration (Galaburda et al. 2006; Fisher & Marcus 2006; Paracchini et al. 2007; Gabel et al. 2010; Scerri & Schulte-Körne 2010; Giraud & Poeppel 2012; Raskind et al. 2013; Adler et al. 2013; Kere 2014; Peterson & Pennington 2015).

In order to understand the precise mechanisms in which these two proteins contribute to such an impairment in neuronal migration, the Molnár and Monaco

laboratories generated a transgenic mouse line carrying a loss-of-function mutation in the homologous mouse gene *Kiaa0319* (*D130043K22Rik*). However, no problems in cortical migration were found to result from altered levels of KIAA0319 in the mouse brain (Martinez-Garay et al. 2017). Robustness against perturbations such as null mutations in gene KOs may be a universal property of biological systems and it is often triggered by functionally overlapping paralogous genes (Ohno 1970; Edelman & Gally 2001; Gu 2003; Kitano 2004; Kafri et al. 2009; Su et al. 2014). Given AU040320 exhibits a similar expression pattern in the developing brain, it shares a number of protein features with the KIAA0319 protein and has also been implicated in neuronal migration (Diez-Roux et al. 2011; Poon et al. 2011b; Platt et al. 2013), compensation by the AU040320 protein is a likely explanation for the normal cortical migration and lamination observed in *Kiaa0319* KO mice. Based on this, Chapter 3 has as its primary research question:

- Do AU040320 and KIAA0319 regulate neuronal migration? Do they interact in a compensatory way during cortical development?

To address this, I start by generating a transgenic mouse line targeting the homologous mouse gene *AU040320/KIAA0319L* to study the role of its encoded protein individually in migration and brain development more generally using a combination of anatomical and histological analyses. Alongside this, I interrogate the putative redundant relationship between KIAA0319 and AU040320 in migration and cortical development using similar approaches and with *in utero* electroporation, an experiment aimed to mimic in the mouse the original findings with RNAi in rats.

Aims of Chapter 4

In order to interrogate the contributions of KIAA0319 and AU040320 on endophenotypes that parallel language-related behaviours in rodents, I performed a series of behavioural experiments to examine potential deficits that the combined deletion of the two proteins may have on mouse behaviour. Given the negative results

of the previous chapter, new hypotheses about the functions of KIAA0319 and AU040320 are needed and these experiments also serve as a way to investigate different neural systems where the two genes may be important. Tests were based on hypothesis-guided questions based on the literature on dyslexia susceptibility genes and human dyslexia endophenotypes such as memory and auditory processing, alongside other tests based on known features and the expression pattern of the two genes. Previous experiments on rats following RNA interference described above pointed towards a role for KIAA0319 in rodent auditory processing and spatial memory and a behavioural screening of *Kiaa0319* KO mice suggested a putative sensorimotor integration impairment.

The chapter starts with a battery of behavioural tests conducted on double KO mice covering locomotor activity, motor learning, spatial memory, olfactory preference, anxiety-like behaviour, sensorimotor gating and auditory processing. In light of results pointing to a deficit in the auditory system, a second round of experiments focusing on this specific question was conducted in an attempt to dissect the individual contribution of KIAA0319 and AU040320 to the observed impairment. This was accompanied by electrophysiological recordings in the auditory brainstem in double and single KO mice to examine the extent to which the different genetic manipulations can affect basic hearing or early auditory processing.

Aims of Chapter 5

In chapter 5, I turn to the role of the AU040320 protein at the level of individual cells. At an early stage of the doctoral work reported here, it became apparent that males carrying no functional copy of *AU040320* were infertile. Whilst the focus of this work is the brain rather than the reproductive system, this observation opened the opportunity to examine the direct contributions of AU040320 at the cellular level. This is particularly important given the paucity of knowledge on this protein so far. Characterising the process which may lead to infertility in *AU040320* KOs could provide a platform to identify (one of) the cellular functions of the encoded protein.

The ultimate goal is to use this as a route to generate new hypotheses about the role this protein may have in brain structure and function. Thus, this chapter provides a characterisation of the infertility phenotype of *AU040320* KO mice with a focus on mutant spermatozoa, alongside putative molecular interactions AU040320 may have.

Aims of Chapter 6

The implications and predictions of the findings of each chapter are discussed individually in specific sections within each chapter. In Chapter 6, I shall give a more general overview of the implications of this work by summarising the findings and outlining their relationship to the neurobiology of dyslexia and language. This chapter also attempts to connect any overlapping points between the relevant findings of each individual chapter and connect the different levels of analyses where appropriate. The questions and new hypotheses that emerge from this thesis are also discussed.

2 Methods

Contents

2.1 General methods 57
2.1.1 Experimental animals 57
2.1.2 Genotyping and PCRs 58
2.1.3 Sanger sequencing 58
2.1.4 Western blot 59
2.1.5 LacZ staining 60
2.2 Chapter 3 methods 61
2.2.1 Immunohistochemistry 61
2.2.2 Nissl-staining 61
2.2.3 *In utero* electroporation 62
2.2.4 Antibodies 63
2.2.5 Image acquisition and statistical analyses 63
2.3 Chapter 4 methods 65
2.3.1 Behavioural testing 65
2.3.2 Auditory brainstem responses 69
2.3.3 Quantification of synapse number by immunohistochemistry 70
2.4 Chapter 5 methods 72
2.4.1 Hematoxylin & eosin staining 72
2.4.2 Giemsa staining 72
2.4.3 Epididymal sperm count 72
2.4.4 Meiotic profile analysis of spermatocytes 72
2.4.5 Immunohistochemistry & Immunofluorescence 73
2.4.6 Antibodies 74
2.4.7 Scanning electron microscopy 74
2.4.8 Transmission electron microscopy 75
2.4.9 GST pulldowns/*in vitro* binding assay 75
2.4.10 Mutation screening in human cases of globozoospermia 76

2.1 General methods

2.1.1 Experimental animals

Animals were housed with *ad libitum* food and water access under a 12 h light/dark cycle with temperature and humidity kept constant. Animal generation, maintenance and procedures took place at the Functional Genetics Facility of the Wellcome Trust Centre for Human Genetics or in the Biomedical Services Building, University of Oxford, with exception of auditory brainstem response recordings which were conducted at The Ear Institute, University College London. All animal experiments were approved by the local ethical boards and followed the regulations detailed in personal and project licenses in accordance with the Animals (Scientific Procedures) Act 1986. Studies were conducted from samples collected from heterozygous breeding pairs for littermate comparisons. In the case of double mutants, double KOs were obtained from crosses between *Kiaa0319* -/-;*AU040320* +/- mice, with controls obtained from a line derived from *AU040320* +/- matings that preceded the crosses with *Kiaa0319* mutants. A detailed description of the generation of these animals, the micro-injections, genetic background and alleles is described in Chapter 3.

2.1.2 Genotyping and PCRs

Genomic DNA was extracted from ear notches and tail clips in the case of young pups or embryos as detailed in French et al. (2007), with some modifications. Protocol consisted of incubating the tissue at 56°C for 2-4h in 0.1 ml ear notch lysis buffer (50 mM Tris-HCl pH 8, 1 mM EDTA, 0.5% Tween-20, 0.5 mg/ml Proteinase K) followed by inactivation of Proteinase K by incubation at 100°C for 15 min and centrifugation at 14,000 rpm for 10 min. The resulting DNA was then diluted 1:5 and 5 μl were used for polymerase chain reactions (PCR) with 20 μl of PCR mix (1 x buffer, 2 mM MgCl2, 0.4 mM dNTPs, 0.4 μM primers, 1% BioTaq DNA polymerase (Bioline Reagents) under the following cycling conditions: an initial denaturation step at 95°C for 15 min, followed by 34 cycles of 30 s denaturation at 94°C, 30 s annealing at 60°C and 45 s elongation at 72°C, with a final elongation step at 72°C for 10 min.

To amplify regions of the 'knockout-first' (KO1) allele, standard PCRs as described above were used in conjunction to long-range PCR using SequalPrep Long polymerase (Life Technologies) according to the manufacturer's instructions. All primers used, from Invitrogen, are listed in Martinez-Garay et al. (2017) for *Kiaa0319* mouse lines and detailed in Table A.1 in Appendix A for *AU040320* transgenic lines.

2.1.3 Sanger sequencing

Sequencing of PCR-amplified fragments was carried out at the sequencing service of the Department of Zoology, University of Oxford, using an ABI 3730xl or ABI 3130 machine according to the following protocol. After DNA amplification by PCR, fragments were checked for the expected size on agarose gels and a clean-up step was performed under the following conditions: 15 μl of PCR reaction, 1 μl of 10X SAP buffer and 1 μl SAP (USB), 0.1 μl Exonuclease I (New England Biolabs), 0.9 μl MilliQ water. Mixes were incubated at 37°C for 30 min and 80°C for 15 min.

Following clean-up, fragments were subjected to a sequencing reaction containing: an average of 2 μl PCR product per reaction (this varied in some cases according to the strength of the PCR reaction), 0.5 μl BigDye v3.1, 1 μl BigDye 5X reaction buffer (Applied Biosystems), 0.5 μl 10 μM primer and MilliQ water to 10 μl. A series of incubation steps were performed starting with 1 min at 95°C followed by 34 steps of 10 s at 95°C, 10 s at 50°C and 4 min at 60°C. Unused PCR reagents were then removed by ethanol precipitation combined with sodium acetate and EDTA. Resulting sequences and chromatograms were analysed using Chromas Lite v2.1.1 (Technelysium Pty Ltd) and Clone Manager 6 (Sci Ed Central) or CodonCode Aligner 6.0.2 (Codon Code Corporation). Each PCR fragment was analysed with both a forward and a reverse sequence.

2.1.4 Western blot

Western blot protein analysis was carried out primarily as previously described in Velayos-Baeza et al. (2008). Samples were collected after culling animal by cervical dislocation and kept at -80°C until processed. Tissue was initially disrupted and

homogenised with a dounce homogeniser using cold RIPA buffer without detergents (50 mM Tris-Hcl pH 7.5, 150 mM NaCl) containing 4X Complete EDTA-free protease inhibitor cocktail (Roche) before being transferred onto a cold Eppendorf. The homogeniser was then washed with RIPA buffer with 2X detergents (2% NP-40, 1% Na-deoxycholate, 0.2% SDS) which was then mixed with the initial homogenate and left on ice for at least 3 h. Lysates were then centrifuged at 6,000 g for 10 min at 4°C and supernatant collected into fresh tubes. Lysate protein concentration was quantified using the Pierce BSA Assay (ThermoFisher Scientific). Proteins were prepared with NuPAGE LDS sample buffer with reducing agent and subjected to electrophoresis using NuPage Novex 4-12% Bis-Tris gels (Invitrogen) following the manufacturer's instructions. Gels were transferred onto PVDF membranes (Invitrogen), checked by Ponceau-staining and processed for Western blot using standard conditions. Primary antibodies were diluted in 1% milk + TBS-Tween 20 and are listed in Table 2.1 and secondary antibodies were goat anti-mouse or anti-rabbit IgG-HRP (Bio-Rad). Immunoreactive bands were visualised with ECL Plus Western Blot Detection Reagent (GE Healthcare).

2.1.5 LacZ staining

For detection of lacZ reporter in *AU040320* or *Kiaa0319* mutant mice, fresh-frozen samples were cut at 30 μm on a cryostat (Jung CM3000; Leica). Sections were post-fixed for 10 min on ice with 0.2% glutaraldehyde (Polysciences) in PBS and slides washed for 10 min in PBS followed by a detergent rinse (0.02% Igepal, 0.01% Sodium Deoxycholate in PBS) and then incubated overnight at 37°C in the dark in the detergent solution containing 1 mg/ml x-gal (Thermo Fisher; plus 5 mM potassium ferricyanide, 5 mM potassium ferrocyanide). Next, slides were post-fixed in 4% PFA for 10 min, washed in PBS and distilled water before Nuclear Fast Red counterstaining (Sigma-Aldrich). Images were taken on a light microscope (Leica DMR/DC-500).

2.2 Chapter 3 methods

2.2.1 Immunohistochemistry

Embryonic brain samples were collected from plug-timed pregnant females and detection of vaginal plug was considered embryonic day 0 (E0). Pregnant females were culled by cervical dislocation, embryos were decapitated and their brains fixed in 4% paraformaldehyde (PFA, Sigma-Aldrich) in 0.1 M phosphate-buffered saline (PBS) pH 7.4 and left at 4°C overnight. For postnatal samples, animals were anaesthetised with pentobarbitone (150 mg/kg, Pentoject, Animal Care Ltd, UK) or by hypothermia on ice before being transcardially perfused with PBS followed by PFA. Samples were stored in PFA overnight at 4°C and transferred to PBS with 0.05% sodium azide (Sigma-Aldrich) until processed for experimentation.

Brain samples were embedded in 4% agarose (Bioline) and sectioned using a vibrating microtome (VT1000S, Leica Systems). Coronal brain sections were cut at 50 μm and sagittal ones at 70-100 μm, and sections were stored in 1X PBS with 0.05% sodium-azide before immunostaining. Selected matching sections were pre-incubated at room temperature for 2 h in blocking solution (4% bovine serum albumin + 3% goat/donkey serum with 0.1% Triton X-100 or 5% goat/donkey serum with 0.1% Triton X-100) before incubation with primary antibodies overnight at 4°C. They were then washed (3 x 10 min in PBS) and incubated with fluorescently-labelled secondary antibodies for 2 h at RT to detect primary antibodies. After three washes they were counterstained with DAPI (4',6-diamidino-2-phenylindole). All antibodies were diluted in blocking solution and omission of primary antibody served as negative control. Slides were mounted with glass coverslips using ProLong Gold Medium (Invitrogen). The antibodies used are listed below in Table 2.1.

2.2.2 Nissl-staining

Vibratome-cut sections processed following the same protocol for immunohistochemistry were mounted on gelatin-coated slides were used for Nissl staining. After defatting in a series of ethanol (95-100%) and chloroform immersion steps of 4 min

each, sections were stained with 1% cresyl violet for 5 minutes, washed in ethanol to dehydrate and cleared in histoclear in several 3 min steps. DePeX mounting medium (WRR) was used to mount with glass coverslips.

2.2.3 *In utero* electroporation

In utero electroporations were performed as described previously (Garcia-Moreno et al 2015), with some minor modifications. Time-mated females were given an intraperitoneal injection of Vetergesic (0.08 mg/kg; Alstoe) for analgesia prior to administration of Isofluorane. Laparatomy was performed at the midline and uterine horns exposed. DNA plasmid was mixed with Fast Green (Sigma) and injected into lateral ventricles with pulled glass capillaries (Harvard Apparatus). Tweezer electrodes (CUY650P3, Nepagene) were used to deliver square pulses (42-45V, 5 $\times$ 50 ms with 950 ms resting periods) using a square pulse generator (Electro Square Porator, Harvard Apparatus). Embryonic sacs were kept warm using PBS along with a heat pad. Uterine horns were then gently placed back inside the abdominal cavity which was closed with surgical incisions sutured using Vicryl 6/0 (Ethicon). Surgical clips were used to hold the skin together during the recovery period. Animals were observed post-anaesthesia until regained normal activity and monitored for a couple of days post-operatively to check for any signs of pain. Expression constructs pCIG-GFP and pCIG-IRES-GFP used for protein expression were already available in the laboratory and are described in Martinez-Garay et al. (2017).

2.2.4 Antibodies

Antibody	Source	Conc.
Rat anti-Ctip2 [25B6]	Abcam (ab18465)	1:250
Rabbit anti-Cux1 [CDP (M-222)]	Santa Cruz (Sc-13024)	1:200
Rabbit anti-Pax6	Covance (PRB-278P)	1:200
Rabbit anti-Tbr2	Abcam (ab23345)	1:500
Rabbit anti-Ki67	Abcam (ab15580)	1:1000
Mouse anti-ph3 (Histone H3)	Abcam (ab14955)	1:2000
Goat anti-Ctgf	Santa Cruz (sc-14939)	1:2000
Mouse anti-Reelin	Chemicon (MAB5364)	1:500
Rabbit anti-Parvalbumin	Swant (PV28)	1:5000
Mouse anti-Somatostatin	GeneTex GTX71935	1:250
Rabbit anti-Calretinin	Swant (7697)	1:2500
Mouse anti-NF-H [SMI32]	Sternberger-Meyer (SMI-32P)	1:2000
Rabbit anti-Calbindin D-28k	Swant (300)	1:2000
Mouse anti-NeuN [A60]	Chemicon (MAB377)	1:100
Mouse anti-Cre	Sigma-Aldrich (7988)	1:200
Guinea pig anti-AU040320	Custom made	1:1000
Mouse anti-actin	BD Transduction (612656)	1:1000
Donkey anti-goat 568	Molecular Probes (A11057)	1:500
Goat anti-rat 488	Molecular Probes (A11006)	1:500
Goat anti-rabbit 488	Molecular Probes (A11008)	1:500
Goat anti-rabbit 568	Molecular Probes (A11011)	1:500
Goat anti-mouse 488	Molecular Probes (A11029)	1:500
Goat anti-mouse 568	Molecular Probes (A11031)	1:500

Table 2.1: List of antibodies used in Chapter 3 for immunofluorescence or Western blotting.

2.2.5 Image acquisition and statistical analyses

Fluorescent images were taken with a laser-scanning confocal microscope (Leica TCS SP8) or a light microscope for non-fluorescently labelled sections (Leica DMR/DC-500). Image processing and analyses used GIMP Image Editor (GIMP Development Team) and ImageJ (Image Analysis in Java, NIH) combined with its Cell Counter plugin. Similarly to Cheung et al. (2010), 100 μm-wide equivalent coronal sections were selected, cortical thickness measured and divided into 10 equally-sized bins for cell counting. For pH3/ki67 quantification, the cortex was divided into two regions only: VZ and the rest (non-VZ). At least three brains

per condition were analysed, with three equivalent sections per brain. For *in utero* electroporation experiments, samples were only considered for analysis when litters contained suitably electroporated test-control pairs in the dorso-lateral cortex. Statistical analyses of cell number/distribution used one-way ANOVAs or paired t-tests to compare group means in PSPP v0.6.1 for Linux (PSPP Development Team), with significance threshold p=0.05. Graphs were generated using LibreOffice Calc (Linux).

2.3 Chapter 4 methods

2.3.1 Behavioural testing

A cohort containing 18 double KO (dKO) mice 18 wildtype controls (9 males, 9 females) was used for behavioural testing. Mutants were derived from *Kiaa0319* -/- ;*AU040320* +/- matings and wildtypes from *AU040320* +/- pairs from a generation used to produce dKOs. Matings were then plug-timed and females were housed as plug-date matched pairs so that mutant and wildtype mice were born and housed together in the same cage. All pups were then genotyped and weaned into cages containing 6 animals, 3 mutants and 3 controls. From this point onwards genotype was kept blind to the experimenter. All behavioural experiments were conducted during the light phase, between 08:00 and 17:00h. Animals were 8 weeks of age at start of testing and lasted 5 weeks following the order in which they appear described below. At least one day of rest between experiments was allowed. Males were always tested before females to avoid interference from the perception of oestrus odours. Statistical analyses were conducted using Unistat 5.6 (Unistat Ltd) or PSPP v0.6.1 for Linux (PSPP Development Team) using paired t-tests, one or two-way ANOVAs. Significance threshold was defined as $p = 0.05$. For all tests, two-way ANOVAs were conducted with genotype and sex as between-subject factors but none of them revealed an effect of sex in the measures tested. Experimental procedures were largely based on previously published protocols (Ufartes et al. 2013), with descriptions for each test following below.

2.3.1.1 Locomotor activity

To measure locomotor activity in a novel environment, mice were placed in Plexiglass cages (20 × 35 cm) equipped with infrared photobeams (San Diego Instruments) over a total of 90 min. Testing always took place in the light phase and started at 10:00 h for all groups. Activity was measured as number of beam breaks and divided into 15 min bins for analysis.

2.3.1.2 Light/dark box

Testing was performed using Med Associates activity chambers (ENV-510) with a perspex dark box insert covering half the area of chamber (27 x 13.9 x 21.5 cm) and a 4 x 4 cm hole placed in the middle at floor level to divide it into light (300 lux) and dark (2 lux) compartments. Animals were started in the light compartment and session lasted 10 min. Animals' performance were automatically scored by Med Associates activity software and measured time spent in each zone, distance travelled, latency to enter dark zone and the number of transitions between zones. Light-dark ratio (LD ratio) was calculated using: time in dark / (time in dark + time in light).

2.3.1.3 Accelerating rotarod

Motor coordination and learning were assessed using an accelerating rotarod (Model 7650, UgoBasile) based on (Jones & Roberts 1968). Mice were placed on a rod moving at 4 rpm that began to accelerate after 10 s at a rate of 20 rpm/min. Latency of animal to fall from the rod was recorded. Mice were given three trials per day over the course of three consecutive days, with a minimum of 60 min inter-trial interval. A habituation phase took place for 30 s one day before testing. Failure to grip in adaptation phase or in initial 10 s of experiment counted as disqualification but all animals passed the test.

2.3.1.4 Olfactory preference task

In order to assess responses to distinct olfactory stimuli, perception of aversive and attractive smells was assessed based on the protocol described in Witt et al. (2009). Briefly, four Plexiglass cages (20 cm x 30 cm) with no bedding were organised in sequence in a safety cabinet and divided with black thick paper to set up partitions and isolate them from each other. Mice were sequentially placed in the first 3 cages for adaptation to the testing environment for 15 min in each cage. Animals then proceeded to test cage where it was presented for 3 min with a 3 x 3 cm square of filter paper dampened with a randomised sequence of water,

peanut butter (dissolved in sunflower oil) used as an attractive odour, or 10% 2-methylbutiric acid (2-MA) as an aversive stimulus. Each scented filter paper was used only once and excess solution removed with Kimwipes (Kimberley-Clark). Inter-trial intervals lasted 1 min between stimulus presentation and stimulus area was cleaned with odourless disinfectant spray (Distel, Starlab), water and dried with paper towels. Time spent sniffing each scented filter paper over the course of 3 min was recorded and excluded instances of chewing. Olfactory preference was calculated by subtracting time sniffing water control from target stimulus (time-sniffing-water – time-sniffing-stimulus).

2.3.1.5 Y-maze spatial novelty

Spatial novelty was assessed in using a perspex Y-maze (30 × 8 × 20 cm arm dimensions). The base arm of the maze was defined as the 'start' arm. In the sampling phase, animals were assigned one of the other two arms (the 'other' arm) counterbalanced for genotype and allowed to explore both 'start' and 'other' arms for 5 min. The animal was then returned to its home cage for 1 min before being placed back in the start arm for a 2 min exploration with access to all three arms. Time spent in each arm, distance travelled and number of arm entries were recorded automatically using a video camera fixed to the ceiling coupled to tracking software AnyMaze (Stoelting).

2.3.1.6 Spontaneous alternations in T-maze

Spatial working memory was assessed using a black wooden T-maze (30 cm x 10 cm, walls 29 cm high). Mice were placed in the start arm and allowed to choose a goal arm. A central partition wall was placed at the end of the start arm which extended the decision-making point 7 cm into the start arm and blocked any experience of the non-visited arms. Once the animal entered the goal arm, a guillotine door was used to confine the animal to it for 30 s for exploration. Arm chosen and latency to enter goal arm were recorded. The animal was then removed from the apparatus for 15 s, guillotine and central partition were removed and the animal was placed back in

the start arm for free exploration in a 'choice' phase. The arm chosen on the second run and latency to enter it were recorded before returning the animal to its home cage. Animals were tested twice a day (morning and afternoon) for 5 consecutive days. Spatial memory was assessed using the percentage of arm alterations – i.e. arm chosen in choice phase was different from the one chosen at exploration.

2.3.1.7 Startle reflex and prepulse inhibition of acoustic startle

An SR-Lab System (San Diego Instruments) was used to measure startle responses and pre-pulse inhibition of acoustic startle. Mice were placed in a Plexiglass cylinder for 5 min exposed to white noise background at 65 dB followed by a habituation phase of 5 x 120 dB stimuli. Test sessions contained a randomised set of stimuli consisting of the following types: stimuli identical to background noise (65 dB) to measure baseline movement, a 40 ms, 120 dB 'pulse' stimulus, 4 single 'prepulse' stimuli at 4, 8, 12 or 16 dB above background noise for 20 ms and, finally, 4 combinations of prepulse-plus-pulse stimuli with a 100 ms delay between them. Six blocks of trials were presented, with each stimulus once in each block. The interval between each trial type varied between 10, 15 and 20 ms. Five 120 dB stimuli were presented at the end of the session. Responses to stimuli were recorded using average startle amplitude for every ms during a 65 ms sampling window starting at the onset of each startle-eliciting sound. Prepulse inhibition was calculated using the following formula: 100 – (prepulse-plus-pulse x 100 / pulse-only).

2.3.1.8 Silent gap detection

To assess the effect of genetic mutations on rapid auditory processing, a silent gap startle paradigm was used following Fitch et al. (2008) and Truong et al. (2014). The protocol is identical to prepulse inhibition design described above with exception of the stimuli, with continuous background noise set at 75 dB. Cued trials consisted of interruptions in white noise (i.e. silent gaps) that varied in duration between 2-100 ms (2, 5, 10, 20, 30, 40, 50, 75, 100 ms) before the presentation of the startle stimulus of 105 dB for 50ms. Stimuli with silent gaps of 0 ms duration were used as uncued,

control trials. Presentation of stimuli was randomised and appeared at inter-trial intervals of 10, 15 or 20 ms. Average startle amplitude was used to calculate an 'attenuation score' according to: (cued-response/ uncued-response) x 100.

2.3.2 Auditory brainstem responses

Auditory brainstem responses (ABR) recordings were performed as described in Anderson & Linden 2016. Briefly, three subdermal needle electrodes were used: a positive electrode at the vertex of the skull, a negative one behind the ear being tested that is oriented toward the speaker, and a ground electrode behind the opposite, contralateral ear (blocked with an earplug to ensure monoaural presentation). Mice were anaesthetised with ketamine and medetomidine, atrophine was given as required and ringers were injected approximately every hour. A homeothermic blanket (Harvard Apparatus) used to maintain body temperature during the procedure.

An isolated sound booth was used for testing (Industrial Acoustics Company, Inc.). A Free-field speaker (Tucker-Davis Technologies, TDT) was used for presentation of auditory stimuli and these were calibrated before experiments started using a Bruel & Kjaer ¼ inch microphone (4939), placed at the location of the ear to be tested to ensure a flat frequency response within +/- 2 dB spanning 2-80kHz. Stimuli were generated and data recorded using RX6 and RX5 signal processors, RA4LI and RA16SD signal amplifiers, PA5 attenuator, and SA1 speaker amplifier (all from TDT) a custom low-pass filter designed to remove attenuation switching transients, and software from TDT (Brainware) and Mathworks (Matlab). All ABR data was analysed with bespoke MatLab software from the Linden Lab at UCL to determine wave peaks and troughs. The wave amplitude was calculated as the height between the wave peak and its following trough. The wave latency was calculated as the latency of the peak of the wave. Only waves I-IV were used as wave V recorded from mice are not always clearly distinguishable.

Click ABRs were recorded using white noise sound bursts at 10-80 dB intensity (increasing in 5-10 dB steps). All clicks were monopolar square waves with a

duration of 50 μs. The inter-onset interval was 100ms for the fast click rate and 500ms for the slow click rate. The results were analysed with a repeated measures ANOVA with genotype as a between-subjects measure and sound level as a repeated, within-subject measure, followed by *post-hoc* Tukey comparisons.

Masker-probe stimuli were all presented at 60 dB SPL. The stimuli were composed of a 'masker', a white noise 200 ms-long sound, followed by a silent gap of varying in duration (8, 20 or 50 ms) which was then followed by a click (probe click). Regardless of the duration of the delay to the probe click, a second click (reference click) was presented 500 ms after the end of the masker white noise.

All clicks were monopolar square waves with duration of 50 μs. Experiments and analyses were all conducted blind to the experimenter. Results were analysed with a repeated-measures ANOVA with genotype as a between-subjects measure and sound level as a repeated, within-subject measure, followed by *post-hoc* Tukey comparisons.

2.3.3 Quantification of synapse number by immunohistochemistry

Analyses of synaptic puncta in the auditory pathway were performed as described in Ippolito & Eroglu (2010) and Risher et al. (2014). This method has been previously validated and confirmed by electron microscopy and electrophysiology (Christopherson et al. 2005; Varoqueaux et al. 2006; Eroglu et al. 2009). Samples from dKO mice and wildtype mice used for behavioural experiments were collected and processed for immunohistochemistry as detailed in section 2.2.1. The following antibodies were used for labelling synaptic puncta: for presynaptic markers, guinea-pig anti-VGlut1 (Chemicon, AB5905; 1:10,000) or guinea-pig anti-VGlut2 (Chemicon, AB5907; 1:2,500); for post-synaptic labelling, mouse anti-PSD-95 (Invitrogen, MA1-046; 1:300). Three independent matching sections per animal were selected for analyses (3 animals per genotype) and confocal images of the relevant area of each section were taken (63x magnification; Leica SP8 SMD X) as 5 μm z-stacks (optical section depth 0.33 μm, 15 sections/z-stack, imaged area/scan = 20,945 μm^2). Maximum projections were then generated for sequences of 3 consecutive

images (1 μm depth) and number of pre-synaptic, post-synaptic and co-localised puncta were calculated in ImageJ with the Puncta Analyzer plugin for ImageJ 1.29 (available at $http://labs.cellbio.duke.edu/Eroglu/Eroglu_Lab/Publications.html$). Briefly, maximum projections spanning 1 μm of depth are separated by channel, background subtracted (with a rolling ball radius = 50) and threshold adjusted so as to allow identification of puncta without noise. Puncta from the two channels are aligned by an algorithm that detects co-localisation and quantifies them.

All analyses were performed blind.

2.4 Chapter 5 methods

2.4.1 Hematoxylin & eosin staining

Animals were culled by cervical dislocation, testis and epididymis dissected out of animals at least 8 weeks old and fixed by immersion in Bouins fixative (Polysciences) for 6 h before being transferred to 70% ethanol. Samples were washed until excess fixative was removed before being embedded in paraffin. Sections were then cut on a microtome at 6-8 μm and stained for hematoxylin and eosin. Briefly, this consisted of dewaxing sections in histoclear and rehydrating them in a series of graded steps of ethanol and water. Slides were then immersed in hematoxylin solution and counterstained with eosin before being dehydrated in ethanol, cleared in histoclear and mounted with glass coverslips. Images were taken using a Nikon wide-field TE2000U Microscope.

2.4.2 Giemsa staining

Smear preparations from sperm samples were prepared by dissecting epididymis of adult mice and releasing sperm cells in 1X PBS. 10 μl of the sperm suspension was applied to a slide mounted in Shandon coverplate holders, air dried and fixed in methanol for 30 s and stained with 4% Giemsa solution (Sigma-Aldrich) in 0.1 M sodium citrate buffer for 2 min.

2.4.3 Epididymal sperm count

To quantify the number of mature sperm in the epididymis of adult mice, the cauda epididymis was dissected, sperm released from the tissue by squeezing and puncturing and incubated for 30 min at 37°C in PBS. The sperm medium was then diluted and cell density quantified using a hemocytometer.

2.4.4 Meiotic profile analysis of spermatocytes

Analysis of spermatocyte meiotic profile was performed by dissecting seminiferous tubules from adult testes into Minimum Essential Medium (MEM, Sigma-Aldrich) with protease inhibitor cocktail (Roche) and pipetting to release cells. Samples

were left on ice and the supernatant collected and centrifuged at 5800 g for 5 min. Cells were resuspended with 0.1 M sucrose in water, spread onto slides coated with 1% PFA and placed in a humidity chamber for 2-3 h. Slides were then rinsed with 0.4% Photo-Flo 200 (Kodak), allowed to air dry and used for immunostaining. Non-specific binding sites were blocked by incubating the cells with 0.2% BSA, 0.2% gelatin, 0.05% Tween-20 in PBS for 1 h at room temperature. Cells were incubated with the primary antibodies (see Table 2.2) overnight at 4°C and secondary antibodies for 2 h at room temperature before mounting.

2.4.5 Immunohistochemistry & Immunofluorescence

For analysis of testis structures and sperm development by immunohistochemistry, adult male mice, at least 8 weeks old, were anaesthetised with pentobarbitone (150 mg/kg, Pentoject, Animal Care Ltd, UK), transcardially perfused with PBS followed by PFA and stored in PFA overnight. Samples were then cryopreserved in 30% sucrose in PBS for at least 24 h before being embedded and frozen in OCT compound (TissueTek). Testes were sectioned at 12-18 μm on a cryostat (Jung CM3000; Leica).

For detection of AU040320 protein, sections were processed for antigen retrieval with boiling sodium citrate buffer for 1 min followed by 4 min in the same buffer at room temperature. To prevent unspecific binding, sections were incubated in blocking buffer (Chemi Blocker, Millipore, and 0.1% Triton-X 100) before incubation with primary antibodies overnight at 4°C in blocking buffer. After PBS washes, slides were incubated with fluorescently-labelled antibodies for 2 h at room temperature and counterstained with DAPI. All antibodies were diluted in blocking buffer and slides were mounted with ProLong Gold Medium (Invitrogen). Images were taken using a Leica SP8 SMD X Confocal Microscope or a Carl Zeiss LSM710 and processed using GIMP Image Editor (GIMP Development Team) and ImageJ (Image Analysis in Java, NIH).

To inspect the morphology of mature epididymal sperm, cells were collected after dissection, squeezing and puncturing of adult epididimi to be released onto

slides and fixed in 4% PFA for 30 min. The procedure then followed the testis immunohistochemistry protocol detailed above in Section 2.4.5

2.4.6 Antibodies

Antibody	**Source**	**Conc.**
Guinea pig anti-AU040320 (# 78)	custom made	1:1000
Rabbit anti-AU040320 (Rb-AU)	ProteinTech (21016-1-AP)	1:1000
Mouse anti-acetylated tubulin	Sigma-Aldrich (T7451)	1:1000
mouse anti-beta-tubulin III (Tuj1)	Abcam (ab14545)	1:1000
sheep anti-rat TGN38	Biorad (AHP499)	1:200
mouse beta-tubulin-CY3	Sigma (C4585)	1:200
Lectin PNA conjugate 488/568	ThermoFisher (L21409/L32458)	1:1000
MitoTracker Deep Red FM	ThermoFisher (M22426)	1:1000
AlexaFluor goat anti-guinea pig 488	Molecular Probes (A11073)	1:1000
AlexaFluor goat anti-guinea pig 568	Molecular Probes (A11075)	1:1000
AlexaFluor goat anti-rabbit 568	Molecular Probes (A11011)	1:1000
AlexaFluor goat anti-mouse 488	Molecular Probes (A11001)	1:1000
AlexaFluor goat anti-mouse 568	Molecular Probes (A11004)	1:1000
Biotinylated goat anti-sheep	Vector (BA-6000)	1:100
Streptavidin-Alexa488	Molecular Probes (S11223)	1:500
Mouse anti-phospho-H2A.X	Millipore (05-636 clone JBW301)	1:500
Rabbit anti-SYCP3	Abcam (ab15093)	1:500
Mouse anti-Pick1	NeuroMab (L20/8)	1:250
Goat anti-Hrb/RIP	Santa Cruz (C-19)	1:500
Mouse anti-AP-1 subunit γ	BD Biosciences (610385)	1:5000
Mouse anti-AP-2 subunit μ	BD Biosciences (611350)	1:500
Rabbit anti-KIAA0319	custom-made	1:1000

Table 2.2: List of antibodies used in Chapter 5 for all experiments

2.4.7 Scanning electron microscopy

For scanning electron microscopy (Fischer et al. 2012), mature sperm cells were released from the epididymis of adult mice and spread onto coverslips before fixation in 2.5% glutaraldehyde (Polysciences) and 2% PFA (Sigma) in 0.2 M sodium cacodylate buffer (pH 7.4). A secondary fixation was performed with 1% osmium dioxide in PBS at 4°C before being dehydrated in a series of graded ethanol incubations. Drying was performed using hexamethyldisilazane and sputter coated with gold. Images were taken with a JEOL-6390 at 5 kV.

2.4.8 Transmission electron microscopy

To visualise the ultrastructure of mature and developing sperm, transmission electron microscopy was utilised (Graham & Orenstein 2007) and adult epididiymis and testis from adult mice were dissected as in Kotaja et al. (2004), cut into 1-2 mm^3 cubes and fixed for at least 24 h in 2.5% glutaraldehyde (Polysciences) and 2% PFA (Sigma) in 0.1 M 1,4 Piperazine bis(2-ethanosulfonic acid) (PIPES) buffer (pH 7.2, Sigma-Aldrich). Samples were washed in PIPES buffer with 50 mM glycine before a second fixation step with osmium tetroxide in PIPES for 1 h at 4°C and a tertiary fixation in 2% uranyl acetate for 2 h at 4°C. Tissue was then dehydrated in gradient steps of ethanol and embedded in epoxy-resin. Ultrathin sections were cut in an ultramicrotome and imaged using a Tecnai 12 (FEI) operated at 20 kV with a OneView CMOS camera (Gatan). Images were adjusted for brightness/contrast with GIMP Image Editor (GIMP Development Team).

2.4.9 GST pulldowns/*in vitro* binding assay

Glutathione S-transferase (GST) experiments used GST-fusion and control GST constructs already available in the Monaco laboratory (using pGEX-6P-3 vectors, Amersham).

These were used to produce purified proteins expressed in *Rosetta E. coli* in LB medium using 0.2 mM isopropyl-β-thiogalactoside for 3 h at 37°C. After harvesting, samples were sonicated for 30 s and incubated with Triton X-100 to a final concentration of 1%. Protein lysates were obtained either from human HeLa cells or adult mouse brain and testis tissue (similarly to the Western blot protocol above in section 2.1.4 but using Pierce IP lysis buffer; Thermo Fisher Scientific). These were pre-cleared with Glutathione S-transferase (GSH) beads (GE Healthcare). 50 μl of GSH beads was incubated with 1 ml bacterial supernatant containing GST proteins in bacterial lysis buffer for 1 h at 4°C for GST-GSH binding and washed in six centrifugation steps. Supernatants containing bound complexes were collected and resuspended in 70 μl of SDS sample buffer and loaded

on a 4-12% Bis-Tris gel electrophoresis with NuPage SDS running buffer (Life Technologies) before Coomassie Blue staining (Life Technologies, LC6060). Western blot was then conducted as above (section 2.1.4).

2.4.10 Mutation screening in human cases of globozoospermia

Patients were screened and samples collected in Prof Pierre Ray & Prof Christophe Arnoult's lab in the Institut Albert Bonniot in Grenoble, France, with samples derived from France and Tunisia. All patients gave their informed consent for the realisation of genetic analyses in view of gaining a genetic diagnosis for their condition. Cases of globozoospermia were defined as patients with more than 80% round-headed spermatozoa, with <5% morphologically normal spermatozoa. All cases had a normal 46, XY karyotype and none carried a deletion (either heterozygous or homozygous) in the *DPY19L2* gene. The analysis was carried out by MLPA as described in Coutton2012.

Genomic DNA was extracted using standard methods and samples were diluted into 8 ng/μl concentration, with 2 μl used for PCR amplification of individual exons of *KIAA0319L*, starting from exon 2 where the transcription start signal lies. Sanger sequencing followed general methods detailed in 2.1.3. Mutation screening was performed by analysis in CodonCode Aligner 6.0.2 (Codon Code Corporation) and used at least two different sequences for each exon (a forward and a reverse read). Primers used are detailed in Table A.2 in Appendix A.

3

Chapter 3

Contents

3.1 Introduction 78
3.2 Results 79
3.2.1 Generation of *AU040320* conditional KO mouse lines . 79
3.2.2 Generation of *Kiaa0319;AU040320* double KO mice . . 88
3.2.3 Normal cortical neurogenesis in *AU040320* and double KOs 89
3.2.4 Absence of *AU040320* does not affect cortical lamination 94
3.2.5 Normal cortical lamination in double KOs 96
3.2.6 Acute knockdown of *Kiaa0319* and *AU040320* does not affect radial migration 100
3.2.7 No changes in position of cortical interneurons following double *Kiaa0319;AU040320* KO 103
3.2.8 Unaltered lamination of hippocampus and cerebellum in the absence of *AU040320* alone and in conjunction with KIAA0319 104
3.3 Discussion 109
3.3.1 Discrepancy with shRNA experiments 109
3.3.2 The neuronal migration hypothesis of dyslexia susceptibility 114
3.4 Conclusion 119

3.1 Introduction

Previous experiments attempting to uncover the neurobiological functions of the dyslexia susceptibility genes *KIAA0319* and *KIAA0319L* have implicated the encoded proteins in neuronal migration processes. A number of studies have found that shRNA-mediated knockdown of *Kiaa0319* via *in utero* electroporation in the developing rat cortex can lead to an arrest in the migration of neuroblasts into the cortical plate and it often results in periventricular nodular heterotopias that persist into adulthood (Paracchini et al. 2006; Peschansky et al. 2010; Szalkowski et al. 2012; Szalkowski et al. 2013; Adler et al. 2013; Centanni et al. 2014a; Centanni et al. 2014b). Similar experiments targeting the homologous gene *Kiaa0319-Like* led to comparable abnormalities in the form of very large nodular periventricular heterotopias (Platt et al. 2013). Neuronal migration deficits have also been seen following knockdown of the rat homologs of two other dyslexia susceptibility genes, *DCDC2* and *DYX1C1* (Meng et al. 2005b; Burbridge et al. 2008; Adler et al. 2013). Combined with evidence from *postmortem* histopathological analyses and behavioural neuroimaging studies in humans, these findings added support to the hypothesis that abnormal neuronal migration is a cellular antecedent to dyslexia (Galaburda et al. 1985; Kaufmann & Galaburda 1989; Humphreys et al. 1990; Chang et al. 2005; Galaburda et al. 2006; Chang et al. 2007; Paracchini et al. 2007; Gabel et al. 2010; Ramus & Ahissar 2012; Kere 2014).

Characterisation of the KIAA0319 and AU040320 proteins and their functional domains provide support for their putative role in neuronal migration given that cell surface glycoproteins are well-known cell adhesion molecules which are key regulators of cell migration (Walsh & Doherty 1997; Sakisaka & Takai 2005; Takeuchi & O'Leary 2006; Ayala et al. 2007; Marín et al. 2010). As such, it is hypothesised that the extracellular region of the two proteins containing five PKD domains, previously linked to cell adhesion (Ibraghimov-Beskrovnaya et al. 2000), may mediate adhesion

between neurons and radial glial fibres during neuronal migration (Paracchini et al. 2006; Velayos-Baeza et al. 2008; Poon et al. 2011b).

With the goal of exploring the putative function of *Kiaa0319* in neuronal migration in more detail, our laboratories have generated transgenic mouse lines carrying a non-functional copy of *Kiaa0319* and our neuroanatomical analyses have revealed that partial or total reduction of KIAA0319 protein does not impair neuronal migration (Martinez-Garay et al. 2017). Robustness against perturbations such as null mutations in gene KOs may be a universal property of biological systems and it is often triggered by functionally overlapping paralogous genes (Ohno 1970; Edelman & Gally 2001; Gu 2003; Kitano 2004; Kafri et al. 2009; Su et al. 2014). In fact, such gene duplicates have been found to be more commonly involved in human genetic disorders than singleton genes (Chen et al. 2013; Dickerson & Robertson 2012). Given *AU040320* exhibits a similar expression pattern in the developing rodent brain, shares a number of protein features with the KIAA0319 protein and has also been implicated in neuronal migration (Diez-Roux et al. 2011; Poon et al. 2011b; Platt et al. 2013), I hypothesised that compensation by AU040320 protein is a likely explanation for the normal cortical migration and lamination observed in *Kiaa0319* KO mice.

Based on this, this chapter aims to investigate the putative functions of both KIAA0319 and AU040320 in neuronal migration and in brain development more generally by examining constitutive and conditional KO mouse lines targeting *AU040320* alone, as well as double *Kiaa0319;AU040320* KO mutants.

3.2 Results

3.2.1 Generation of *AU040320* conditional KO mouse lines

Transgenic mouse lines were generated from embryonic stem (ES) cell clones (EPD0726-2-H05 and EPD0726-2-F06; Pettitt et al. (2009)) targeted at the mouse homologous gene *AU040320* or *Kiaa0319-Like* (I shall refer to it as *AU040320* to clearly distinguish it from *Kiaa0319*) obtained from the European Conditional Mouse

Mutagenesis Program (EUCOMM, www.eucomm.org) under the International Knockout Mouse Consortium (Project ID 27003).

The *AU040320* locus in these cells was modified by inserting a reporter-tagged transgene to generate a 'Knock-Out First' (KO1; Skarnes et al. 2011) conditional allele (C57BL/6N-$AU040320^{tm1a(EUCOMM)Wtsi}$ or AU^{ko1}; Fig. 3.1A) targeting exon 3 by gene trapping (with respect to the ENSMUST00000102608 transcript of *AU040320*). The KO1 strategy permits bypassing potential early lethality by utilising the '3 loxP' system to generate conditional KO animals. The inserted KO1 transgene cassette contains a sequence of sites including a splice acceptor (SA), internal ribosome entry site (IRES), *lacZ* reporter gene, a poly-adenylation site to signal termination of transcription, the β-actin promoter and a *Neomycin* resistance gene; the cassette also contains two FRT (short flippase recognition target) and three loxP (locus of X-over P1) sites (Fig. 3.1A).

The Transgenic Core at the Wellcome Trust Centre for Human Genetics, University of Oxford, performed microinjections of these modified ES cells (from an agouti C57BL/6N strain) into blastocysts obtained from a C57BL/6J mating and transferred to 2.5 day pseudo-pregnant CD1 foster females. These injections were performed with ES cell clone EPD0726-2-H05 using three different foster females, resulting in 10 pups being born, whilst injections using clone EPD0726-2-F06 into two foster female produced 11 pups (Table 3.1). All females pups were discarded given that ES cells were XY and transmission of mutation would be highly unlikely. From ES clone EPD0726-2-H05, three males were found to be chimeric based on coat colour (mutant mice should have mixed agouti-black coats) and had 10%, 75% and 30% contribution from injected ES cells. The first (10% chimeric) male was discarded due to low chimerism and germline transmission of the targeted mutation was checked by mating and genotyping PCRs for the remaining two but could not be confirmed. From the second clone, EPD0726-2-F06, two of the pups were male and had ~95% and ~80% contribution from ES cells to coat colour (Table 3.1). These two animals were crossed with C57BL6/J females and germline transmission

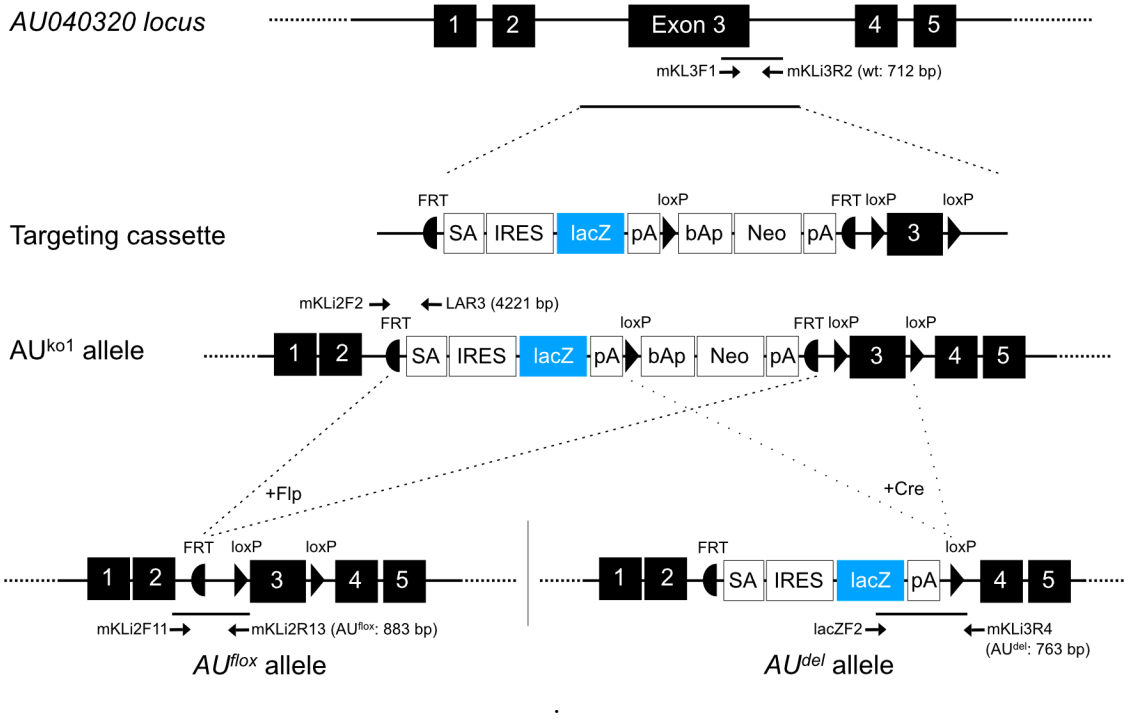


Figure 3.1: Generation of *AU040320* mouse lines: *AU040320 locus*. (A) Schematic representation of the *AU040320 locus*, the targeting cassette and the different alleles obtained. Region of wild-type allele replaced by the targeting cassette after homologous recombination is indicated by a horizontal line under exon 3; exons are shown as black boxes; primers used for genotyping PCRs are indicated with arrows, and the PCR name and product size indicated shown in brackets.

was found in both of them by the presence of F1 pups with agouti coat colour and/or positive result in PCRs specific for the KO1 allele. These F1 animals have a mixed C57BL/6J;C57BL/6N background. From this point onwards, all back-crosses to maintain this and the other alleles described were done with C57BL6/J mice.

	EPD0726_2_H05			**EPD0726_2_F06**	
	♀1	♀2	♀3	♀1	♀2
Embryos implanted	27	22	22	18	10
Pups born	4	6	0	6	5
Pups weaned	4	6	0	6	5
♂ chimeras	1 (10%)	2 (75%, 30%)	-	1 (95%)	1 (80%)
♀ chimeras	1(80%)	1 (50%)	-	1 (70%)	1 (40%)

Table 3.1: ES cells injections and chimeras obtained per ES cell clone

Although EUCOMM performs quality control tests on clones, a series of PCR

reactions were performed to verify the presence of the full targeting construct in these two chimeric males as well as the correct integration of the full region between both homology arms in the *AU040320 locus*. The combinations of primers used to cover the length of the KO1 allele are detailed in Fig. 3.3A – primers are listed in Table A.1 in Appendix A. Pups obtained after breeding of the '95% chimera' were positive for a number of PCRs covering different sections of the KO1 allele and its flanking regions (Fig. 3.3A), suggesting pups contained the cassette integrated into the *AU040320 locus* as expected.

The sequence of the inserted fragment was also checked by Sanger sequencing of some of these PCR products, with only one minor change in relation to the expected sequence: the insertion of an A at the *IRES* region, which does not affect any of the critical regions. The full sequence of the KO1 cassette in the relevant region of the *AU040320* locus is included in Appendix A in section A.2. The correct integration of the targeting cassette in the *AU040320 locus* was further confirmed by long-range PCR to amplify a 4.2 kb fragment of the AU^{ko1} allele using a primer outside the homology arm of the targeting cassette in intron 2 and another primer specific for this cassette to cover the entire 5'-region of homologous recombination (Fig. 3.2A). On the other hand, pups derived from the '80% chimera' were found to carry only a small fragment of the transfected construct, more specifically, an *IRES-lacZ* sequence. None of the other regions could be detected by PCR (Fig. 3.3B). This is likely to result from some degree of heterogeneity within the ES cell clone which might have contained some cells with this 'partial insert'. These cells may have originated after a partial integration of the transfected construct, possibly at a random genomic site, or after a complex recombination event in a cell during the expansion of the F06 clone; no further investigations were performed on this issue. Mice derived from this male were therefore culled.

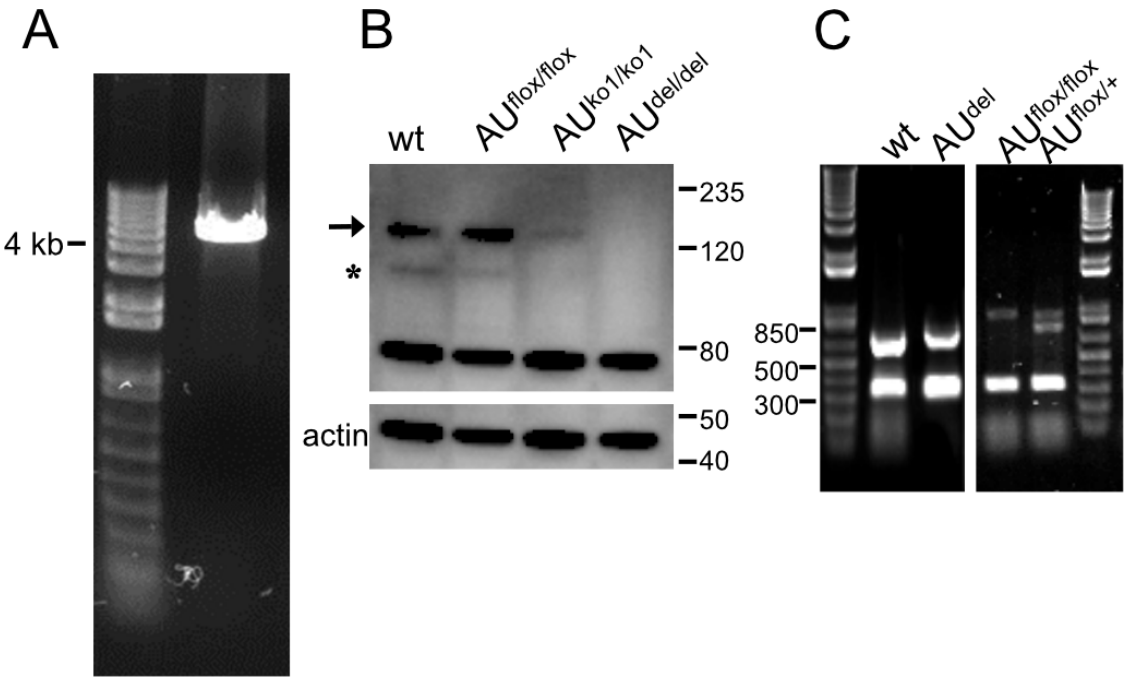


Figure 3.2: Generation of *AU040320* mouse lines: Western blot and PCRs. (A) Long-range PCR product used to confirm correct integration of targeting construct in the *AU040320*-KO1 using a forward primer upstream the 5' homology arm present in the targeting cassette (mKLi2F2, in A) and a reverse primer specific for the targeting cassette (LAR3). (B) Western blot using a custom-made polyclonal antibody with brain lysates from P21 animals homozygous for the different alleles generated. Normal protein levels at the target band (~150 kDa, indicated by an arrow) are detected for *AU*-flox, residual protein is seen in *AU*-KO1 and no protein product for the KO allele *AU*-del; some unspecific bands are also detected, and the main one is indicated by an asterisk. Bottom panel shows anti-alpha-actin used as loading control. (C) Example of PCRs used to genotype the wildtype, floxed and del alleles corresponding to the primer combinations shown in Fig.1A; bottom band (324bp) in all lanes represents an internal control.



Figure 3.3: Schematic representation of PCR approach for analysis of *AU040320* transgenic alleles. (A) Details of PCR fragments obtained and used for Sanger sequencing to confirm the sequence of the trapping cassette and its integration into the *AU040320 locus* in animals generated from '95% chimera' obtained from ES clone F06; regions covered by each fragment are schematically represented in black bars. (B) Regions of the trapping cassette detected (black) and not detected (grey) in animals derived from the '80% chimera'. (C) PCR fragment used to sequence the *AU040320*-flox allele. (D) Fragment used to confirm sequence of the *AU040320*-del allele. Length of shown regions and PCR fragments not to scale.

Animals homozygous for the AU^{ko1} allele were found to be viable and with no obvious differences compared to wildtype and heterozygous littermates. However, all homozygous males AU^{ko1} were found to be infertile (described in Chapter 5), with females showing no signs of impairment in fertility.

The AU^{ko1} allele is predicted to generate a transcript that would lead to loss-of-function via the new splicing driven by the acceptor site in the KO1 cassette inserted in intron 2 which would result in a very short, truncated protein (p.D48GfsX102) containing only the signal peptide sequence. Western blotting analyses of P21 brain lysates show that this AU^{ko1} allele leads to a clear reduction of AU040320 protein but traces of residual expression are observed (Fig. 3.2B), possibly due to a residual normal splicing that skips the splicing acceptor site on the trapping cassette.

To ensure a total elimination of normal protein production, a global KO allele line lacking the targeted exon 3 was obtained by crossing a male heterozygous for the AU^{ko1} with a Sox2-Cre transgenic female (B6.Cg-Tg(Sox2-Cre)1Amc) (Hayashi et al. 2002; Vincent & Robertson 2003). Sox2-Cre mice express Cre recombinase under the control of the mouse SRY-box containing gene 2 (*Sox2*) promoter in epiblast cells at embryonic day 6.5 to induce recombination and create a null allele; however, a female is required to ensure transgene activity in all progeny, irrespective of Sox2-Cre transmission as its expression is active in the female germline – if a male is used, recombination only takes place in embryos that inherit the transgene, not in all of them (Hayashi et al. 2002). Thus, crossing Sox2-Cre females with the AU^{ko1} male will trigger the excision of *loxP*-flanked sequences (here, exon 3 and the Neomycin-resistance gene) to produce a null allele, denoted here as AU^{del} (C57BL/6J-$AU040320^{tm1b(EUCOMM)Wtsi}$; Skarnes et al. (2011)). These mice were then back-crossed onto C57BL/6J animals for at least 8 generations before AU^{del} animals were used for experimentation. In the interest of simplicity and clarity, mice heterozygous and homozygous for this allele are referred here as *AU040320* +/- (or AU+/-) and *AU040320* -/- (or AU -/-), respectively. The main transcript derived from this allele is expected to be the same as that of the AU^{ko1} allele since

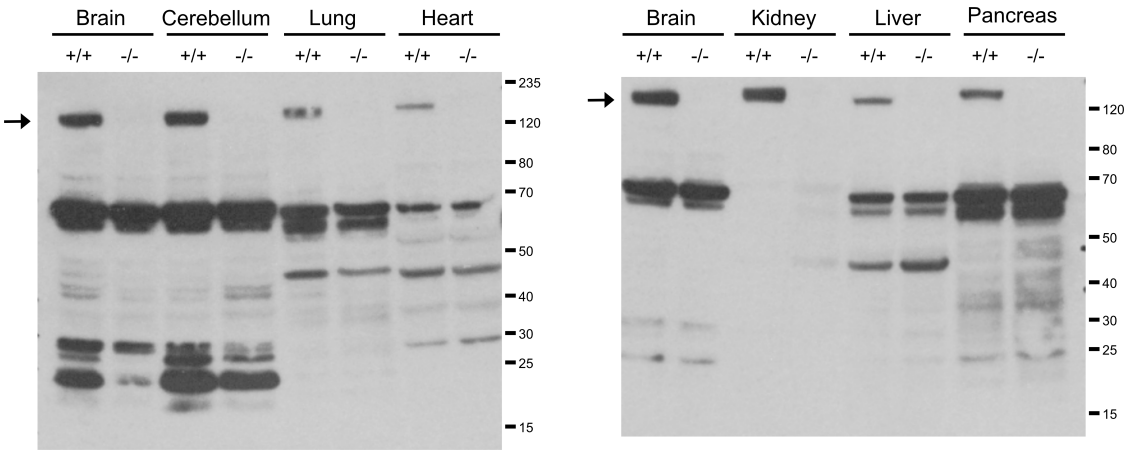


Figure 3.4: Western blot of multiple tissues to detect AU040320 protein in wildtype (+/+) and $AU^{del/del}$ KO (-/-) animals shows the protein is present throughout the mouse body. KO animals exhibit the expected absence of the target protein at ~150 kDa (indicated by arrow). The used custom-made antibody also detects a number of unspecific bands, both in WT and in KO lysates.

the trapping cassette is conserved. However, it bypasses potential residual protein as seen with the KO1 allele as any transcripts would lack exon 3 in this new allele. Removal of this exon also involves a shift in the reading frame which leads to an early stop codon: the effect would be a truncated protein (p.D48GfsX14) similarly as in the KO1 allele above, or total absence of this protein after degradation of the transcript via nonsense-mediated mRNA decay (Brogna & Wen 2009). Western blots of brain lysates from *AU040320* -/- mice indicate this allele leads to a complete elimination of AU040320 protein (Fig. 3.2B). I also verified expression of *AU040320* in various other tissues in mice, alongside its elimination in the *AU040320* KOs (Fig. 3.4).

Mice carrying the AU^{del} allele, similarly to the AU^{ko1} mutants, were viable and with no apparent differences compared to littermates. Genotyping of litters from intercrosses of $AU^{del/+}$ animals for presence of the AU^{del} allele revealed positive fragments (Fig. 3.2C) and genotype ratios similar to the expected 25:50:25 (%) Mendelian rates: Table 3.2 shows the number of pups born (and percentages) for pups born from *AU040320* +/- matings. Body weight was measured for early

postnatal animals and no differences were found across genotypes (Table 3.3; for P2, $n = 30$, $p = 0.61$, $F = 0.29$; for P10, $n = 25$, $p = 0.41$, $F = 0.71$). In addition, the overall brain organisation and morphology of these animals is normal, as revealed by Nissl-stained sections (Fig. 3.5A-C). Male infertility persisted for homozygous male mutants (*AU040320* -/-).

Genotype	No. of mice (%)
AU +/+	39 (31%)
AU +/-	49 (38%)
AU -/-	39 (31%)
Total	127 (100%)

Table 3.2: Genotype analysis of progeny from crosses of *AU040320* +/- mice.

	Body weight (g)	
Genotype	P2	P10
AU +/+	2.01 (± .10)	5.41 (± .35)
AU +/-	1.76 (± .08)	5.18 (± .32)
AU -/-	1.81 (± .05)	5.58 (± .22)

Table 3.3: Weight of AU040320 mutants during early development.

In addition to this, constitutive AU^{del} null allele, animals carrying a "floxed" allele AU^{flox} (C57BL/6J-$AU040320^{tm1c(EUCOMM)Wtsi}$) for conditional KO potential were obtained by crossing the same $AU^{ko1/+}$ male mentioned above with a female carrying a *Flp* recombinase transgene (B6.Cg-Tg(ACTFLPe)9205Dym/J; Rodríguez et al. (2000)). Expression of FLP induces recombination between the two FRT sites to remove the *IRES;lacZ* trapping cassette and the *Neo* resistance gene. The result is an allele expected to behave as the wild type allele but where exon 3 is flanked by two loxP sites (as shown above in Fig. 3.1A). Western blots of brain lysates for homozygous floxed mice $AU^{flox/flox}$ demonstrated protein levels equivalent to wildtypes as expected (Fig. 3.1C). $AU^{flox/flox}$ animals were used for spatio-temporally controlled, *in vivo*, KO using Cre-recombinase via *in utero* electroporation experiments which induces excision of the critical exon 3 to produce a different type of 'null' allele AU^{null} ($AU040320^{tm1d(EUCOMM)Wtsi}$). The sequences

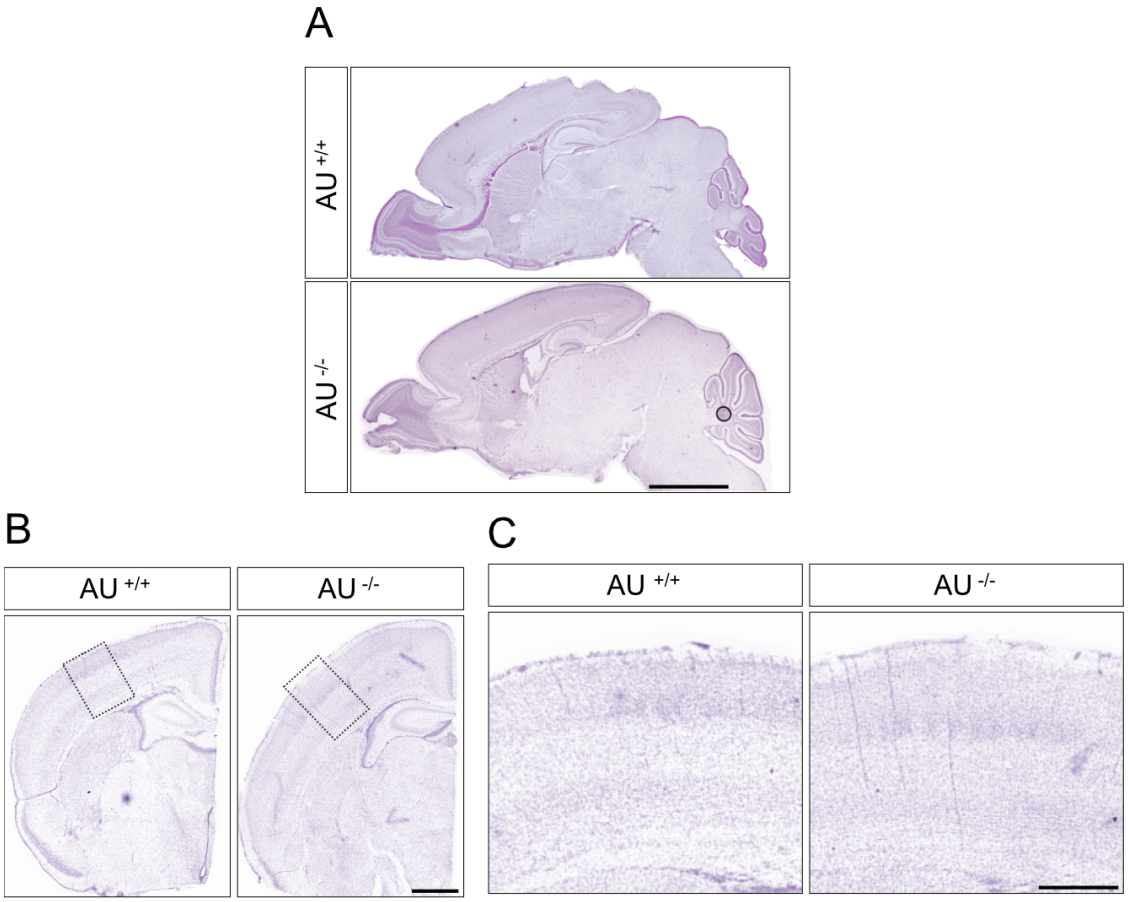


Figure 3.5: Generation of *AU040320* mouse lines: Nissl stainings. (A-C) Cresyl-violet stained sections of wildtype and AU-/- brains show no gross morphological defects resulting from the *AU040320* deletion. Scale bars: 500 μm (E), 50 μm (F), 200 μm (G).

of the AU^{del} and AU^{flox} alleles were confirmed by PCR and Sanger sequencing and contained no changes from the expected sequences (data not shown).

Given the residual presence of full-length AU040320 protein in the AU^{ko1} allele, the constitutive KO AU^{del} line was selected for analyses of effect of loss-of-function mutations in *AU040320* and floxed AU^{flox} mice were reserved for conditional KO experiments.

3.2.2 Generation of *Kiaa0319;AU040320* double KO mice

Besides the characterisation of mice targeted at the *AU040320* locus reported here, I also investigated double transgenic mice targeted both at *AU040320* and *Kiaa0319*. The mouse lines obtained for this purpose were: (a) the double KO (dKO), carrying

the tm1b allele (AU^{del} and KA^{del}); and (b) the double floxed line with the tm1c (AU^{flox} and KA^{flox}) alleles, respectively. For the dKO line, the first mating was between a $KA^{del/del}$ female and a $AU^{del/+}$ male. A second step involved backcrossing of F1 double heterozygous ($K^{del/+}$; $AU^{del/+}$) with homozygous $K^{del/del}$ animals (both male x female and female x male variations used). This led to the generation of $K^{del/del}$; $AU^{del/+}$ mice. Finally, inter-crossing between these animals was used to obtain [$K^{del/del}$;$AU^{+/+}$, $K^{del/del}$;$AU^{del/+}$ and $K^{del/del}$;$AU^{del/del}$ animals. A similar breeding protocol was followed to obtain the double floxed line.

3.2.3 Normal cortical neurogenesis in *AU040320* and double KOs

Previous work from the Monaco laboratory has revealed the KIAA0319 and KIAA0319L proteins have a number of features suggesting a potential role in signalling pathways and which closely resembles those of Notch receptors (Levecque et al. 2009; Velayos-Baeza et al. 2010). Given Notch signalling is a key regulator of neurogenesis (Ables et al. 2011) and both *Kiaa0319* and *AU040320* are expressed in the VZ of the developing neocortex in humans and rodents (Paracchini et al. 2006; Diez-Roux et al. 2011; Miller et al. 2014), it is possible that these proteins may play a role in cell proliferation and the emergence of neuronal progenitors.

To investigate this, I first analysed the embryonic brains of wildtype, heterozygous and homozygous *AU040320* KO mice at E15 when upper layer neurons are being generated as well as at E18 during the last wave of neurogenesis and the start of astrogliogenesis. Cycling and mitotic cells were immunostained with antibodies against Ki67 (antigen KI-67) and ph3 (phospho-histone H3), respectively, and the number of cells within 100 μm of the dorsal cortical wall was quantified based on their position within the VZ or elsewhere (non-VZ). The majority of cells positive for ph3 and ki67 were located in the VZ in the samples examined and no differences between these two cell populations were found in brains lacking AU040320 when compared to wildtype controls at E15 (Fig. 3.6A-C) nor at E18 (Fig. 3.6D-F). Similar results have been found for *Kiaa0319* KO mice (Martinez-Garay et al. 2017).

Given the possibility of functional redundancy and compensation between KIAA0319 and AU040320, I then applied the same methods to investigate potential impairment in cell proliferation in dKOs at these two developmental stages. Statistical analyses using one-way ANOVAs revealed the number of cycling and mitotic cells in these germinative zones of the neocortex of dKO mice was also unaltered (Fig. 3.6G-L).

Next, I examined whether loss of functional copies of these genes could specifically affect the neuronal progenitor pools by labelling radial glia progenitors with antibodies against Pax6 (paired box protein 6) and intermediate progenitors with Tbr2 (T-box brain protein 2/Eomes). First, *AU040320* mutants were examined and progenitor cells appeared in the germinative areas as expected, with Pax6+ cells in mutant brains being found primarily in the first two bins of the E15 cortex (roughly corresponding to the VZ; Fig. 3.7A-B) whilst Tbr2+ cells were found predominantly in the region immediately above it (bins 2-5; Fig. 3.7D-E). Cell quantification revealed no differences between the three genotypes in the number of cells for each of the ten bins dividing the cortical wall (Fig. 3.7C, F). Similar analyses were performed in *AU040320*-deficient mice at E18 which revealed neither Pax6+ or Tbr2+ cell populations displayed alterations when compared to wildtypes (Fig. 3.7G-L). To assess potential compensatory interactions in neurogenesis between AU040320 and KIAA0319 during development, I then examined these two progenitor populations in the neocortex of dKO mutants. Both Pax6+ and Tbr2+ cells displayed a normal distribution along the germinative regions of the dorsal cortex of mutant mice and quantifications revealed there were no differences between dKOs and wildtype controls at E15 or E18 (Fig. 3.8A-L). These results indicate that absence of AU040320 alone or in conjunction with KIAA0319 does not affect cortical neurogenesis.

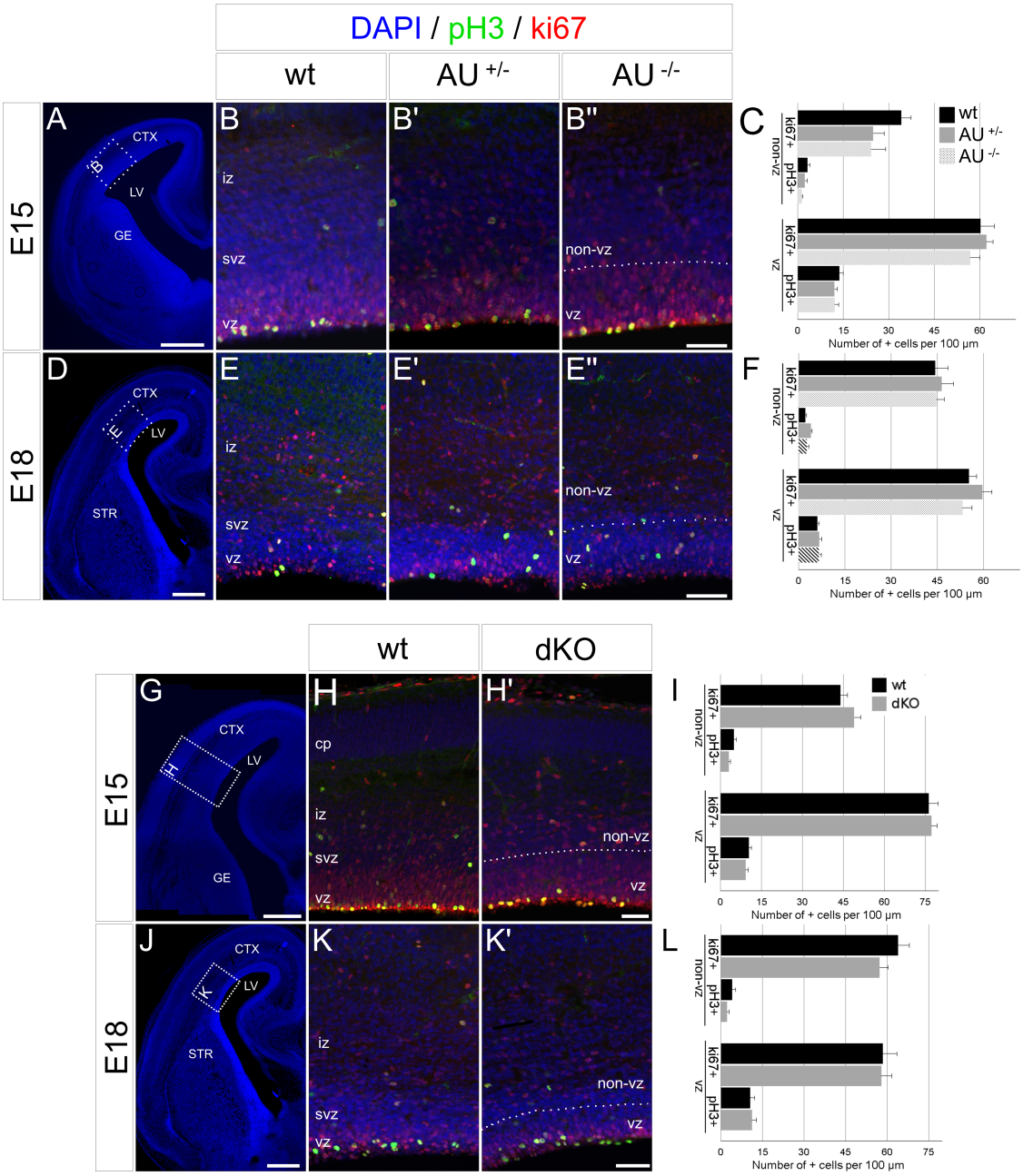


Figure 3.6: Normal cell division profiles in *AU040320* and double KOs. DAPI panels show regions selected for analyses (A, D, G, J). Cycling cells labelled with ki67 (red) and cells in M-phase with ph3 (green) form similar bands at the VZ at E15 (B, H) and E18 (E, K). Quantifications of cell number within VZ and non-VZ regions show no differences across genotypes at either age for *AU040320* mutants (C, F) or dKOs (I, L) (One-way ANOVAs, $n = 3, p > 0.05$). Data shown as mean ± SEM. CTX, cortex; LV, lateral ventricle; GE, ganglionic eminences; STR, striatum; cp, cortical plate; iz, intermediate zone; svz, subventricular zone; vz, ventricular zone. Scale bars: 400 μm (A, D, G, J); 50 μm (B, E, H, K).

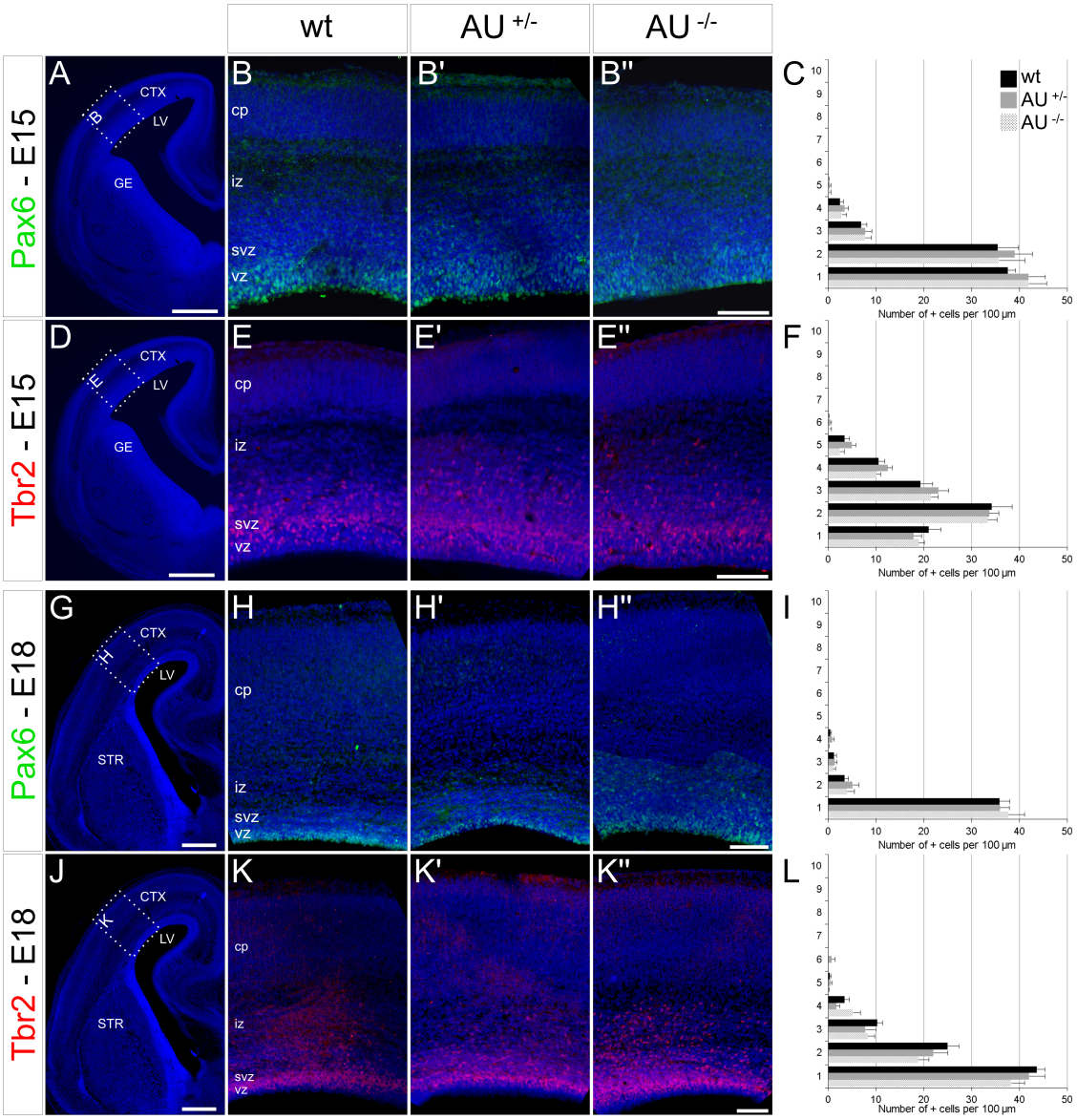


Figure 3.7: Radial glial and intermediate progenitors are unaffected in *AU040320* KO. DAPI panels show regions selected for analysis at E15 and E18 (A, D, G, J). Representative images of the cortices of wildtype (wt), heterozygous (+/-) and homozygous KOs (-/-) show mutants exhibit a similar composition of Pax6+ radial glial cells clustering primarily in the VZ at E15 and E18 (B, H). Mutants also exhibit a normal population of Tbr2+ intermediate progenitors in the germinative region of the cortex when compared to controls at both stages (E, K). Quantification of cell number dividing cortex into ten equal bins spanning 100 μm is shown for all ages and cell populations (C, F, I, L) and indicate no significant differences in any of the conditions (One-way ANOVAs, $n = 3, p > 0.05$). Data shown as mean ± SEM. CTX, cortex; LV, lateral ventricle; GE, ganglionic eminences; STR, striatum; cp, cortical plate; iz, intermediate zone; svz, subventricular zone; vz, ventricular zone. Scale bars: 400 μm (A, D, G, J); 100 μm (B, E, H, K).

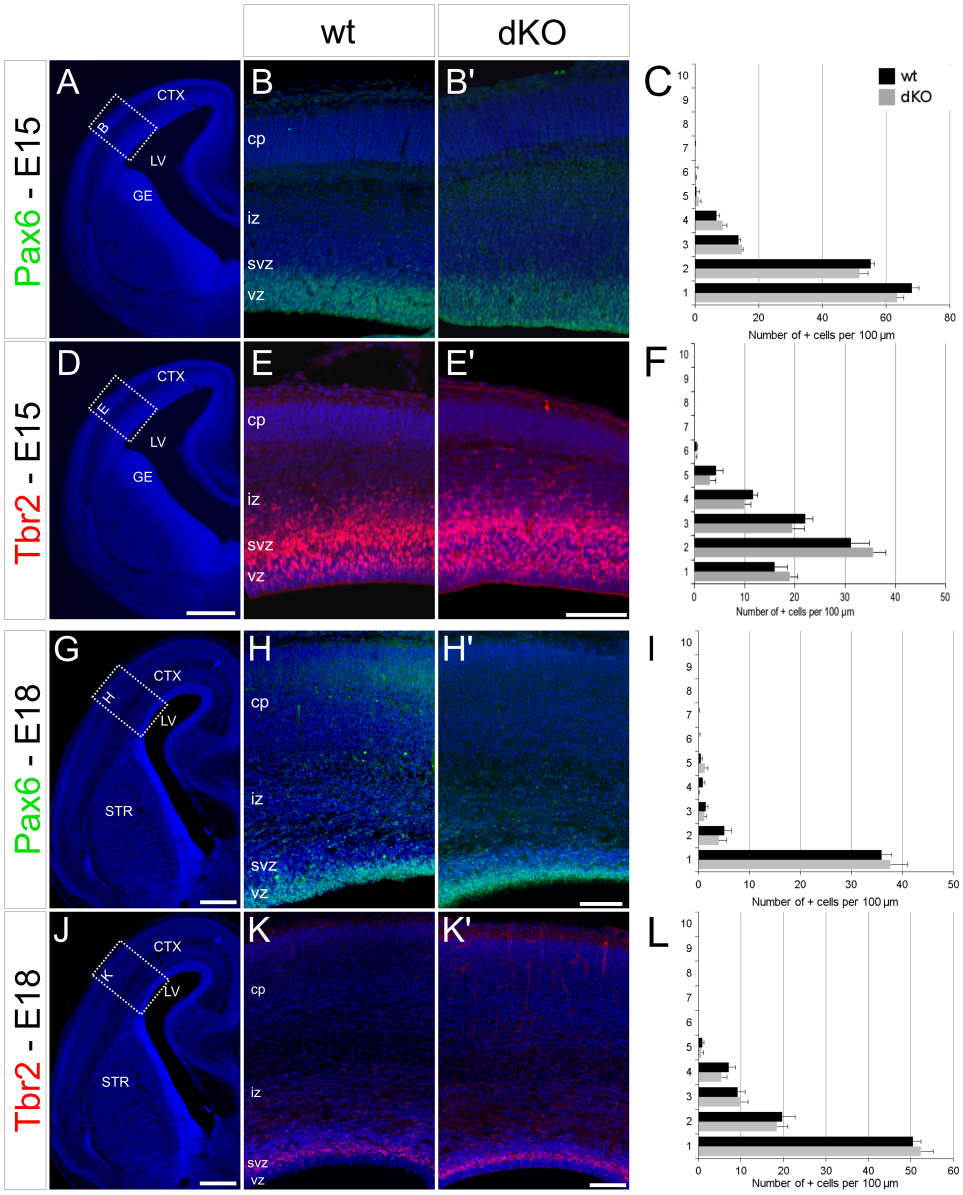


Figure 3.8: Normal progenitor pool in the developing cortex of dKO mice. DAPI panels show regions selected for analysis at E15 and E18 (A, D, G, J). Distribution of Pax6+ radial glial cells and Tbr2+ intermediate progenitors appear similar in dKO and wildtype (wt) animals at both E15 and E18, with Pax6+ cells occupying the region immediately adjacent to the lateral ventricle (B, H) and Tbr2+ progenitors forming a band of cells centered primarily in the SVZ (E, K). Graphs showing quantification of cell number per bin are also shown (C, F, I, L) and results revealed no differences between genotypes for any of the conditions (One-way ANOVAs, $n = 3, p > 0.05$). Data shown as mean ± SEM. CTX, cortex; LV, lateral ventricle; GE, ganglionic eminences; STR, striatum; cp, cortical plate; iz, intermediate zone; svz, subventricular zone; vz, ventricular zone. Scale bars: 400 μm (A, D, G, J); 100 μm (B, E, H, K).

3.2.4 Absence of *AU040320* does not affect cortical lamination

Previous work has reported that knockdown of the *KIAA0319L* rat homologous gene during cortical development using shRNA *in utero* transfection can lead to problems in radial migration resulting in peri-ventricular heterotopias (Platt et al. 2013). This would suggest that the AU040320 protein is necessary for the normal migration of cortical neurons from the embryonic VZ to the CP. To investigate this in detail, I first examined the laminar organisation of pyramidal neurons in the cortices of *AU040320*-deficient mice using immunohistochemistry. Cells destined to the layers V-VI of the neocortex were labelled with an antibody against Ctip2 (Bcl11, B-cell lymphoma/leukeamia 11B) and those destined to layers II-IV with one against Cux1 (Cut Like Homeobox 1, Molyneaux et al. 2007). If *AU040320* plays a role in neuronal migration, the spatial distribution of these cell populations would be affected in the absence of the protein.

First, the distribution of cells across the length of the cortical wall was examined at early postnatal stages: at P2 when neurons destined to deep cortical layers have settled in their final position and upper layer cells are still migrating and at P10 when migration is fully complete (Fig. 3.9A-B, E-F). Quantification of the percentage of cells per bin showed no differences between wildtype, *AU040320* +/- and *AU040320* -/- brains (Fig. 3.11C-D, G-H). However, it is possible that absence of AU040320 causes simply a delay in the migration of these cells despite their normal final position. To verity this, I examined the distribution of migrating cells per bin at E18 when Ctip2+ cells are mostly settled and Cux1+ have only started to arrive in the CP, and also at E15 when only deep layer cells have occupied the CP (Fig. 3.11I-J, M-N). At both stages, the percentage of cells in each of the bins did not differ across the three genotypes (Fig. 3.9K-L, O). These results indicate that partial reduction of AU040320 protein levels or its total elimination does not affect the laminar patterning of the neocortex.

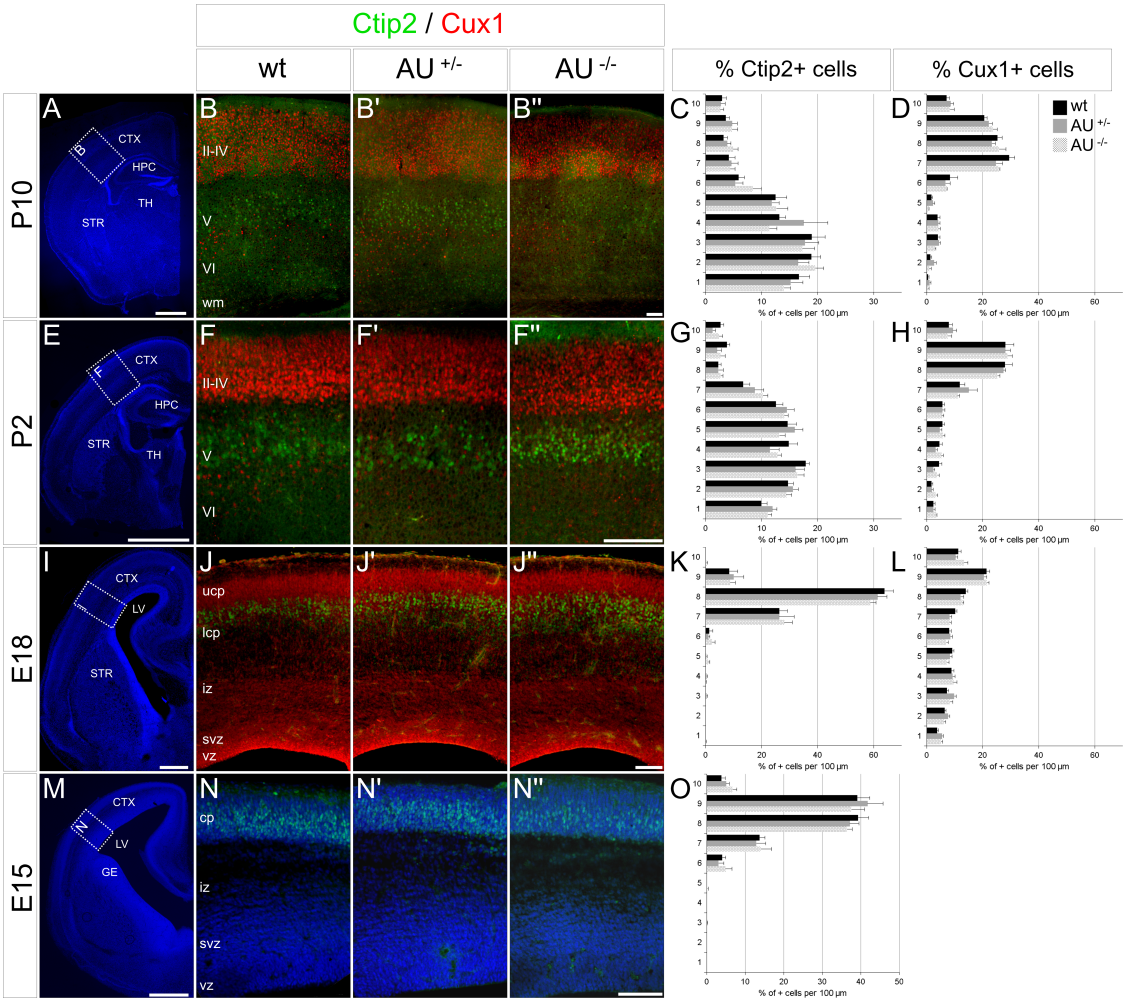


Figure 3.9: Normal cortical lamination in *AU040320* KOs throughout development. DAPI panels (A, E, I, M) show somatosensory cortex regions selected for analysis. At P10 (A) and P2 (E), Cux1+ cells (red) equally occupy layers II-IV and Ctip2+ cells (green) occupy layers V-VI in wildtype (wt), *AU040320* +/- and *AU040320* -/- sections (B, F). At E18 (I, J), Ctip2 is strongly expressed in the lower cortical plate (lcp), whilst Cux1+ cells are seen in the upper cortical plate (upc), migrating through the intermediate zone (iz) and in germinative areas (svz, vz). At E15 (M, N), Ctip2+ cells occupy the cortical plate in a similar arrangement across genotypes (N). Quantification of Ctip2+ (C, G, K, O) and Cux1+ (D, H, L) cells reveal no differences in the percentage of cells occupying each of the ten bins (One-way ANOVAs, $n = 3, p > 0.05$). Data shown as mean ± SEM. CTX, cortex; TH, thalamus; HPC, hippocampus; LV, lateral ventricle; GE, ganglionic eminences; STR, striatum; cp, cortical plate, lower (lcp) and upper (ucp); iz, intermediate zone; svz, subventricular zone; vz, ventricular zone; wm, white matter. Scale bars: 1000 μm (A, E); 400 μm (I, M); 75 μm (B, F, J, N).

3.2.5 Normal cortical lamination in double KOs

The data above are in contrast with the previous reports linking AU040320 and neuronal migration in rats (Platt et al. 2013) and it parallels previous work from the laboratory showing a similar contrast with respect to *Kiaa0319* (Paracchini et al. 2006; Peschansky et al. 2010; Adler et al. 2013; Martinez-Garay et al. 2017). Given gene duplicates are well-known sources of functional compensation (Edelman & Gally 2001; Kitano 2004), it is possible that the observed discrepancy is due to (partially) overlapping functions of KIAA0319 and AU040320 that may compensate for the absence of one of these proteins in the single KO experiments.

To examine this possibility, I first inspected Nissl-stained serial sections spanning the rostro-caudal length of double mutants lacking both KIAA0319 and AU40320 as well as wildtype brains to examine potential alterations in cortical organisation. Histological analyses revealed no major anatomical abnormalities caused by the combined absence of both proteins (Fig. 3.10A-B). Also, molecular layer (type 2) ectopias or periventricular heterotopias were not detected in the cortices of the mutant or wildtype adult brains examined in serial sections (n=3; Fig. 3.10) as well as in the other analyses of lamination over development (Fig. 3.9 and Fig. 3.11), despite their common occurrence in many inbred wildtype samples generally (Ramos et al. 2008).

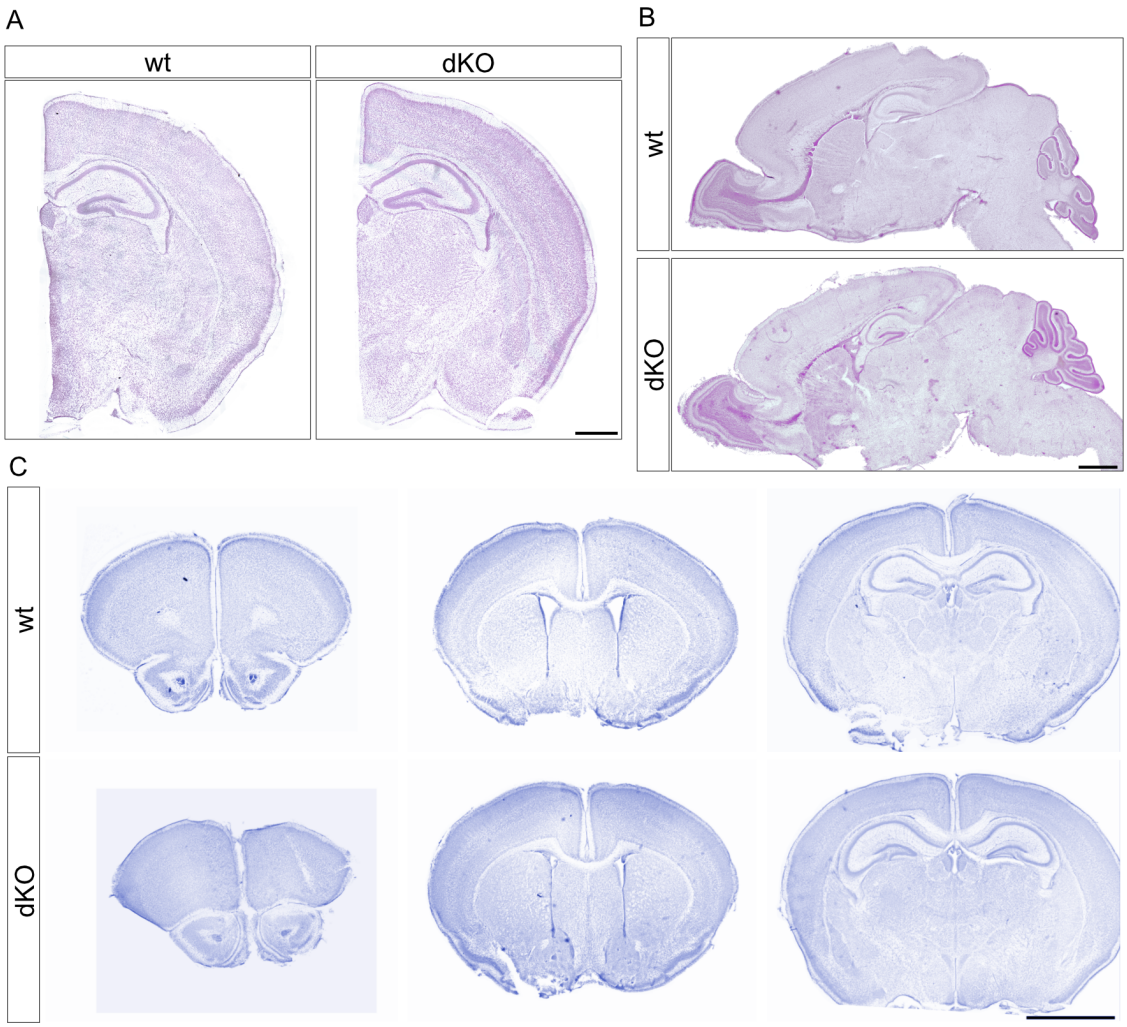


Figure 3.10: Double KOs exhibit normal overall brain anatomy and no cortical ectopias. (A-B) Coronal and sagital P10 sections stained with Cresyl violet show dKOs have no major neuroanatomical defects. (C) Coronal sections of wildtype and dKO P10 brains used in serial section analyses (every third section at 50 μm) examining presence of cortical ectopias ($n = 3$ per genotype). Scale bars: 500 μm (A, C); 200 μm (B).

Following this, I investigated putative deficits in cortical lamination in dKOs by immunohistochemistry, similarly to the experiments for *AU040320* described above. Immunolabelling in sections of early postnatal stages (P2 and P10) revealed both infra- and supra-granular layers (Ctip2+ and Cux1+, respectively) exhibited comparable distribution between dKOs and wildtypes (Fig 3.9B, F). Quantifying the percentage of cells per bin along the cortical wall confirmed there were no differences between the two genotypes (Fig. 3.9C-D, G-H).

To exclude the possibility of a developmental delay, I labelled migrating projection neurons at E18 with Ctip2 and Cux1 antibodies and results revealed lower layer neurons in dKOs had occupied the CP without alterations and migration of upper layer neurons (Cux1+) progressed similarly unaffected (Fig. 3.11I-L). In addition, the subplate, one of the first neuronal populations to migrate and occupy the developing neocortex, exhibited no apparent differences at P10 as indicated by immunostaining with the subplate-specific marker Ctgf (connective tissue growth factor) alongside the pan-neuronal marker NeuN (Fig. 3.12). These images also clearly demonstrate that mutant brains exhibit the expected formation of barrel fields in layer IV of the somatosensory cortex, indicating no gross defects of ingrowth of thalamocortical fibres (Fig. 3.12). Together, these results suggest that systemic KO of both *Kiaa0319* and *AU040320* does not alter lamination of the neocortex.

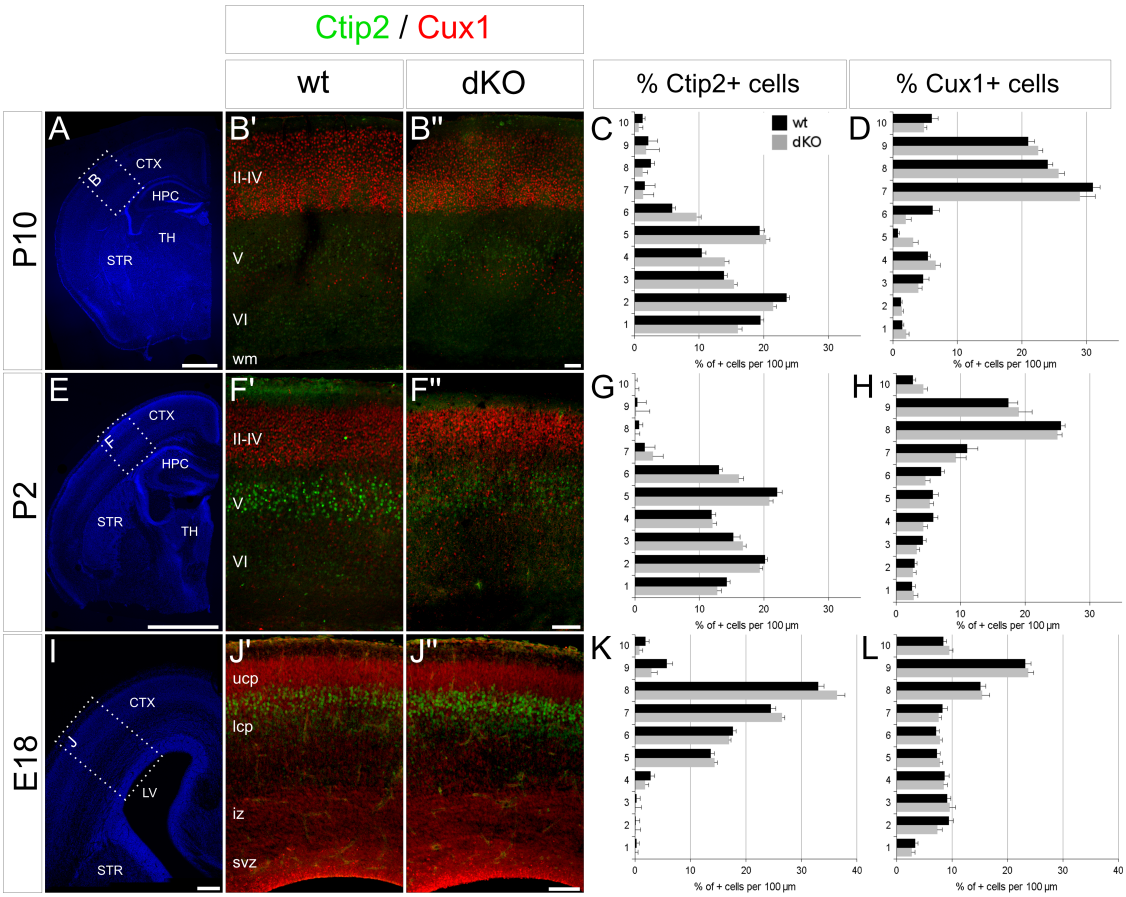


Figure 3.11: Coronal sections including somatosensory cortex selected for analysis (A, E, I). Representative images of P10 (B) and P2 (F) brains, show Cux1+ (red) and Ctip2+ (green) cells occupy layers II-IV and V-VI, respectively, exhibiting a comparable pattern between wildtypes (B', F') and dKOs (B", F"). At E18, dKOs (J") show Ctip2+ cells occupying the lower cortical plate (lcp) similarly to wildtypes (J') and Cux1+ cells are seen in upper cortical plate (ucp), migrating through intermediate zone and svz/vz. Graphs show percentage of labelled cells for each bin with no significant differences between controls and dKOs (C-D, G-H, K-L; one-way ANOVAs, $n = 3, p > 0.05$). Data shown as mean + SEM. CTX, cortex; TH, thalamus; HPC, hippocampus; LV, lateral ventricle; GE, ganglionic eminences; STR, striatum; cp, cortical plate, lower (lcp) and upper (ucp); iz, intermediate zone; svz, subventricular zone; vz, ventricular zone; wm, white matter. Scale bars: 1000 μm (A, E); 200 μm (I); 100 μm (B, F, J).

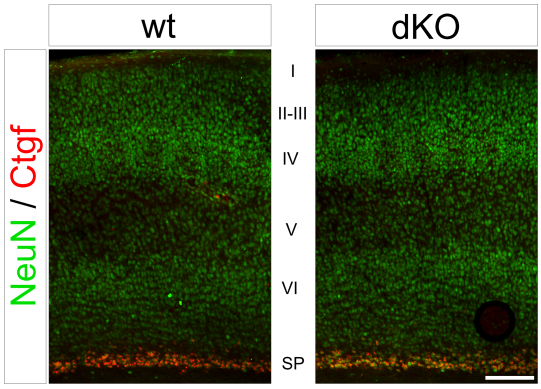


Figure 3.12: Normal subplate in absence of KIAA0319 and AU040320. At P10, the subplate layer of the dKO neocortex appears normal as indicated by labelling with subplate-specific Ctgf (red). All other neurons are labelled with NeuN (green). Images also demonstrate the presence of barrel fields in layer IV, indicating no major defects in thalamic innervation of the neocortex. Scale bar 150 μm.

3.2.6 Acute knockdown of *Kiaa0319* and *AU040320* does not affect radial migration

These results remain in contradiction with previous reports showing the involvement of both *Kiaa0319* and *AU040320* in radial migration (Paracchini et al. 2006; Peschansky et al. 2010; Platt et al. 2013; Adler et al. 2013). One possible explanation for this may lie in the different developmental time points in which the function of the gene is affected: whilst shRNA experiments target mRNA at the point in which migration is taking place, the experiments presented here so far disrupt protein levels from embryogenesis. The constitutive KO of KIAA0319 and AU040320 in the KO mice studied above eliminates the protein product of a gene from developmental onset and may allow for regulatory changes to compensate for the absence of certain protein (see e.g. Rossi et al. 2015).

In order to acutely eliminate KIAA0319 and AU040320 from migrating neurons and mimic the original the developmental course of the shRNA experiments, I performed *in utero* electroporation to deliver Cre recombinase to the telencephalon of double *Kiaa0319;AU040320* floxed embryos ($KA^{flox/flox}$;$AU^{flox/flox}$). Plasmids already available in the laboratory (used in Martinez-Garay et al. (2017)) were used

to simultaneously express Cre and EGFP under the chicken β-actin promoter (pCIG-Cre-IRES-GFP) or just EGFP (pCIG-GFP) as a control condition. Electroporations were performed at E14.5 to target migrating upper layer neurons and brains were harvested at E18.5, allowing four days for cells to migrate (Fig. 3.13A). Samples were only considered for analysis if a test-control pair with electroporated cells was present in the same litter – so that the same amount of time post-transfection is passed for migration to take place. The majority of targeted cells in both conditions occupied the upper CP and the IZ, with a few cells in the lower CP and ventricular regions (Fig. 3.13B). The percentage of neurons in the VZ/SVZ, IZ, lower CP and upper CP were then quantified and results revealed no significant differences between brains transfected with Cre-EGFP and those with GFP only (Fig. 3.13C). Expression of Cre from pCIG-Cre plasmids was confirmed by immunohistochemistry which showed a number of Cre+ cells present in the electroporated region (Fig. 3.13D). In the absence of an antibody that reliably detects the AU040320 protein in fixed brain tissue, the proper activity of Cre upon the floxed allele was confirmed by Western blot in samples from homozygous null animals ($AU^{null/null}$) showing total absence of the AU040320 protein (Fig. 3.13E). The effect of Cre on the floxed *Kiaa0319* allele has already been demonstrated in Martinez-Garay et al. (2017). The combination of the lamination and migration results presented here indicate that KIAA0319 and AU040320 do not play an essential role in radial migration in the developing mouse neocortex.

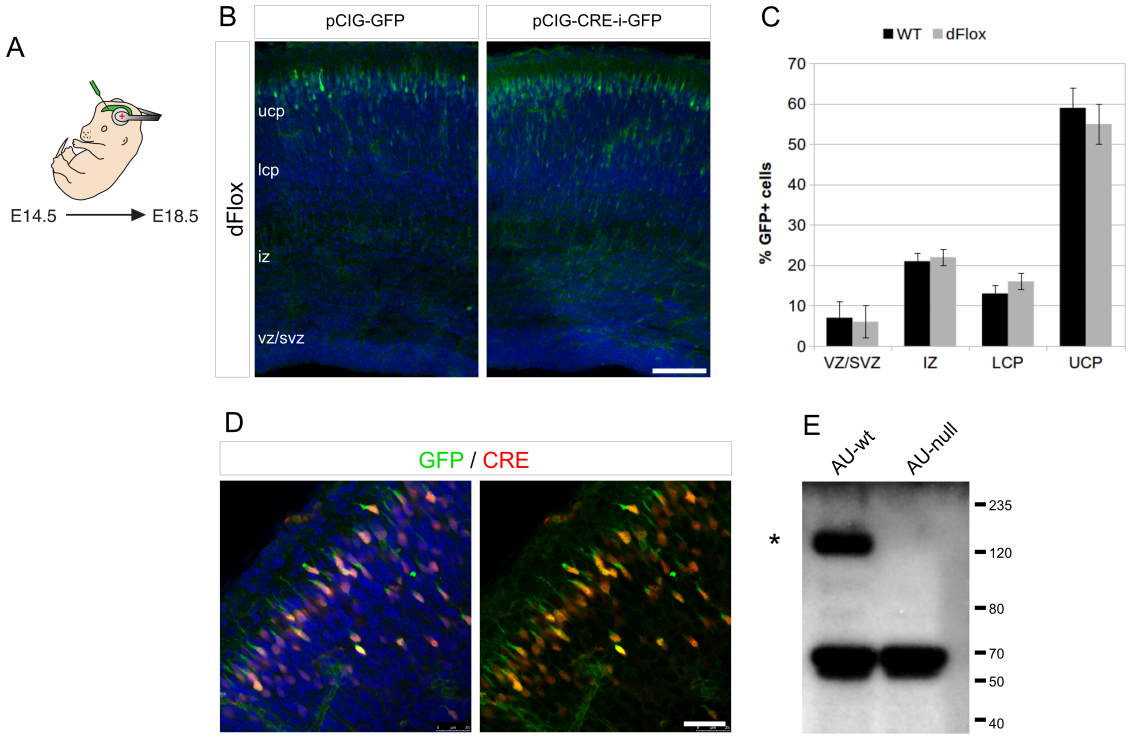


Figure 3.13: Acute KO of *Kiaa0319* and *AU040320* does not affect neuronal migration. (A) Electroporations were performed at E14.5 and brains harvested at E18.5 in double *Kiaa0319;AU040320* floxed animals (double Flox; dFlox). (B) Panels show representative images of the cortices of double floxed mice transfected with Cre for knockout (pCIG-CRE-i-GFP) and GFP only for control tests (pCIG-GFP). The majority of transfected neurons in both conditions are seen in the upper cortical plate (ucp), with some neurons seen in the lcp, iz and in the germinative areas. (C) Graphs showing quantification of percentage of cells in individual regions of the developing neocortex. There are no statistically significant differences between the two conditions (n=3, $p>0.05$). (D) A section of neocortex electroporated with plasmids expressing GFP and Cre recombinase and immunostained with anti-Cre antibody (red) to confirm expression as expected. (E) Western blot with brain lysates (30 μg/lane) of adult control wildtype (AU-wt) and homozygous *AU040320*-null mice (AU-null) showing that normal AU040320 protein (molecular weight indicated with an asterisk) is not produced in the 'null' allele after Cre-induced recombination between loxP sites in floxed allele (see Fig. 1A). Antibody used is the custom-made anti-AU040320 (at 1:3000 concentration) also used in Figure 1 of this chapter. Scale bars: 150 μm (B), 25 μm (D).

3.2.7 No changes in position of cortical interneurons following double *Kiaa0319;AU040320* KO

The previous sections report a series of experiments showing that radial migration is unaffected by the partial or total elimination of KIAA0319 or AU040320 proteins. However, the migratory processes that take place in the developing neocortex are not restricted to the radial displacement of projection neurons but extend also to the appearance of cortical interneurons originating from the subpallium. Given the expression of *Kiaa0319* and *AU040320* in this region and the putative role of these proteins in cell migration, I examined the cortices of dKO brains for the presence of distinct interneuron populations after their migration has completed.

Amongst the several interneuron subtypes, three cell groups from the two main germinative regions were selected for analysis: parvalbumin and somatostatin-positive cells derived from the medial ganglionic eminence (PV+ and SST+, respectively) and calretinin-positive cells (CR+) which originate primarily in the caudal ganglionic eminence (Marín 2013). Brain sections were analysed at P15 when interneurons have largely completed their migration into the neocortex and their radial distribution across the cortical layers. PV+ cells were found to cluster mainly in layers IV to VI (Fig. 3.14A), CR+ neurons primarily in the upper cortical layers (Fig. 3.14B) and SST+ cells mostly in the deep layers (Fig. 3.14C). No major differences in the spatial distribution of these three interneuron subtypes were observed between dKOs and wildtype samples. In addition, I examined the brains of dKO mutants at P10 by immunolabelling with Reelin, a marker for a subset of interneurons as well as Cajal-Retzius cells which are also derived from extra-cortical regions (Bielle et al. 2005; García-Moreno et al. 2008b). Mutant brains were found to have a distribution of Reelin+ cells that was largely similar to controls (Fig. 3.14D). These results suggest that absence of KIAA0319 and AU040320 does not lead to gross abnormalities in the tangential migration of cortical interneurons.

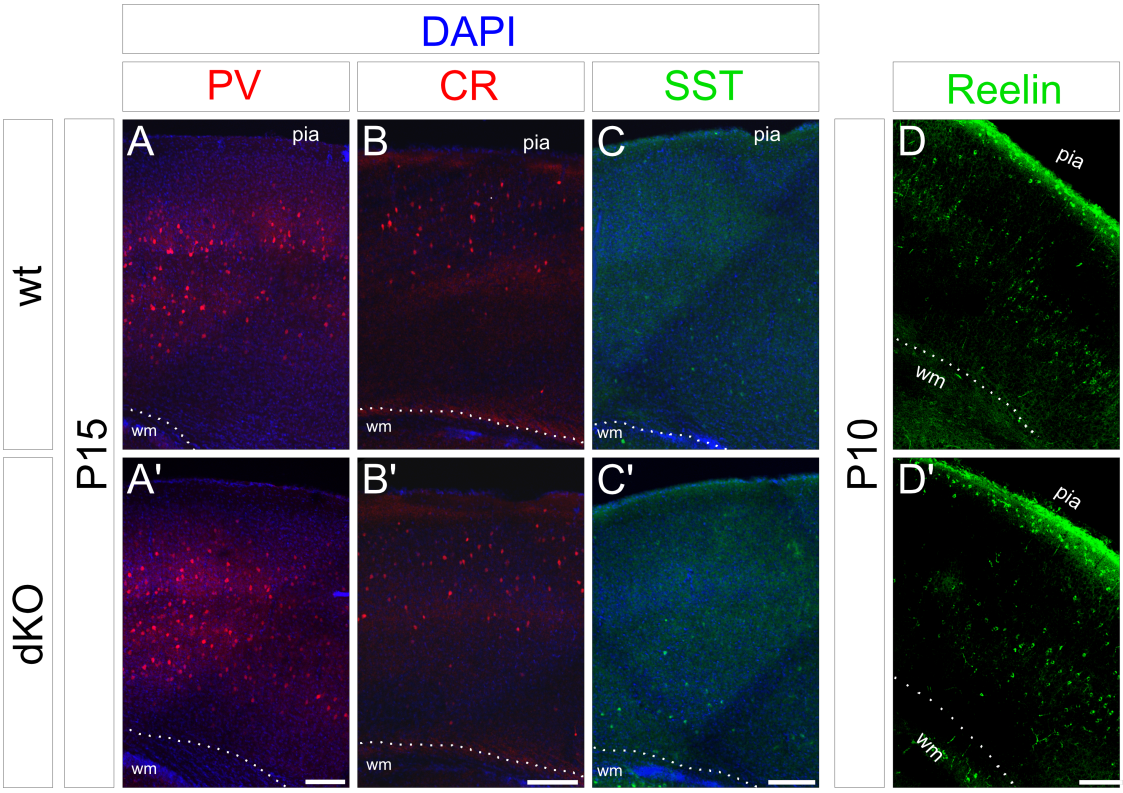


Figure 3.14: Normal distribution of interneurons in the dKO neocortex. PV+ (red, A), CR+ (red, B) and SST+ (green, C) interneurons exhibit a similar pattern of occupation in the neocortex of dKO and wildtypes at P15 after their tangential migration has largely been completed. At P10, Reelin+ cells (green, D) derived from various extra-cortical regions via tangential migration occupy the cortical plate and marginal zone in both wildtype and dKO samples, without gross differences. Dentate gyrus morphology is also unaltered. DAPI counter staining is shown in blue. Wm, white matter. Scale bar: 150 μm.

3.2.8 Unaltered lamination of hippocampus and cerebellum in the absence of *AU040320* alone and in conjunction with KIAA0319

Given cell migration is not restricted to cortical neurons and both *Kiaa0319* and *AU040320* are also expressed in other areas of the developing brain, I examined the lamination and general morphology of the hippocampus in the mutant brains under study here. This is particularly important given that mouse mutants for the *Lis1* and *Dcx* genes were found to contain only minor abnormalities in cell distribution in the hippocampus despite widespread rearrangement of the neocortex in human patients with mutations in the *LIS1* or *DCX* genes (Corbo et al. 2002;

Keays 2007). Analyses were conducted by inspecting the P10 Nissl-stained sections shown above for any gross morphological alterations (Fig. 3.1 and 3.10 above) as well as by immunohistochemistry. These experiments labelled hippocampal pyramidal neurons positive for calbindin (CB) and cells migrating through the subiculum to CA1 and CA3 with antibodies against Smi32 (Neurofilament H) at two developmental timepoints: P2 when migration is still under way and once it has settled at P10 (Nowakowski & Rakic 1981; Rakic & Nowakowski 1981; Altman & Bayer 1990a; Altman & Bayer 1990b). Examining *AU040320* mutants first, the laminar pattern of the hippocampus and the localisation of these two cell populations appeared unaltered in comparison with wildtype hippocampi at P2, with Smi32+ cells migrating through the subiculum and tangentially through CA1 and CA3 alongside CB+ pyramidal cells which delineate the different hippocampal layers as well as labelling the granule cells layer of the dentate gyrus (Fig. 3.15A-C). After its complete formation at P10, CB+ cells formed a distinct uniform layer across the hippocampus and a clear bundle of Smi32+ cells projected through CA3 (Fig. 3.15D-F). The absence of abnormalities prompted the examination of hippocampi of *Kiaa0319;AU040320* KOs at P10 and results revealed a similarly normal lamination and overall morphology (Fig. 3.16; see also Nissl-stained sections in Fig. 3.10).

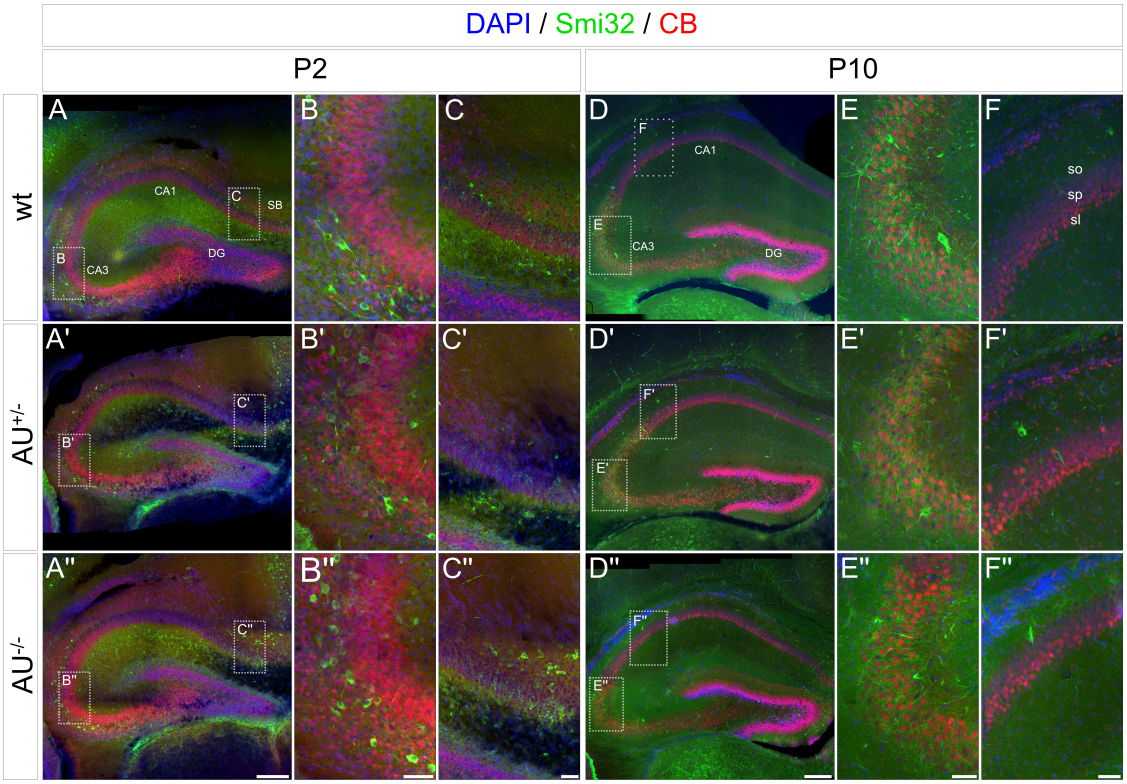


Figure 3.15: Normal hippocampal morphology in *AU040320* KO mice. Staining of neurofilament H protein (Smi32, green) and calbindin+ cells (CB, red) shows overall organisation of developing and mature hippocampus. DAPI counter staining is shown in blue.
At P2, Smi32+ cells are seen migrating through CA3 (B) and subiculum (C) and later settle in CA3 at P10 to project across CB+ neurons (E). CB+ cells are seen to distribute across hippocampal layers in the CA1 at P10 in wildtype and AU040320 mutants (F). DG, dentate gyrus; SB, subiculum; so, stratum oriens; sp, stratum pyramidale; sl, stratum lucidum. Scale bars: 200 μm (A, D); 75 μm (B, C, E, F).

Next, I turned the attention to the cerebellar cortex to study two main cell populations derived from different migratory streams: (i) Purkinje cells originating in the germinal zone in the cerebellar anlage and which migrate tangentially to form the Purkinje cell layer (Sotelo & Rossi 2013); and (ii) granule cell precursors born in the rhombic lip and occupy the external granule/molecular layer where they proliferate and differentiate into post-mitotic granule neurons, before start descending radially across Purkinje cells to form the inner granule cell layer (Sotelo et al. 2013). To visualise these cell groups and their corresponding layers, I immunolabelled Purkinje cells with a CB antibody and post-mitotic neurons with

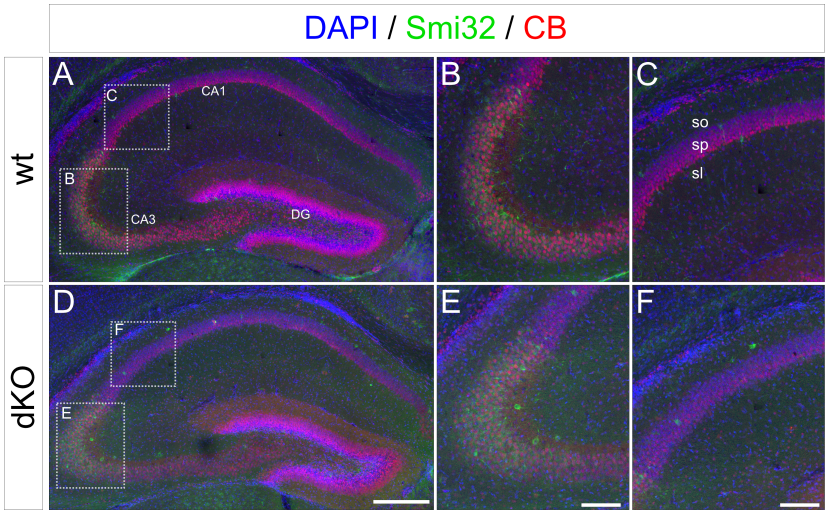


Figure 3.16: Hippocampus of P10 dKOs exhibit normal lamination pattern. Neurofilament H+ cells (Smi32, green) which migrate via the subiculum and CA1, occupy CA3 to project across calbindin+ pyramidal cells (CB, red; B). CB+ neurons in (C) are seen to delineate the predicted layers around CA1: stratum oriens (so), stratum pyramidale (sp) and stratum lucidum (sl). Dentate gyrus morphology is also unaltered. DG, dentate gyrus; SB, subiculum. DAPI counter staining is shown in blue. Scale bars: 200 μm (D); 75 μm (E, F).

the neuronal marker NeuN at P2 and P10.

Examination of *AU040320* KOs revealed both heterozygous and homozygous mutant cerebella exhibit a normal pattern of calbindin-positive Purkinje cells in the process of their maturation, an external granule layer containing predominantly precursors cells (DAPI+) and NeuN+ granule cells in the internal granule layer (Fig. 3.17A-C). The cerebellar cortex of *Kiaa0319;AU040320* KOs at P2 also exhibit no major malformations in the distribution of these cells (Fig. 3.17D). At P10, when the laminar organisation of the cerebellum appears more similar to its mature form, no gross abnormalities were detected in either *AU040320* mutants or in dKOs: foliation, lamination and the invasion of granule cells into the internal granule cell layer all appeared normal (Fig. 3.17E-H). Combined, these results suggest that KIAA0319 and AU040320 are not required for normal migration and lamination of the hippocampus and cerebellum in mice.

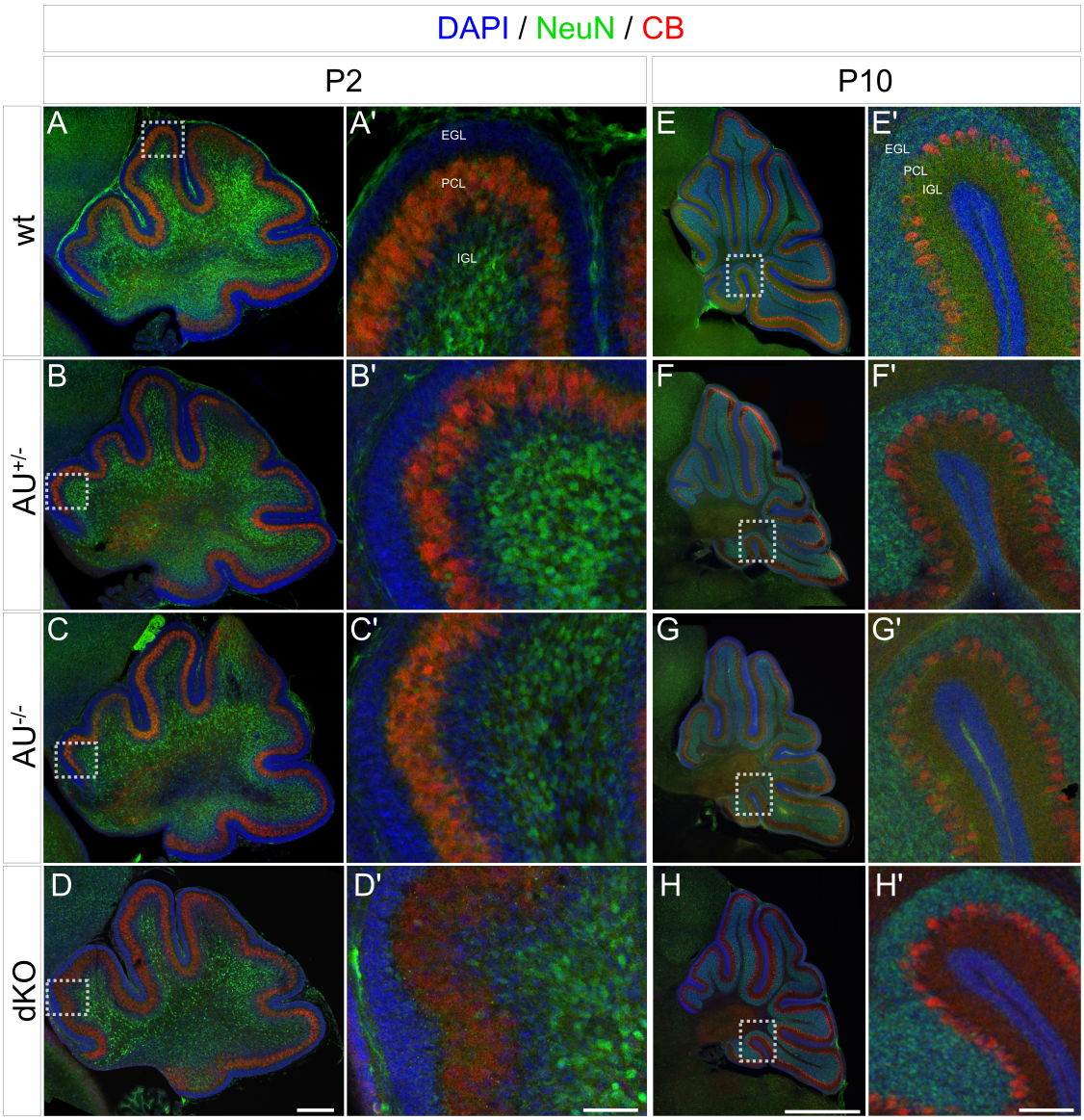


Figure 3.17: Normal cerebellar anatomy in *AU040320* and double KOs. Developing mutant cerebella show normal foliation pattern at P2 (A-D) and P10 (E-H). DAPI counter staining is shown in blue. Thickness of external granule layer (EGL), Purkinje cells (calbindin+, red) are layered as expected (PCL) and internal granule layer (predominantly NeuN+ cells, green) are similar across genotypes at P2 and P10. Purkinje cells show the same degree of variation and scatter across genotypes. Scale bar: 200 μm (D); 50 μm (D'); 1000 μm (H); 50 μm (H').

3.3 Discussion

The results described in this chapter show that absence of AU040320 alone or in conjunction with KIAA0319 does not lead to major neurodevelopmental anatomical defects or neuronal migration during cortical development, a process where these proteins had been strongly implicated previously (Paracchini et al. 2006; Peschansky et al. 2010; Szalkowski et al. 2012; Adler et al. 2013; Platt et al. 2013). The data presented here shows that *AU040320* as well as double *Kiaa0319;AU040320* KO mice do not exhibit abnormalities in the lamination of projection neurons in the cortex or in the distribution of cortical interneurons. Moreover, bypassing potential developmental compensatory mechanisms with the use of acute genetic knockdown via the expression of Cre recombinase in double floxed mice did not affect radial migration in the neocortex. Neurogenesis in the neocortex was also found to be unaffected by the partial or total reduction of AU040320 levels or by removal of both KIAA0319 and AU040320. In addition, other brain structures whose formation depends on cell migration, the cerebellum and the hippocampus, also exhibited normal overall morphology and lamination. Thus, the results presented here indicate that KIAA0319 and AU040320 are not required for neuronal migration in the mouse cortex or in the brain more generally.

3.3.1 Discrepancy with shRNA experiments

These findings are in stark contrast with previously published work using shRNA knockdown which suggests that altered levels of KIAA0319 or AU040320 can significantly impair neuronal migration in the developing rat neocortex (Paracchini et al. 2006; Peschansky et al. 2010; Platt et al. 2013; Adler et al. 2013, amongst others). Whilst rat-mouse species-differences could potentially account for this discrepancy (see below), mismatches between RNAi and genetic deletions are well-known in the literature, including in the context of dyslexia susceptibility genes. ShRNA-mediated knockdown of the rat homologs of *DCDC2* and *DYX1C1*, two other well-established dyslexia candidate genes, have been shown to result in strong

deficits in radial migration (Meng et al. 2005b; Wang et al. 2006; Burbridge et al. 2008; Adler et al. 2013). However, as shown to be the case here for *KIAA0319* and *AU040320*, mice carrying germline loss-of-function mutations for either *Dcdc2* or *Dyx1c1* displayed no deficits in the lamination of the cortex (Wang et al. 2011b; Rendall et al. 2015). The only dyslexia susceptibility gene for which there has been concordance between migration defects in RNAi and KO experiments is *ROBO1* (Gonda et al. 2013). For *Dyx1c1*, constitutive KOs exhibit severe neuroanatomical defects due to severe hydrocephalus resulting from ciliary motility abnormalities but conditional KO induced by forebrain-specific Emx1-Cre did not affect cortical lamination (Tarkar et al. 2013; Rendall et al. 2015). In the case of *Dcdc2*, only when shRNA was used to target *Dcx*, another member of the same gene family, did absence of DCDC2 indicate susceptibility to migration abnormalities: *Dcdc2* KOs displayed a stronger impairment in radial migration following knockdown of *Dcx* than the wildtype controls (Wang et al. 2011b). Given doublecortin family members are known to have partially overlapping functions (Deuel et al. 2006; Koizumi et al. 2006), it may be possible that functional compensation takes place in the case of *Dcdc2* KOs and *Dcx* knockdown. The possibility of functional compensation by paralogous genes was tested for *Kiaa0319* and *AU040320* with both constitutive and acute KO but the results revealed no deficits in cortical lamination or neuronal migration.

Whilst functional overlap of paralogous genes is a common source of compensation (Ohno 1970; Gu 2003), robustness against null mutations is a key property of biological systems which may be triggered by other buffering mechanisms intrinsic to their design (Edelman & Gally 2001; Kitano 2004; Kafri et al. 2009). Accordingly, a recent study has shown that such compensatory network may be more susceptible to activation in the case of null mutations than compared to knockdown methods by exploiting the plasticity of gene circuits (Rossi et al. 2015). This could explain the discrepancy in observed phenotypes between the two approaches - in zebrafish at

least, the mismatch in phenotypes seen between genetic mutants and (morpholino) knockdowns has been estimated to amount to around 80% (Kok et al. 2015).

The strategy employed here with the use of *in utero* electroporations to express Cre recombinase in floxed mice aims to circumvent such potential developmental compensatory mechanisms. This approach recapitulates in mice the same developmental conditions of the shRNA knockdown experiments performed in rats for *Kiaa0319* and *Kiaa0319-Like/AU040320*. The two methods differ only (aside from the species difference) with respect to the molecular stage where gene function is disrupted – targeting mRNAs or DNA, leading to either a transient or a permanent manipulation, respectively. Note that the size of electroporations (e..g number of transfected cells, vectors delivered, etc) are not easily comparable across animals. However, the electroporation experiments simultaneously genetically targeting *Kiaa0319* and *AU040320* in floxed mice reported here led to no observable defects in neuronal migration. Similar results have been obtained for *Dcdc2* using floxed mice although this result was somewhat sidelined given parallel knockdown of *Dcx* triggered migration abnormalities (Wang et al. 2011b).

One possibility for the discrepancy between the results described here and previous experiments lies in potential for off-target effects which may be triggered by the use of shRNA methods. Whilst RNA interference has been a powerful tool for functional genetics and it is widely used, specificity concerns have been a constant focus of investigation (see e.g. Jackson & Linsley 2010; Harrison 2013). More recently, it has been shown that neuronal migration deficits can emerge from unintended targets of shRNAs. Baek et al. (2014) has found that knockdown of *Dcx* led to migration defects in the form of cortical dyslamination that were indistinguishable when anti-*Dcx* shRNA vectors were delivered to developing cortex of wildtypes and *Dcx* KO mice, where no functional *Dcx* mRNA should be present. Scrambled shRNA sequences, a common control method in knockdown experiments, elicited similar effects and RNA profiling of electroporated cells revealed that the presence of shRNA vectors led to significant disruption of microRNAs which were

responsible for the arrest in cell migration. Interestingly, the authors reported that the observed toxicity effects did not appear when using shmiRNA, a next generation type of knockdown vector – when shmiRNAs were used to target *Dcx*, no migration phenotype was observed. Another example of cortical migration abnormalities triggered by off-target effects of shRNA has been demonstrated with the schizophrenia susceptibility gene *DISC1*, for which similar knockdown-knockout discrepancies had been previously noted (Brandon et al. 2009; Kamiya et al. 2005; Kubo et al. 2010). When mouse *Disc1* was targeted with shRNA in the developing neocortex, electroporated neurons failed to migrate even in the absence of DISC1 in gene KOs (Tsuboi et al. 2015). Although dosage can play a significant role in triggering of off-target effects (Caffrey et al. 2011), there are several other reports of similar effects following the use of shRNA affecting other processes such as spine formation and microglial response (Alvarez et al. 2006; McBride et al. 2008).

These studies also serve as a point for comparison between potential species differences. Aside from the experimental technique used (RNA interference vs genetic deletions), it is possible that the discrepancies observed may emerge from differences between mice and rats. For *Kiaa0319* or *AU040320*, there are no shRNA-knockdown experiments conducted in mice or genetic deletions in rats. However, it has been shown that RNA interference methods produce similar alterations in neuronal migration when performed in mice as well as rats when targeting *Dcx* (Bai et al. 2003; Ramos et al. 2006; Baek et al. 2014) and *Disc1* (Kvajo et al. 2012; Tsuboi et al. 2015). As mentioned above, shRNA knockdown has been shown to lead to neuronal migration defects due to off-target effects (Baek et al. 2014; Tsuboi et al. 2015). Whilst this has not been directly tested, the most parsimonious explanation is that these artefacts are responsible for neuronal migration abnormalities in rats in a similar way to mice. It is likely that the same is true for the experiments with *Kiaa0319* and *AU040320*, as well as other dyslexia susceptibility genes. Alternatively, it is possible that the discrepancies observed may be due to subtle differences in the compensatory mechanisms triggered by gene

circuits between mice and rats, or in complexity of the mechanisms underlying cell migration in these species – however, this has not been demonstrated before, and thus do not appear to be a main factor in driving these differences.

The knockdown studies on *Kiaa0319* and *AU040320* attempted to demonstrate target specificity by using multiple shRNA vectors as well as performing rescue experiments by overexpressing the targeted protein. However, in light of the methodological concerns outlined here, it is possible that the reported migration abnormalities are triggered by the response of the RNAi machinery rather than specific target knockdown. As such, those results should be interpreted with caution, particularly in light of growing concerns for reproducibility in the biological sciences and in scientific research more generally (e.g. Ioannidis 2005; Bustin 2014; Open Science Collaboration 2015).

The emergence of new technologies to interrogate gene function should assist and promote the use of more reliable methods. The advent of modern genome-editing techniques such as CRISPR/Cas9 may provide an 'off the shelf' system similar to RNAi but without its undesired side effects (although specificity can also be an issue; see Hsu et al. (2013), Fu et al. (2013), Cradick et al. (2013), and Lin et al. (2014). In fact, *in utero* manipulations have already been published using this method (Shinmyo et al. 2016; Kalebic et al. 2016) and this could allow probing into the putative functions of KIAA0319/AU040320 in neuronal migration in a number of other species beyond rodents, particularly those whose neocortex resemble more the human one such as sheep and ferrets who are also gyrencephalic. Although neither *KIAA0319* nor *KIAA0319L* have been directly implicated in neuronal migration in humans, the results described here (and those recently reported in Martinez-Garay et al. (2017)) cannot rule out such possibility for either or both genes. In fact, there are severe migration disorders in humans that emerge from mutations in genes such as *LIS1*, *TUBA3* and *DCX* which present no cortical migration defects in the corresponding KO mouse (Corbo et al. 2002; Keays 2007). The association of *KIAA0319* with dyslexia differs from these cases in that it is

based on SNPs rather than coding mutations with direct consequences on protein function. Cerebral organoids, which recapitulate cortical development in vitro from pluripotent stem cells (Lancaster et al. 2013), may be a valuable tool to directly assess a putative function of *KIAA0319* and *KIAA0319L* in neuronal migration or brain development more generally - note, however, that cell migration has not yet been explicitly demonstrated in such models.

It is important to note also that, whilst the migration effects found in rats treated with shRNA against *Kiaa0319* are clear and robust, the effect observed with *Kiaa0319-Like/AU040320* are very mild at best. In their report, Platt et al. (2013) describe that knockdown of *Kiaa0319-Like* did not affect cortical lamination and only led to periventricular nodular heterotopias in 25% of cases – and the control experiments with scrambled shRNA sequences contained only half the number of animals (n=16 for anti-*Kiaa0319-Like* and n=8 for controls). In addition, the rescue condition examined only 4 samples and 2 of those exhibited heterotopias (Platt et al. 2013), raising further questions on the reliability of the original results. It is important to note also that the study reported here investigated only 3 pairs of mutant-control embryos for putative migration defects (3 other mutants were examined and showed no signs of impaired neuronal migration, although these did not have control litter mates for direct comparison and quantification).

In sum, the results of this study combined with shortcomings of shRNA methods suggest that *Kiaa0319* and *AU040320/Kiaa0319-Like* do not play the role in neuronal migration as previously hypothesised. Moreover, given similar questions arise with the two other main dyslexia candidate genes implicated in neuronal migration before, *DCDC2* and *DYX1C1*, the view that the dyslexia susceptibility genes operate in neuronal migration should be re-evaluated.

3.3.2 The neuronal migration hypothesis of dyslexia susceptibility

The hypothesis that dyslexia is a disorder of neuronal migration has two lines of evidence at its cornerstone: functional genetics on a handful of susceptibility

genes and human neuropathological examinations of dyslexic specimens (Galaburda et al. 2006; Paracchini et al. 2007; Gabel et al. 2010; Ramus & Ahissar 2012; Kere 2014). The previous sections put to question the first part of the hypothesis given methodological issues and the failures in replicating the original findings. In this section, I outline key issues that emerge from the second aspect of the neuronal migration hypothesis given the original neuropathological *postmortem* analyses and the related neuroimaging studies suffer from what could be interpreted as important flaws – thus, casting further doubt onto dyslexia as a neuronal migration disorder.

In a series of publications, a group at Harvard Medical School led by Albert Galaburda reported the examination of the brains of 8 individuals diagnosed with dyslexia which were found to contain a high incidence of focal cortical malformations, mostly in the form of layer I ectopias but also some focal dysplasia and polymicrogyria – all features that emerge from deficits in neuronal migration during cortical development (Galaburda & Kemper 1979; Galaburda et al. 1985; Humphreys et al. 1990; Guerrini & Parrini 2010; Blümcke et al. 2011). Although these micro-abnormalities were found in different regions of the neocortex, they clustered around the left peri-sylvian fissure. Two other similar cases were also reported by other groups (Drake 1968; Levine et al. 1981; Cohen et al. 1989). Based on this, it was hypothesised that subtle cortical malformations are one of the neuroanatomical basis of dyslexia (Galaburda et al. 1985; Kaufmann & Galaburda 1989; Humphreys et al. 1990). Although no further studies have been conducted, the idea received support from later findings from behavioural structural neuroimaging studies demonstrating reading difficulties in individuals with periventricular nodular heterotopias (Chang et al. 2005; Chang et al. 2007).

However, there are important shortcomings with these two sets of studies which call for careful consideration. Firstly, the histopathological analyses of the putatively dyslexic samples did not include the examination of control samples which were only reported later on (Kaufmann & Galaburda 1989) and, as such, analyses were not conducted blind. Although the authors report control samples contain a markedly

lower incidence of cortical micro-abnormalities, subtle defects such as ectopias require systematic procedures for examination. Secondly, whilst the initial 4 cases reported in Galaburda et al. (1985) had a large number of defective foci (30 to 140 per brain), the subsequent 3 patients from Humphreys et al. (1990) contained between 4 and 11, levels which are comparable to the range reported in some non-dyslexic brains by other groups (Morel & Wildi 1952; Levine et al. 1974) . However, the control cases examined by the Galaburda team reported only 1-2 ectopias per brain (Kaufmann & Galaburda 1989; Humphreys et al. 1990). A further problem comes from whether the dyslexic subjects are representative of the dyslexia population: one individual in Galaburda et al. (1985) was noted to suffer from 'notable language difficulties', not specific to reading, which could indicate a high degree of co-morbidity with other neurodevelopmental disorders such as specific language impairment (Bishop & Snowling 2004). Another individual studied is reported to have suffered from a significant delay in language acquisition, with possible ADHD, whilst a further case had been diagnosed with severe depression. Similar concerns have been raised by others which have also questioned the unclear diagnostic criteria used for categorisation of dyslexia (Beaton 1997; Beaton 2002; Altarelli et al. 2014).

In addition, the first reported patient in Galaburda & Kemper (1979) had a history of epileptic seizures and the same issue arises with the individuals with periventricular nodular heterotopias in the neuroimaging studies of Chang et al. (2005) and Chang et al. (2007) (the first one of which, incidentally, did not contain a control group to compare performance in the reading behavioural task). Whilst mild learning disabilities can occur in cases of periventricular heterotopias, more severe defects, particularly epilepsy, are a well-established feature of this phenotype (Kabat & Król 2012; Guerrini & Dobyns 2014). More importantly, there appears to be only one further case linking periventricular heterotopias and reading impairment since the two studies (Reinstein et al. 2012, which also presents a case of dissociation between the two phenotypes), even despite hundreds of MRI images of dyslexic brains (e.g. Krafnick et al. 2014; Jednoróg et al. 2015). Naturally, it is possible

that micro-abnormalities in cortical organisation resulting from neuronal migration impairment may be present in these samples but are too small to be detected with current *in vivo* neuroimaging methods. Technological and statistical advances (such as variations/improvements of 7T MRI) may allow this question to be specifically tackled in the future, with some promises of improvement already reported in the literature (Wagner et al. 2011; Thesen et al. 2011; Hong et al. 2014; Pardoe & Kuzniecky 2014; Wang et al. 2015). On the other hand, some studies have reported an increased incidence of polymicrogyria in individuals with language impairment more generally, not specific to reading, although this has not been consistently replicated (Guerreiro et al. 2002; Hage et al. 2005; Oliveira et al. 2008; Webster et al. 2008; Leventer et al. 2010; Jansen et al. 2016). The one neuroanatomical feature that has been consistently reported in structural imaging studies is the deviation in the asymmetry of the planum temporale as originally reported in the *postmortem* histopathological studies 30 years ago (Galaburda et al. 1985; Humphreys et al. 1990; Bloom et al. 2013; Altarelli et al. 2014). Nonetheless, it is not clear how a tendency for symmetry in the *planum temporale* could result from abnormalities in neuronal migration.

The value of the *postmortem* analyses conducted by Galaburda and his colleagues is undeniable and represent the first investigations into the neuroanatomical basis of dyslexia. However, the results need to be interpreted with caution in light of the issues outlined above and require replication using carefully controlled samples examined in a systematic way following modern standards (Bishop 2012). However, availability of suitable *postmortem* tissue is extremely limited for a study with the necessary minimum of 20 specimens, thus, lowering the odds for such a study to be conducted.

Another important issue in this debate lies with respect to the limited understanding of genetic variants implicated in dyslexia upon which the neuronal migration hypothesis is based. The standard formulation of the hypothesis of dyslexia as neuronal migration disorder, from the perspective of functional genetics,

lies on evidence related to at most five genes putatively implicated in neuronal migration (*KIAA0319*, *DCDC2*, *DYX1C1*, *ROBO1* and *KIAA0319L*). Whilst some of these correspond to the strongest candidates revealed so far and comprise the majority of genes implicated in dyslexia at the time the migration hypothesis was first proposed (Galaburda et al. 2006; Paracchini et al. 2007), these are likely to be a very small subset of the genes responsible for susceptibility to a highly heterogeneous and complex disorder such as dyslexia. Molecular genetics has advanced significantly in recent years and our understanding of the genetic architecture of complex disorders has been redrawn as a result of it, with many different types of genetic alterations being implicated (Mitchell 2012). As it has been shown for other neurodevelopmental disorders such as autism and schizophrenia (Mitchell 2012; Bourgeron 2015), it is likely that several hundreds of genes varying in frequency, penetrance and type of variant (SNPs, point mutations, CNVs) are involved in susceptibility to dyslexia and, as such, the 4-5 candidates linked to neuronal migration represent only a fraction of it.

There is a growing body of work uncovering new genes putatively implicated in dyslexia and these are associated with a range of different neurodevelopmental and neuronal functions such as regulation and function of ion channels, glucose transport or synaptic plasticity. Whilst neuronal migration may turn out to be one of the cellular mechanism underlying susceptibility to dyslexia, it is likely that other neurobiological pathways and processes play a role in the disorder – such as, for example, altered formation and function of primary cilia that has been recently suggested (Tarkar et al. 2013; Massinen et al. 2011; Brandler & Paracchini 2014).

The next chapters explore the putative roles of KIAA0319 and AU040320 from the point of view of animal behaviour, electrophysiology and cell biology. The combination of findings reported there points to a new direction for the cellular and molecular function of these proteins.

3.4 Conclusion

This chapter described the generation of AU040320 transgenic mouse lines and the examination of the role of the AU040320 and KIAA0319 proteins in neuronal migration in the mouse brain using a variety of methods. The results failed to replicate previous findings suggesting KIAA0319 and AU040320 are involved in cell migration and revealed that absence of these two proteins does not lead to neuroanatomical malformations in the developing mouse brain. Furthermore, detailed evaluation of the evidence derived from human neuropathological and imaging studies highlights a number of inconsistencies and issues underlying them which put to question the strength of its support for the neuronal migration hypothesis of dyslexia. Since the publication of functional genetics studies in the mid-2000s, this has been the prevalent view on the neuroanatomical basis of dyslexia and has been championed in numerous publications (as a measure, Scopus lists 110 articles with neuronal migration and dyslexia as part of title, abstract or keywords). Whilst the findings reviewed here do not directly disprove the hypothesis, it highlights a growing body of evidence pointing towards a shift in the current paradigm. When the first functional genetics results from *in utero* electroporations in rat embryos emerged, the convergence between those experiments and the parallels to the human studies were remarkable and generated great excitement in the language sciences community. It is now time to be equally interested in discussing its shortcomings and focus on studying other biological pathways in the challenge to understand the molecular and cellular basis of susceptibility to dyslexia.

4

Chapter 4

Contents

4.1 Introduction 122
4.2 Results 123
4.2.1 Locomotor activity in a novel environment 123
4.2.2 Accelerating rotarod 124
4.2.3 Spatial memory tests 125
4.2.4 Anxiety-like behaviour in the light-dark box 126
4.2.5 Olfactory response 129
4.2.6 Startle response, PPI and rapid auditory processing in dKO mice 130
4.2.7 Startle response, PPI and rapid auditory processing in single *Kiaa0319* and *AU040320* KOs 133
4.2.8 Impaired auditory brainstem responses in *AU040320* and double KO mice 136
4.2.9 Expression of *Kiaa0319* and *AU040320* in the lower auditory pathway 148
4.2.10 Synapse number in the auditory pathway of dKO mice . 151
4.3 Discussion 155
4.4 Conclusion 164

4.1 Introduction

Previous experiments attempting to assess the role of *Kiaa0319* in mediating language-related behaviours in rodents have implicated this gene in spatial memory and complex auditory processing tasks following shRNA-mediated knockdown in the developing rat cortex (Szalkowski et al. 2012; Centanni et al. 2014a; Centanni et al. 2014b). These results are paralleled by similar findings in shRNA-treated rats for the rodent homologs of two other main dyslexia susceptibility candidate genes, *DCDC2* and *DYX1C1* as well as their respective KO mice (Threlkeld et al. 2007; Wang et al. 2011b; Szalkowski et al. 2011; Szalkowski et al. 2013; Truong et al. 2014; Rendall et al. 2015). Together, these findings point towards a role for dyslexia susceptibility genes in modulating the function and/or structure of neural circuits important for learning and memory as well as auditory processing.

With regards to *Kiaa0319*, previous experiments from our laboratory have shown that constitutive KO of this gene does not lead to significant behavioural abnormalities in mice. *Kiaa0319* KOs exhibited performance comparable to wild-types when assessed for their baseline locomotor activity (LMA), social interaction, performance in the accelerated rotarod, T- and Y-maze, object recognition task, amongst others (Martinez-Garay et al. 2017). On the other hand, there was suggestive evidence that partial or total absence of KIAA0319 may lead to subtle alterations in two behavioural domains: (a) KIAA0319-deficient mice exhibited decreased anxiety-like behaviour in the initial stages of the light/dark box task, although no similar alterations were detected in other anxiety-related tests; (b) a subtle deficit in sensorimotor integration or attention as measured in the prepulse inhibition/facilitation task; this specifically affected males in conditions of long delay between cue and startle-eliciting stimulus (between 400-800 ms). However, the effects observed in these two tests were mild and based on a relatively small sample size (7-9 per group); thus, they must be interpreted with caution and require further validation.

Based on this and on the possibility raised earlier of functional overlap between KIAA0319 and AU040320, I performed a range of tests on dKO mice and wildtype controls to investigate potential behaviours which may be affected by the combined deletion of these two proteins. These tests were driven primarily by hypothesis-guided questions based on the literature on dyslexia susceptibility genes and human dyslexia endophenotypes (see e.g. Kere 2014; Peterson & Pennington 2015) as well as known features of the KIAA0319 and AU040320 proteins. They also served as a way to interrogate different neural systems where the two genes may be important and to generate new hypotheses in light of the negative findings in neuronal migration outlined in the previous chapter.

4.2 Results

4.2.1 Locomotor activity in a novel environment

In order to measure baseline activity and assess exploratory behaviour following exposure to a novel environment, I performed locomotor activity (LMA) testing on dKOs and wildtype mice. Measuring the number of beam breaks in the initial 5 minutes of the task immediately following exposure to the test arena, the two groups performed similarly, with one-way ANOVAs revealing no differences between them (Fig. 4.1A; $F=1.19$; $p=0.28$). Total ambulation over the duration of the 90 min also revealed no differences (Fig. 4.1B; $F=0.21$; $p=0.85$). Figure 4.1C shows the distribution of beam breaks for each of the 10 minutes of the task, where there were also no significant differences based on repeated measures ANOVAs with genotype as a between-subject factor and time bin as a within-subject factor ($F=0.20$; $p=0.65$).

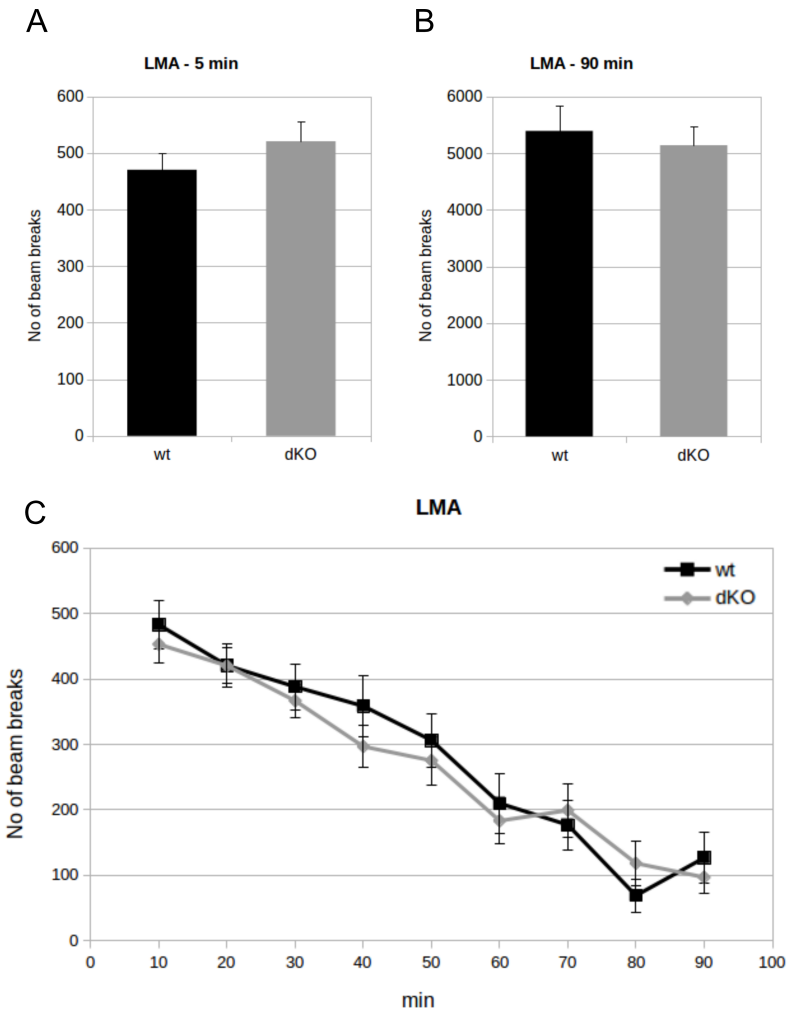


Figure 4.1: Double KOs exhibit normal locomotor activity in a novel environment. (A) Total beam breaks during the first 5 minutes of exposure to the arena, and (B) for the duration of the entire 90 minutes of the task. (C) Number of beam breaks per group for each 10 minute period; (n=18 per group). Data shown as means; error bars indicate ±SEM.

4.2.2 Accelerating rotarod

Procedural and motor learning deficits have been hypothesised to underlie the deficit in language ability seen in language-impaired populations, including in dyslexia (Stein 2001; Ullman & Pierpont 2005; Lum et al. 2013). Given the relevant systems rely heavily on cerebellar function and both *Kiaa0319* and *AU040320* are expressed in the cerebellum, I interrogated whether absence of functional copies of these genes may affect motor function and learning in the accelerating rotarod task.

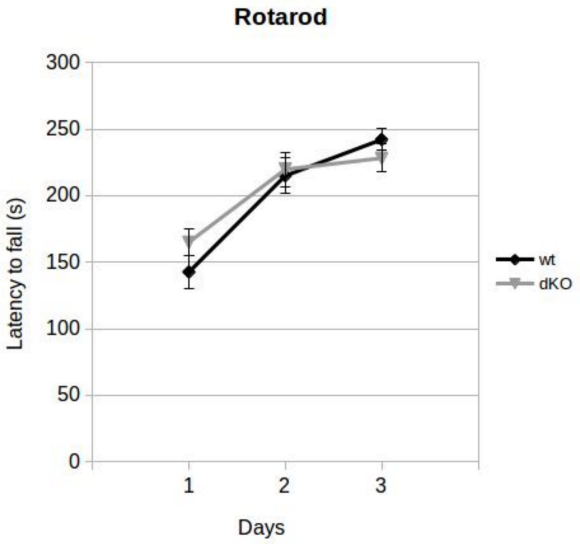


Figure 4.2: Motor coordination and learning in accelerating rotarod is unaffected in dKOs. Latency to fall (s) from rotating rod during the 5 minute period of acceleration of the apparatus for each of the three consecutive days; (n=18 per group). Data shown as means; error bars indicate ±SEM.

Basic motor coordination in the cohort was assessed by comparing latency to fall from the apparatus in the first day of testing, where the performance of dKO and wildtype animals did not significantly differ (Fig. 4.2; F=2.05; p=0.16). Mice were tested over the course of another two consecutive days to assess learning and both animal groups showed improved performance by staying in the apparatus for longer in the test, although not reaching the 300 s limit (Fig. 4.2). Statistical comparisons revealed there were no differences between the two genotypes reaching the significance threshold (Day 2, F=0.07, p=0.8; Day 3, F=1.1; p=0.30).

4.2.3 Spatial memory tests

In order to assess the spatial memory ability of dKO mice, animals were tested on two different tasks. Spatial memory defects were previously reported for rats treated with shRNA against *Kiaa0319* during cortical development (Szalkowski et al. 2012) but no such deficit was found in *Kiaa0319* KO mice (Martinez-Garay et al. 2017). In the Y-maze, spatial memory was tested by assessing exploration of a novel maze arm as opposed to the 'other' arm, which was previously sampled during the habituation

period. Firstly, there was a difference in control measures of activity during the test (in the 'arm choice' phase) as measured by the overall distance travelled during the 2 min session, with dKO mutants covering less territory than controls (Fig. 4.3A; F=6.98; p=0.01). However, there was no such difference when considering only the novel arm, suggesting exploration of the target area was comparable between the two groups (not shown; F=0.13; p=0.72). With respect to preference to a novel environment which can be used as a measure of memory recall, mutants and controls spent a similar amount of time exploring the novel arm (Fig. 4.3B; F=1.85; p=0.18) as well as in the number of entries into it (Fig. 4.3C; F=0.55; p=0.46).

Short-term spatial memory was tested using the spontaneous alternation test in the T-maze. Successful entry to the arm previously unexplored in the sample phase counted as an alternation and animals were assessed on the percentage of alternations over the 10 trials (2 per day over 5 consecutive days). Both groups of animals alternated arms around 60% of the time, just above the 50% chance level (Fig. 4.3E; wt, t(17)=-3.72; p=0.009); dKO, t(17)=-3.16, p=0.01). There were no significant differences between the means of the two groups (Fig. 4.3D; F=0.13; p=0.72). These results suggest that absence of KIAA0319 and AU040320 does not lead to major impairments in spatial memory.

4.2.4 Anxiety-like behaviour in the light-dark box

Previous experiments from our laboratory have raised the possibility of a subtle reduction in anxiety-like behaviour in *Kiaa0319* KO mice in the light-dark box, although the sample size was relatively small and the finding was not confirmed in other tests such as the elevated plus maze, open field and in social interaction (Martinez-Garay et al. 2017). Given the relationship between anxiety and learning disability and the co-morbidity of dyslexia with other developmental and psychiatric disorders (Al-Yagon & Mikulincer 2004; Cantwell & Baker 1987; Schulte-Körne 2010; Sundheim & Voeller 2004), I decided to probe into this putative anxiolytic effect of KIAA0319 and test this cohort of double KO mice in the light-dark box.

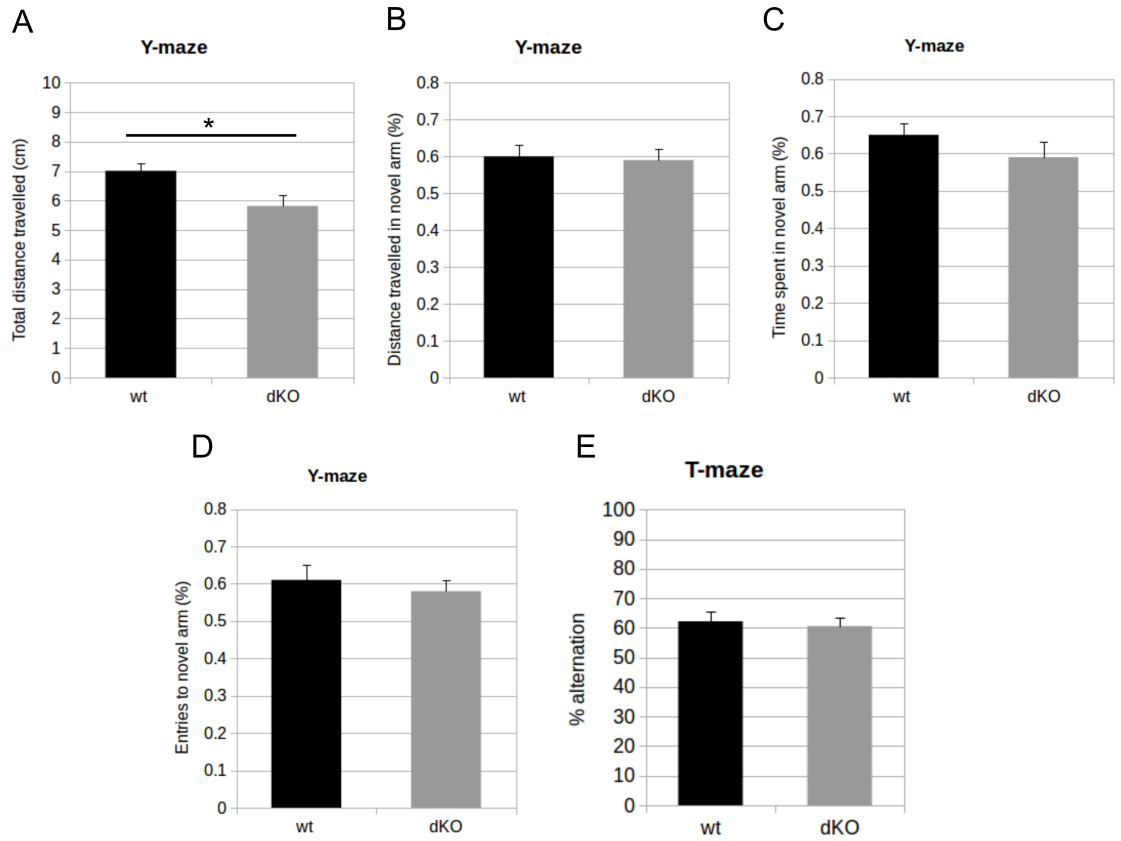


Figure 4.3: Normal spatial memory and exploration in dKOs. (A) The mutant group travelled less than wildtypes during the duration of the test phase (* denotes $p = 0.01$). (B) Percentage of time spent in the novel arm as compared to the rest of the apparatus in the test phase. (C) Ratio of entries to the novel arm in relation to the 'other' arm; ($n = 18$ wt, $n = 17$ dKO). (D) Percentage of alternation to unexplored arm in the T-maze. Data shown as means; error bars indicate ±SEM.

Results of control locomotor activity measures revealed a significant difference between the two groups as dKOs covered a shorter distance during the task across the whole arena (Fig. 4.4A; F=7; p=0.01), with an effect size generally considered to be large (Cohen's d=0.89). When path length was interrogated specifically for each side of the apparatus, the difference was revealed to be driven by distance travelled in the light zone (Fig. 4.4B; Light area: F=4.21; p=0.05; d=0.70); Dark area: F=3.14; p=0.09; d = 0.6). There were no differences detected in the number of transitions between the two zones (Fig. 4.4C; F=2.08; p=0.16).

With respect to anxiety measures, dKOs showed signs of a suggestive increase in anxiety levels as mutants spent more time in the dark zone during the 10

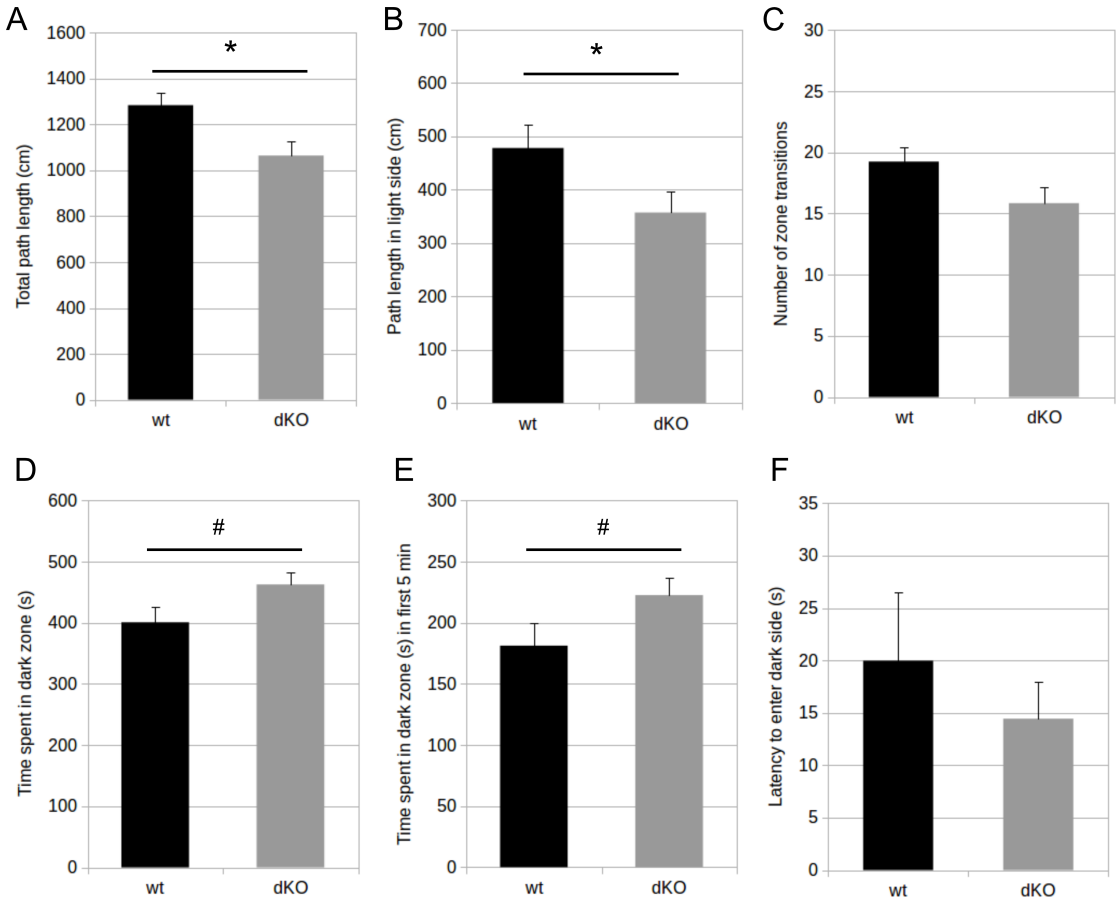


Figure 4.4: Double KOs display a mild increase in anxiety-levels in the light-dark box. Mutants travelled shorter distances in the total arena (A) as well as only in the light zone (B). Number of transitions between dark and light zones was similar between the two groups (C). Measuring changes in anxiety levels with time spent in the different areas showed a suggestive effect from dKOs spending more time in dark areas during the entire task (D) and the first 5 minutes (E). Latency to leave light area and enter dark area (F); * denotes $p < 0.05$; # denotes p = 0.06-0.08; (n = 18 wt, n=17dKO). Data shown as means; error bars indicate ±SEM.

min duration of the task (Fig. 4.4D), although the difference did not hold below the statistical significance threshold level (p=0.05) but it showed a considerable effect size (F=3.76; p=0.06, d=0.66). Similar results hold when considering only the initial 5 min of the session (Fig. 4.4E; F=3.23; p=0.08; Cohen's d=0.61). Furthermore, the performance of dKOs did not differ from controls in the latency to leave the light zone and move to the dark area (F=0.54; p=0.42). Combined, these results suggest that the absence of KIAA0319 and AU040320 together may

trigger a subtle anxiogenic effect in mice.

4.2.5 Olfactory response

A number of studies have linked dyslexia candidate genes with cilia structure and function (Ivliev et al. 2012; Massinen et al. 2011; Tarkar et al. 2013; Kere 2014). In relation to *Kiaa0319*, some studies have associated this protein to this organelle: its expression is enriched in ciliated tissues such as airways and Fallopian tubes, but not in brain (Ivliev et al. 2012); during cell division in ES cells, it may localise to the centrosome from which ciliary basal bodies of cilia will form (Silvia Paracchini, unpublished data); and a study of the proteome of olfactory sensory neurons reported its specific expression in the ciliary membrane of these cells (Kuhlmann et al. 2014). In addition, *AU040320* has been detected in olfactory sensory neurons and it is expressed in the developing olfactory epithelium at E14.5 (Diez-Roux et al. 2011). Combined, this suggests the possibility of a function for these proteins in mediating cilia function in olfactory sensory neurons. In order to test this, I performed an olfactory preference test of dKO and wildtype mice (Witt et al. 2009). This task measures the time spent by an animal in smelling an attractive stimulus (e.g. peanut butter) and an aversive one (e.g. 2-methylbutiric acid, 2-MA) and it serves as an initial characterisation of olfactory behaviour.

The results shown in Figure 4.5 indicate that both animal groups considerably avoided the aversive stimulus, measured by time spent with target stimulus minus time spent sniffing water as control (4.5A). However, animals did not display a significant preference for the supposedly attractive smell of peanut butter as values floated around zero (time spent with peanut butter minus time spent with water; 4.5A). Nonetheless, the performance between the two groups did not exhibit statistically significant differences for either of the two stimuli (2-MA: $F=0.42$; $p=0.52$; peanut butter: $F=0.14$; $p=0.71$). As a measure of control, I compared the total time spent exploring all stimuli but performance did not differ for this measure

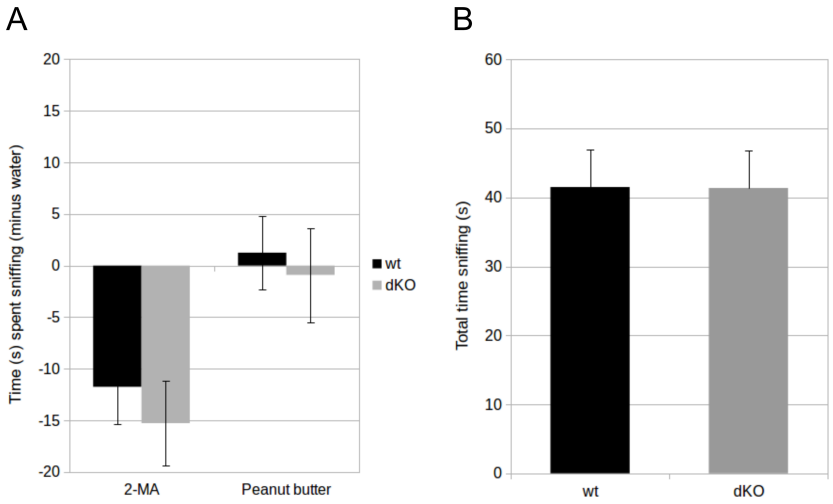


Figure 4.5: No change in olfactory preference test in Double KOs. (A) Time spent sniffing aversive stimulus 2-MA or attractive peanut butter (minus time spent sniffing water). (B) Total time spent with all stimuli; ($n = 12$ wt, $n = 12$ dKO). Data shown as means; error bars indicate ±SEM.

either (Fig. 4.5B; F=0.11; p=0.99). These results suggest that absence of KIAA0319 and AU040320 does not lead to a major deficit in olfactory behaviour in mice.

4.2.6 Startle response, PPI and rapid auditory processing in dKO mice

Knockdown of *Kiaa0319* using shRNA in rats has been reported to lead to deficits in the processing of rapidly-changing auditory stimuli using a silent gap detection paradigm as well as more complex tasks such as frequency modulation sweeps (Szalkowski et al. 2012). Similar deficits have been found after manipulation of other language-associated genes in rats and mice (Threlkeld et al. 2007; Szalkowski et al. 2013; Truong et al. 2014; Truong et al. 2015). Based on these findings, I decided to subject dKOs to a similar silent gap detection task to assess rapid auditory processing using the same modified prepulse inhibition (PPI) paradigm used in the aforementioned studies and depicted in Figure 1.12 in Chapter 1 (Fitch et al. 2008; Truong et al. 2014).

First, a standard PPI test was conducted as a control experiment to measure baseline startle reflexes and sensorimotor gating. Previous experiments on *Kiaa0319* KO mice have shown a very mild effect on sensorimotor integration but only at

very long gaps between cues (400-800 ms Martinez-Garay et al. 2017). A potential deficit in startle reflex and PPI could obscure the relevance of the findings in the silent gap detection task which attempts to interrogate the auditory system more specifically. Results revealed the expected startle reflex responses in both dKO and wildtype groups upon presentation of simple white noise sound bursts of different intensity levels above the background sound (69, 73, 77 and 81 dB SPL; background noise 65 dB SPL) with reflex responses increasing at higher sound levels as expected (Fig. 4.6A). Repeated-measures ANOVA indicated there was no effect of genotype on these responses, both across stimuli (stimulus as a within-subject factor; F=0.13; p=0.71), or with genotype x stimulus as factors (F=0.22; p=0.95).

In the PPI test, presentation of loud prepulse cues led to the expected increase in inhibition of the startle response in wildtypes (Fig. 4.6B). Mutant mice responded with slightly higher inhibition in all conditions (Fig. 4.6B) but these did not significantly differ from controls as there was no effect of genotype in repeated-measures ANOVA (with stimulus as a within-subject factor, F=1.89; p=0.17; or genotype x stimulus as between-subject factors; F=0.15; p=0.93). Together these results indicate that the startle reflex system in dKOs is intact.

Given this, I proceeded with the silent gap detection task to assess auditory processing in dKOs. An attenuation score was used as a measure of inhibition which inversely correlates with startle inhibition: higher attenuation scores indicate lower inhibition of acoustic startle and weaker perception of the cue. Both animal groups displayed the expected decrease in attenuation score as gap duration increased - longer gap duration allows more time for perception/reactivity (Fig. 4.6C). In most gap durations, attenuation scores of dKOs were higher than wildtypes, indicating higher startles and, thus, less sensitivity to the cue. Comparison of attenuation scores using repeated-measures ANOVA revealed that performance in the task overall, across all conditions, indicated an effect of genotype on performance across stimuli types (genotype as a between-subject factor and gap duration as a within-subject factor; F=2.12; p=0.03). *Post-hoc* Tukey analyses revealed significant

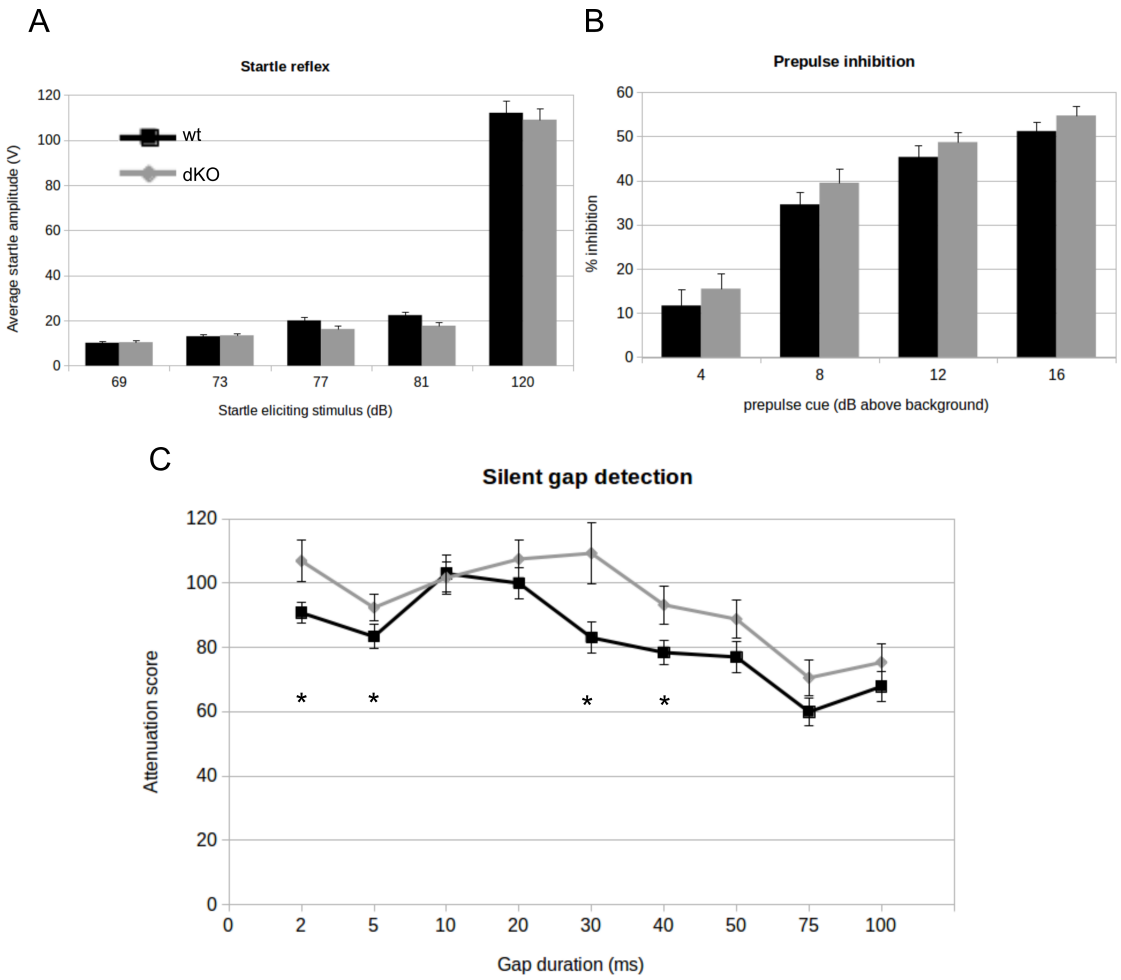


Figure 4.6: Double KOs have normal startle reflex and prepulse inhibition but impaired silent gap detection. (A) Amplitude of startle reflex (measured in V) in response to noises of different sound intensity levels. (B) Measurements of inhibition of startle-eliciting stimulus (%) when preceded by cues (prepulses) of different sound intensity levels above background. Mutants exhibited increased inhibition for all conditions but these did not differ statistically from controls. (C) Double KOs exhibit increased attenuation scores in the silent gap detection task for a subset of stimuli which tended to be in the shorter gap range (2, 5, 30, 40). p values and Cohen's d for each gap: 2: p=0.03; d=0.76; 5: p=0.04; d=0.57; 10: p=0.53; d=0.05; 20: p=0.41; d=0.30; 30: p=0.01; d=0.84; 40: p=0.04; d=0.77; 50: p=0.12; d=0.52; 75: p=0.13; d=0.51; 100: p=0.31; d=0.34. * denotes p<0.05; ($n = 18$ wt, $n = 17$ dKO). Data shown as means; error bars indicate ±SEM.

differences in responses to the following gap durations: 2, 5, 30, 40 ms ($p<0.05$; $d=0.57$-0.84; detailed in legends to Fig. 4.6). There was no effect on responses at longer latencies (50-100 ms gaps). These results indicate an impairment in the gap detection ability of dKOs.

4.2.7 Startle response, PPI and rapid auditory processing in single *Kiaa0319* and *AU040320* KOs

A question that immediately emerges from these findings is whether the observed gap detection deficit also occurs in the absence of only one of the two genes. Single KO mice for either *Kiaa0319* or *AU040320* have not been subjected to this specific task. In the previous study from our laboratory on *Kiaa0319* KO mice, (Martinez-Garay et al. 2017) used a PPI paradigm where cues were prepulses (of 81 dB) of fixed durations with a variable delay to the startle-eliciting stimulus. *AU040320* KOs have not been subjected to any behavioural testing. Based on this, I generated a small cohort of 9-10 single KO mice for *Kiaa0319* and *AU040320* by crossing pairs heterozygous mutants for the loss-of-function allele for each gene. Wildtype littermates from each crossing served as controls.

Baseline/control measurements of sensorimotor gating were conducted first as above. Measures of startle reflex using prepulses only were comparable between *Kiaa0319* KOs and its corresponding wildtype group and repeated measures ANOVA revealed no effect of genotype in the task (Fig. 4.7A; $F=0.35$; $p=0.55$) and similarly for the *AU040320* cohort (Fig. 4.7B; $F=0.02$; $p=0.87$). Differences were also absent in the PPI condition where prepulses served as cues to the startle-eliciting stimulus (Fig. 4.7C, D; $F=0.25$; $p=0.88$ for *Kiaa0319*; $F=1.8$; $p=0.18$ for *AU040320*).

In the absence of deficits in these tests, single KO mice were subjected to the silent gap detection task. The decrease in attenuation score was observed for all groups as gap duration increased (indicating reduced startle reflex and, therefore, increased inhibition; Fig. 4.8A, B). Repeated-measures ANOVA with gap duration as a within-subject factor revealed no differences between *Kiaa0319* KOs and wildtypes ($F=1.99$; $p=0.16$) or between *AU040320* KOs and wildtypes

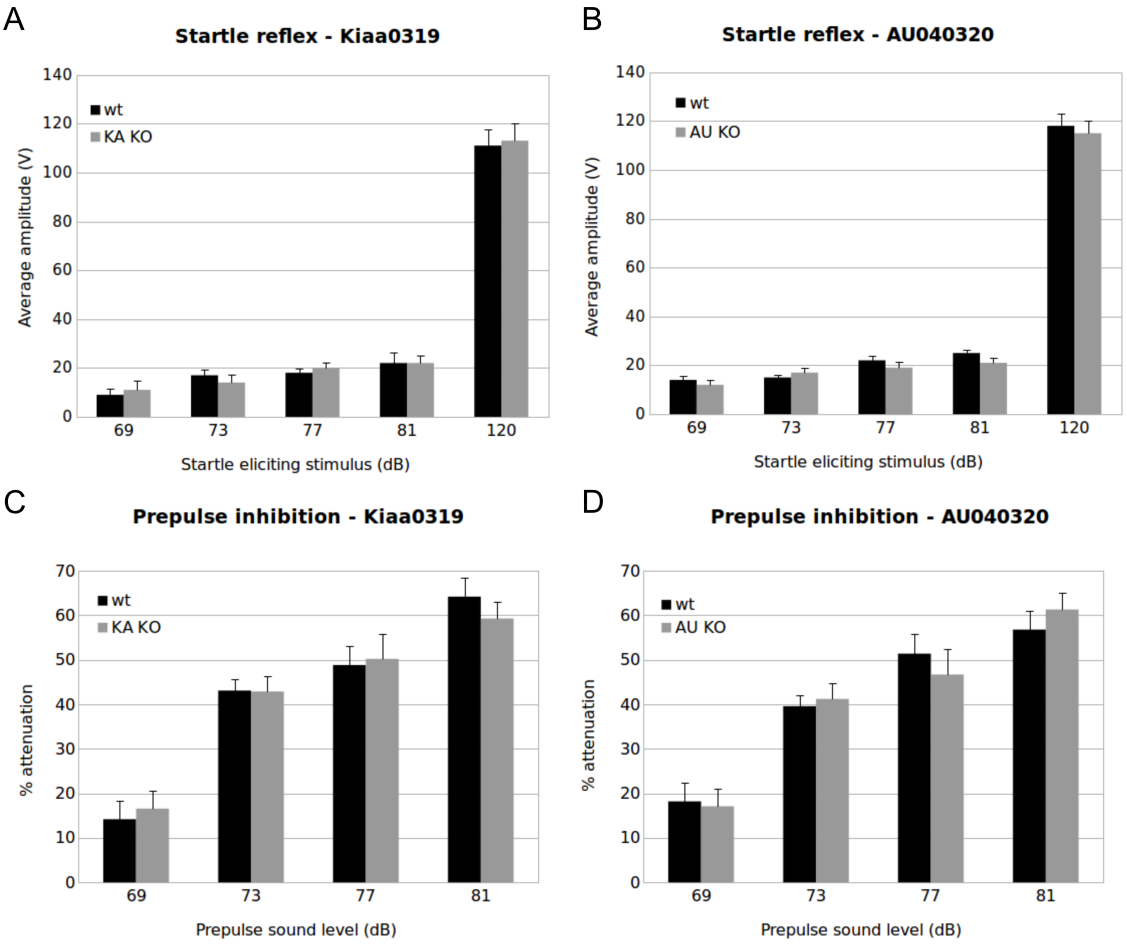


Figure 4.7: Normal startle reflex and prepulse inhibition in *Kiaa0319* and *AU040320* single KOs. (A, B) Startle reactivity (V) to simple pulses at different sound pressure level intensities for *Kiaa0319* (A) and *AU040320* (B) single KOs. (C, D) Percentage inhibition of startle reflex when preceded by prepulse cues of different sound intensity levels above background noise (dB) for *Kiaa0319* (C) and *AU040320* (D); *Kiaa0319*, n=9 per genotype; *AU040320*, n=10 per genotype. Data shown as means; error bars indicate ±SEM.

(F=1.2; p=0.28). No significant effect was found when considering genotype x gap duration as between-subject factors either. These results indicate that absence of KIAA0319 or AU040320 alone does not impair startle reflex and sensorimotor gating or lead to a deficit in gap detection.

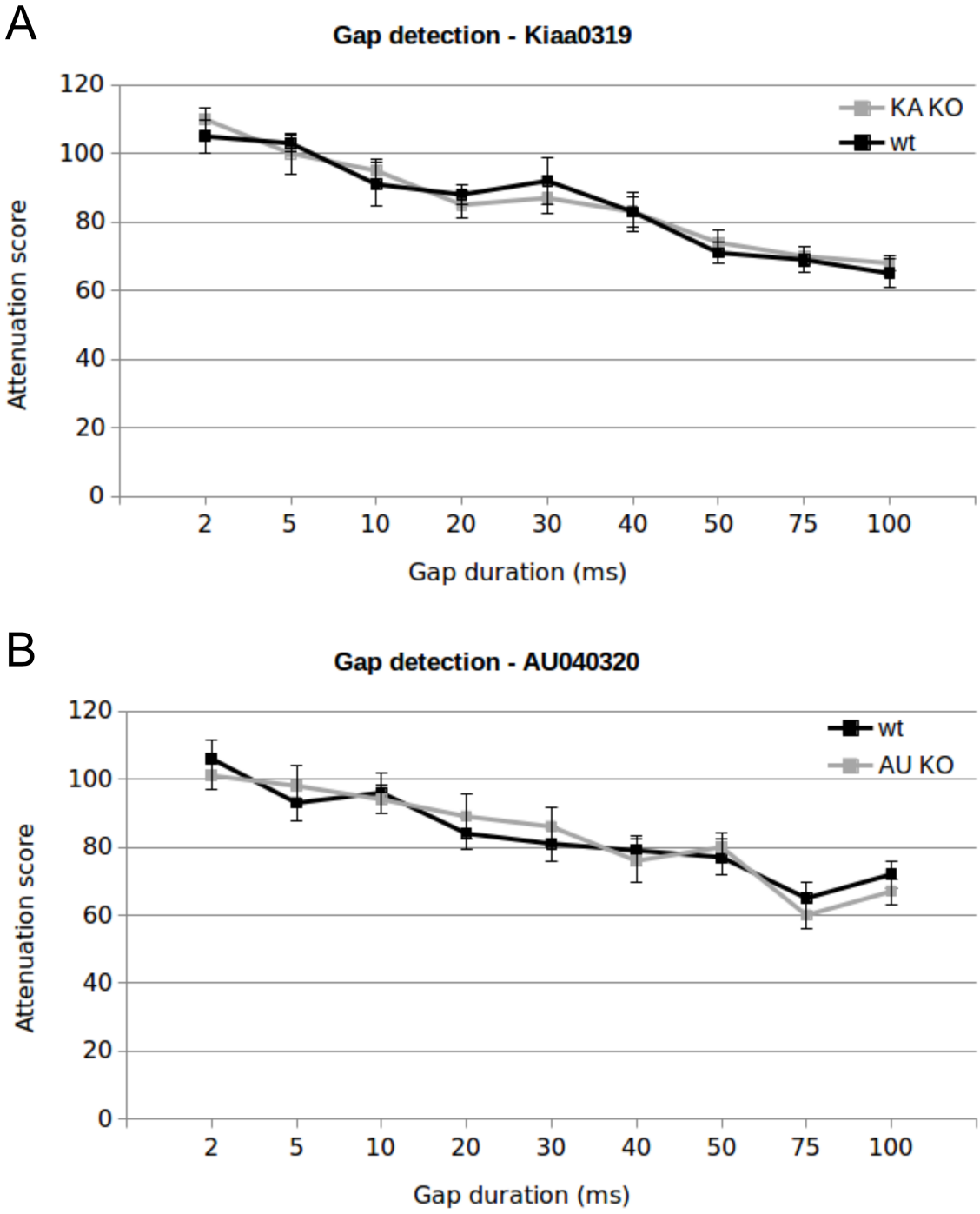


Figure 4.8: Normal silent gap detection in single Kiaa0319 and AU040320 KO mice. Both Kiaa0319 (A) and AU040320 (B) cohorts exhibit the expected decrease in attenuation score (indicating higher inhibition of startle) as gap duration increases; Kiaa0319, n=9 per genotype; AU040320, n=10 per genotype. Data shown as means; error bars indicate ±SEM.

4.2.8 Impaired auditory brainstem responses in *AU040320* and double KO mice

The results above indicate that auditory processing is impaired in dKO mice. However, a deficit in gap detection may result from alterations in a number of different points along the auditory pathway, from a basic hearing deficit affecting the ear/cochlea such as in tinnitus to problems at higher levels in the auditory thalamus and the cortex (Fournier & Hébert 2013; Weible et al. 2014; Anderson & Linden 2016). Given both *Kiaa0319* and *AU040320* are expressed in the cochlea (Scheffer et al. 2015; Liu et al. 2014; Kwan et al. 2015), I decided to assess whether the absence of the two encoded proteins may affect auditory processing at low levels in the pathway by recording auditory brainstem responses (ABRs). ABR is an evoked measure of electrophysiological activity in the peripheral areas of the auditory system (cochlea/auditory nerve) and the lower parts of the central auditory system such as the cochlear nuclei, lateral lemniscus, superior olivary complex and the inferior colliculus. It provides information on the synaptic activity of neuronal populations along the afferent auditory pathway and, in mice, it is typically characterised by 4-5 consecutive potentials (waves I to V; Fig. 4.9), each roughly corresponding to different components of the peripheral auditory system (Henry 1979).

Experiments were conducted in two different age-matched cohorts: (a) a first cohort of dKOs vs wildtype animals obtained in the same way as the behavioural cohorts described above were tested at 10-12 weeks old, preceding the onset of age-related hearing loss in C57BL/6J that initiates around 12-14 weeks (Hunter & Willott 1987; Ison et al. 2007); (b) following that, groups of single KO for *Kiaa0319* and for *AU040320* with littermate wildtype animals pooled together as controls were tested at slightly older age (~14 weeks old). Tests used a number of different stimulus types using white noise click sounds at different sound intensity levels (dB SPL). Each cohort included both male and female animals (for details, see Materials and Methods). There were only minor effects of either gender or age on the ABR measures used for analysis of genotype effects. All data is shown in

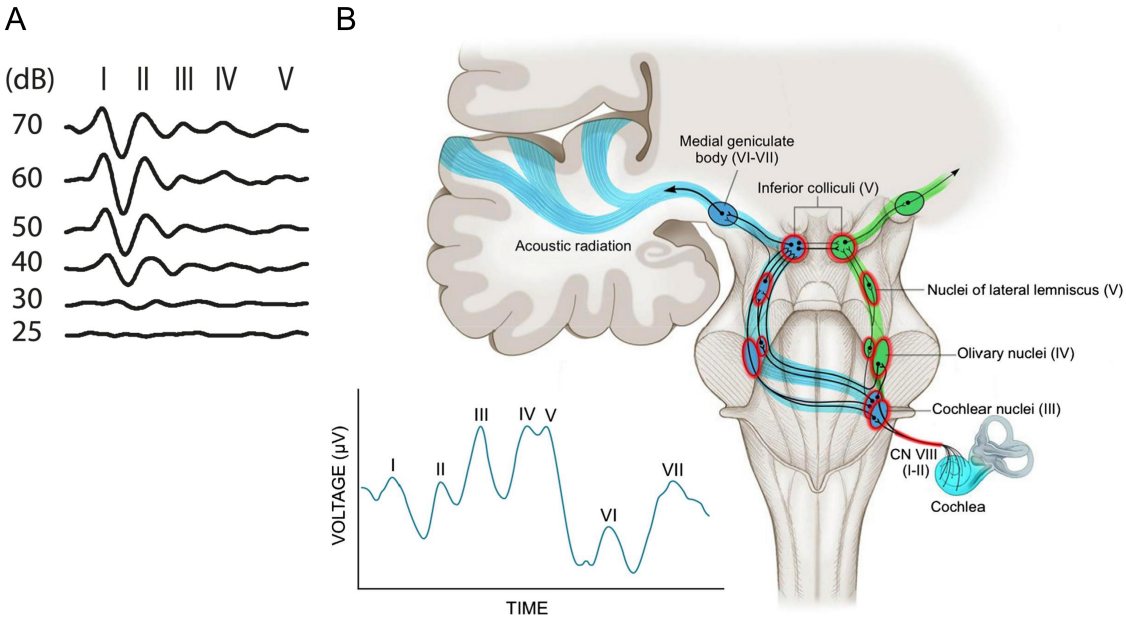


Figure 4.9: Auditory brainstem responses. (A) Example of raw traces of ABRs recorded in mice using simple noise clicks at different sound intensity levels (dB). Labels I-V indicate different wave peaks. Adapted from Li et al. 2015. (B) Schematic representation of components of the auditory pathway in humans with a proposed correspondence between anatomical location and ABR wave. The afferent pathway is represented in blue whilst green indicates efferent pathway. Note that the precise relationship between ABR wave and anatomical sites is a matter of dispute (Henry 1979); image adapted from the Hearing Foundation of India (http://www.hearingfoundation.in/).

the appendix with graphs and tables of statistical tests conducted (see Appendix section B. The only significant differences observed were in click ABR experiments: between dKO and dWT for wave III latency (RM-ANOVA (group x sound level x gender) p=0.01; F=7.971), and between age and wave I amplitude for AU040320 KO mice (C, p=0.004). Given these effects are very small, all comparisons were conducted with groups collapsed from here onwards.

4.2.8.1 ABR thresholds

As an initial examination of hearing, ABR thresholds for noise click stimuli were calculated for the different animal groups. Threshold was defined as the lowest sound level where 2 ABR wave peaks elicited by clicks could be reliably detected. The majority of animals exhibited a threshold of 30-40 dB SPL. Figure 4.10 shows the percentage of animals for each threshold value within this range. No significant

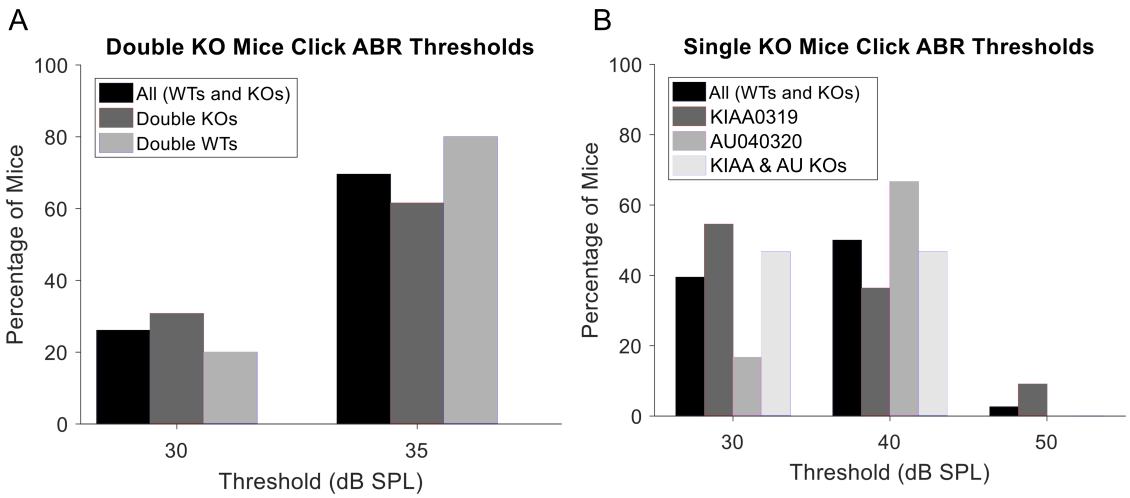


Figure 4.10: Click ABR thresholds (A) Bar chart showing percentage of animals showing 30 and 35 dB SPL thresholds for dKOs (dark grey), wildtype (light gray) and all animals together (black). (B) Bar chart for percentage of animals within the 30, 40 and 50 dB SPL thresholds for all animals (black), *Kiaa0319* KOs (dark gray), *AU040320* KO (medium gray) and wildtype littermates (light gray).

differences were detected for animals within the groups or between them (non-parametric tests, Wilcoxon rank-sum; $p > 0.05$). These results indicate that the overall hearing sensitivity of the tested animals is similar.

4.2.8.2 Reduced wave amplitudes indicate altered auditory processing in *AU040320* and dKO mice

Responses were then assessed for amplitude and latency for each wave at the different sound intensity levels to which animals were exposed. These measures were determined from wave peaks and their corresponding troughs identified manually. Each wave was scored three times for each dataset and their mean was used for subsequent analyses.

For wave amplitudes in the dKO cohort, repeated measures ANOVA with genotype as a between-subject factor and sound level as within-subject factor revealed a significant effect in wave I (4.11A; F=5.536, p=0.002) and *post-hoc* Tukey tests with genotype x sound level as factors revealed a significant reduction in responses at 80 dB only (p=0.02). For wave II, comparisons across sound levels were also significant (F=2.855, p=0.043) but Tukey tests did not reveal significant

differences when comparing responses to individual sound levels. No differences were detected across sound levels for waves III and IV (p=0.317 and p=0.258, respectively). *Post-hoc* Tukey tests showed an effect of genotype x sound level in wave III for each condition (50dB p=0.01, 60dB p=0.01, 70dB p=0.019, 80dB p=0.036) but none for wave IV. Analyses of peak latencies for the dKO cohort did not reveal any significant differences when compared to wildtype controls (Fig. 4.11B).

It is important to note that the significant differences in wave amplitudes identified are relatively small, particularly in light of the multiple statistical tests involved. Whilst this may mean that the observed differences could be obtained by chance and the results must be interpreted with caution, they suggest a subtle but consistent shift towards lower response amplitudes in dKO animals compared to wildtypes.

In the single KO cohorts, *Kiaa0319* mutants displayed no differences in any wave amplitudes or latencies at any of the sound levels tested (Fig. 4.12). However, for *AU040320* KOs, whilst comparisons across sound levels revealed no amplitude differences between the genotypes, small but significant differences were identified in *post-hoc* Tukey tests for wave III in responses to clicks at 50, 60 and 80 dB, as well as in wave IV for 80 dB (all, $p<0.05$). In all these conditions, as it in the case of dKOs above, the amplitude of responses from *AU040320* mutants were lower than those of wildtypes (Fig. 4.12A). For wave IV latency, however, *AU040320* mutants displayed higher amplitude (Fig. 4.12A). Comparison of latencies of the responses in *AU040320* KOs by repeated-measures ANOVA only showed a difference for latencies to wave II, irrespective of sound level (F=3.241, p=0.027), although these did not hold when individual comparisons were performed. Moreover, inspection of means shows the effect to be inconsistent: whilst at 50 dB *AU040320* mutants display a higher average mean latency to wave II than wildtypes, the opposite pattern is observed for means at 80 dB (Fig. 4.12B, top right).

These results indicate *AU040320* KOs may have impaired wave amplitude responses within the central auditory system. However, similarly to the case of

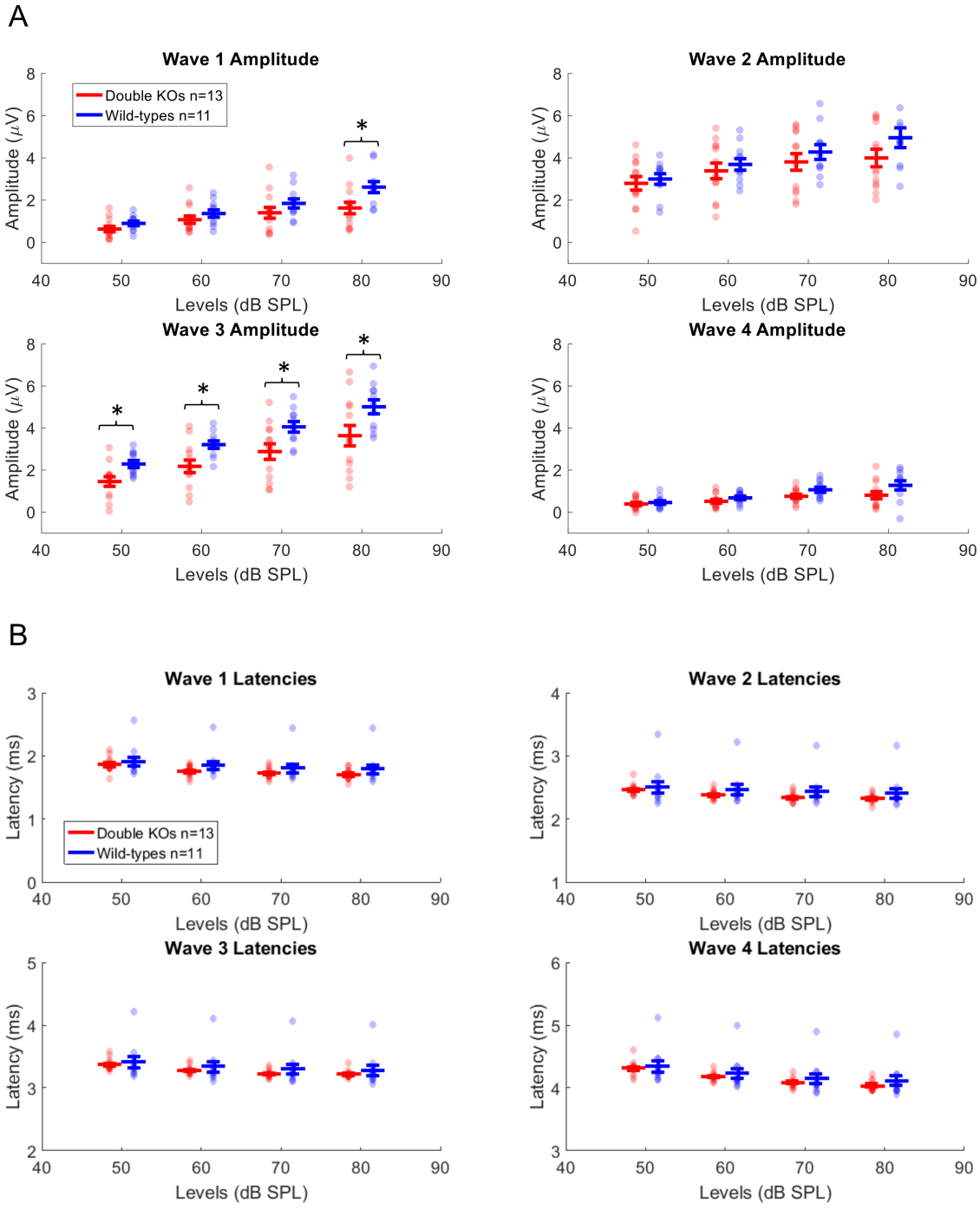


Figure 4.11: Peak amplitudes and latencies for dKO and wildtype controls in click ABRs (10 clicks/sec). Scatter plots showing amplitude (A, μV) and latency (B, ms) for each animal per genotype (wt, blue; dKO, red) at different supra-threshold sound levels (dB SPL). Straight lines indicate group mean; error bars ± SEM. * denote significant differences in *post-hoc* Tukey tests ($p<0.05$).

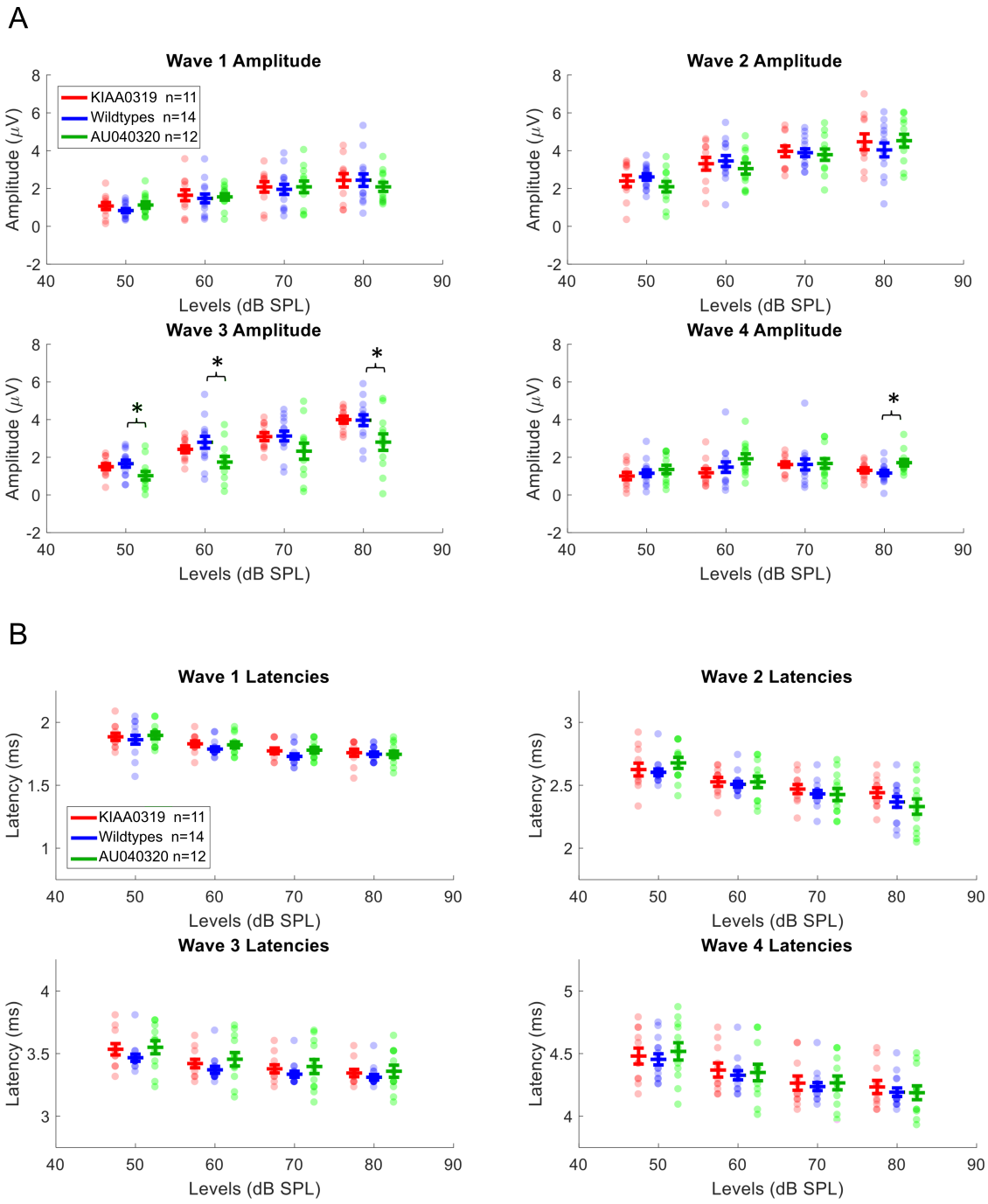


Figure 4.12: Peak amplitudes and latencies for wildtype, *Kiaa0319* and *AU040320* KO mice in click ABRs (10 clicks/sec). Scatter plots showing amplitude (A, μ V) and latency (B, ms) for each animal per genotype (wt, blue; *Kiaa0319* KO, red; *AU040320* KO, magenta) at different supra-threshold sound levels (dB SPL); straight lines indicate group mean; error bars ± SEM. * denote significant differences in *post-hoc* Tukey tests ($p<0.05$).

dKOs above, caution is required when considering these results given the large number of statistical tests performed on the same data.

In order to probe into this putative deficit further, animals were tested on a similar sequence of click stimuli but with a slower click rate, with an inter-trial interval of 500 ms (10 clicks/sec), as opposed to the 100 ms in the 'fast' click rate of the experiments above (2 clicks/sec). Such longer interval between each click allows more time for neurons responding to the previous stimulus to recover and return to its baseline state by the time the next click is presented (Abbas & Gorga 1981). If there are indeed subtle deficits as the data above indicates, these experiments should be able to detect them more reliably. However, only single KO mice were subjected to this task.

Similarly to the experiments above, responses from *Kiaa0319* KO mice did not display significant differences from those of wildtype controls in amplitude or latency. For *AU040320* mutants, repeated-measures ANOVA across sound levels did not reveal significant differences for any of the wave amplitudes. However, results for wave III almost reached the statistical significance threshold (p=0.056) and *post-hoc* Tukey tests comparing responses between mutants and controls for each sound level revealed significant differences for all conditions (Tukey tests: 50 dB p=0.024; 60 dB p=0.002; 70 dB p=0.01; 80 dB p=0.011). In each of them, wave III amplitudes in *AU040320* KOs were lower than in wildtypes, as it was the case in the 'fast' click rate above (Fig. 4.13A). No other waves displayed significant differences.

With respect to wave latencies in these *AU040320* mutants, comparisons of means by repeated-measures ANOVAs identified marginally significant differences in wave II and III (F=2.75, p=0.048; F=2.75, p=0.048, respectively) but no statistically significant differences were observed in *post-hoc* Tukey tests for individual sound levels (Fig. 4.13B). Whilst these results are not very robust statistically, they confirm the findings of impaired wave III amplitudes in *AU040320* KOs observed in the faster click rate above. This is also consistent with the findings obtained

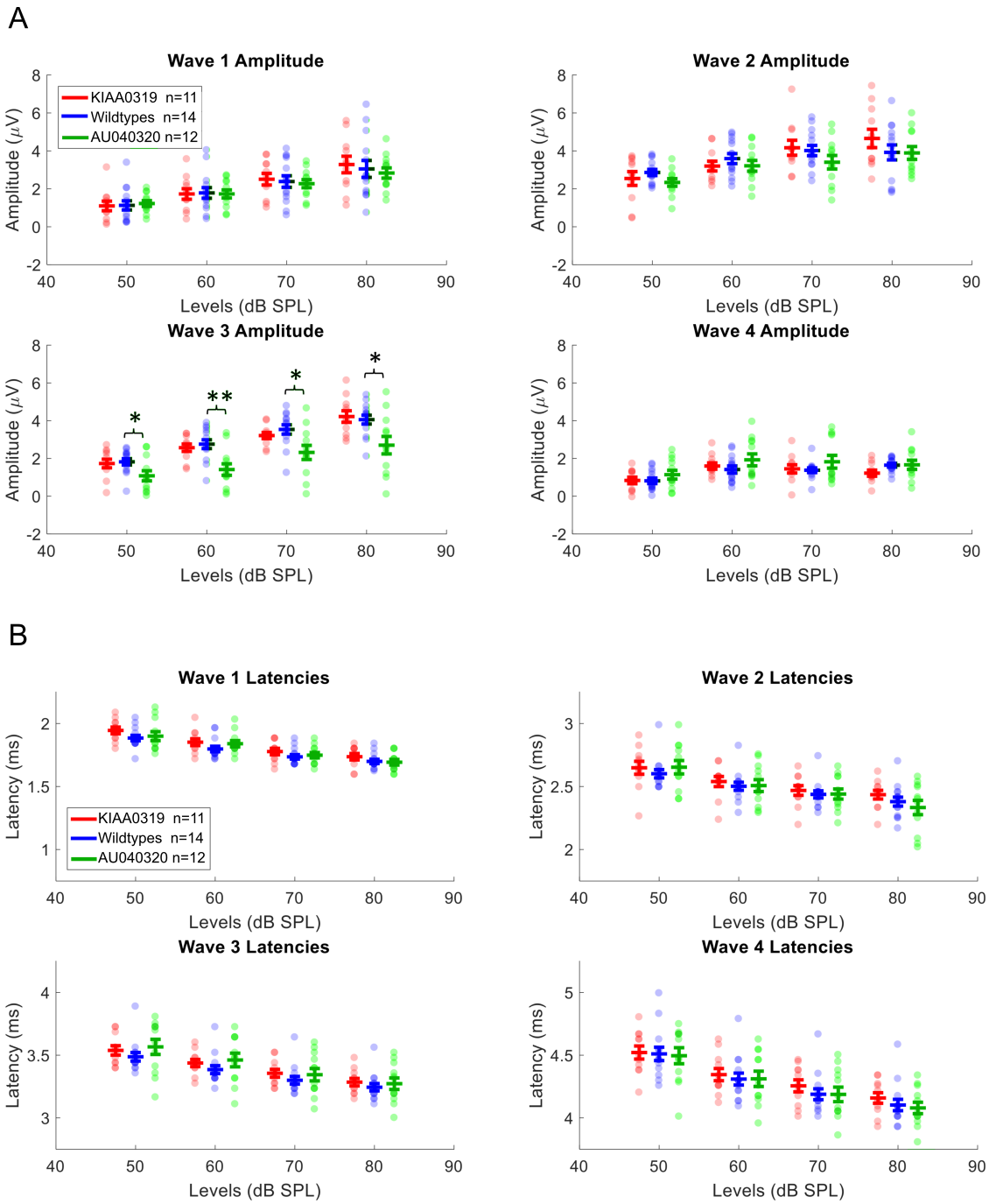


Figure 4.13: Peak amplitudes and latencies for wildtype, *Kiaa0319* and *AU040320* KO mice in click ABRs a slow click rate (2 clicks/sec). Scatter plots showing amplitude (A, μ V) and latency (B, ms) for each animal per genotype (wt, blue; *Kiaa0319* KO, red; *AU040320* KO, magenta) at different supra-threshold sound levels (dB SPL); straight lines indicate group mean; error bars ± SEM. * denote significant differences in *post-hoc* Tukey tests ($p<0.05$).

with dKOs and may indicate the presence of a small deficit in the firing pattern of these animals that are hard to detect in an indirect measure like the ABR.

4.2.8.3 ABR deficits in *AU040320* and double KOs in response to sounds in noise suggest impaired temporal processing

In light of the putative temporal processing deficit identified by the silent gap detection experiments above (see section 4.2.6) and the suggested impairment in waves II and III in the ABR experiments just described, more fine-grained tests were performed to probe into the putative auditory processing deficit in the mutants examined here. For this, responses were recorded from clicks presented at different time points following a noise burst of 200 ms: the first click (probe click) followed the noise by 20 ms, whilst the second stimulus (reference click) was presented at 500 ms after the end of the noise (see Fig. 4.14A). Such 'masker-probe' experiments compare the responses to clicks preceded by noise (i.e. probes; the first click, 20 ms after the end of noise) to the responses to clicks preceded by silence (i.e. references; the second click, 500 ms after the end of noise). Such stimuli are often used to assess more temporal aspects of auditory processing (Lasky 1991; Mai et al. 2015) and have been shown to reveal deficits in cases of language-impaired individuals (Rosen 2003; Basu et al. 2010). All stimuli were of 60 dB SPL. Responses (amplitudes or latencies) to reference and probe clicks were then plotted for each wave and a best fit line was calculated to describe the wildtype responses. The number of KO responses deviating from this best fit line was then calculated and statistical comparisons performed using a binomial cumulative distribution function to determine any significant deviations.

Similarly to the simple clicks above, responses from *Kiaa0319* KO mice showed no alterations in comparison to controls. For *AU040320*, there was a statistically significant difference in the amplitudes of wave II alone (binomial cumulative distribution, p=0.006). The amplitudes of responses in mutants were found to generally fall below the best fit line determined from wildtypes, showing that responses to probe clicks had smaller amplitudes than in wildtype controls, despite

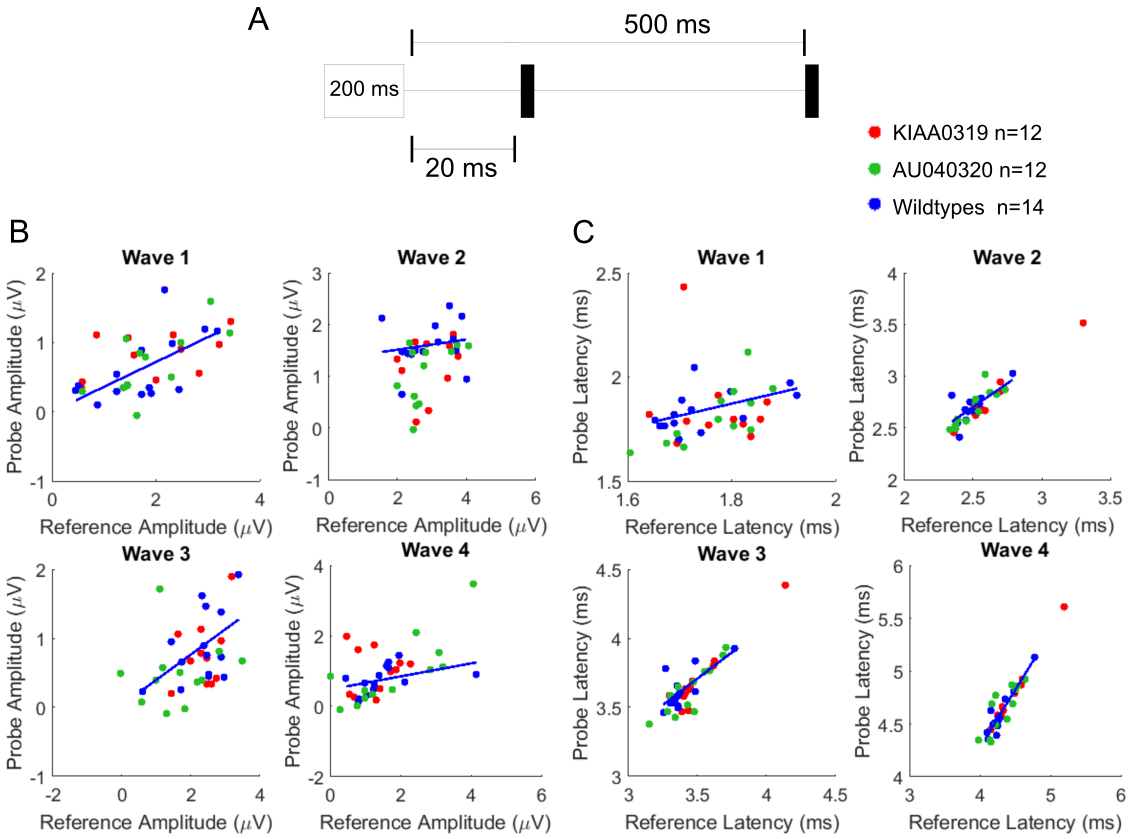


Figure 4.14: Comparisons of responses to sound clicks following noise (probe click) with responses to clicks following silence (reference click) in wildtype (blue), *Kiaa0319* (red) and *AU040320* (green) KO mice. Scatterplots with individual animal responses in masker-probe experiments showing wave amplitudes (B) and latencies (C). Blue line indicates best fit for wildtype animals and number of mutants deviating from this were used for statistical comparisons with binomial test. *AU040320* KO mice showed impaired wave II amplitudes.

similar responses to reference clicks (Fig. 4.14B). All other wave amplitudes in *AU040320* mutants appeared normal and similarly for their corresponding wave latencies (Fig. 4.14C). Note that some data points of the *Kiaa0319* KO group fall considerably distant from most of the data and thus have high leverage, particularly in the latency plots. Whilst this could perhaps skew results slightly, it appears unlikely that these data points are masking real differences between the groups as the rest of the data points appear to cluster similarly to wildtypes.

In the case of dKOs, wave amplitudes were comparable to those of wildtypes (Fig. 4.15A) but differences were observed in the case of latencies of wave II and III

(binomial tests, p=0.003 in both cases). In both cases, the latency to wave peaks in probe clicks (y-axis) are longer in dKOs than in wildtypes (Fig 4.15B). For wave III, latencies to reference clicks in dKOs also appear longer than in wildtypes. Similarly to the case of *Kiaa0319* KOs above, wildtype data appears to contain a measure with high leverage that falls further from the main cluster of data points. Thus, it is possible that this animal is driving or obscuring possible differences.

Double *Kiaa0319;AU040320* mutants were also tested on variants of this masker-probe stimulus where different delays to probe clicks were used. Whilst the probe clicks in the previous tests followed the offset of noise by 20 ms (detailed in Fig. 4.14A), these new stimuli had probe clicks presented either 8 or 50 ms after the noise bursts.

For probe delays of 8 ms, the responses of dKOs and wildtypes did not differ (data not shown). However, longer probe delays, at 50 ms, led to altered responses in dKOs in wave III for both amplitude and latency (p=0.003 and p<0.001, respectively). The plotted data shows that most dKO animals had wave III amplitudes that were considerably smaller for both probe and reference clicks as they fell below the best fit line of wildtypes (Fig. 4.15C). Small wave III amplitudes were also detected in the simple click experiments above (section 4.2.8.2). With respect to the observed differences in wave III latency, responses to probe clicks in dKO clustered altogether (some data points overlap) and they did not diverge dramatically from wildtypes, but the majority of them had values above the best fit line (Fig. 4.15D). However, it is possible that the wildtype data point with high leverage may be skewing the best fit line and, consequently, the statistical difference.

A flow chart detailing the experimental progression and experience of each of the two cohorts is shown in Fig. 4.16 for clarity.

Altogether, these data indicate that absence of AU040320 alone can lead to altered brainstem responses in wave III (but not in earlier waves) and that its combined absence with KIAA0319 can lead to more profound effects in early auditory processing that may be linked to temporal processing.

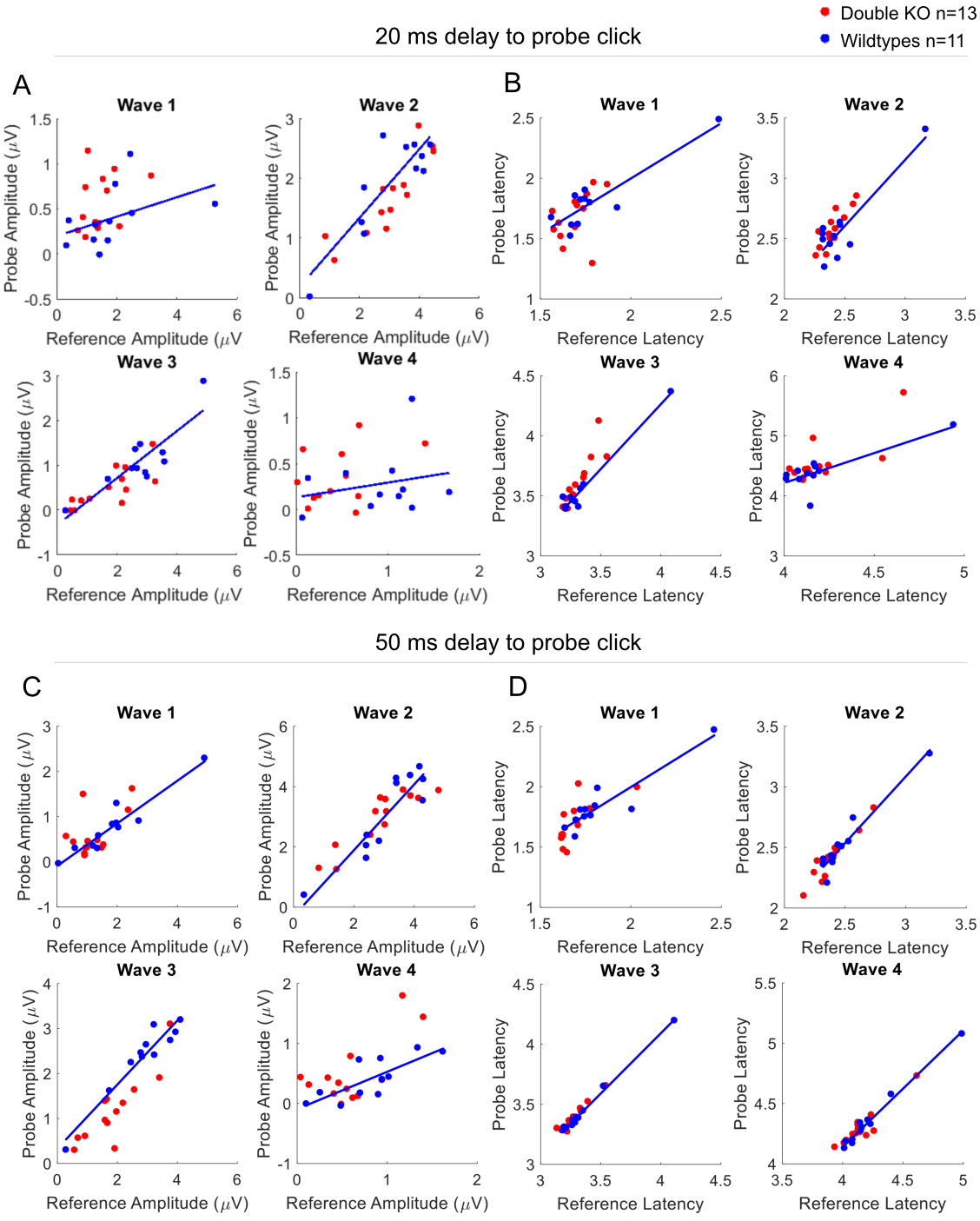


Figure 4.15: Double KO mice show impaired wave III in responses to clicks 20 and 50 ms after noise. (A, B) Comparisons of responses between clicks following noise and following silence in wildtype (blue) and dKO (red) mice. Scatterplots with individual responses in 20 ms condition showing wave amplitudes (A) and latencies (B). Double KO showed differences in latencies to wave II and III. (C, D) Comparisons of responses to clicks 50 ms after noise showing amplitudes (C) and latencies (D). In both cases, there were significant differences in wave III. Blue line indicates best fit for wildtype animals.

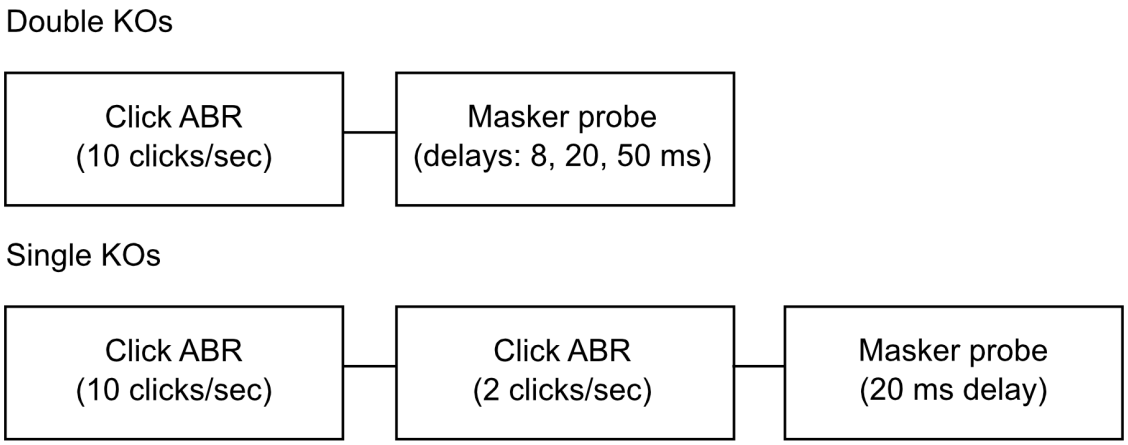


Figure 4.16: Flow-chart of experimental progression of double and single cohorts in ABR experiments.

4.2.9 Expression of *Kiaa0319* and *AU040320* in the lower auditory pathway

These results indicate the presence of structural or functional abnormalities in the auditory pathway of *AU040320* and *Kiaa0319;AU040320* mutants, with defects in wave III often associated with activity between the cochlear nucleus and the inferior colliculus. In order to gain a better insight into its nature and possible structural abnormalities, I decided to validate the expression of *Kiaa0319* and *AU040320* in the auditory lower pathway by using the *lacZ* reporter gene in the trapping cassette of the KO alleles of both mutant lines (see Chapter 3 and Martinez-Garay et al. (2017)). X-gal stainings show very low and limited expression of *Kiaa0319* as positive cells were only observed in the areas around the superior olivary complex but not in the cochlear nuclei or the inferior colliculus (IC; Fig. 4.17B). For *AU040320*, x-gal staining was virtually ubiquitous across the different brain regions and strongly observed in the cochlear nuclei (Fig. 4.17D), superior olivary complex (Fig. 4.17E) and the different compartments of the inferior colliculus (Fig. 4.17F).

Beyond the brainstem, genome-wide expression studies of cells in the inner ear in the Shared Harvard Inner Ear Database (SHIELD, https://shield.hms.harvard.edu/; Shen et al. 2015) show that both *Kiaa0319* and *AU040320* have detectable but low expression in hair cells and auditory nerve cells over the course of development,

although they are upregulated in postnatal stages (Scheffer et al. 2015; Liu et al. 2014). On the other hand, *AU040320* appears to have considerably strong expression in otic cells (within the top 10% of most highly expressed genes), the progenitor population in the inner ear that will give rise to hair cells and supporting neurons (Kwan et al. 2015).

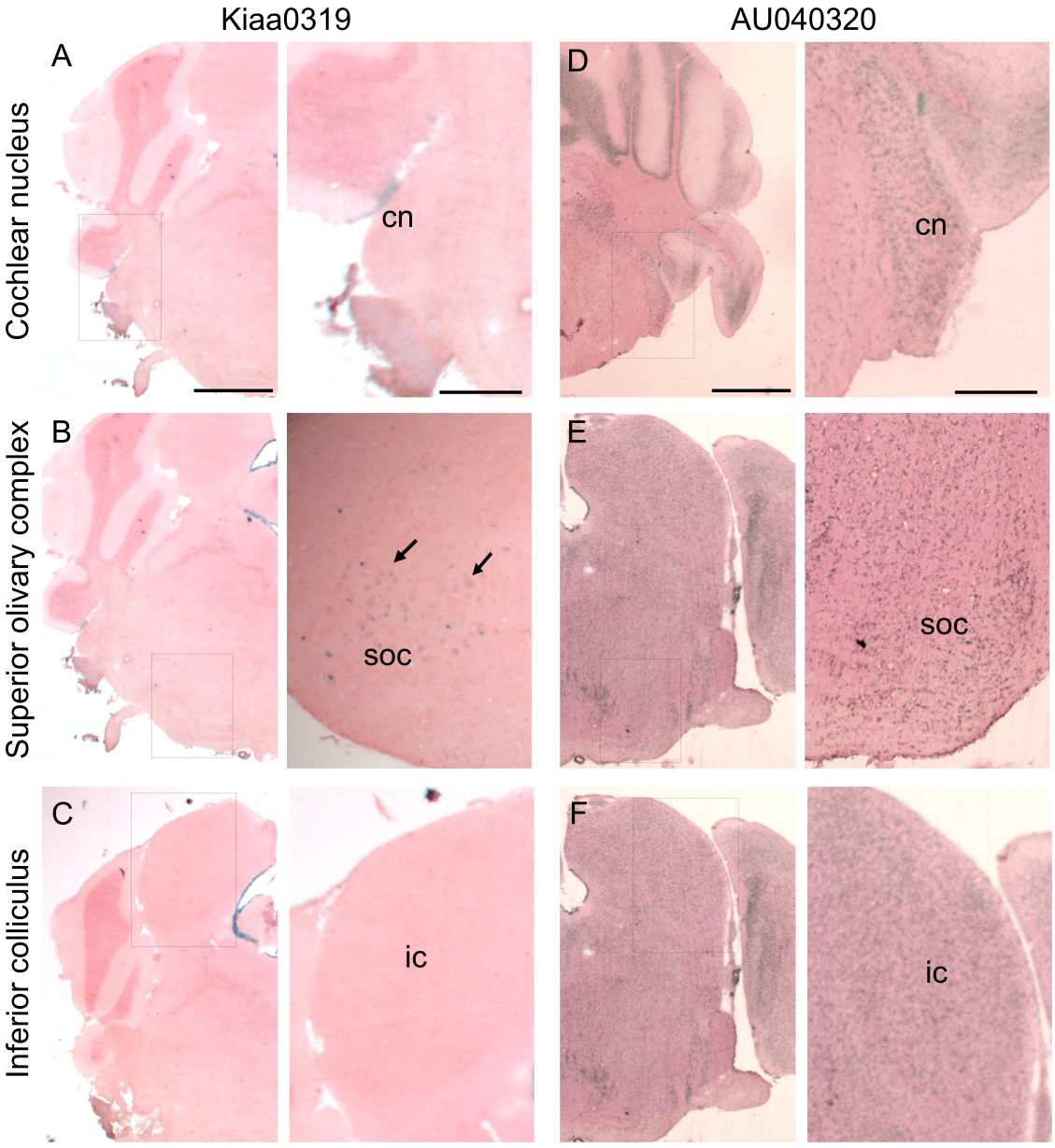


Figure 4.17: Expression of *Kiaa0319* and *AU040320* in the adult lower auditory pathway by X-gal staining. (A-C) Expression of X-gal in *Kiaa0319* mutants is only detected in a few cells around the superior olivary complex (B, arrows) but absent in the cochlear nuclei and the inferior colliculus. (D-F) *AU040320*-induced X-gal expression displays widespread distribution across different areas of the midbrain. Cn, cochlear nuclei; soc, superior olivary complex; ic, inferior colliculus. Scale bars: 1000 μm; insets, 600 μm

4.2.10 Synapse number in the auditory pathway of dKO mice

Several lines of evidence point towards a potential role for *Kiaa0319* and/or *AU040320* in synaptogenesis: (a) both proteins are predicted to be adhesive cell surface glycoproteins with Ig-like domains, features commonly seen in proteins important for synaptogenesis, maintenance and plasticity (Gerrow & El-Husseini 2006; Dalva et al. 2007; Katidou et al. 2008; Missler et al. 2012); (b) expression of *Kiaa0319* peaks during early development across the brain when synaptogenesis is taking place (see Fig. 1.9 in section 1.4.4); (c) KIAA0319L has been reported to interact with Nogo receptor (*NgR*) which has been previously linked to synapse number (Wills et al. 2012) and work from the Monaco laboratory suggests potential interactions with other proteins linked to synapse formation such as NCAM, SrGAP2, Neurexin I, although this remains to be confirmed. To assess whether impaired synaptogenesis may be a cellular correlate of the behavioural and physiological deficits identified in the auditory system of *Kiaa0319/AU040320* mutants, I investigated whether absence of these proteins may alter the number of synapses in three parts of the adult auditory system: the ventral cochlear nucleus (VCN), the central nucleus of the inferior colliculus (CIC) and the ventral nucleus of the medial geniculate body (MGBv) of the thalamus. The first corresponds to an easily identifiable anatomical structure that may correspond to the defect in wave III (Henry 1979), although the specific correspondence between ABR wave and anatomical location is imprecise and still a matter of debate (Møller et al. 1981). Earlier analysis also indicated a putative effect on wave V of ABRs but the corresponding signals are not robust enough for a precise analyses - nonetheless, I included this structure in the study of synaptic number as a way to assess this in more detail; and MGB was used as a point to assess putative deficits higher in the auditory pathway. The same animals tested in the behavioural task were used for these experiments. This initial investigation used an immunohistochemical method to determine the number of synaptic puncta by co-localisation of a pre-synaptic marker, VGlut1 or VGlut 2 (vesicular glutamate

transporter 1/2), and a post-synaptic one, PSD-95 (post-synaptic density protein 95) across a 5 μm depth of a specific anatomical location using co-localisation of the differently coloured pixels. This approach exploits the distinct localisation of these markers in synapses (axons and dendrites, respectively) as well as their close proximity to show them as co-localising (Varoqueaux et al. 2006; Ippolito & Eroglu 2010; Cao et al. 2013; Risher et al. 2014).

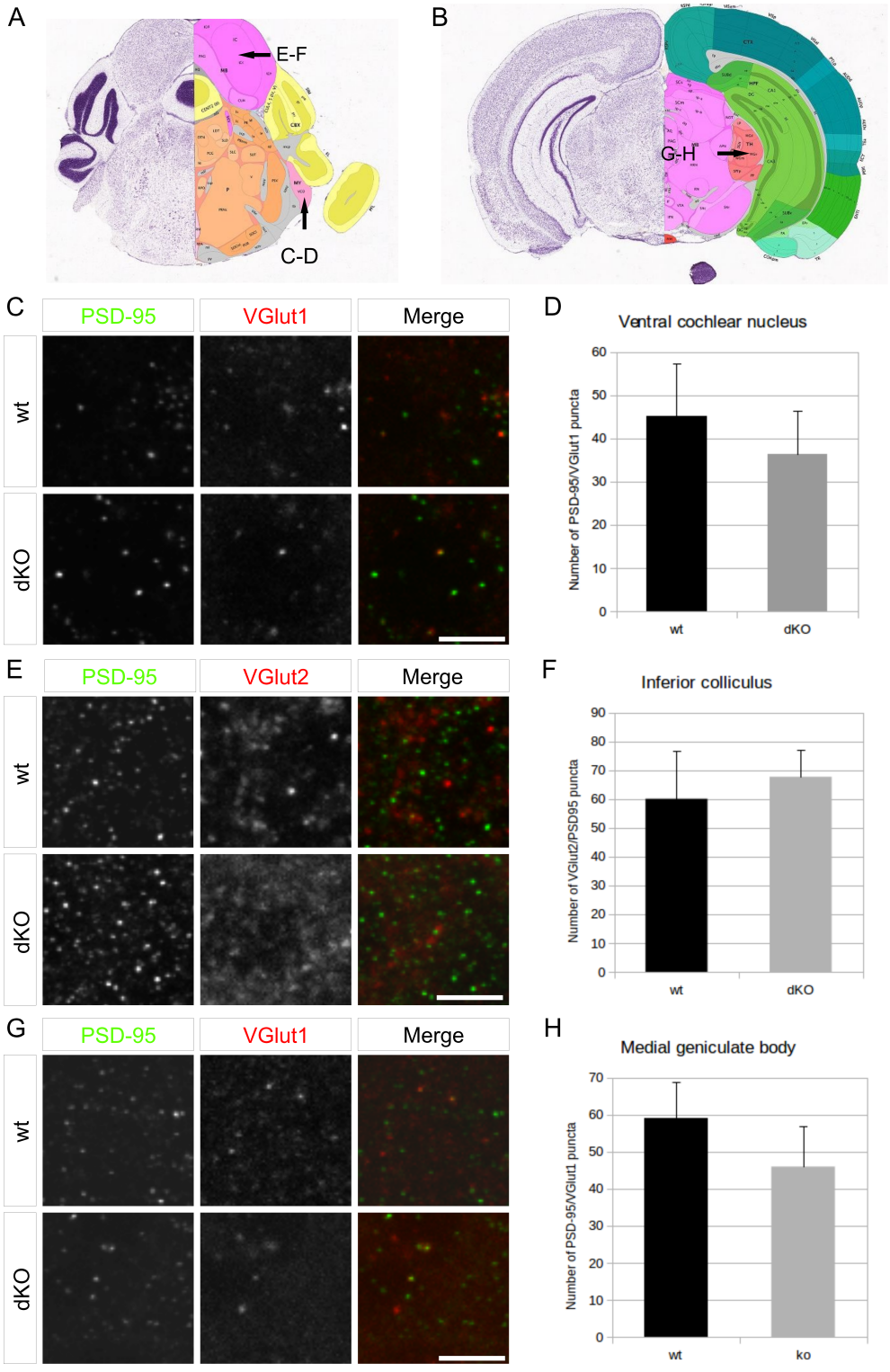

A
E-F
C-D
B
G-H
C
PSD-95
VGlut1
Merge
wt
dKO
D
Ventral cochlear nucleus
Number of PSD-95/VGlut1 puncta
0
10
20
30
40
50
60
wt
dKO
E
PSD-95
VGlut2
Merge
wt
dKO
F
Inferior colliculus
Number of VGlut2/PSD95 puncta
0
10
20
30
40
50
60
70
80
90
wt
dKO
G
PSD-95
VGlut1
Merge
wt
dKO
H
Medial geniculate body
Number of PSD-95/VGlut1 puncta
0
10
20
30
40
50
60
70
wt
ko

Figure 4.18: Absence of KIAA0319 and AU040320 does not affect the number of synaptic puncta in the ventral cochlear nucleus, inferior colliculus and medial geniculate body. (A-B) Images from the reference atlas of the Allen Institute (http://brain-map.org/) indicating brain regions used for analyses showing the ventral cochlear nucleus (C-D), central nucleus of the inferior colliculus (E-F) and the medial geniculate body (G-H). (C-H) Immunohistochemical quantification of synapses by co-localisation of post-synaptic marker PSD-95 (green) and presynaptic markers VGlut1 or VGlut2 (red) at different points of the auditory pathway. (D, F, H) Graphs indicating number of co-localised puncta for each of the regions examined where no difference between mutants and controls were identified (n=3, 3 sections/brain and 3 brains/genotype; $p>0.05$). Error bars indicate ± SEM. Scale bars: 5 μm.

Analyses were first conducted in the VCN as it corresponds to one of the regions likely to correlate to the ABR deficits described above. Comparison of the number of co-localised VGlut1/PSD-95 puncta between dKOs and wildtype cochlear nuclei did not significantly differ between the two conditions (Fig. 4.18C-D; n=3, F=0.65; p=0.56). The central nucleus of the inferior colliculus was examined next (indicated in Fig. 4.18A) given it is the main target of fibers coming from the cochlear nuclei, the superior olivary complex and from the descending thalamic and cortical projections; and, thus, it is a synapse-rich region critical for auditory function (Nakamoto et al. 2008). Given there is no VGlut1 expression in the adult IC, VGlut2 was used as a pre-synaptic marker. There was no effect of genotype in quantifications of the number of co-localised puncta in the IC (Fig. 4.18E-F; F=0.16; p=0.69). I then turned to the primary auditory nucleus in the thalamus, the MGB, specifically the ventral nucleus as it is the most easily distinguishable anatomically (Fig 4.18B). Quantifications also revealed no differences in the number of VGlut1/PSD-95 puncta between the two genotypes (Fig. 4.18G-H; F=0.8; p=0.38). These results indicate that absence of KIAA0319 and AU040320 does not lead to major impairment in the number of synapses in these components of the auditory pathway.

4.3 Discussion

The series of experiments described here investigated potential behavioural deficits that might result from the absence of KIAA0319 and AU040320 in mice, with a particular focus on auditory processing. The results reveal that double KO mice displayed normal levels of locomotor activity in the open field and unaltered performance in the accelerating rotarod, in olfactory preference and spatial memory, whilst a potential mild increase in anxiety levels was detected in the light-dark box test. Moreover, auditory tests in the modified PPI gap detection task identified an impairment in psychophysical discrimination of rapidly changing stimuli in these double KOs but which was absent in single *Kiaa0319* or *AU040320* mutants. This deficit was accompanied by altered evoked responses to simple sounds in brainstem electrophysiological recordings that affected predominantly wave III for both *AU040320* and double KOs. More profound effects were detected in the latter case with effects also seen in waves I and II, in line with their more profound genetic manipulation. These results suggest that loss-of-function mutations in *Kiaa0319* and *AU040320* can lead to auditory deficits via underlying abnormalities in the brainstem that result in reduced activity and affect sensory processing early in the pathway.

Although its specific nature remains highly controversial (phonology vs. sensory vs attentional, cortical vs. subcortical, and so on), deficits associated to the auditory system are a hallmark of dyslexia (Ramus 2003; Giraud & Ramus 2013; Goswami 2014; Peterson & Pennington 2015). Impaired temporal acuity and rapid auditory discrimination have been argued to form part of the mechanisms underlying these deficits (Tallal 1980; Temple et al. 2000; Choudhury & Other 2007; Raschle et al. 2014; de Groot et al. 2015; but see also e.g. Breier et al. 2003; Georgiou et al. 2010; Protopapas 2014). The gap detection PPI paradigm used here is specifically designed to exploit parallel temporal sampling processes that are relevant to rodent auditory processing based on mismatch negativity measures and by isolating potential confounds from attention and learning (Friedman et al.

2004; Fitch et al. 2008; Threlkeld et al. 2008; Fitch et al. 2013). Accordingly, genes associated with language disorders such as *DCDC2* and *CNTNAP2* have been linked to impaired temporal auditory processing in rodent models of gene function using this paradigm (Truong et al. 2014; Truong et al. 2015). Similar findings have been reported for rats treated with shRNA against *Dyx1c1* (Threlkeld et al. 2007; Szalkowski et al. 2013), although this has not been confirmed in the genetic KO in mice (Rendall et al. 2015).

With specific reference to *Kiaa0319*, *in utero* knockdown in the developing rat neocortex was reported to lead to subtle deficits in detection of silent gaps of very brief duration (up to 10 ms; but not in longer gaps) as well as in responses to more complex stimuli such as frequency modulating sweeps (Szalkowski et al. 2012). The experiments reported here identified a gap detection deficit within the shorter range of gaps tested (up to 50 ms) but this was only following manipulation of both *Kiaa0319* and *AU040320*, not in single KOs. However, these findings do not preclude the possibility that these mutants are affected in more complex auditory tasks if they could be tested – differences between the rat-mouse auditory system (Rendall et al. 2015), in technology available at the University of Oxford and in Home Office licence regulations impose restrictions on directly testing this. It is expected that the attested gap detection deficit observed in double *Kiaa0319;AU040320* mutants would be accompanied by further problems as task difficulty increases (Friedman et al. 2004; Fitch et al. 2008; Fitch et al. 2013, cf.), as it was the case for *Kiaa0319*-shRNA treated rats (Szalkowski et al. 2012).

These animals were also found to suffer from deficits in spatial memory when tested in the Morris Water maze (Szalkowski et al. 2012). Whilst this specific test was not conducted with the mouse mutants investigated here, testing in the T- and Y-maze did not provide indications of parallel deficits. However, given that shRNA-treated animals only showed impaired memory in cases of hippocampal malformations, it is likely that such behavioural differences result from the wider disruptions caused by this, particularly given the well-known role of the hippocampus

in spatial memory (Martin & Clark 2007). But perhaps more importantly, the differences between shRNA-treated rats and KO mice alongside the issues with shRNA-specificity discussed in Chapter 3 calls for caution when comparing results obtained with these different methods.

The gap detection deficits reported here also expose previous links made in rodents between rapid auditory processing deficits, particularly gap detection, and cortical migration abnormalities such as ectopias and polymicrogyria as they seemed to co-occur (Ison et al. 1991; Fitch et al. 1994; Clark et al. 2000; Frenkel et al. 2000; Peiffer et al. 2004; Higgins et al. 2008; Giraud & Ramus 2013; Truong et al. 2015; Anderson & Linden 2016). A similar overlap has also been proposed for language-impaired populations more generally (Boscariol et al. 2010; Boscariol et al. 2011). However, impaired gap detection in dKOs was not accompanied by cortical migration malformations (see Chapter 3), and parallel results have been observed for *Dcdc2* KO mice in a modified version of the task, for which no deficits in neuronal migration have been found (Wang et al. 2011b; Truong et al. 2014). On the other hand, abnormalities in rapid auditory processing have been reported for *Cntnap2* KOs where a subtle dyslamination of the neocortex has been reported (Peñagarikano et al. 2011; Truong et al. 2015). Thus, the combination of these findings indicates that the relationship between rapid auditory processing and cortical migration abnormalities is weaker than previously thought, if related at all. In any case, this does not rule out a role for cortical abnormalities in gap detection given there is strong evidence for the involvement of the neocortex in this task (Weible et al. 2014).

However, the impaired auditory responses recorded from the brainstem in the mutants under investigation here suggest a more general impairment in auditory processing which occurs even in the context of simple sounds like noise clicks. This highlights that an auditory processing deficit is already present at the lower stages of the auditory pathway. Although there are questions over the statistical robustness of some of the specific differences observed with simple click stimuli, a consistent shift towards lower amplitudes in wave III was detected in both *AU040320* and double

KOs. Moreover, these changes persisted in the more subtle masker-probe tests, including alterations in wave II for double KOs. These animals also presented a small deficit in wave I in responses to simple clicks, although this was not confirmed with the forward-masking experiments.

The locations from which ABR waves originate are still a matter of debate but, in mice, wave I is often thought to represent neural activity in the most peripheral regions in the cochlea and auditory nerve, whilst waves II and III typically correspond to activity derived at some point along the cochlear nuclei and the superior olivary complex, also sometimes along the inferior colliculus (Henry 1979; Møller et al. 1981). Altogether, these results show that absence of AU040320 alone affects neural activity in the auditory brainstem which, when combined with absence of KIAA0319, produce more profound defects in early auditory processing. Evoked responses in the auditory brainstem have been shown to be altered in dyslexic and language-impaired populations more generally (McAnally & Stein 1996; Chandrasekaran et al. 2009; Basu et al. 2010; Hornickel & Kraus 2013) and, interestingly, there are also reports of similar inconsistent responses in pre-reading children carrying specific genetic variants in *KIAA0319* and *DCDC2* (Neef et al. 2015).

This is the first time a gene linked to dyslexia has been shown to affect auditory responses at such early levels in the rodent auditory processing pathway without affecting basic hearing. Previously, mice carrying mutations in another language-related gene, *Foxp2*, has been implicated in brainstem-level auditory deficits using ABR recordings, with more profound effects in earlier waves such as wave I (Kurt et al. 2009). Previous functional genetics work using animal models has followed studies of language-impaired populations that typically focuses on the neocortex and have interrogated the role of the relevant genes in modulating responses in the auditory cortex or in stimuli whose processing are considered to be dependent on higher components of the pathway (Threlkeld et al. 2007; Szalkowski et al. 2012; Szalkowski et al. 2013; Centanni et al. 2014a; Truong et al. 2014; Truong et al. 2015; Rendall et al. 2015; Centanni et al. 2016).

In a series of tests, Centanni et al. (2014a) and Centanni et al. (2014b) reported that altered levels of KIAA0319 in the rat embryonic cortex lead to an impairment in the discrimination of speech sounds in both behavioural and electrophysiological measures. These recordings were performed exclusively in neurons of the primary auditory cortex, although it is unclear whether this region is affected by the cortical lamination abnormalities associated with shRNA knockdown of *Kiaa0319* previously reported (Paracchini et al. 2006; Peschansky et al. 2010). Moreover, although the experiments use primarily speech sounds as stimuli, responses to simple sound bursts like the ones used in the ABR experiments reported here were also degraded. Bearing in mind potential issues with RNAi methods, these results are generally consistent with the findings reported here with double KOs and, given deficits were observed already in much lower levels of the auditory pathway, it would be expected that similar results would be found in recordings from the auditory cortex. Whilst experiments with single KOs did not identify any effect of the absence of KIAA0319 protein, results from dKOs suggest that the role of KIAA0319 in rodent auditory processing may not be limited to the neocortex as suggested by Centanni et al. (2014a), highlighting the need for a less cortex-centered approach to study the neurobiology of language (Krishnan et al. 2016).

It is likely that the impaired responses in the auditory brainstem underlie psychophysical gap detection deficits and that it has an impact on processing at higher levels in the auditory pathway in the thalamus and auditory cortex. Moreover, the fact that the most robust effect on ABRs was observed with the masker-probe stimuli indicate the effect may be sensitive to temporal processing, given that such forward masking stimuli and gap detection are key measures of temporal sound acuity (Werner et al. 2001). This is particularly relevant in the context of suggestions that impaired temporal sampling may underlie dyslexia and other language-related disabilities as mentioned above (Tallal 1980; Temple et al. 2000; Choudhury & Other 2007; Raschle et al. 2014). Such temporal sensitivity may also explain why a deficit is observed in the gap detection task but not in basic

startle and PPI, even though they share circuitry components early in the pathway (Swerdlow et al. 2001). Gap detection requires fine-grained temporal information to which the startle/PPI circuit may not be so sensitive.

The neuronal activity recorded by ABRs is considered to reflect the summation of post-synaptic events occurring synchronously in a population of neurons at distinct auditory nuclei (Parham et al. 2001). Alterations in the strength or synchrony of firing of these neurons are thought to lead to smaller amplitudes and longer latencies in the respective waves. Whilst their precise relationship and correspondence is not very well understood, deficits in gap detection are often interpreted as similar reductions in the activity of neuronal populations or as 'sluggish processing' (Anderson & Linden 2016). Although no deficit was identified in the absence of only KIAA0319 in our experiments, this is generally consistent with the findings from Centanni et al. (2014a) where KIAA0319 knockdown was found to result in degraded firing in KIAA0319-deficient neurons in the auditory cortex. There are a number of different alterations at the cellular and circuit level which could lead to a reduction in the strength or synchrony of neural activity detected by ABRs, be it via a reduction in synaptic activity in individual neurons, a reduction in the pool of neurons that are active and so on (Don et al. 1994). Although the mechanisms through which AU040320 and KIAA0319 may lead to such deficits are currently unclear, there are a number of routes for future investigation based on the current knowledge of these two proteins.

One of these, briefly explored here, is that the altered responses recorded may result from a difference in the synaptic profile of mutants as the encoded proteins share a number of features with other molecules involved in the formation and maintenance of synapses, many of which are also cell surface adhesive glycoproteins (Gerrow & El-Husseini 2006; Dalva et al. 2007; Katidou et al. 2008; Missler et al. 2012). The reported interaction of AU040320 with the Nogo receptor NgR1 (Poon et al. 2011b) also supports this given that NgR1 has been shown to regulate synapse number (Wills et al. 2012). However, measurements of synapse number

by immunohistochemistry in dKOs did not reveal any major alterations in the key regions of the early central auditory system analysed here (ventral cochlear nucleus, inferior colliculus and medial geniculate body) - nonetheless, a more subtle deficit could be present and may be detected with alternative methods such as quantification of key synaptic molecules by Western blot, qPCR or synapse counting via electron microscopy. The reported interaction between AU040320 and NgR1 also suggests the possibility of abnormal connectivity in these mutants through other routes. Nogo receptors are key regulators of axonal growth and dendritic branching in the developing nervous system (Schwab 2010) and a defect in extension and targeting of axons could alter local auditory circuits and lead to a change in activity in the relevant areas. Interestingly, NgR1 is also known to be important in myelin formation (McGee & Strittmatter 2003; McDonald et al. 2011) and a recent single-cell RNAseq analysis of cortical cells has revealed *AU040320* expression to be enriched in oligodendrocytes as well as neurons in the neocortex (Zeisel et al. 2015). Such possibility of impaired axonal targeting is supported by evidence reporting that the KIAA0319 protein is a regulator of axonal growth via Smad2, an activator of the Nogo signalling pathway (Schwab 2010; Franquinho et al. 2017). The Molnár and Monaco laboratories are currently investigating whether KIAA0319 and/or AU040320 may regulate dendritic branching and spine formation dynamics (Melissa Bailey, unpublished data).

Another possibility suggested by the changes in ABR wave amplitudes of *AU040320* and double KOs comes from potential changes in cell intrinsic properties rather than in circuit-level malformations. It has been reported that knockdown of *KIAA0319* via shRNA in the rat auditory cortex leads to changes in the electrophysiological properties of transfected cells which show higher input resistance and excitability, resulting in increased firing variability (Centanni et al. 2014a). One mechanism through which this may take place at the molecular level lies in the significant degree of homology between KIAA0319/AU040320 proteins and members of the polycystin gene family which also encode transmembrane glycoproteins with

PKD domains such as polycystin-1 (PKD1), polycystin-2 (PKD2) and polycystin-1 Like 1 (PKD1L1). These proteins have been shown to function as transient ion channels regulating cell-internal calcium levels via the primary cilium (Hughes et al. 1995; Decaen et al. 2013; Patel 2015). There are a number of suggestive links between KIAA0319 (and AU040320) and cilia such as the enriched expression of KIAA0319 in ciliated tissues (though not in the brain; Ivliev et al. 2012), its localisation to the ciliary membrane in olfactory sensory neurons (Kuhlmann et al. 2014), as well as *AU040320* KO mice displaying male infertility, a well-known characteristic of ciliopathies (Fliegauf et al. 2007). The two other main dyslexia susceptibility genes, *DCDC2* and *DYX1C1*, have both been shown to affect cilia function and/or structure (Massinen et al. 2011; Tarkar et al. 2013; Kere 2014; Grati et al. 2015). The link between cilia and candidate genes of language disorders provide an interesting connection with the much-debated role of cerebral asymmetry in language impairment and development (Bishop 2013; Brandler & Paracchini 2014; Newbury et al. 2014). However, there is so far no direct association between KIAA0319, AU040320 and altered structure or function of cilia. And a preliminary analysis of primary cilia in cortical neurons revealed no major structural abnormalities (Appendix A.3), although detailed quantification of cilia number and length would be required to discard more subtle malformations.

A separate but related alternative lies in the relationship between KIAA0319 and KIAA0319L with the clathrin endocytic pathway (Levecque et al. 2009, and unpublished data). Clathrin-mediated endocytosis is the predominant mechanism through which synaptic vesicles are recycled following the release of neurotransmitters (Heuser & Reese 1973; Maycox et al. 1992; Granseth et al. 2006; Saheki & De Camilli 2012; Watanabe et al. 2014) and both KIAA0319 and KIAA0319L have been shown to interact with adaptor protein 2 (AP-2), a key molecule involved in the recruitment of transmembrane vesicle proteins for the proper function of synaptic vesicles (Südhof & Rothman 2009). Given KIAA0319 and KIAA0319L also localise to the trans-Golgi network and early endosomes, from which synaptic

vesicles originate, it is possible that these two proteins play a role in the normal function and processing of synaptic vesicles. A putative deficit in vesicle recycling could impair the rapid turnover of the vesicular pool in neurons in a way that affects its restoration to baseline and, thus, affects more time-sensitive firing. This possibility is discussed in more detail in Chapter 6.

Aside from the deficits in auditory processing, the series of behavioural tests performed on dKO also revealed a mild effect of *Kiaa0319;AU040320* KO in the performance in the light-dark box, with mutant animals showing a subtle increase in anxiety-like behaviours by spending more time in the dark area and reduced area exploration. These findings are interesting in light of a previously identified change in anxiety levels in *Kiaa0319* KOs, although this was found exclusively in the initial stages of the test (Martinez-Garay et al. 2017). However, the effect observed in that study had the opposite effect to the one identified here: whilst *Kiaa0319* KOs displayed a subtle reduction in levels of anxiety-like behaviour, the putative effect of absence of both KIAA0319 and AU040320 was anxiogenic and, thus, in the opposite direction. The differences between dKOs and controls had considerable effect sizes but no confirmation was obtained with other anxiety-related tests. In the adult human brain, *KIAA0319* expression appears at some of its strongest levels in the amygdala (Hawrylycz et al. 2012), a key region in the regulation of emotional behaviour and fear (Shin & Liberzon 2010). It is possible that KIAA0319 (and AU040320) plays a role in anxiety-associated circuits in the amygdala and this requires further exploration. The fact that an increase in anxiety levels has been found to be common in populations with learning or language disability including dyslexia (possibly linked to the high degree of comorbidity with other developmental disorders; Cantwell & Baker 1987; Sundheim & Voeller 2004; Greenham 1999; Schulte-Körne 2010) highlights the potential importance of this finding.

A main limitation of the study reported here lies in that, in order to generate a cohort of double mutant mice that is large enough to obtain robust results with strong statistical power, separate breeding lines were required for ethical and

financial reasons. Whilst it is possible that results may have been influenced by subtle epigenetic differences, this is standard practice in studies using double KO mice and strong precautions have been taken to minimise potential external factors: (a) mutant and wildtype animals were derived from very closely related lines (3 generations apart), all traceable to a set of *AU040320* heterozygous KO parents, so that potential genetic background differences were kept to a minimum; (b) despite having different parents, dKO and wildtype animals were *de facto* littermates (they are 'cage-mates') as plug-timed pregnant females were matched and paired in the same cages so that wildtype and dKO-generating mothers gave birth in the same place with a maximum of 24 h apart; this ensured that pups were exposed to the exact same environmental conditions and experiences from birth (and most of gestation) such as cage cleaning routines, ear clipping, and so on.

4.4 Conclusion

In sum, the study reported here points towards a role for AU040320, and to a lesser extent KIAA0319, in the proper function of the rodent auditory system starting already at the level of the brainstem, similar to findings in human dyslexic populations (Hornickel & Kraus 2013). Thus, KIAA0319 and AU040320 may underlie the firing and connectivity of circuits relevant for sensory processing of sounds in human dyslexia, a topic of much debate in dyslexia neuropsychology (Ramus & Ahissar 2012; Goswami 2014). Nonetheless, it is possible that this deficit is not specific to the auditory system and may affect other sensory modalities such as vision. Whilst most work examining the function of language-related genes in animal models tend to focus on putative deficits in the neocortex (as it is the case with human language studies), this highlights the importance of going beyond the cortex and examining lower-level processes which may also be present (Krishnan et al. 2016).

5

Chapter 5

Contents

5.1 Introduction 166
5.1.1 Introduction to spermatogenesis 166
5.1.2 Spermiogenesis: acrosome development 169
5.1.3 Disorders of acrosome formation: globozoospermia . . . 170
5.2 Results 172
5.2.1 Expression of AU040320 in the reproductive system . . 172
5.2.2 *AU040320* KO leads to male infertility 173
5.2.3 Normal meiotic progression of spermatocytes is unaffected following *AU040320* KOs 173
5.2.4 Absence of *AU040320* leads to abnormal sperm morphology with globozoospermia-like features 175
5.2.5 Impaired acrosome biogenesis in *AU040320* KO mice . . 178
5.2.6 Failure in vesicle transport and fusion in *AU040320*-deficient spermatids 180
5.2.7 Normal Sertoli cells & manchette in *AU040320* KOs . . 182
5.2.8 AU040320 localises to the trans-Golgi network 184
5.2.9 Interaction with proteins involved in acrosome development and intracellular trafficking 186
5.2.10 Mutation screening in human globozoospermia 189
5.3 Discussion 191
5.4 Conclusion 197

5.1 Introduction

Very little is currently known about the KIAA0319L protein and its putative functions. Aside from the previous association to neuronal migration in brain development examined and discussed in Chapter 3, there were no other links to its function until Pillay et al. (2016) revealed it can serve as a receptor for AAV entry into cells. In the attempts to uncover how the mouse homolog *AU040320* modulates neuronal migration, I found that its total absence in constitutive KO mice led to male infertility in all cases as no pups were born from matings with *AU040320* -/- (more detail below). Faced with this and the paucity of knowledge on this protein to date, I decided to probe into this phenotype in order to uncover the cellular functions of the AU040320 protein - with the ultimate goal of generating hypotheses about its role in brain structure-function and in underlying susceptibility to dyslexia. Such efforts were initially strongly guided by previous suggestions of a link between dyslexia susceptibility genes and cilia (Newbury et al. 2014) as male infertility is a key feature of ciliopathies (Fliegauf et al. 2007), although no direct evidence for this has been found either in this study or others.

This chapter provides a characterisation of the infertility phenotype of *AU040320* KO mice which shares features with cases of globozoospermia cases in humans. My identification of *AU040320* as a novel globozoospermia gene in mice prompted the examination of a cohort of human cases of globozoospermia in which no causative mutations have been found so far. The chapter starts with an introduction to the relevant areas of sperm development and infertility: spermatogenesis, acrosome development and globozoospermia. The results obtained shed light onto a putative new function of AU040320 in the vesicular trafficking and fusion which may also contribute to the debate regarding the developmental origin of the sperm acrosome.

5.1.1 Introduction to spermatogenesis

The spermatozoon is a unique cell type in mammals due to its functional specialisation and structural complexity which derives from a highly complex developmental

program regulating cell morphology, biochemistry, transcriptome and so on (Russell et al. 1990; Abou-Haila & Tulsiani 2000; Cooke & Saunders 2002). Mammalian spermatozoa are generated in the seminiferous tubules of the testis where they proliferate and differentiate before entering the seminiferous lumen and translocate into the epididymis where they become fully mature (Fig. 5.1A).

Seminiferous tubules contain a number of different cell types which are divided into supporting Sertoli and Leydig cells and germ cells from which spermatozoa will develop (Fig. 5.1A). Spermatogenesis starts with proliferating germ cells called *spermatogonia* that line the epithelium of the seminiferous tubules and follow several steps of mitosis and meiosis to generate *primary spermatocytes*. These, in turn, undergo meiosis to produce haploid, *round spermatids* (Fig. 5.1B, C) before starting a complex differentiation process that will lead to the formation of the sperm *acrosome* surrounding the nucleus and the elongation of the sperm head. During this process, round spermatids associate with Sertoli cells as they move towards the seminiferous lumen and become elongated, mature spermatozoa (Russell & Clermont 1976; Guttman et al. 2004). A fully formed spermatozoon is subdivided into the following cell compartments: (a) a sperm tail or flagellum with a 9 + 2 microtubular axoneme; (b) a midpiece region packed with mitochondria to provide energy for tail motility; and (c) a sperm head containing the nucleus surrounded by a sperm-specialised membranous organelle called *acrosome* (Fig. 5.1D Grootegoed et al. 1995; Cooke & Saunders 2002; Jan et al. 2012).

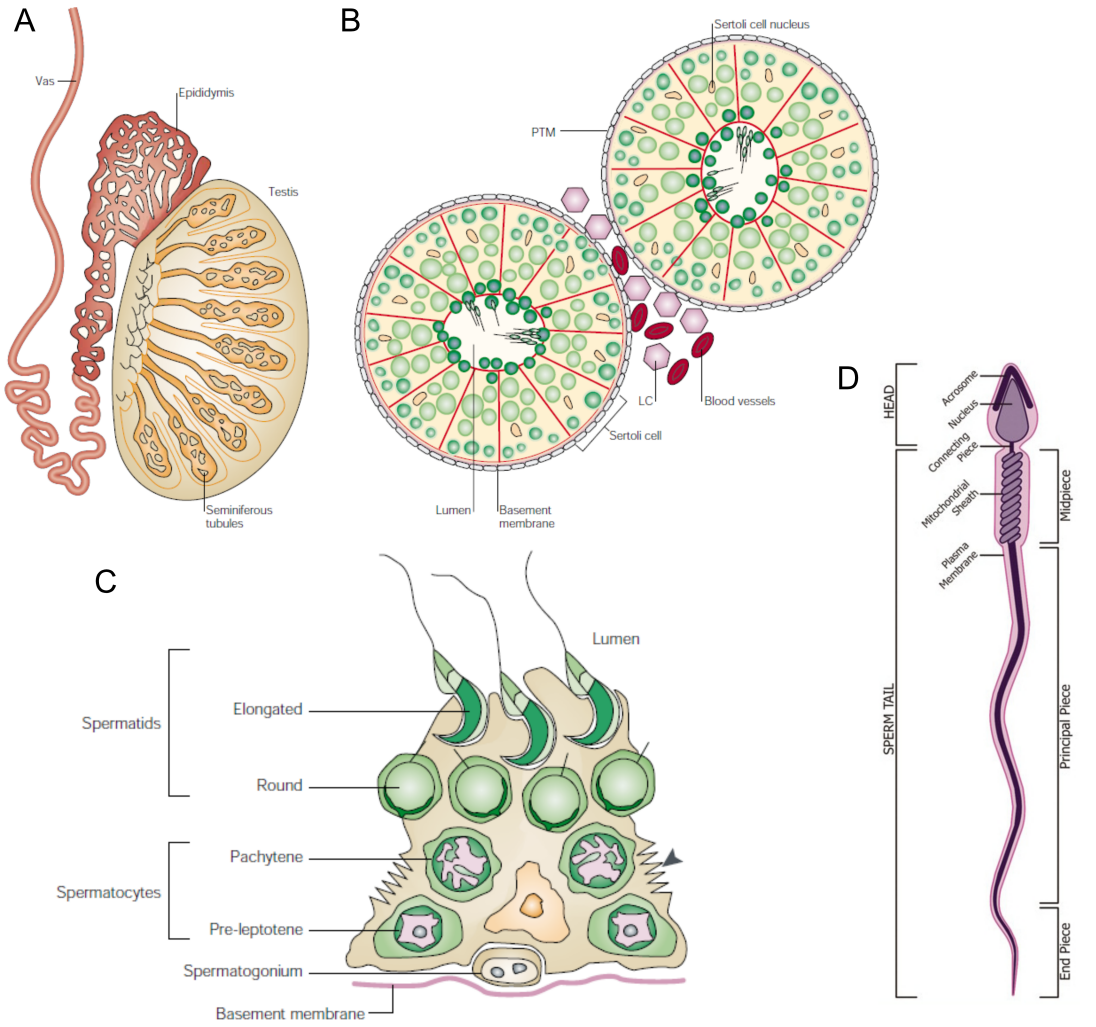


Figure 5.1: The male reproductive system and spermatogenesis in mammals. (A) Cross-section showing the overall organisation of the mammalian reproductive system in males which is composed of testis packed with seminiferous tubules that are responsible for the production of spermatozoa, and the epididymis which is responsible for the maturation of spermatozoa and for their later transport onto the vas deferens. (B) Seminiferous tubules are luminal structures based around an epithelium formed by Sertoli cells (yellow) that support tubules and contain spermatogenic cells (green). Tubules are supported by Leydig cells (pink) which are responsible for hormonal production. (C) Diagram of a Sertoli cell (arrowhead) associated with the different spermatogenic cell types (green). Progenitor cells (spermatogonia) are adjacent to the epithelial membrane and will give rise to diploid spermatocytes and eventually post-meiotic spermatids, in an arrangement where the cell in maturation lies closer to the seminiferous lumen. Elongated spermatids dissociate from Sertoli cells and are released onto the lumen before translocation onto the epididymis. DNA is represented in pink. (D) Subdivisions of a mature human spermatozoon. The head contains the acrosome and the cell nucleus, whilst the sperm tail is composed of the midpiece, packed with tightly arranged mitochondria, and a flagellum. Adapted from Cooke & Saunders 2002 (A, B, C) and Borg et al. 2010 (D).

5.1.2 Spermiogenesis: acrosome development

The acrosome was first identified in the early 1920s (Bowen 1924) and it is a large vesicular compartment bound to the anterior part of the nucleus. It contains digestive glycosylated enzymes such as hyaluronidase that facilitate sperm penetration into the egg by breaking down the egg's outer membrane after sperm-egg binding to initiate fertilisation. Acrosomes vary in size and morphology across mammals, from the sickle shape in rodents to cap-like structure in humans, although their basic structure is well-conserved (Yanagimachi 1994; Abou-Haila & Tulsiani 2000; Moreno & Alvarado 2006; Berruti & Paiardi 2011; Berruti 2016).

The development of the acrosome starts in the *Golgi phase* with the formation of a single, large compartment called the *acrosomal granule* where acrosomal content is stored (Fig. 5.2). As it progresses through to the *cap phase*, the developing acrosome becomes larger and attaches to the acroplaxome, an adhesive actin and keratin-rich structure lining the nuclear envelope (Kierszenbaum et al. 2003; Kierszenbaum et al. 2011). Its increase in size is accompanied by the flattening of the vacuole along the nuclear surface to adopt a hemispherical shape before initiating elongation - in what is called the *acrosome phase*. This is achieved in coordination with a transient structure called *manchette*, a microtubular network anchoring the acrosome, that assists in head elongation during the remodelling of the cell nucleus. In its final step, the *maturation phase*, the acrosome adopts its final shape and the cytoplasm is eventually discarded (Fig. 5.2).

The process of acrosome biogenesis is typically considered to originate from the direct transport of Golgi-derived vesicles, known as *proacrosomal vesicles*, which are continuously shipped to the emerging acrosomal granule and coalesce to form a single structure (Aguas & da Silva 1985; Abou-Haila & Tulsiani 2000; Moreno et al. 2000). However, recent evidence has revealed extra-Golgi trafficking routes which contribute to the acrosome involving the endocytic and lysosomal pathways, bringing a revival of the idea that the acrosome is a lysosome-related organelle

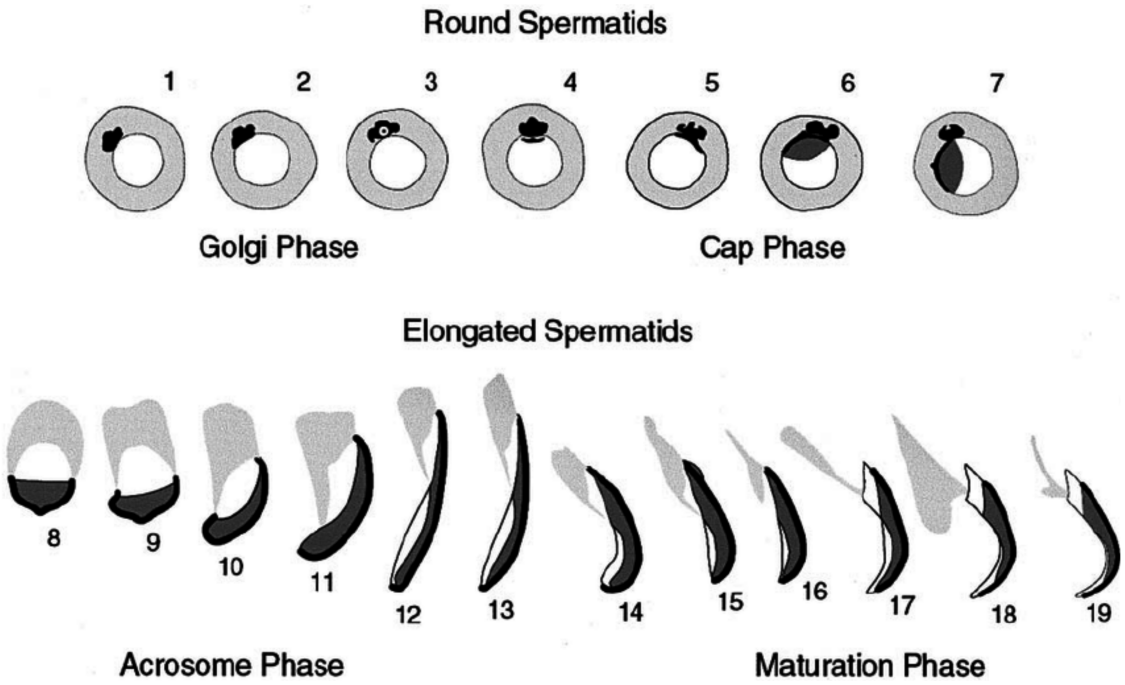


Figure 5.2: Schematic representation of rodent spermiogenesis. The differentiation process of round spermatids into elongated, fully formed spermatozoa, depicting the formation of the acrosome (black and dark grey), the cytoplasm (light grey) and cell nucleus (white). Note the growth of the acrosome between the Golgi phase and Cap phase, and the remodelling of the acrosome and cell nucleus during elongation. Adapted from Abou-Haila & Tulsiani 2000.

(Allison & Hartree 1970; Ramalho-Santos et al. 2002; Moreno & Alvarado 2006; Berruti & Paiardi 2011; Berruti 2016).

5.1.3 Disorders of acrosome formation: globozoospermia

Abnormalities in acrosome development can lead to severe morphogenetic defects in spermatozoa and eventually infertility. Malformation of the acrosome typically results in a rare but severe disorder called *globozoospermia*. Globozoospermic spermatozoa are characterised by a rounded head lacking an acrosome (Fig. 5.3A) and accompanied by abnormal nuclear condensation and impaired sperm motility (Baccetti et al. 1977; Dam et al. 2007a; Coutton et al. 2015a). Acrosomeless spermatozoa are impaired in their ability to bind and fertilise eggs which results in reduced fertility. Although general male infertility is a multifactorial disorder which can affect up to 12% of men (Brugo-Olmedo et al. 2001; Agarwal et al. 2015),

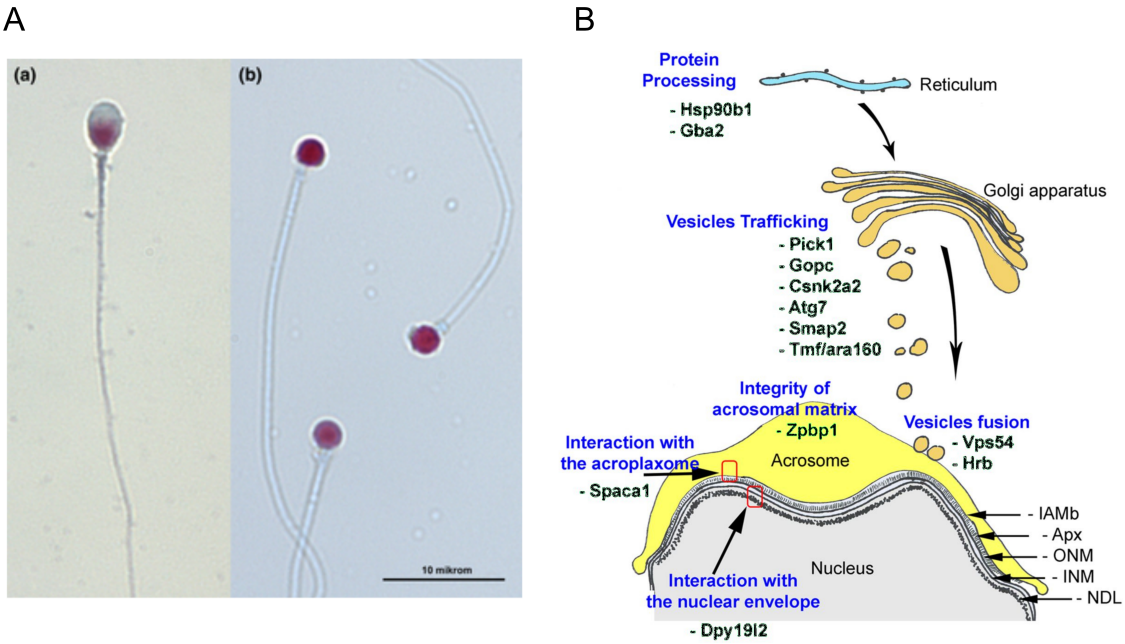


Figure 5.3: Human globozoospermia and proteins involved in globozoospermia in mice. (A) Example of a normal oval-shaped sperm head stained with Spermac®. in (a), and a globozoospermic sample with the characteristic round head in (b); adapted from Vozdova et al. 2014. (B) Proteins and cellular compartments known to be involved in acrosome formation and which can lead to globozoospermia in mice. The classical intracellular pathway for acrosome formation involves the processing of proteins in the endoplasmic reticulum followed by their trafficking in vesicles from the Golgi apparatus before they fuse and attach onto the acroplaxome to form the acrosomal granule. Disruption in any of these steps can lead to severe disruption in acrosome biogenesis and its absence in mature spermatozoa. Protein/gene abbreviations: heat shock protein 90 kDa beta 1 (Hsp90b1); glucosidase, beta (bile acid) 2 (Gba2); protein interacting with PRKCA 1 (Pick1); golgi-associated PDZ and coiled-coil motif containing (Gopc); casein kinase 2, alpha prime polypeptide (Csnk2a2); autophagy related 7 (Atg7); small ArfGAP 2 (Smap2); TATA element modulatory factor 1; (Tmf1 or ARA160); zona pellucida binding protein (Zpbp or Zpbp1); vacuolar protein sorting 54 (Vps54); ArfGAP with FG repeats 1 (Hrb), sperm acrosome associated 1 (Spaca1). Apx, acroplaxome; ONM, outer nuclear membrane; INM, inner nuclear membrane; NDL, nuclear dense lamina; IAMb, inner acrosomal membrane. From Coutton et al. 2015a.

globozoospermia is an inherited autosomal recessive condition estimated to affect less than 0.1% of the male population (Dam et al. 2007a; Coutton et al. 2015a).

Several genes have been reported to lead to globozoospermia in mice following genetic KO, with at least 13 genes affecting different stages of acrosome biogenesis – from protein processing in the ER and vesicle trafficking to acrosome adhesion

onto the nuclear envelope (Fig. 5.3B; see Coutton et al. 2015a; de Boer et al. 2014, for recent reviews). In humans, however, only two genes have been shown to carry causative mutations leading to globozoospermia. *SPATA16* was the first gene linked to the disorder by the identification of a homozygous missense mutation, although only recently its pathogenicity has been confirmed (Dam et al. 2007b; Karaca et al. 2014; ElInati et al. 2016). The majority of cases identified so far result from alterations in the *DPY19L2* gene in the form of point mutations or deletions specifically affecting this gene (Harbuz et al. 2011; Koscinski et al. 2011; Coutton et al. 2012; Elinati et al. 2012; Zhu et al. 2013; Ghédir et al. 2016). Recent estimates indicate that changes to *DPY19L2* may account for 80% of pathological alleles, although consanguinity is common factor in analysed samples and such high incidence may be due to founder effects (Coutton et al. 2015b).

In light of this, this chapter aims to address the following questions:

1. What is the nature of the infertility of *AU040320* male KO mice?
2. At which point is the developmental programme of spermatogenesis disrupted in these mutants?
3. What molecular and cellular functions may AU040320 be responsible for?
4. Can mutations in *KIAA0319L* also lead to similar pathology in humans?

5.2 Results

5.2.1 Expression of AU040320 in the reproductive system

Firstly, expression of *AU040320* in the reproductive system was confirmed by Western blot. AU040320 protein was detected in lysates of the testis and at low level in the epididymis, with the expected absence in the KO samples (Fig. 5.4A). No AU040320 protein was detected in isolated mature spermatozoa collected from the cauda epididymis, although protein levels are considerably low due to limited amount of cells that can be collected and it is possible that some AU040320 may be present but remain undetected. To interrogate the cell types where AU040320

protein is present, I made use of the lacZ reporter gene in the $AU040320^{del}$ allele of mutants and performed X-gal staining in testis sections. LacZ expression was found virtually ubiquitously in the tissue and it was detected in supporting Sertoli and Leydig cells, precursor spermatogonia and developing spermatids (Fig. 5.4B). These results are in line with available transcriptomic data reporting that *AU040320* transcripts are detected in isolated supporting cells and in germ cells, with its expression peaking at the onset of spermatid differentiation (Shima et al. 2004; Laiho et al. 2013; Sanz et al. 2013).

5.2.2 *AU040320* KO leads to male infertility

The generation of mice carrying the targeted deletion of *AU040320* was described in Chapter 3. Mating of these *AU040320* mutants revealed that homozygous males (*AU040320* -/-) are infertile as no pups were born after mating for several weeks and despite detection of vaginal plug in females (Fig. 5.4C). The fertility of mutant females and heterozygous KO males appear to be unaffected. Testes of *AU040320* -/- males exhibited no major structural abnormalities, with both size and weight comparable to that of wildtypes (Fig. 5.4D, E). Histological examination of sections stained with hematoxylin and eosin revealed mutant seminiferous tubules and epididymi did not display any gross structural malformations (Fig. 5.4F). No major change in the number of spermatozoa was observed in these sections but quantification of cells isolated from the cauda epididymis revealed a significant reduction in the number of mature spermatozoa in AU040320-deficient samples (Fig. 5.4G; n=4, p=0.04). Motility of epididymal spermatozoa was verified by live microscopy and found to be significantly reduced, although some motile cells were also observed (data not shown).

5.2.3 Normal meiotic progression of spermatocytes is unaffected following *AU040320* KOs

Given the expression of AU040320 in spermatocytes and the observed difference in epidydimal spermatozoa, potential deficits in cell proliferation and meiosis of

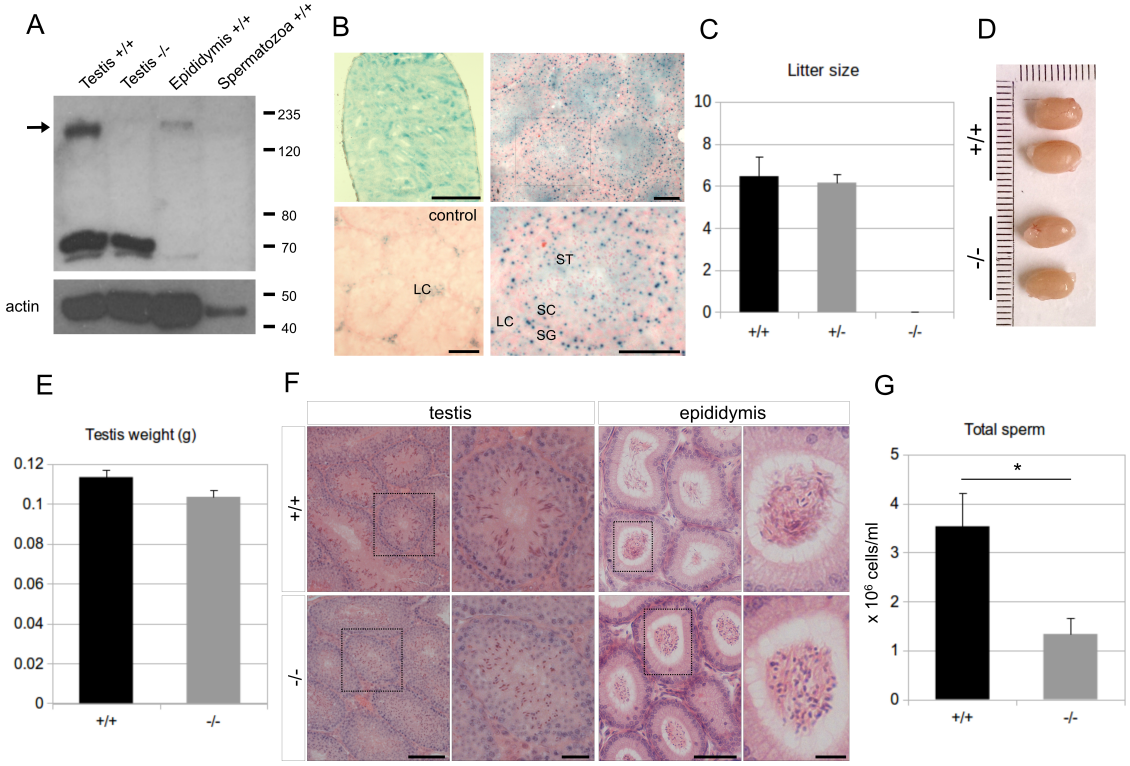


Figure 5.4: Absence of AU040320 leads to male infertility. (A) Western blot demonstrating expression of AU040320 in the testis of wildtype (+/+) and its absence in *AU040320* KO mice (-/-). The protein could also be detected in wildtype lysates of the epididymis but not in isolated spermatozoa from the epididymis, although this may be due to small quantities of cells that can be collected. Actin was used as loading control. (B) X-gal staining of testis sections of *AU040320* -/- mice which carry the *lacZ* reporter gene. Image of a whole testis section (top left) shows reporter gene has a widespread expression which can be seen in the majority of cells of seminiferous tubules (insets, right panels), including spermatogonia (SG), spermatocytes (SC) and spermatids (ST). Control (wildtype) samples display signal only in Leydig cells (LC), likely unspecific, but not inside seminiferous tubules. Nuclei are counterstained with Nuclear FastRed. (C) Average number of pups born from matings with males wildtype, heterozygous (+/-) and homozygous (-/-) for the *AU040320* KO allele (n=10 wildtype; n=12 for +/- and -/- mutants). (D) Representative images of testis of wildtype and *AU040320* -/- mice show no major morphological abnormalities. (E) Average weight of individual testis are comparable between wildtype and mutant mice (n=8). (F) Histological sections of Bouins-fixed testis and epididimis of wildtype (top row) and *AU040320* -/- (bottom row) mice (n=8 per genotype). (G) Quantification of sperm number (x 10^6 cells/ml) revealed a reduction in the number of spermatozoa released from the cauda epididymis of *AU040320* KOs (* denotes $p < 0.05$; n=3 per genotype). Scale bars: 250 μm (B, top left), 25 μm (B, others); 125 μm (F); 25 μm (F, insets).

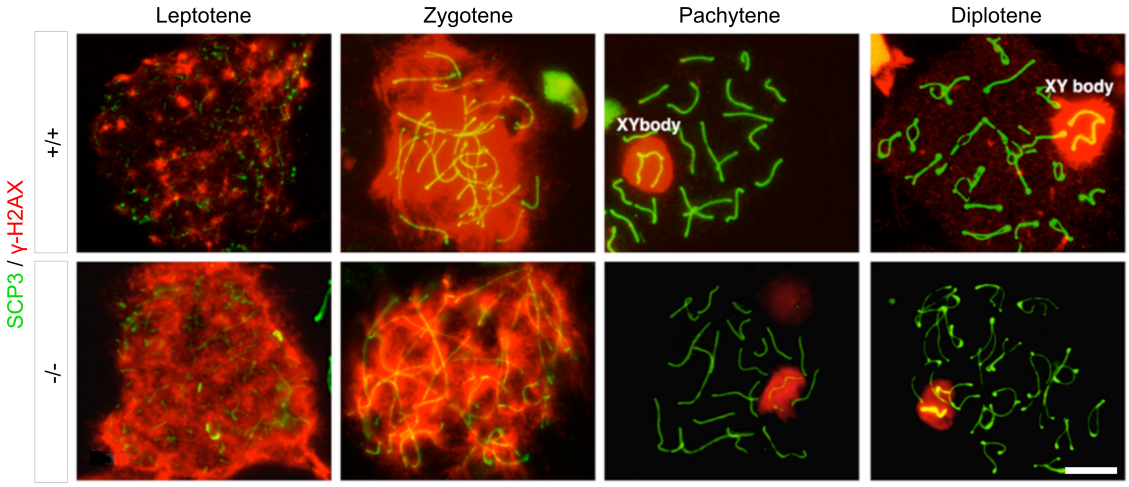


Figure 5.5: Normal meiotic progression of spermatocytes is unaffected following *AU040320* KO. Immunostaining of dissociated spermatocytes from wildtype and AU040320-deficient mice labelling of XY bodies with γ -H2AX (red) and paired chromatids with SCP3 (green) revealed no gross abnormalities in chromatid rearrangement during meiosis. Scale bar: 10 μm.

precursor cells were verified by immunofluorescence. Dissociated cells from the seminiferous tubules of wildtype and mutant animals were immunostained with an antibody against phospho-γ-H2AX to label the XY body and detect potential recombination problems during prophase 1 progression. The specific stages of meiosis of these cells were identified by labelling synaptonemal complex 3 (SCP3). These experiments were conducted as an initial characterisation and included only one sample per genotype but approximately 50 cells per sample were analysed. Staining with γ-H2AX revealed a normal chromatid recombination pattern over the course of meiosis, with the formation of XY bodies as expected (Fig. 5.5). These results suggest that the reduced epididymal sperm count of *AU040320* -/- males are not due to major problems in cell proliferation and may occur at some later stage between the testes and epididymis.

5.2.4 Absence of *AU040320* leads to abnormal sperm morphology with globozoospermia-like features

Initial examination of mutant spermatozoa in H & E-stained sections (Fig. 5.4F) and Giemsa stainings (Fig. 5.6A) indicated an abnormal morphology of mature

spermatozoa as they had a globular appearance, rather than the sickle shape characteristic of rodent spermatozoa. In order to gain a better understanding of the nature of this defect, the different subdivisions of spermatozoa were visualised by immunofluorescence using DAPI to label the nucleus, lectin (peanut agglutinin, PNA) as an acrosomal marker and acetylated tubulin to detect the sperm tail. Wildtype spermatozoa exhibited the expected acrosome shape lining the cell nucleus and the long tail attached to its base (Fig. 5.6B). On the other hand, no lectin staining was detected in AU040320-deficient spermatozoa and tails were found coiled around the head - this feature was found in all spermatozoa from every mutant analysed (n=10). When the midpiece was labelled with the mitochondria marker MitoTracker, midpiece dysplasia in mutant sperm became apparent as they did not display the characteristic compact and structured sheath extending from the nucleus (Fig. 5.6C). These findings were confirmed in the ultrastructure of mutant epididymal spermatozoa. Scanning electron microscopy (SEM) images revealed that *AU040320* -/- cells did not have the characteristic sickle-shaped head found in rodent sperm and instead displayed a round morphology and a smaller size, indicative of altered nuclear condensation (Fig. 5.6D). All mutant spermatozoa analysed displayed this morphology. Midpiece also appeared disarranged and tails were also coiled in these samples. Transmission electron microscopy (TEM) confirmed the absence of the acrosome, alongside the rounded cell nucleus and mitochondrial dysplasia (Fig. 5.6E). Given the motility impairment observed in mutants, the axoneme of the flagellum was examined but the 9 + 2 microtubular structure of the flagellum's axoneme appeared intact, with dynein arms clearly visible (Fig. 5.6F). Altogether, these results show that total loss of AU040320 leads to abnormal head morphology and absence of the acrosome, features that parallel the morphological defects observed in human cases of globozoospermia (Dam et al. 2007a).

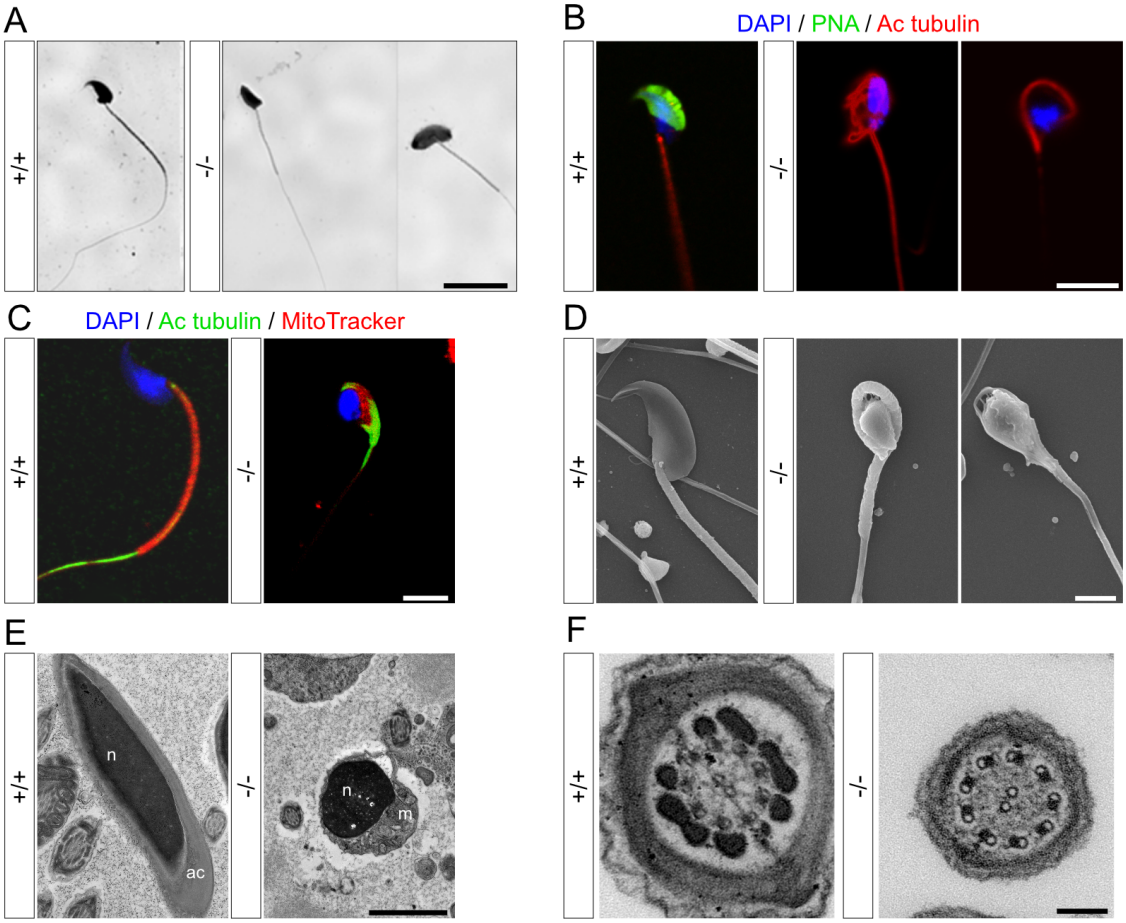


Figure 5.6: AU040320-deficient spermatozoa exhibit globozoospermia-like features. (A) Giemsa staining reveals rounded, mushroom-shaped sperm heads in *AU040320* -/- spermatozoa. (B) Immunostaining of dissociated epididymal spermatozoa shows that AU040320-deficient cells have rounded nuclei (DAPI, blue) instead of characteristic sickle shape, lack an acrosome (PNA, green) and tails (acetylated tubulin, red) coil around the sperm head. (C) Mitochondrial midpiece (MitoTracker, red) in mutant spermatozoa is disarranged given that it does not form the normal elongated thin structure at the base of the cell nucleus and extending with the flagellum (acetylated tubulin, green). (D) SEM images of wildtype and AU040320-deficient spermatozoa demonstrate the rounded nuclear shape and lack of acrosome in all spermatozoa analysed (100% spermatozoa of each animal). (E) Ultrastructure of spermatozoa obtained with TEM reveals the absence of the acrosome in rounded-head mutant spermatozoa in all cases. Ac, acrosome; m, mitochondria; n, nucleus (F) The microtubular organisation of the axoneme of mutant flagella appears normal, containing the 9 outer doublets and the 2 central pair. Some radial spokes extending to the central pair and dynein arms are also visible. Note that the images in the control sample are at the level of the midpiece given that the mitochondria can be seen. For all conditons, least 3 animals per genotype were analysed but often included n>10 animals per genotype. Scale bars: 10 μm (A), 5 μm (B, C), 2.5 μm (D); 2 μm (E), 100 nm (F).

5.2.5 Impaired acrosome biogenesis in *AU040320* KO mice

The abnormal morphological characteristics described above suggest a morphogenetic defect during spermatid development in *AU040320* -/- germ cells. Given globozoospermia often results from abnormalities in acrosome formation, I interrogated the developmental course of acrosome biogenesis in *AU040320* mutants to examine whether disruption in this process may be responsible for the deficits observed. Spermatogenesis follows continuous cycles in adulthood (in mice, spermatozoa develop over the course of 35 days) and occurs at different phases across sections of seminiferous tubules, permitting the identification of spermatids at different developmental stages in the same section. Identification of stage-specific cells can be achieved by examination of the degree of nuclear condensation and from cell morphology. To observe the developmental course of the spermatid acrosome, testes sections were labelled with acrosome-specific marker PNA and images revealed that acrosome formation showed signs of defect already in the early Golgi phase.

In wildtype tubules, the developing acrosome displayed its characteristic clustering in one face of the cell nucleus whilst mutant spermatids displayed less uniform and more sparse PNA signal that did not form a single homogeneous compartment (Fig. 5.7, top). The abnormalities were more evident at the next developmental stage where, instead of the thin cap-like layer enveloping the nucleus seen in wildtypes, the lectin staining in mutants displayed a non-uniform, punctated pattern along the nuclear surface (Fig. 5.7, middle). As spermatids entered the acrosome phase, the sperm head was seen to clearly elongate in wildtypes, with parallel remodelling of the acrosome and cell nucleus (Fig. 5.7, bottom panel). In contrast, an accumulation of disarranged acrosomal content was observed at the base of the head in mutant spermatids, likely reflecting the distribution of acrosomal content within the cytoplasm in the process of being discarded (Fig. 5.7, bottom panel). In some very few cases, the nucleus of mutant spermatids displayed an elongating nuclear shape (indicated by arrows) but these are likely to be attempting

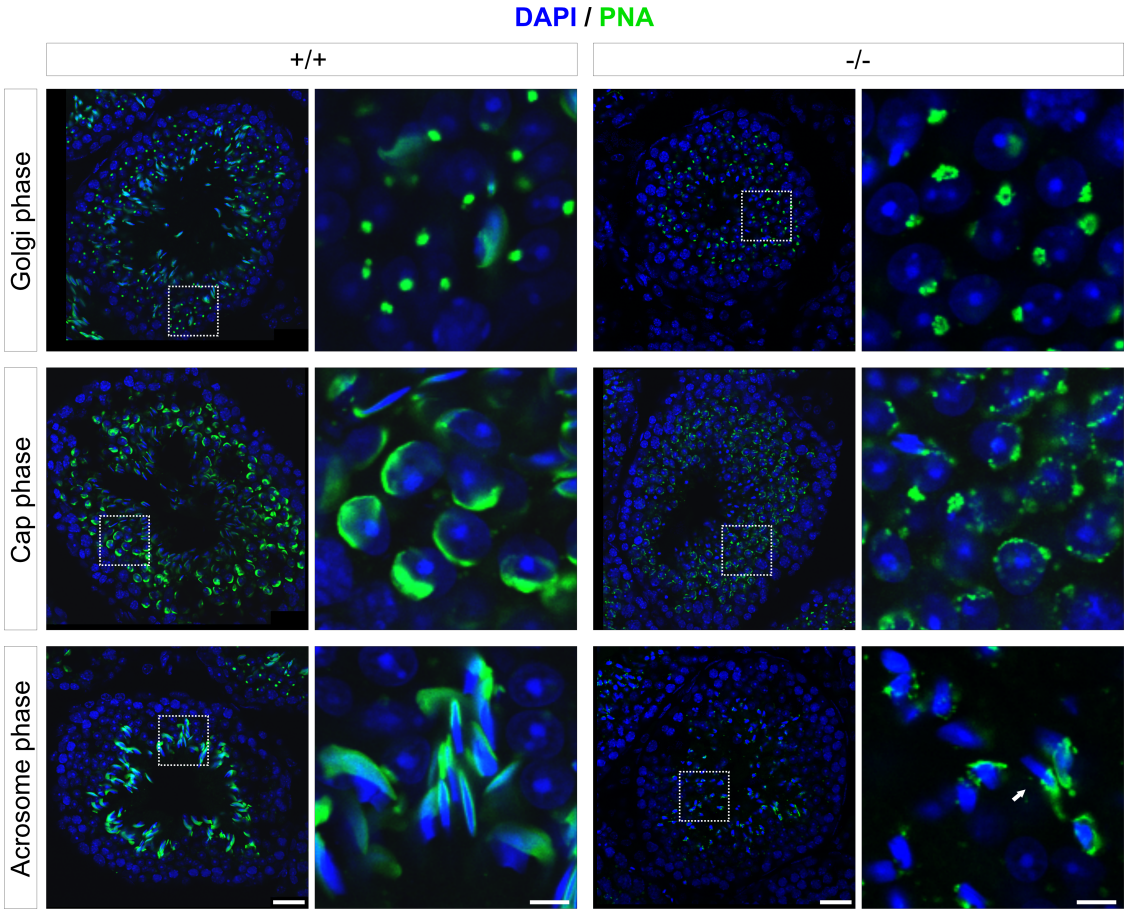


Figure 5.7: Developmental course of the acrosome is disrupted in AU040320-deficient mice. Adult testes sections from wildtype (+/+, left panels) and KO (-/-, right panels) samples stained with PNA (green) to label developing acrosome and DAPI for cell nuclei (blue) to identify stage-dependent cell types (spermatid development stage labelled on left panels). Non-homogeneous early acrosomes are observed in Golgi phase mutant spermatids which develop into a punctate pattern in the cap phase. Elongating spermatids do not exhibit an acrosome or have it misshaped. Scale bars: 25 μm (leftmost and inner right panels), 5 μm (inner left and rightmost panels).

to elongate into mature spermatozoa - testicular sperm were predominantly round (>95%) and all epididymal sperm observed were round-headed. These results indicate that *AU040320* KO leads to a disruption of the normal formation of the acrosome as early as in the Golgi phase.

5.2.6 Failure in vesicle transport and fusion in *AU040320*-deficient spermatids

The formation of the acrosome involves the fusion of proacrosomal vesicles typically derived from the TGN for the formation of a single, large acrosomal vesicle attached to the nuclear envelope and the acroplaxome on the Golgi face of the cell nucleus (Abou-Haila & Tulsiani 2000; Berruti et al. 2010). Given the disruption in acrosome formation observed above, I examined spermatids at different stages of acrosome development to identify the subcellular structures and processes which may be affected by *AU040320* KO.

Wildtype spermatids exhibited the characteristic progression of acrosome development with the formation of the acrosomal granule in the Golgi phase and its subsequent thinning and growth into a cap-like structure followed by elongation (Fig. 5.8A-C). However, no acrosomal granule was detected in *AU040320* -/- spermatids. Instead, in the Golgi phase, vesicles accumulated along the perinuclear region facing the Golgi stacks without forming a single granule-like structure, although some slightly larger vesicles were visible (Fig. 5.8D, arrows). In the cap phase, vesicles continued to cluster along the nuclear surface adjacent to the nuclear envelope but failed to form a homogeneous structure (Fig. 5.8E). Some spermatids exhibited curvatures on the edges of the acroplaxome, suggesting the microtubular manchette may not be affected (Fig. 5.8E, arrowheads). As *AU040320* -/- spermatids started to elongate, vesicles continued to line the nuclear surface despite the lack of an acrosome (Fig. 5.8F; arrows), with the flattened nuclear envelope face detected in some spermatids suggesting the acroplaxome may be present (Fig. 5.8F).

Although no acrosome was detected in *AU040320* -/- spermatids, a pseudo-acrosomal structure in a layer-like arrangement lining the nuclear envelope was observed in a few cases (Fig. 5.9). Such features have been observed in other globozoospermia-like mouse mutants and may result from the displacement of the ER and its attachment to the acroplaxome (Kierszenbaum 2004; Roqueta-Rivera et al.

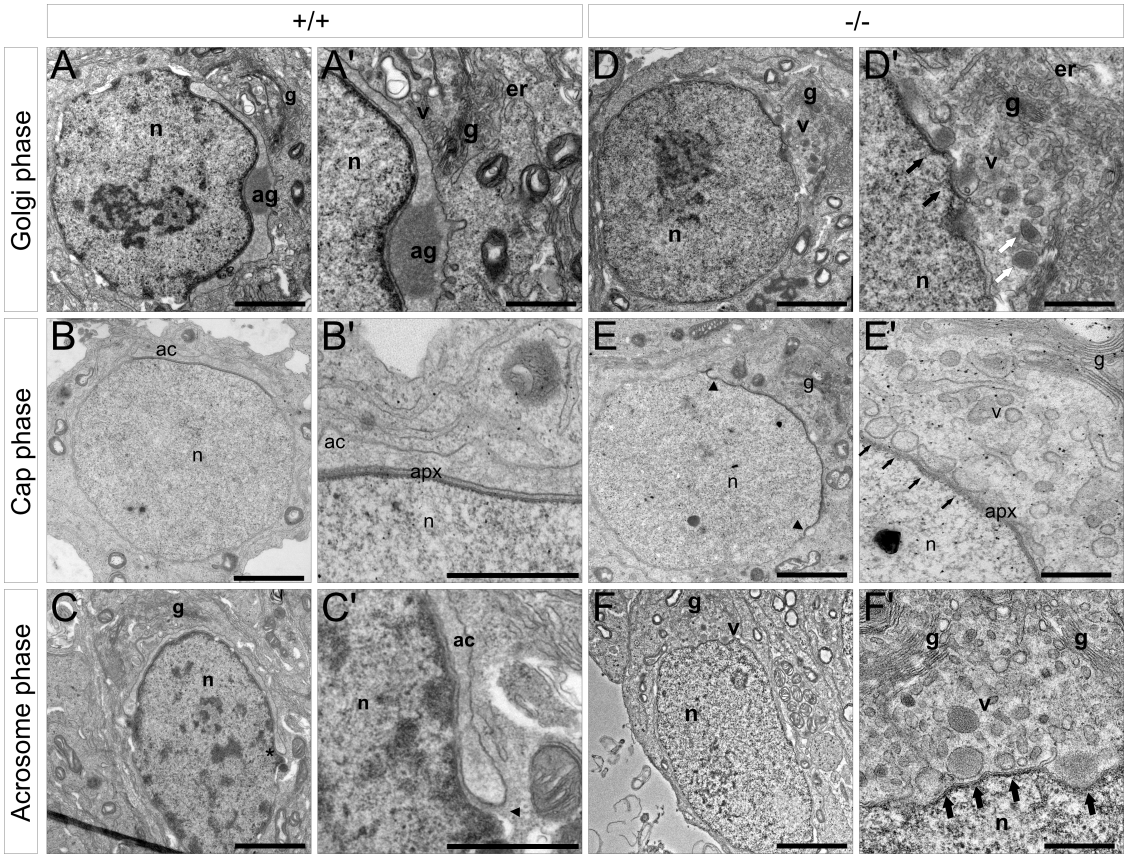


Figure 5.8: Ultrastructure of developing acrosomes shows impaired vesicle fusion in *AU040320* mutants. (A-C) Wildtype sperm exhibit the characteristic developmental path of the acrosome, with proacrosomal vesicles fusing together to form a large acrosomal granule (A) which becomes flattened along the acroplaxome and the nuclear face in the cap stage (B) before sperm elongation (C). In mutant spermatids on the other hand, vesicles containing proacrosomal material (D', white arrows) are seen to approach the Golgi face of the nucleus and form multiple points of indentations on it (D', black arrows) but fail to coalesce into a single acrosomal granule. Over the course of their development, round spermatids continue to show no acrosomal structure despite the continuous arrival of proacrosomal vesicles to the nuclear face (black arrows, E-F). The curvatures observed at the end of the acroplaxome in these cells (black arrowheads) indicate the presence of the manchette (E). Scale bar: 2 μm; insets, 1 μm. n, nucleus; g, Golgi; er, endoplasmic reticulum; ac, acroxome; apx, acroplaxome; ag, acrosomal granule.

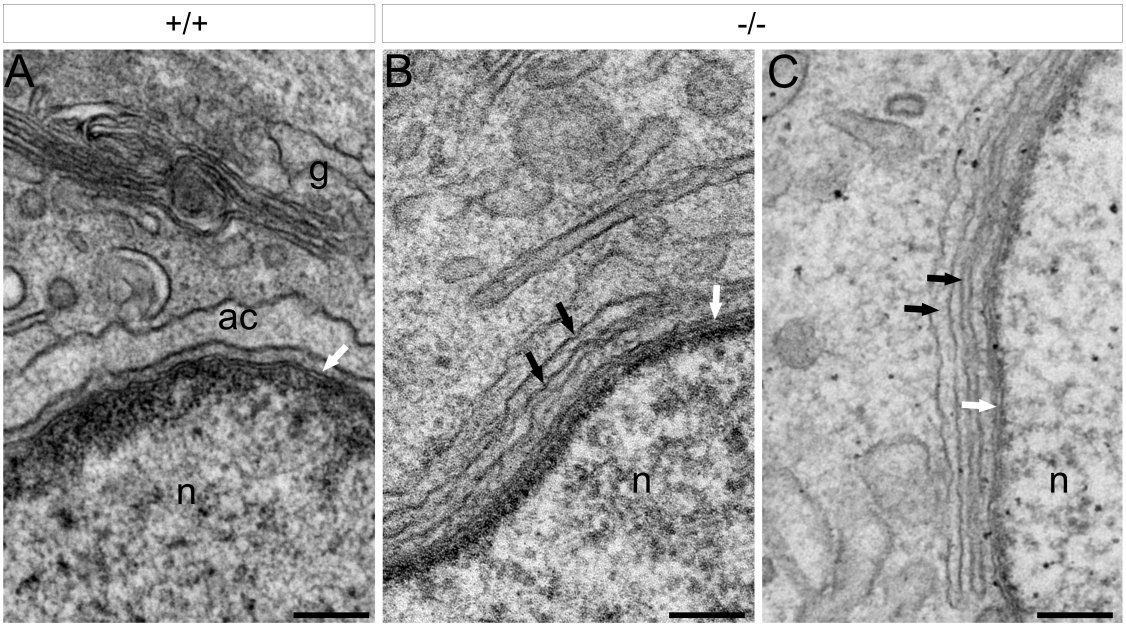


Figure 5.9: Pseudoacrosomal structures in *AU040320* -/- mice. (A) The acrosome (ac) and acroplaxome (white arrows) are observed in TEM images of wildtype round spermatids. (B-C) In AU040320-deficient spermatids, developing acrosomes appear to contain a normal acroplaxome (white arrows) which is surrounded by saccules (black arrows) that seem to attach in a layered fashion. Scale bars: 200 nm.

2011). These observations suggest that impaired acrosome formation in *AU040320* -/- may result from a failure in the fusion or docking of proacrosomal vesicles.

5.2.7 Normal Sertoli cells & manchette in *AU040320* KOs

Acrosome formation and spermatid differentiation involve a highly complex developmental program and defects in other processes beyond vesicle trafficking and docking have been known to cause globozoospermia in mice such as microtubular organisation in the manchette and acrosome adhesion to the nuclear envelope (Dam et al. 2007a; de Boer et al. 2014; Coutton et al. 2015a). Thus, it is possible that impaired acrosome biogenesis is accompanied or caused by other abnormalities. As such, I examined the overall arrangement of Sertoli cells in AU040320-deficient testes given the interaction of these cells with round spermatids is essential during spermatid translocation to the seminiferous lumen - they form a specialised adherens junction involving a combination of actin-based scaffold and adhesion molecules

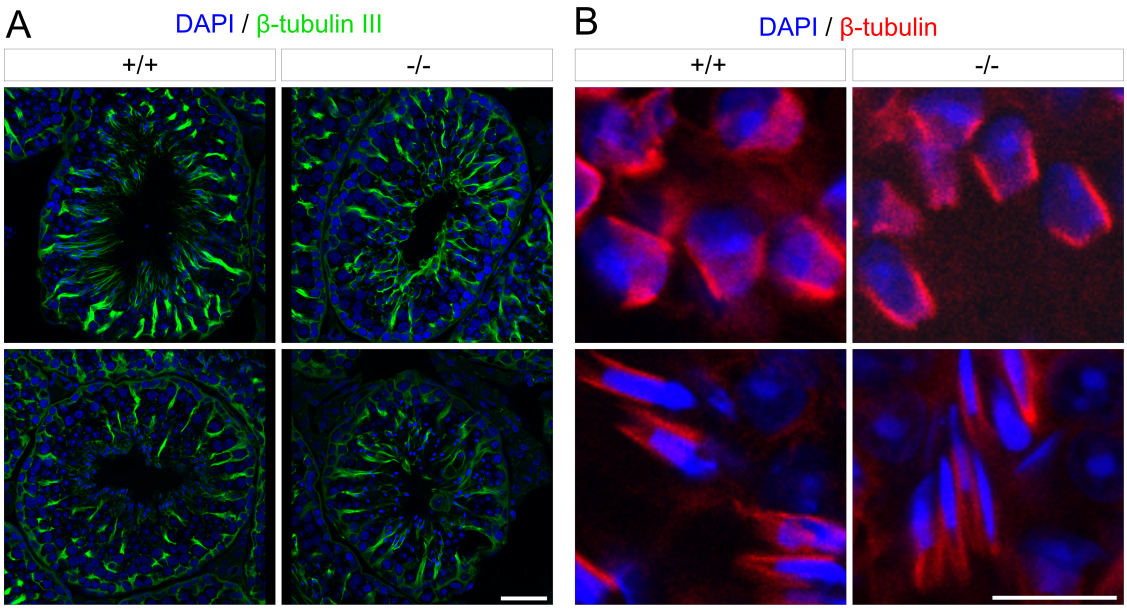


Figure 5.10: Cytoskeletal arrangement of Sertoli cells and developing manchette appears unaltered. Immunohistochemistry labelling the microtubular supporting structures of Sertoli cells (β-tubulin III, green) in seminiferous tubules of wildtype (+/+, left panel) and AU040320-deficient (-/-, right panel) mice. (B) Labelling of the manchette (β-tubulin, red) in developing spermatids at different stages (top and bottom panels) by immunohistochemistry in +/+ and -/- samples. DAPI, blue. Scale bars: 50 μm (A); 12 μm (B).

(de Boer et al. 2014). Immunostaining with an antibody against tubulin III (Tuj1), a Sertoli cell marker, revealed overall cytoskeletal structure of Sertoli cells do not exhibit gross defects and the arrangement in the seminiferous epithelium of AU040320-deficient testes appeared to be uniform, extending into the luminal region in a way that compared to wildtypes (Fig. 5.10A).

Another structure known to be critical in sperm maturation is the manchette, a transient microtubular complex associated to the acrosome and the acroplaxome to generate a complex interplay of contractile tension that shapes the sperm head during elongation (Kierszenbaum 2004). Labelling of the manchette with an antibody against β-tubulin in developing spermatids revealed the manchettes of mutants emerged at the base of the nucleus and extended towards the acrosome in the characteristic hemispherical shape observed in wildtype cells (Fig. 5.10B, top panels). In elongating spermatids (Fig. 5.10B, bottom panels), mutant manchettes

appeared elongated in parallel with the nucleus. Whilst these results do not exclude the possibility of more subtle deficits, they indicate that absence of AU040320 does not cause major cytoskeletal abnormalities and that the overall organisation of the manchette and Sertoli cells is not majorly affected.

5.2.8 AU040320 localises to the trans-Golgi network

KIAA0319L, the human homolog of AU040320, has been previously shown to localise in HeLa cells to the plasma membrane, endosomes and the *trans*-Golgi network (Levecque, unpublished; Hirst et al. 2012; Pillay et al. 2016). In order to verify the specific distribution of this protein during spermiogenesis, immunohistochemistry was performed in testis sections using two different antibodies recognising distinct regions of the AU040320 protein. Knockout samples served as negative controls for antibody specificity. The first antibody (named here # 78) is a custom-made one raised in guinea-pig that targets the C-terminus of the protein and was used for the Western blots presented here in this thesis (see e.g, Fig. 5.4). The second one (named here as Rb-AU) is a commercial antibody that recognises an epitope in the juxta-membrane position on the extracellular side of the full-length protein (detailed in Table 2.2 in Chapter 2).

Immunohistochemical stainings revealed that both antibodies displayed the same pattern of distribution in the distinct cell types suggesting the detection of the full-length protein (Fig. 5.11A). No distinguishable signal was detected in the *AU040320* -/- samples. These antibodies were then used in conjunction with a marker of the *trans*-Golgi network (TGN38) which revealed co-localisation between AU040320 and the TGN (Fig. 5.11B). AU040320 also seems to associate with early acrosomal structures based on a partial overlap with PNA in spermatids at the Golgi phase (Fig. 5.11C, top panels). In later stages, after the spreading of the acrosomal cap, AU040320 and acrosomal proteins appear to occupy different cell compartments as their distribution does not coincide (Fig. 5.11C, middle

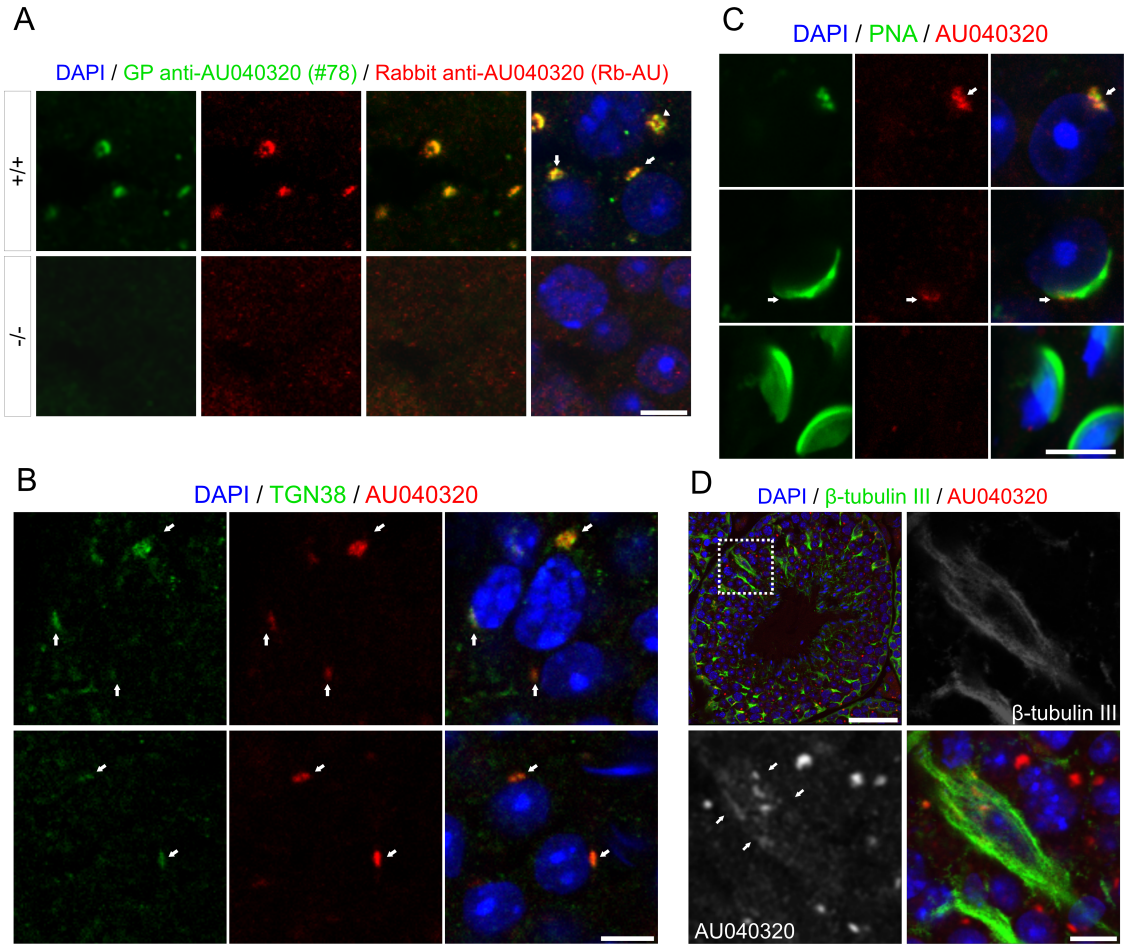


Figure 5.11: Immunohistochemistry of AU040320 and its subcellular localisation. (A) Immunostaining to label AU040320 with an antibody raised in guinea pig (#78, green) and one in rabbit (Rb-AU, red) displays overlapping signal (white arrows). DAPI counter-staining is shown in blue. (B) Double immunohistochemistry of guinea pig anti-AU040320 (red) and trans-Golgi marker TGN38 (green) shows co-localisation (white arrows). (C) Localisation of AU040320 protein (with #78, red) in relation to PNA (green) over the course of acrosome development reveals association with early acrosomal structures in Golgi phase spermatids (indicated by white arrows). (D) AU040320 protein (#78, red) exhibits a pattern with some overlap (indicated by arrows) with the structure of Sertoli cells (beta-tubulin III, green), suggesting AU040320 is also present in these cells. Scale bars: 5 μm, except top left in D (25 μm).

and bottom panels). In Sertoli cells, AU040320 was also detected with a pattern consistent with a membrane distribution (Fig. 5.11D).

Whilst these results indicate that AU040320 in round spermatids localise in the TGN, it is possible that residual AU040320 may be present in proacrosomal vesicles or in the developing acrosome but at levels which cannot be detected by

immunohistochemistry. Immunogold labelling was attempted in order to probe into this possibility directly but no reliable signal could be detected in these experiments. This is likely to result from the harsh tissue treatment necessary for antigen retrieval which considerably degrades the tissue, a condition found necessary for reliable detection of AU040320 in immunohistochemistry.

5.2.9 Interaction with proteins involved in acrosome development and intracellular trafficking

Previous work from the Monaco Laboratory has shown that intracellular transport of KIAA0319 follows the classical clathrin-endocytic pathway mediated by Rab5 and interaction with adaptor protein 2 (AP-2; Levecque et al. 2009). Parallel results have been found for KIAA0319L (Levecque, unpublished data). AP-2 is part of a family of adaptor complex proteins and it is an essential component of the clathrin endocytic pathway (Park & Guo 2014). Clathrin-coated vesicles and small GTPases such as Rab5 and Arf proteins are involved in intracellular trafficking and contribute to acrosome formation (Griffiths et al. 1981; Moreno et al. 2000; Ramalho-Santos et al. 2001; Berruti & Paiardi 2011). Whilst AP-2 has not been reliably detected in developing spermatids (Kang-Decker et al. 2001), another adaptor complex protein, adaptor protein 1 (AP-1), is known to localise to the TGN and in proacrosomic vesicles in these cells (Kang-Decker et al. 2001). AP-1 mediates trafficking between the TGN and other cellular compartments (Nakatsu & Ohno 2003; Park & Guo 2014) and it has been proposed to retrieve KIAA0319L from the peripheral endosomal compartment to the TGN (Hirst et al. 2012). Based on this, a putative interaction between KIAA0319L and AP-1 was interrogated in order to probe into a potential underlying molecular mechanism responsible for the observed failure in vesicle trafficking and fusion in AU040320-deficient spermatids.

For this, GST-pulldown experiments were performed using a GST-fusion protein containing the cytoplasmic domain of the human KIAA0319L protein containing the normal sequence (wildtype, wt; GST-KLc wt) or a Tyr to Ala mutation (Y>A, position 995; GST-KLc Y>A) at the consensus endocytic signal YXXØ. Fusion

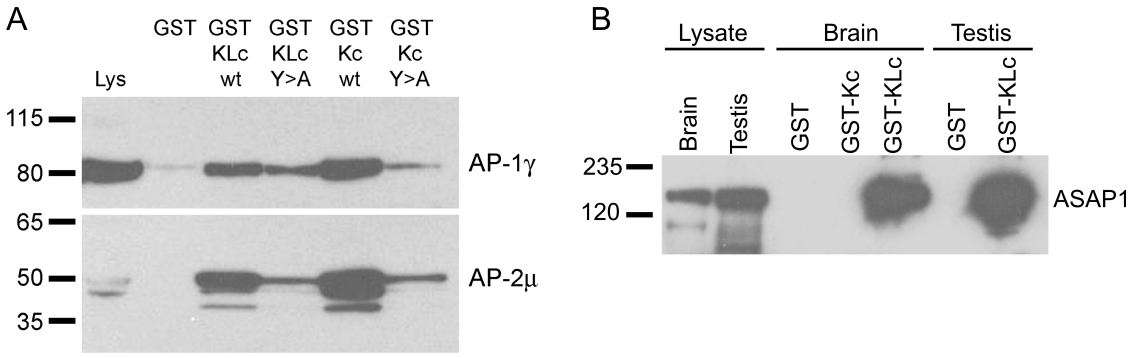


Figure 5.12: The C-terminal domain of human KIAA0319L protein is pulled-down with intracellular trafficking proteins AP-1, AP-2 and ASAP1 by GST pull-downs. GST pulldowns were performed to verify a potential interaction of the cytoplasmic domain of human KIAA0319 proteins with candidate interacting partners using GST (negative control) and GST-fusion proteins containing the cytoplasmic domain of human KIAA0319 (GST-Kc) and KIAA0319L (GST-KLc) with either the normal sequence (wt) or a Tyr to Ala mutation (Y>A, positions 995 and 968, respectively) at the consensus endocytic signal YXXØ (Y, Tyrosine; X, any residue; Ø, amino acid with a bulky hydrophobic side chain). (A) Putative interactions with AP-1 and AP-2 were probed using protein lysates from HeLa cells and Western blot with antibodies against the specific subunits (AP-1, γ; AP-2, μ). Both subunits were detected after pulldown with the wt GST-fusion proteins, suggesting a potential interaction. A clear reduction in protein levels were detected when compared to wildtype samples when Y>A mutant proteins were used. (B) Western blot showing expression of ASAP1 protein in lysates from wildtype adult mouse brain and testis and detection of ASAP1 in both tissues following pulldown with GST-KLc (wt only; no mutant). ASAP1 was not detected after pulldown with GST-Kc in brain lysates. Lys, original HeLa protein lysate.

proteins, alongside a control GST-only protein, were incubated with protein lysates from HeLa cells. Western blots revealed that subunits of both AP-1 (γ) and AP-2 (μ) could be detected after pulldown of the GST-KLc fusion protein, as well as with similar GST-KIAA0319 fusion constructs (GST-Kc; Fig. 5.12A). When Y>A mutant proteins were used instead of wildtype KIAA0319L, a clear reduction in protein levels was observed in the case of AP-2, indicating this site may mediate some of the interaction, whilst only a marginal reduction was observed for AP-1.

GST-pulldowns were also used to probe into a potential interaction of KIAA0319L with another candidate linked to intracellular transport, ASAP1. This protein has been identified as a promising candidate in a screening targeting potential interactors with the C-terminus of KIAA0319L (KLc) using a combination of GST-pulldowns

and mass spectrometry assays (data not shown). ASAP1 (ArfGAP with SH3 domain, ankyrin repeat and PH domain 1) is a member of the Arf GTPase activating protein (Arf GAP) family which are known to play a crucial role in regulating intracellular trafficking, membrane morphology and the assembly of vesicle coat proteins (Nie et al. 2006). As such, ASAP1 appears to be a promising candidate alongside AP-1 as a potential mediator of the failure of vesicle fusion in AU040320-deficient spermatids.

Expression of ASAP1 in both testis and brain were verified by Western blots using tissue lysates (Fig. 5.12B). Following this, pulldowns of the GST-KLc fusion proteins were performed and presence of ASAP1 could be detected by Western blot both in brain and testis (Fig. 5.12B). Interestingly, ASAP1 was not detected after pulldown of GST-fusion proteins containing the C-terminus of KIAA0319 (GST-Kc; 5.4). This data provides initial support for an interaction between KIAA0319L with AP-1/2 and with ASAP1, raising the possibility that a disruption of such interactions may underlie the failure in vesicle fusion and acrosome development observed in AU040320-deficient spermatids.

In order to gain further understanding of the molecular role AU040320 performs in spermatid and acrosome development, I sought to probe into a potential relationship between AU040320 and other proteins associated with mouse globozoospermia by examining whether they localise to the same cellular compartments. PICK1 and HRB are two proteins whose absence leads to phenotypes that mimic those observed for AU040320-deficiency. PICK1 has been shown to be required for the transport of Golgi-derived vesicles and their budding from the TGN (Xiao et al. 2009; He et al. 2015), whilst Hrb is an Arf-GAP protein required for vesicle fusion (Kang-Decker et al. 2001). Double immunohistochemistry revealed AU040320 and PICK1 exhibit some overlap in round spermatids (Fig. 5.13A), consistent with a previous report that PICK1 localises to the TGN and proacrosomic vesicles (Xiao et al. 2009). On the other hand, no association between AU040320 and Hrb could be detected as they appear to occupy different cellular compartments and Hrb expression does not appear detectable in the Golgi (Fig. 5.13B; see also Kang-Decker et al. 2001). In

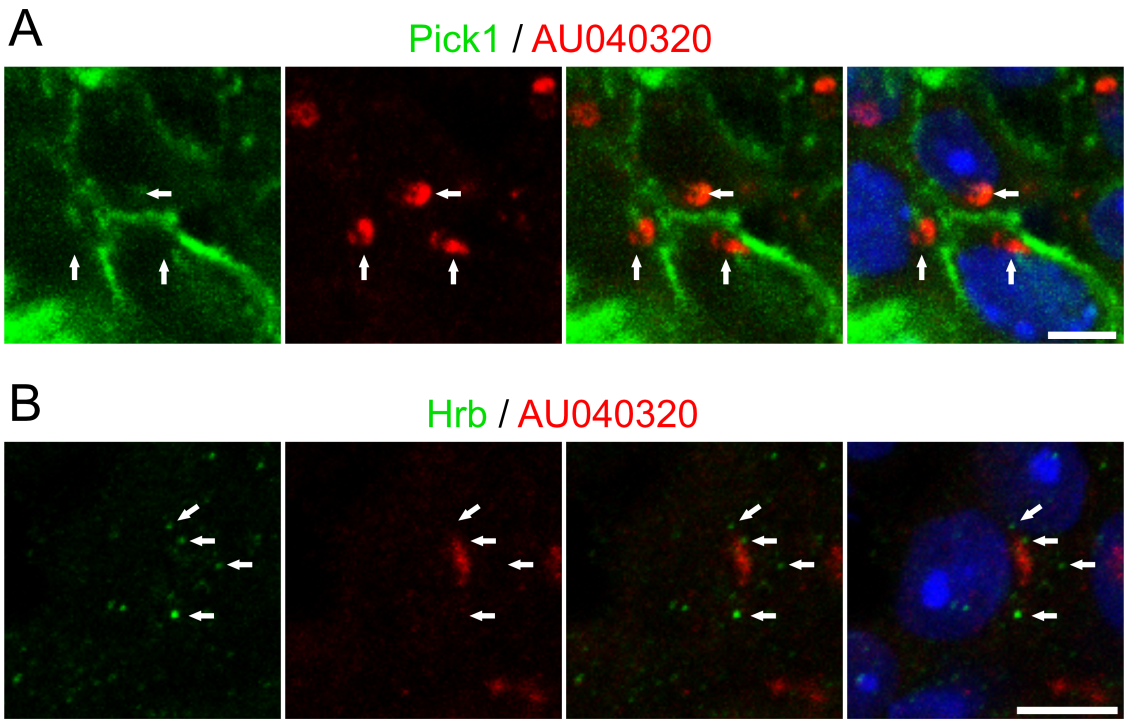


Figure 5.13: Co-localisation of AU040320 with other mouse globozoospermia-associated proteins. (A) AU040320 (#78, red) and PICK1 (green) seem to only display partial co-localisation in the region of the TGN in round spermatids. (B) Punctate staining of Hrb-positive proacrosomal vesicles does not appear to overlap with AU040320 in the TGN. Scale bars: 5 μm.

addition, SMAP2 and GOPC, two other globozoospermia-linked proteins (Yao et al. 2002; Funaki et al. 2013) were probed for co-localisation with AU040320 but no reliable signal could be detected for the antibodies used (data not shown).

Whilst preliminary, the combination of these results suggest the possibility of a relationship between AU040320 and proteins known to play a role in vesicle function and acrosome development.

5.2.10 Mutation screening in human globozoospermia

The identification of the globozoospermia phenotype on mice raised the question whether mutations in *KIAA0319L* leads to globozoospermia in humans. *KIAA0319L* has not been previously implicated in male infertility but there are suggestive associations. A recent study has found a significant difference in methylation patterns in this gene in samples from men undergoing IVF treatment when compared

to normal controls (Aston et al. 2015; Jenkins et al. 2016) and chromosome 1, where *KIAA0319L* is located, shows an enrichment for breakpoints in cases of chromosomal rearrangements in cases of male infertility (Bache et al. 2004). In globozoospermia more specifically, most identified mutations lie in the *DPY19L2* gene but several patients remain without a known genetic diagnosis (Coutton et al. 2015a).

Given this, a collaboration was established with the laboratory of Prof Pierre Ray and Prof Christophe Arnoult at the Université Joseph Fourier, Grenoble, France, who have published several reports of cases of human globozoospermia (Koscinski et al. 2011; Harbuz et al. 2011; Coutton et al. 2012; Coutton et al. 2013; Coutton et al. 2015b; ElInati et al. 2016). Genomic DNA samples were obtained from 16 males with globozoospermia for which no genetic abnormalities have been previously identified. Cases of globozoospermia were defined as patients with more than 80% round-headed spermatozoa, with <5% morphologically normal spermatozoa. All cases had a normal 46, XY karyotype and none carried a deletion (either heterozygous or homozygous) in the *DPY19L2* gene. The analysis was carried out by MLPA as described in Coutton2012.

Screening of mutations was performed by PCR-amplification of each of the 20 coding exons individually (start codon *ATG* lies in exon 2) from each patient followed by Sanger sequencing. Fragments were amplified to span the entire exons with a small flanking intronic region. A number of synonymous changes/SNPs were found in these samples but no potential pathogenic mutations such as missense, small insertions/deletions or nonsense changes were detected. Whilst this approach can reliably detect point mutations in coding regions and possible deletions of particular exons if they are homozygous, it cannot capture heterozygous deletions, duplications, larger rearrangements or intronic mutations leading to alternative splicing.

5.3 Discussion

The study reported here shows that absence of AU040320 in male mice leads to infertility and gross cell morphology abnormalities characterised by all mutant spermatozoa displaying a rounded head lacking an acrosome, features reminiscent of human globozoospermia (Dam et al. 2007a; Coutton et al. 2015a). The formation of the acrosome in AU040320-deficient males was disrupted in round spermatids as proacrosomal vesicles failed to fuse and coalesce into a single acrosomal vesicle, leading to an accumulation of vesicles around the nuclear face. The AU040320 protein localises to the trans-Golgi network of germ cells and it interacts with AP-1, suggesting that presence of AU040320 may be required for the normal function of proacrosomal vesicles. The abnormalities in nuclear condensation and head morphology observed in AU040320-deficient spermatozoa are likely to be a secondary effect given the importance of the acrosome in head elongation (Kierszenbaum 2004). Coiling of sperm tails may be a similarly collateral consequence as it has been shown to be induced by passage of globozoospermic spermatozoa into the epididymis (Suzuki-Toyota et al. 2004).

Loss-of-function mutations in several mouse genes have been found to cause phenotypes resembling human globozoospermia such as *Hrb, GOPC, Pick1, C2K2, Hsp90b1, Vps54, Dpy19l2, Atg7, Zpbp1/Zpbp2, Spaca1, Mfsd14a, Smap2* and *Fads2* (Xu et al. 1999; Kang-Decker et al. 2001; Yao et al. 2002; Yildiz et al. 2006; Lin et al. 2007; Xiao et al. 2009; Audouard et al. 2011; Fujihara et al. 2012; Pierre et al. 2012; Funaki et al. 2013; Wang et al. 2014; Doran et al. 2016). A typical feature of globozoospermia is the absence of the acrosome in mature spermatozoa. The acrosome is formed from the accumulation of proacrosomal vesicles derived from intracellular trafficking pathways that form a large vesicular organelle anchored to the nuclear envelope (Abou-Haila & Tulsiani 2000). The genetic models mentioned above have shown that disruption in a number of different processes during acrosome biogenesis can lead to globozoospermia, from protein processing in the endoplasmic

reticulum and fusion of proacrosomal vesicles to the adhesion of acrosome with nuclear structures (de Boer et al. 2014; Coutton et al. 2015a).

The main mechanism underlying the failure of acrosome formation in AU040320-deficient spermatids appears to be a failure in the fusion of proacrosomal vesicles between the TGN and the nucleus. Amongst the other globozoospermia mouse mutants, the abnormalities observed in *AU040320* -/- mice phenocopy those observed for *Hrb*, *Gopc*, *Mfsd14a* and *Fads2* mutants, with strong similarities also in the case of *Pick1* (Kang-Decker et al. 2001; Yao et al. 2002; Xiao et al. 2009; Roqueta-Rivera et al. 2011; Doran et al. 2016). In all these cases including AU040320, proacrosomic vesicles fail to coalesce and instead line up the nuclear surface without the clustering as a single acrosomal granule. Amongst the proteins involved, only HRB has been directly linked to vesicle fusion via its interaction with VAMP7, a member of the SNARE complex which mediates vesicle fusion and docking (Doria et al. 1999; Chaineau et al. 2008; Pryor et al. 2008; Südhof & Rizo 2011). On the other hand, GOPC and PICK1 are involved in the budding of vesicles from the TGN and their trafficking, whilst Fads2 is an enzyme involved in the synthesis of fatty acids, suggesting that the failure in the fusion of vesicles in these mutants may be the result of abnormalities in some preceding steps of vesicle formation (Yao et al. 2002; Xiao et al. 2009; Roqueta-Rivera et al. 2011; He et al. 2015; Lu et al. 2015).

It appears that the impairment in vesicle fusion in AU040320-deficient mice results from similarly indirect mechanisms. The protein encoded by *AU040320* is a transmembrane glycoprotein with five immunoglobulin-like domains (Ig-like) of the PKD family that lie in the protein's ectodomain and which have been linked to cell adhesion (Ibraghimov-Beskrovnaya et al. 2000). Adhesive glycoproteins such as zona pellucida proteins 1-4 (ZP1-4) in the reproductive system are generally associated with sperm-egg binding in the zona pellucida of the *ovum* rather than vesicles (Wassarman 1988; Gupta et al. 2012). Whilst other proteins with Ig-like motifs have been shown to mediate membrane fusion events, these tend to occur at cell-cell junctions (Grobler & Hurley 1997; Chen & Ghosh 2005; Martens &

McMahon 2008). Such cellular interactions in spermatogenesis are most clearly seen in the transient association between Sertoli cells and developing spermatids via the ectoplasmic specialisation, an actin-based specialised adherens junction that forms between them (Yan et al. 2007), and which is often mediated by transmembrane glycoproteins with adhesive properties, including those of the Ig superfamily (Wong et al. 2008). However, the abnormalities detected in AU040320-deficient mice differ considerably from those that directly affect the ectoplasmic specialisation as these do not normally affect spermatid differentiation and tend to emerge during the onset of elongation, rather than the early stages of acrosome formation (de Boer et al. 2014).

The fact that AU040320 appears to localise mainly in the TGN and could not be detected in proacrosomal vesicles (or in the acrosome itself) is consistent with the hypothesis that AU040320 does not directly operate during vesicle fusion. Thus, the failure of proacrosomal vesicles to fuse in AU040320-deficient spermatids is likely to result from some defect that precedes the fusion events, in the processing and formation of vesicles. The associations observed between KIAA0319L and AP-1 as well as with ASAP1 in the pulldown experiments are in line with this.

AP-1 is an adaptor protein for clathrin-coated vesicles which are responsible for regulating intracellular trafficking from the TGN, endosomes and plasma membranes (Cai et al. 2007; Park & Guo 2014). Components of vesicle coats mediate vesicle budding, the shaping of vesicular membranes and the recruitment of cargo proteins by specific sorting signals (Bonifacino & Glick 2004; Park & Guo 2014). After their formation, vesicles are transported within the cell by an interplay of motor proteins, cytoskeletal network and Rab family members until they initiate docking and fusion with the membrane of their cellular target via interaction with SNARE proteins (Rizo & Rosenmund 2008; Südhof & Rizo 2011). The delivery and fusion of proacrosomal vesicles in developing spermatids have been shown to be dependent upon this complex molecular machinery (Griffiths et al. 1981; Moreno et al. 2000; Ramalho-Santos et al. 2001; Kang-Decker et al. 2001; Funaki et al. 2013).

AP-1 is a member of this molecular network and it is present in the TGN and vesicles of developing spermatids (Kang-Decker et al. 2001). As such, one possibility is that an interaction between AU040320 and AP-1 in the TGN is necessary for proacrosomal vesicles for the recruitment of cargo proteins or perhaps the proper budding of vesicles - and a disruption in this interaction by the absence of AU040320 may lead to abnormal vesicular formation and/or molecular composition. SMAP2 and HRB, two other proteins linked to globozoospermia have also been shown to interact with clathrin-related proteins such as AP-1, AP-2, EPS15 and CALM (Kang-Decker et al. 2001; Chaineau et al. 2008; Funaki et al. 2013). However, the exact molecular mechanisms through which AU040320 deficiency may affect the formation of proacrosmal vesicles remains to be further investigated. The AU040320 protein is a type I transmembrane protein with its N-terminal region containing the MANEC and PKD domains situated extra-cellularly at the plasma membrane or facing the lumen of membrane organelles such as the Golgi or vesicles in the secretory pathway; thus, leaving the small C-terminal region facing the cytosol. This conformation resembles that of transmembrane receptors for vesicle cargo or other membrane proteins that associate with adaptor proteins in larger complexes during vesicle assemble.

Members of the SNARE protein complex are likely candidates to be affected in the vesicles of AU040320-deficient spermatids given their observed inability to fuse as expected. Other proteins involved in acrosome formation that localise to the Golgi apparatus and proacrosomal vesicles such as GOPC, PICK1 and SMAP2 may also be involved (Yao et al. 2002; Xiao et al. 2009; Funaki et al. 2013). Although no direct interaction with PICK1 has been detected so far, their partial co-localisation in the TGN would be consistent with this possibility, particularly given the known role of PICK1 in vesicle budding and transport (Xiao et al. 2009; He et al. 2015). Another option comes from potential functional similarity with a low-density lipoprotein (LDL) receptor, LRP11, as it shares a number of biochemical and structural features with AU040320 such as the presence of an extracellular MANEC domain, a PKD

motif and a transmembrane domain. LDL receptors typically bind cholesterol, a key component of biological membranes, and their presence has been shown to modulate calcium-regulated vesicle fusion by focal recruitment of SNARE proteins to membranes so as to promote efficient vesicle docking and fusion (Churchward et al. 2005; Lang et al. 2001). A putative role for AU040320 in the recruitment of SNARE proteins remains a topic for further investigation.

The potential interaction with ASAP1 observed in GST-pulldown experiments is in line with the hypothesis that absence of AU040320 leads to a defect in vesicle function and/or formation. ASAP1 (ArfGAP with SH3 domain, ankyrin repeat and PH domain 1) is a member of the Arf GTPase activating protein (Arf GAP) family which, together with Arf family GTP-binding proteins, play crucial roles in regulating intracellular membrane trafficking (Nie et al. 2006; Nie & Randazzo 2006). ASAP1 has been linked to the promotion of tumour motility (Liu et al. 2002; Muller et al. 2010) and it was shown to regulate the formation and sorting of vesicles targeted to specialised organelles like primary cilia (Wang et al. 2012). This process is dependent on the formation of a coat complex in the TGN by interaction with Arf4 and Rab11, proteins previously shown to regulate membrane transport alongside other protein coats, adhsesive proteins and SNARES (Cai et al. 2007; Wang et al. 2012). The ASAP1 proteins contain a number of different functional domains such as Arf GAP domain, pleckstrin homology, SH3, proline-rich and N-terminal BAR domain (Brown et al. 1998). Several Arf GAP proteins contain BAR domains and this structural component has been shown to be important in the induction or sensing of membrane deformations and binding to it (Peter et al. 2004; Jin et al. 2006); thus, contributing to the regulation of coat assembly and disassembly (Nie & Randazzo 2006).

A number of studies have shown that ASAP1 can modulate membrane morphology and curvature via its BAR domain (Nie & Randazzo 2006; Nie et al. 2006), adding to the evidence that the protein could be a component of membrane-deforming vesicle coats (Deretic & Wang 2012). This raises the suggestion that the

observed failure in vesicle fusion in AU040320 mutants may be due to the malformation of proacrosomal vesicles as the disrupted interaction between AU040320 and ASAP1 could affect the normal composition of vesicle coats or their ability to deform their membranes or those of the acrosomal granule. Interestingly, BAR domains are also encoded in *PICK1*, a gene linked to globozoospermia in both human (Liu et al. 2010) and mice, whose knockout phenocopies that of *AU040320* (Xiao et al. 2009; He et al. 2015).

The predominant view of acrosome formation is that it originates from proacrosomal vesicles transported directly from the TGN (Aguas & da Silva 1985; Abou-Haila & Tulsiani 2000; Moreno et al. 2000). However, there is mounting evidence that extra-Golgi vesicles derived from other routes and trafficked along the endocytic pathway also contribute to the development of the acrosome via the involvement of several different proteins: regulator of lysosomal delivery SPE-39, SH3P13 which is involved in clathrin-mediated endocytosis of membrane receptors, a transmembrane protein (AFAF) present in the acrosome and in endosomes, amongst others (Zhu et al. 2009; Li et al. 2009; Li et al. 2006; Berruti & Paiardi 2011). Members of the Rab family of small GTPases have also been linked to acrosome formation and are well-known factors in the regulation of the endosomal system and formation of lysosome-related organelles (Ramalho-Santos et al. 2001; Raposo et al. 2007). These findings led to a revival of the idea that the acrosome is a lysosome-related organelle due to a number of features it shares with other specialised lysosomes (Hartree 1975; Moreno et al. 2000; Berruti & Paiardi 2011; Berruti 2016).

Although the study reported here does not directly support this, previous findings showing trafficking of the human homolog KIAA0319L are consistent with this idea and an old hypothesis that plasma membrane proteins play a role in acrosome development (West & Willison 1996; Berruti 2016). Endocytosis of KIAA0319L from the plasma membrane into early endosomes is dependent on Rab5 and an interaction with AP-2 via a tyrosine-based motif (Levecque, unpublished; Pillay et al. 2016), both of which have been shown to regulate the sorting of

endosomes and the formation of acrosomes and lysosome-related organelles (Moreno & Alvarado 2006; Raposo et al. 2007; Delevoye et al. 2009). It is possible that the AU040320 protein traffics outside the TGN but remains undetected due to low levels or its rapid relocation to the TGN (Pillay et al. 2016). Transcriptomic analyses of sperm development support this possibility given that expression of *AU040320* is upregulated around P21 when spermatid differentiation and acrosome development initiates, with an expression profile that is similar to that of other proteins involved in vesicle trafficking/fusion and globozoospermia such as PICK1 and HRB (Kang-Decker et al. 2001; Shima et al. 2004; Xiao et al. 2009; Laiho et al. 2013). Further investigations into the localisation and function of AU040320 may provide further insight and potential support for an extra-Golgi origin of the acrosome. This avenue is particularly interesting given that the hypothesis of the acrosome as a lysosomal-related organelle draws an intriguing parallel with the nervous system through its similarities with neuronal synaptosomes, another type of secretory vesicle (Cosker et al. 2008; Berruti & Paiardi 2011).

5.4 Conclusion

In conclusion, the study reported here identifies *AU040320* as a new gene involved in globozoospermia in mice. No evidence of mutations in the human homolog *KIAA0319L* was found in 16 human samples analysed. Thus, *AU040320* joins a number of other genes known to cause globozoospermia in mice without a clear relationship with the disorder in humans (Coutton et al. 2015a). The globozoospermia-like defects observed in *AU040320* -/- are characterised by the absence of the acrosome due to a failure in the fusion of proacrosomal vesicles during its development. The subcellular localisation of AU040320 in the TGN and the putative molecular interactions of AU040320 with proteins involved in intracellular trafficking suggest AU040320 may be important in the proper formation of TGN-derived vesicles and/or their cargo in developing spermatids.

6

General Discussion

Contents

6.1 Introduction 200
6.2 Summary of findings & final considerations 200
6.2.1 The role of KIAA0319 & KIAA0319L proteins in neuronal migration 200
6.2.2 The role of KIAA0319 & AU040320 in mouse behaviour and auditory processing 202
6.2.3 Subcellular function of AU040320 and a new hypothesis 204
6.3 Unresolved questions and future work 207
6.4 Final conclusion 212

6.1 Introduction

The aim of this thesis was to elucidate the function of dyslexia susceptibility candidate genes *KIAA0319* and *KIAA0319L* in brain structure and function. The important position of *KIAA0319* within the range of dyslexia susceptibility genes identified through classic association studies and its homology with *KIAA0139L* indicates that advancing our knowledge of the role of the two encoded proteins may provide important insights into the nature of the language/reading-ready brain as well as how these genes may contribute to susceptibility to dyslexia and associated language-related disorders.

This thesis attempted to tackle the problem of gene function from multiple levels of 'granularity', from the perspective of molecular and cellular biology to the modulation of animal behaviour. This involved the interrogation of a variety of neural systems in the mouse brain (cortical development and cell migration, rodent behaviour and auditory processing, spermatogenesis and subcellular functions) based on the specific questions raised by the current knowledge on KIAA0319 and KIAA0319L, and as a way to generate new hypotheses about their function. Below, I provide a brief summary of my findings and some final considerations.

6.2 Summary of findings & final considerations

6.2.1 The role of KIAA0319 & KIAA0319L proteins in neuronal migration

In order to test the hypothesis that the KIAA0319 and KIAA0319L proteins regulate the migration of neurons during cortical development, I first generated a transgenic (conditional) knockout mouse line targeting the *AU040320* gene. The effect of the introduced loss-of-function mutation was studied both alone and in conjunction with *Kiaa0319* KO, so as to assess potential functional redundancy that may exist between the two proteins.

Analyses of the developmental progression of the cortex in these mutants using immunohistochemistry, histology and *in utero* electroporation revealed no evidence

for a contribution of the two proteins during neuronal migration as the distribution of cortical projection neurons and interneurons in the cortex was found to be normal, with similarly unaffected lamination of the hippocampus and cerebellum. Moreover, no periventricular heterotopias or molecular layer ectopias were detected in any of these animals with the methods used. In addition, cortical neurogenesis in both *AU040320* and double KOs was found to be normal as the mitotic profile of cells in the early cortex was found to be unaltered in the mutants, and similarly for their neuronal progenitor populations (Pax6+ and Tbr2+ cells).

These results indicate that neither KIAA0319 nor AU040320 are required for neurogenesis or neuronal migration in the mouse brain, findings which go against the hypothesis that the two proteins could interact in compensatory ways during cortical development (Martinez-Garay et al. 2017). Moreover, these findings stand in contrast to previous reports of a role for both KIAA0319 and KIAA0319L in cortical migration in rats (Paracchini et al. 2006; Peschansky et al. 2010; Adler et al. 2013; Platt et al. 2013), as it is the case for the two other main dyslexia susceptibility genes, *DYX1C1* and *DCDC2* (Meng et al. 2005b; Burbridge et al. 2008; Wang et al. 2011b; Rendall et al. 2015). Although species differences could potentially account for some of it, I argued that these discrepancies are likely to result from methodological artefacts of shRNA-knockdown techniques that trigger migration abnormalities via off-target effects (see Baek et al. 2014).

More importantly, there has been no replication so far for the role of these candidate genes in neuronal migration using alternative methods or by a group other than the one who made the original findings. At a time when the scientific community is striving to improve reproducibility and reliability (Freedman et al. 2015; McNutt 2014), it is imperative that we place the necessary importance on these issues and publish studies with negative findings, particularly when it addresses specific existing hypotheses.

Moreover, I argued that these problems are exacerbated when combined with a careful evaluation of the evidence from human neuropathology and neuroimaging

studies on dyslexia which face key issues with respect to methodology. Based on this, I proposed a careful reconsideration of the view of dyslexia as a neuronal migration disorder (Galaburda et al. 2006; Fisher & Marcus 2006; Paracchini et al. 2007; Gabel et al. 2010; Scerri & Schulte-Körne 2010; Giraud & Poeppel 2012; Raskind et al. 2013; Adler et al. 2013; Kere 2014; Peterson & Pennington 2015), and that the presentation of this hypothesis in the future must be done in conjunction with its shortcomings.

Recently, there has been growing interest in the relationship between these very same dyslexia susceptibility candidate genes and the structure/function of primary cilia, offering a promising alternative on the research direction of the field, particularly given potential relationships with brain asymmetry (Kere 2014; Newbury et al. 2014; Brandler & Paracchini 2014; Paracchini et al. 2016; Trulioff et al. 2017). However, in relation to KIAA0319 and KIAA0319L, this relationship remains speculative and lacks substantive evidence - for example, the studies of subcellular function of KIAA0319L/AU040320 in Chapter 5 did not identify a link to the cilium, despite male infertility being one of the key features of ciliopathies (Fliegauf et al. 2007). Moreover, as argued in the discussion to Chapter 3, our understanding of the genetic architecture of dyslexia and its associated genes/variants remains hugely limited – there are still very few genes identified and the associations do not hold the challenge of robust, genome-wide, powerful statistical testing. Moreover, it would be surprising if all associated genes perform a function in the very same process, especially for a heterogeneous disorder like dyslexia. Therefore, caution must be taken in order to avoid an over-enthusiasm similar to what may have happened to the case of neuronal migration.

6.2.2 The role of KIAA0319 & AU040320 in mouse behaviour and auditory processing

In Chapter 4, I performed a series of behavioural tests on a cohort of double *Kiaa0319;AU040320* KO mice to assess potential deficits that the combined deletion of the two proteins may have on mouse behaviour. This was motivated not only as

a way to interrogate how they may mediate language-related endophenotypes with parallel processes in mice (e.g. auditory processing, motor learning, etc), but also as a strategy to identify neural circuits in which they may play an important role. This was particularly important given the little knowledge on the two proteins beyond neuronal migration and the need to generate new hypotheses about their function.

The results of this chapter revealed that double KO mice had normal levels of locomotor activity in the open field and unaltered performance in the accelerating rotarod, in olfactory preference and spatial memory. A putative increase in anxiety levels was detected in the light-dark box test, although no further evidence for the defect was identified in other tests. On the face of evidence for a role of *Kiaa0319* in auditory processing (albeit derived from shRNA studies) (Szalkowski et al. 2012; Centanni et al. 2014a; Centanni et al. 2014b), I also probed the auditory system of these dKO mice and found an impairment in psychophysical discrimination of rapidly changing stimuli in a silent gap detection task. This prompted a more detailed examination of the auditory system of these animals which revealed altered evoked responses to simple sounds in the brainstem using ABRs. These predominantly affected the latency and amplitude of wave III for both mutants *AU040320* and double KOs, but more profound effects were detected in the latter case as I identified deficits in wave II, in line with their more profound genetic manipulation. These results suggest that loss-of-function mutations in *Kiaa0319* and *AU040320* can lead to auditory deficits via underlying abnormalities in the brainstem that result in reduced activity and affect sensory processing early in the pathway. No anatomical differences were detected in this pathway, particularly in relation to the number of synapses present in key structures of the auditory system investigated (cochlear nucleus, inferior colliculus, medial geniculate body).

Although its specific nature remains highly controversial (phonology vs. sensory vs attentional, cortical vs. subcortical, and so on), deficits associated to the auditory system are a hallmark of dyslexia (Ramus 2003; Giraud & Ramus 2013; Goswami 2014; Peterson & Pennington 2015). The gap detection test and masker-probe

ABR recordings performed here provide important insights into how *Kiaa0319* and especially *AU040320* may contribute to the normal function of the auditory circuit in humans, particularly in relation to temporal acuity and rapid auditory discrimination (Tallal 1980; Temple et al. 2000; Choudhury & Other 2007; Raschle et al. 2014; de Groot et al. 2015; but see also e.g. Breier et al. 2003; Georgiou et al. 2010; Protopapas 2014). In addition, these results point towards the importance of going beyond the standard cortico-centric approach of much work in neurobiology of language (see also Krishnan et al. 2016). In the case of dyslexia and auditory processing, deficits in neural activity and representation of sounds in the brainstem have been reported before (Hornickel & Kraus 2013) and my results here suggest a potential relationship between AU040320 and KIAA0319 with such deficits.

The relationship between the observed ABR deficits with a reduction in activity in the auditory pathway was also discussed in relation to its potential cellular correlates, and a preliminary analysis of the number of synapses in dKO mutants revealed no observable defects using immunohistochemistry. In this context, I outlined a number of possible ways in which the AU040320 and KIAA0319 proteins may operate and lead to the type of impairment observed in ABRs, ranging from synaptogenesis, axonal growth, calcium/ion-channel regulation, synaptic vesicle release, and so on. The experiments reported in Chapter 5 served as a parallel way to probe into this by investigating the function of AU040320 at the cellular level.

6.2.3 Subcellular function of AU040320 and a new hypothesis

On the face of the paucity of knowledge on the AU040320/KIAA0319L protein, Chapter 5 aimed to examine its function at the level of individual cells by exploiting the window into its role within cells opened by the fertility abnormality observed in male *AU040320* -/- mutants. This phenotype offered an opportunity to dissect the contributions of this protein in subcellular processes with the final goal of generating new hypotheses on cellular functions that could potentially be translated/interrogated to the brain.

I showed that AU040320 protein is expressed abundantly in the testis, with expression observed across the different cell types of seminiferous tubules from where spermatozoa develop. The overall organisation of the seminiferous tubules and of the epididymis in *AU040320* -/- mutants was unaltered, but a reduction in the number of mature spermatozoa in the epididymis was detected (about half the expected amount). Given no defect in cell division in spermatocytes was observed through immunohistochemical analysis of its meiotic progression, I turned to examine the morphology of spermatozoa which were found to display gross morphological alterations in all the examined samples . These displayed sperm heads that were round-headed and lacked an acrosome – features that mimic a human condition called globozoospermia. Examination of the developmental progression of developing spermatids found that acrosome formation was impaired from the early stages and ultra-structural analyses revealed this to be due to a failure in proacrosomic vesicles to coalesce and fuse along the surface of the cell nucleus. No major defects were observed in other structures known to lead to globozoospermia such as the sperm manchette or in Sertoli cells. Immunohistochemical analyses of AU040320 localisation found that the protein localises to the TGN and I presented preliminary evidence for a potential interaction with proteins involved in acrosome formation and Golgi-derived intracellular transport such as PICK1, ASAP1 and AP-1/2. Screening of a cohort of 16 human cases of globozoospermia did not identify potential causative mutations in the *KIAA0319L* gene.

Based on this, I outlined the view for a potential role for AU040320 in the proper formation and/or fusion of TGN-derived vesicles in developing spermatids, possibly via interaction with proteins essential for vesicle coat assembly, fusion or cargo recruitment. Whilst the evidence for this requires further investigation, this hypothesis extends naturally to the nervous system. Similarities between the sperm acrosome and synaptosomes have been noted by a number of groups before for the intriguing parallels in their secretory functions (Ramalho-Santos et al. 2001; Redecker et al. 2003; Moreno & Alvarado 2006; Cosker et al. 2008; Berruti & Paiardi

2011). Interestingly, this overlap extends to the molecular level as several members of the SNARE protein family and others involved in vesicle release have been shown to play a role in both synaptic and acrosomal release (e.g. Ramalho-Santos et al. 2001; Li et al. 2009). Much of intracellular trafficking in developing spermatids is mediated by the clathrin-endocytic pathway which is widespread across cell types in the body, but it is also known to play a major role in the regulation of synaptic vesicles, particularly in their recycling at synaptic terminals (Heuser & Reese 1973; Saheki & De Camilli 2012; Watanabe et al. 2014). The Monaco group had previously published a report on the transport of KIAA0319 protein along the clathrin pathway (Levecque et al. 2009), with similar but unpublished evidence for AU040320 (Levecque, unpublished), and this was considered to be linked to the regulation of the availability of the protein at the cell membrane for cell adhesion during migration. The findings reported in this thesis on impaired vesicle fusion in the absence of AU040320 and its link to intracellular trafficking proteins indicates that this protein may have some other function before it reaches the cell membrane, although it is possible that such a function may be limited to specific cell types such as spermatids.

Interestingly, PICK1 (Protein that interacts with C kinase 1), a protein previously shown to lead to globozoospermia in mice (Xiao et al. 2009; He et al. 2015), provides a clear example of a molecule that plays a role in intracellular trafficking both in developing spermatids and neurons. Several groups have reported PICK1 is important in the regulation of synaptic plasticity through regulating the trafficking of AMPA receptors at synaptic terminals (Xia et al. 1999; Terashima et al. 2008; Xu et al. 2014), with much of the control of these receptors at the synaptic membrane being dependent on the clathrin-endocytic pathway (Anggono & Huganir 2012; Madasu et al. 2015). In Chapter 5, I already noted the strong similarities between spermatids lacking PICK1 and AU040320 and also provided preliminary evidence for their co-localisation in spermatids, suggesting the possibility of their interaction. Thus, whilst further evidence is required to identify the precise relationship between AU040320

and vesicle structure-function in developing spermatids, it is possible that the role AU040320 plays in vesicle structure/function in cells of the reproductive system may extend also to neurons, just as it is the case for PICK1. A potential function in vesicle recycling or receptor trafficking could perhaps be one of the mechanisms underlying the reduction in neuronal firing observed in the electrophysiological recordings of ABR in Chapter 4.

6.3 Unresolved questions and future work

Whilst this thesis addressed some key questions with respect to the function of KIAA0319 and AU040320, there are a number of points that remain unanswered or which have emerged as a result of the work presented in this thesis. This section outlines a series of experiments to be conducted to address them, resolve pending problems and investigate new hypotheses.

Putative alternative isoforms. Western blots using an anti-AU040320 antibody revealed a number of additional smaller bands present in various different tissues in both wildtype and knockout samples. The majority of these bands are thought to be unspecific targets of this polyclonal antibody, but it is possible that they represent other isoforms that continue to be produced by the transgenic null allele. There are several ways to address this:

- Load protein samples from KO tissue onto a gel to separate bands and perform mass spectrometry on gel outs to identify KIAA0319L/AU040320 peptides that may be present
- Use different antibodies detecting AU040320 for a Western blot and compare bands with the original blot – bands which overlap may indicate potential persistent isoforms
- Purify the aforementioned antibody to increase specificity of target. Performing a Western blot with a purified antibody would be expected to produce

signal that is more specific to the target protein and would be better at revealing potential protein isoforms

- The question of isoforms should also be addressed at the level of RNA. This can be achieved by generating cDNA to perform RT-PCR using a combination of primers to cover different exonic regions which may be present (e.g. target exons 4-5, 5-6, 6-7, and so on). These experiments are currently being conducted in the Monaco and Molnár laboratories.

Species differences in neuronal migration. As noted in Chapter 3, there is a discrepancy between experiments probing neuronal migration in rats in the literature and the mouse ones reported here. I argued that it is likely that this divergence results from off-target effects of shRNA vectors used in rats, rather than differences between species in gene function and/or cortical development. But there are several experiments which can be conducted relatively easily to test this in more detail:

- Perofrm in mice the same shRNA knockdown design used for the rat experiments, both in wildtype and in KO mice

- Conversely, CRISPR-based knockdowns to be performed in rats for a replication of the original experiments with a method that is 'cleaner' than shRNA

- Knockdown experiments should be combined with Western blots to validate the efficiency of knockdown of the relevant proteins using whole brain or cortex only (for increased sensitivity/detection); alternatively single cell RNA-seq of electroporated cells can be used to investigate potential protein levels as well as dysregulation of unintended pathways. These *in utero* electroporation experiments would provide robust further tests of the putative function of Kiaa0319 and Kiaa0319-Like/AU040320 in neuronal migration.

Auditory deficits. The mechanisms underlying abnormal ABR responses, particularly in relation to adaptation to noise, might well involve not only the auditory brainstem structures where ABR waves originate, but also higher auditory areas including the cortex. In the auditory system, there are extensive descending connections from cortical to subcortical structures (Winer 2005; Lou et al. 2008), as well as olivocochlear projections from the superior olivary nuclei into the sensory transduction machinery of the cochlea (Guinan 2006). As such, further behavioural and electrophysiological tests in the auditory pathway are necessary to further dissect the deficits observed here:

- At the behavioural level, the gap detection experiments reported used cues with variable gap duration (i.e. noise onset) which maintained delay from gap to startle eliciting stimulus constant (100 ms). Given there is evidence for the auditory thalamus to be particularly sensitive to noise offset but not noise onset (Anderson & Linden 2016), repeating this task and using variable noise offset (between 0-100 ms) may reveal a potential role for the thalamus in the deficit

- Perform PPI-based auditory experiments with stimuli consisting of complex variation of tones or frequency-modulating sweeps, stimuli whose processing is more dependent on the cortex and, thus, can interrogate other deficits at a higher level in the auditory pathway

- Conduct extracellular multi-unit recordings in the generators of wave II and III (cochlear nucleus and superior olivary complex, respectively) in *AU040320* and/or dKOs using multichannel electrode arrays in response to clicks or more complex sounds

- Recording local field potentials from the auditory cortex to probe whether reduced neural activity detected in the ABR persists higher in the pathway and/or display a different profile to that observed in the brainstem. Such

experiment would also serve as replication of the deficits reported by Centanni et al. (2014a) showing reduced neural responses following *Kiaa0319*-shRNA knockdown

- To dissociate potential top-down effects from the cortex onto the brainstem, local field potential (LFP) recordings from the brainstem (e.g. cochelar nucleus) can be combined with focal stimulation in the auditory cortex to assess whether cortical stimulation modulates brainstem LFPs (see e.g. Lou et al. 2008)

Anxiety-like behaviour. Martinez-Garay et al. 2017 reported that absence of Kiaa0319 alone leads to increased anxiety. Here, it was reported here that double KO of Kiaa0319 and AU040320 may lead to subtle reduction in anxiety levels in the light dark box, but no further anxiety test was conducted. Based on this, I would propose:

- Performing a more comprehensive screening of other anxiety tests in *Kiaa0319* and *AU04032* KOs as well as dKOs which include a number of experiments such as: illuminated open-fied, elevated plus maze, light-dark box, hypo-neophagia

Infertility in AU040320 -/- mutants. In reference to the infertility phenotype of AU040320 KO male mice, several questions remain open and require further investigation for a better understanding of the underlying causes of the deficits described here:

- Perform immunogold labelling in round spermatids to detect potential presence of AU040320 protein in proacrosomic vesicles or other cellular compartments

- Co-immunoprecipitation of AU040320 and several other proteins in lysates from mouse testis: AP-1, AP-2, ASAP1, HRB, PICK1, and other globo-zoospermia proteins

- These proteins should also be probed further in co-localisation experiments with AU040320 using immunohistochemistry in mouse testes sections

- Sample a wider population of human globozoospermia for potential mutations in KIAA0319L using a method with bigger coverage than Sanger sequencing such as whole exome sequencing – thus, increasing the likelihood of detecting CNVs which may be present, as well as mutations in other genes

Putative AU040320 function in synaptic vesicles. The experiments described in Chapter 5 outline a link between AU040320 and the function of intracellular vesicles/trafficking. Given the relationship between the human homologous KIAA0319L protein (as well as KIAA0319; Levecque et al. 2009; Levecque, unpublished) in the clathrin-pathway, this has raised the question of whether AU040320 may influence the normal function of vesicles in neurons. To investigate this possibility, the following experiments would be performed:

- Localisation: is the AU040320 protein present in the secretory-related organelles beyond spermatids and, more specifically, in neurons? Determine sub-cellular localisation of AU040320 in neurons by optimising anti-AU040320 antibodies for detection in brain sections (e.g. auditory brainstem) with immunohistochemistry or use cultured neurons (e.g. cortex, hippocampus). Perform double immunolabelling with TGN markers (e.g. TGN38), synaptic vesicles (e.g. synaptophysin).

- Ultrastructural analyses with TEM to investigate localisation and number of vesicles within neurons of the auditory brainstem (or other regions, or neuronal cultures) in *AU040320* KO samples

- Live cell imaging of cultured neurons to examine exocytosis and endocytosis using fluorescent markers (e.g. pHluorin) in AU040320 KO and wildtype samples. Use stimulation trains to generate a large number of action potentials

to elicit peak pHluorin responses (see e.g. Miesenbock et al. 1998) and use signals for quantification of rate of synaptic vesicle endocytosis. These can be combined with drugs that block vesicle recycling (e.g. Bafilomycin A1) to assess synaptic vesicle pool available to synapses and its recycling rate (cf. Marland et al. 2016)

- A basic characterisation of the intrinsic properties of AU040320 -/- neurons using acute *in vitro* brain slices (e.g. brainstem or cortex) would be performed by injecting depolarising or hyperpolarising current steps to assess action potential dynamics and membrane properties (rheobase, risetime, threshold, amplitude, input resistance, resting potential, and so on)

- This would serve as basis for further experiments testing vesicle recycling ability of AU040320-deficient neurons by recording changes in membrane capacitance following endo/exo-cytosis in cultured adult neurons (e.g. Lou2008)

6.4 Final conclusion

In this thesis, I presented three distinct contributions to the understanding of the function of dyslexia susceptibility candidate genes *KIAA0319* and *KIAA0319L* using the mouse as a tool for investigation. In Chapter 3, I show that neither KIAA0319 nor AU040320 play a role in neuronal migration during brain development, in contrast to previous reports. In Chapter 4, I characterised the basic behavioural functions of *Kiaa0319;AU040320* KO mice and demonstrate their impairment in rapid auditory processing, which is accompanied by more profound deficits in auditory processing present in the brainstem using auditory brainstem recordings. In Chapter 5, I investigate the subcellular function of the AU040320 protein by examining the infertility deficit of *AU040320* mutants and show that the protein is required for the normal fusion of proacrosomic vesicles.

The result of this is strong evidence against the role for these two proteins in neuronal migration which, when combined with previous reports, adds further

doubt to the view that dyslexia is a neuronal migration disorder. In addition, the deficits observed in auditory function indicate that KIAA0319 and particularly AU040320/KIAA0319L may play a role in auditory dysfunction through deficits at very low levels in the auditory pathway. The results obtained in Chapter 5 in the characterisation of globozoospermia in *AU040320* KO mice raise the possibility that the auditory deficits observed here may stem from altered structure/function of vesicles that results from absence of AU040320/KIAA0319.

Appendices

A

Appendix 1

Contents

A.1 List of primers 217
A.2 Sequence of the AU040320-KO1 allele and flanking regions 220
A.3 Primary cilia in double KO cortical neurons 229

A.1 List of primers

Primer			
Name	Sequence		Reverse complementary to
mKLi2F2	CCACAGGTTAGTGACCATCT	20	
mKLi2F7	TGGCAGACTGGCTTCCATAC	20	
mKLi2F11	AGTTCACCGTTGCATGTCTC	20	
SA-F1	AAGGCGCATAACGATACCAC	20	
SA-F3	ATGCCAGAGACTCAGTGAAG	20	
IRES-F1	GCCACGTTGTGAGTTGGATA	20	
IRES-F2	CGAAGCCGCTTGGAATAAGG	20	
lacZ-F5	GTTCAGATGTGCGGCGAGTT	20	
lacZ-F8	AATCAGGCCACGGCGCTAAT	20	
lacZ-F1	TGGCGAGCGATACACCGC	18	
lacZ-F2	GCCCGTCAGTATCGGCGG	18	
lacZ-F3	AATCGCCTTGCAGCACATCC	20	
lacZ-F9	GACCAGCGAATACCTGTTCC	20	
Neo-F1	CGCCACCATGATTGAACAAG	20	
Neo-F4	TCGCCTTCTTGACGAGTTCT	20	
PNF	ATCCGGGGGTACCGCGTCGAG	21	
R2R	TCTATAGTCGCAGTAGGCGG	20	
mKL3F1	TCTGCCTGCCACGCTCTATG	20	
mKL3F2	AGTCACCACCAGAGCTTACT	20	
mKLi3F4	GCAGCAGCTCTGGCATCGAA	20	
mKLi3F11	TGCTGGCCTGCATCTTCTTC	20	
AGp-F2	AGAGCCTCTGCTAACCATGT	20	
Cre-F2	GGTCGATGCAACGAGTGATG	20	
Cre-F3	AGGCGTTTTCTGAGCATACC	20	
oIMR7338	CTAGGCCACAGAATTGAAAGATCT	23	
oIMR1348	CACTGATATTGTAAGTAGTTTGC	22	
mSry-F1	ATACAGAGATCAGCAAGCAGC	21	
mSry-F	TGGGACTGGTGACAATTGTC	20	
mIL3-F	GGGACTCCAAGCTTCAATCA	20	
mKLi2R11	GCAAGCAGGTGACAGATACT	20	AGTATCTGTCACCTGCTTGC
LAR3	CACAACGGGTTCTTCTGTTAGTCC	24	GGACTAACAGAAGAACCCGTTGTG
SA-R2	GGTTGCTGGAGTCTAGCTAC	20	GTAGCTAGACTCCAGCAACC
IRES-R1	AAGCGGCTTCGGCCAGTAAC	20	GTTACTGGCCGAAGCCGCTT
IRES-R3	CTGCTTCCTTCACGACATTC	20	GAATGTCGTGAAGGAAGCAG
lacZ-R2	ACGACTGTCCTGGCCGTAAC	20	GTTACGGCCAGGACAGTCGT
lacZ-R3	GTTCAACCACCGCACGATAG	20	CTATCGTGCGGTGGTTGAAC
lacZ-R5	GACATCCAGAGGCACTTCAC	20	GTGAAGTGCCTCTGGATGTC
lacZ-R7	AGGAGTCGTCGCCACCAATC	20	GATTGGTGGCGACGACTCCT
bAp-R1	CATCCTAGGTGTGGACATCT	20	AGATGTCCACACCTAGGATG
Neo-R2	GCAGGAGCAAGGTGAGATGA	20	TCATCTCACCTTGCTCCTGC
R2R-R	CCGCCTACTGCGACTATAGA	20	TCTATAGTCGCAGTAGGCGG
mKL3R3	AGCCTAGCCTCAGAAGATGT	20	ACATCTTCTGAGGCTAGGCT
mKLi3R2	AACTTGACGGCAGCTACACC	20	GGTGTAGCTGCCGTCAAGTT
loxP3R	GATGGCGAGCTCAGACCATA	20	TATGGTCTGAGCTCGCCATC
mKLi3R4	AGTGCCTGGCAAGTAGTAAC	20	GTTACTACTTGCCAGGCACT
mKLi3R6	TCGACCTGAGTGAGAATGTG	20	CACATTCTCACTCAGGTCGA
mKLi3R11	CCAGGTAGTGGTAGTGCATA	20	TATGCACTACCACTACCTGG
mKLi3R13	GACTGGTGTGAGGTGGAATC	20	GATTCCACCTCACACCAGTC
mKLi3R14	CCAGCAGTGGAGGAGTGTTC	20	GAACACTCCTCCACTGCTGG
oIMR7339	GTAGGTGGAAATTCTAGCATCATCC	25	GGATGATGCTAGAATTTCCACCTAC
oIMR1349	CTAGTGCGAAGTAGTGATCAGG	22	CCTGATCACTACTTCGCACTAG
mSry-R1	GTGTGCAGCTCTACTCCAGTC	21	GACTGGAGTAGAGCTGCACAC
mSry-R	GAGTACAGGTGTGCAGCTCT	20	AGAGCTGCACACCTGTACTC
mIL3-R	TGGAGGAGGAAGAAAAGCAA	20	TTGCTTTTCTTCCTCCTCCA

Table A.1: List of primers for genomic AU040320 and transgenic gene trapping cassette.

Primer			
Name	Sequence		Reverse complementary to
KLg02F1	GTGCAACCTCTTCTCCTCAA	20	
KLg03F2	GGTCTCCATGGCAGGAACTC	20	
KLg04F1	GGCGTGAGCCACCATGCTTA	20	
KLg05F1	GAAGCCACTGAGATGTGAGA	20	
KLg06F1	AGCTGAGTCAGCAGCATTCG	20	
KLg07F1	GCTGGTCTTGAACTCAGGAA	20	
KLg08F1	CTGCCTCCTGTCAGATCAGT	20	
KLg09F1	GGTTGCCTGTGTTGGAGTTC	20	
KLg10F1	GCAGTGCCTAGCACATCATA	20	
KLg11F1	AGACTGGCCTTGGTAATCTC	20	
KLg12F1	CAGAAGGCACCGATCCATAG	20	
KLg13F1	GACCAGCAGGCAGCCTGTAT	20	
KLg14F1	TGCAGACCTCCAGACATAAG	20	
KLg15F1	GGCTGCAATGCTGTTCCGTA	20	
KLg16F1	GCACTGCCAGTTGCACAGAG	20	
KLg17F1	GATCTGGCTCTGCCATAATC	20	
KLg18F1	AAGTGAAGACAGGCTGGAAG	20	
KLg19F1	CCGTGCTGTAGCCTAATGGA	20	
KLg20F1	TCCGTGCCAAGGTGGTCATA	20	
KLg21F1	GGTGTGCTCTCATCCGTACT	20	
KLg02R1	TGCTGAGTGCTGTGCTACAT	20	ATGTAGCACAGCACTCAGCA
KLg03R1	CCGCAAGCATCAGCTTCATT	20	AATGAAGCTGATGCTTGCGG
KLg04R1	TAAGCTGGAGGCCTGCTGAG	20	CTCAGCAGGCCTCCAGCTTA
KLg05R1	CCAGGAGTGGTAGTGTATGC	20	GCATACACTACCACTCCTGG
KLg06R1	ACCATGCTGGTACAGTCTTC	20	GAAGACTGTACCAGCATGGT
KLg07R1	ATGTGTCCAGCTCAGCATTC	20	GAATGCTGAGCTGGACACAT
KLg08R1	AAGAAGGCCTGTCTGGTGTG	20	CACACCAGACAGGCCTTCTT
KLg09R1	CTGTGGCAGATCCTGATCTA	20	TAGATCAGGATCTGCCACAG
KLg10R1	ATTACAGGCGCACGCCACTA	20	TAGTGGCGTGCGCCTGTAAT
KLg11R1	AAGTCACCAGAGGCTCTATG	20	CATAGAGCCTCTGGTGACTT
KLg12R1	CCATCCTGCCTCTCAAGTGT	20	ACACTTGAGAGGCAGGATGG
KLg13R2	GTCTGGAGGTCTGCATATCT	20	AGATATGCAGACCTCCAGAC
KLg14R1	GCCTACAACTGCTAGGATCA	20	TGATCCTAGCAGTTGTAGGC
KLg15R1	TGGAACAGACGGTCTCTATG	20	CATAGAGACCGTCTGTTCCA
KLg16R1	CGCATGTCACCTGCACTAGA	20	TCTAGTGCAGGTGACATGCG
KLg17R1	GCTCACAGCCTTCTGAACAC	20	GTGTTCAGAAGGCTGTGAGC
KLg18R1	GGCTGTAACTGGCATTGGAT	20	ATCCAATGCCAGTTACAGCC
KLg19R1	GGCTACAGTGTGGTGCATTA	20	TAATGCACCACACTGTAGCC
KLg20R1	AGCGGAAGTAGCACGCGAAG	20	CTTCGCGTGCTACTTCCGCT
KLg21R1	CCTGGAGGACGTCTCTGGAT	20	ATCCAGAGACGTCCTCCAGG

Table A.2: List of primers for genomic KIAA0319L.

A.2 Sequence of the AU040320-KO1 allele and flanking regions

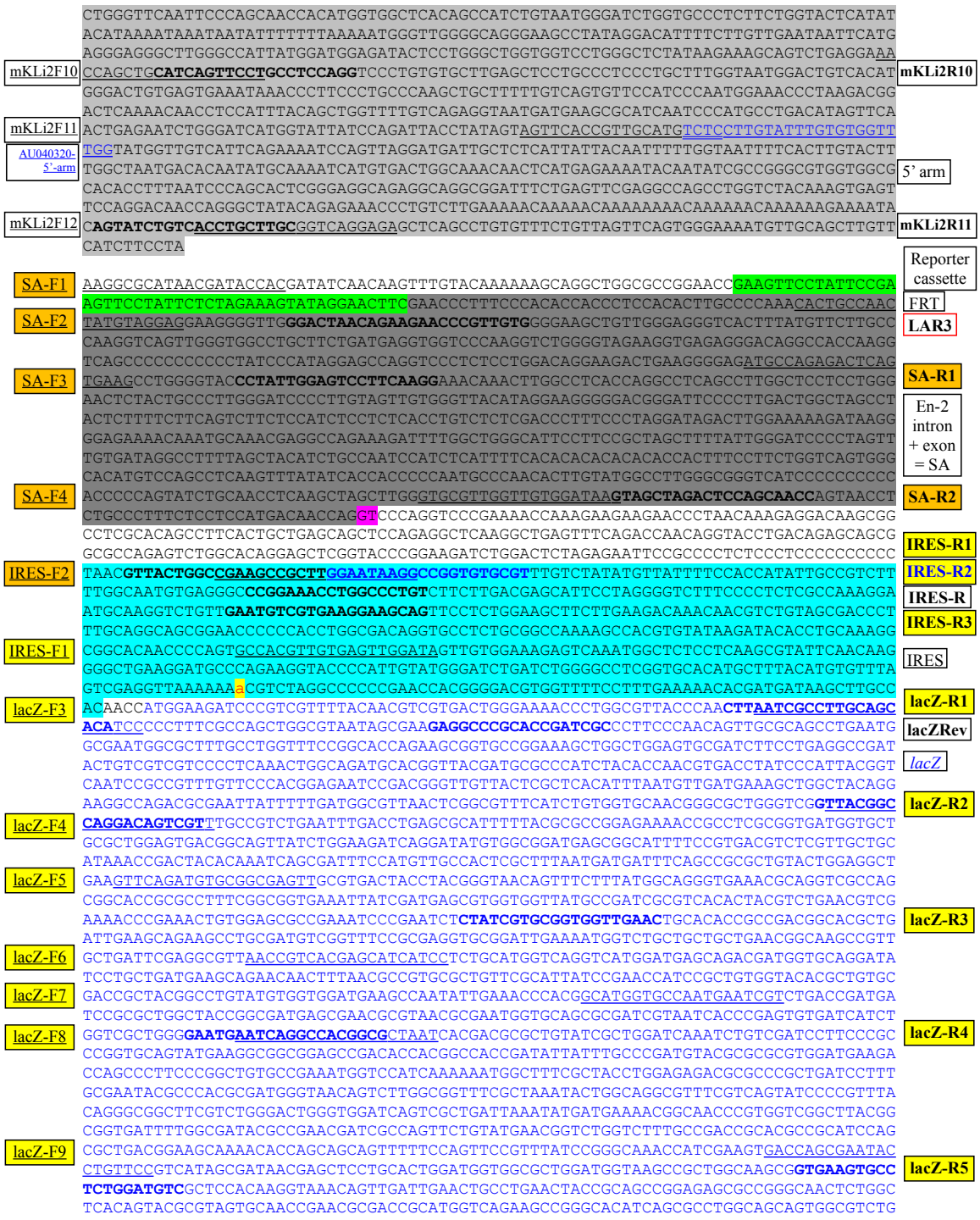
***AU040320* gene, knockout first allele, gDNA, from +19143 in intron 2 to +15396 in intron 3**

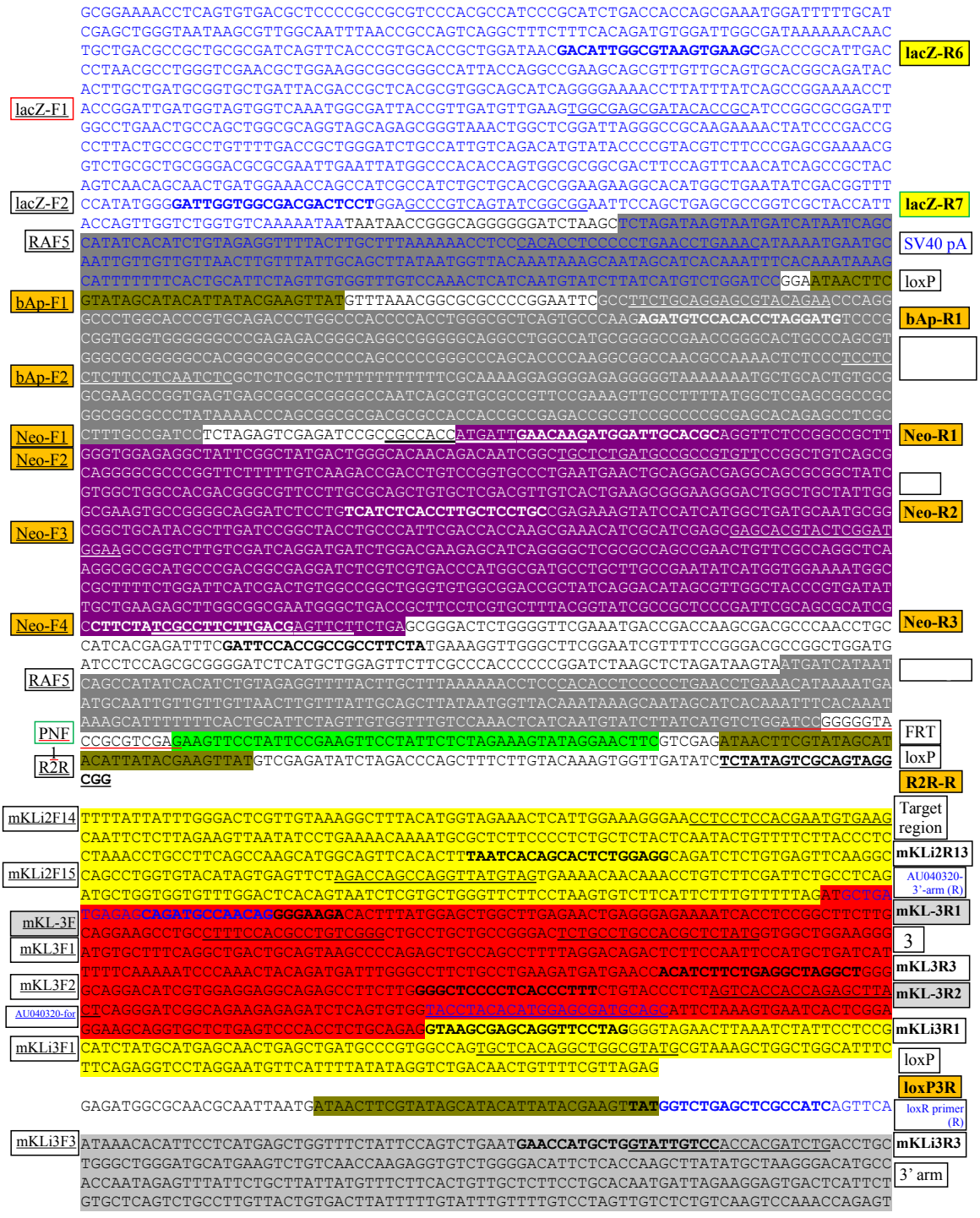
5′arm upstream region: 1-11338 = 11338 bp from Intron 2 (+19143 to +30480)
5′arm: 11339-15050 = 3712 bp from Intron 2 (+30481 to +34192)
Synthetic cassette: 15051-22172 = 7122bp replacing 121bp from Intron 2 (+34193 to +34313)
Critical Region: 22173-23269 = 1097 bp
Intron 2: +34314 to +34706 (-393 to -1)
Exon 3: 521 bp (target exon)
Intron 3: +1 to +183
loxP site: 23270-23349, replacing 163 bp from Intron 3 (+184 to +346)
3′arm: 23350-27434 = 4085 bp from Intron 3 (+347 to +4431)
3′arm downstream region: 27435-38399 = 10965 bp from Intron 3 (+4432 to +15396)
Total = 38399bp

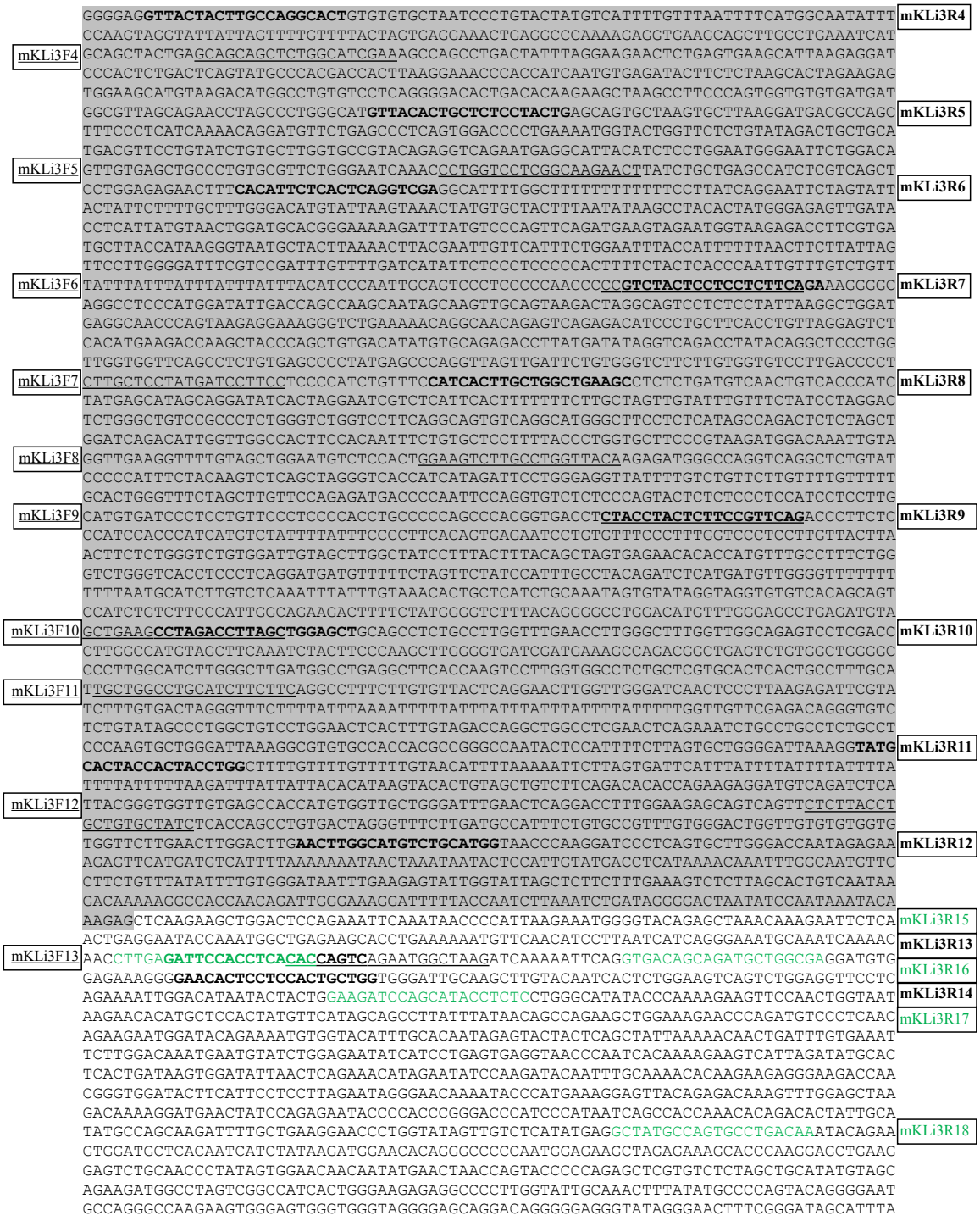
CTCAGGTGAAGATCTCCAGGATCATGAATTCCCCTGTCAATCACAAGGGGACTAGACAGTACCATAGATAAGAAGGAGTT
CCCCTTGATGGGGAGTTAGCCAGCACTGATGGTGTCTAAGGAGTGTGAAGTGGAGCAACCCTGGCCGAGACCCGACTGAA
GCTCTGGACCTCTGTCCCTAAGGATGGTGCTGGAGCGTCTTGCCTGGTTCCCCTGGAAAACTCACTCTGCAGACATTGTT
TCCAGGAATGTTCTTCCAGCTGGCTCGATGTTATGTTTTGATTCTAGCGCACAACACATTTTGGTTGAGATAAATGTGTG
CTCCCAAGTTCTCTCACCTGTAGGTAGTAAAGGGGGAGGTGAGAGGAGGAGTGGGGTTTCCATTGCTTTTTTTTTTTAAA
TAAAATATTGTTGAGGAATTTTTTAAATTTAATTTTATTTGTAATTCATTTTTTACACTCCATATTCTATTCCCTGCCCC
TCCCCTCCCACCCTCCAACTGTTCCACATCCCACACCTCCTCCCCACCACACCCCATCTCCACATGGATGCCCCCACCCT
CCACCCCATCTGACCTCTAAACTCCCTTGGGCCCCCAGTCTCTTGACGGATAGGTGCATCATCTCTGAATAAACACAGAC
CTGGAAGTCCTCTACAGTATGTGTGTTGGGGGCCTCATATCAGCTGGTGTATACTGTCTGTTTGGTGGCCCAGTGTTTGA
AAGATCTCGGGGGTCCAGATTAATTGAGACTGCTGGTCCTCCTATAGGATCGCCCTTCTCCTCAGCTTCTTTCAGCCTTC
CCTAACTCAACAACAGGGCTCAGCTGCTTCTGTCCATTGGTTGGGTTAGTGTTCATTTCTGATTCGGGTTTTACAGTTTT
AAGGGAACTGTTCTCTACCTGTTAAAAATGCCCACTAGCCCACAACTCACTGTTTATTGACCGAAAGCAACCCGAGTCAG
CTGGAGGCTATGGAAATGGGCCTGCCAGCGTGAATGAGTCTTAATCAGAATAAATGAAGCTGCCTTGTACATAGGCACTC
AAGAGCCATATTCCATTTCATAAAATCAAGTAATTTGTATCCTGTAGGGTCAGTCTTCGGCATCTGGTCTGTAACTTGCA
ACTCCGAGTCTGCACTACAGCAGCCCAGCTTGCCTCTCCCTGTGTGCTCCCCTCTACCAGCTCCTGACTGCTTGGCTTTC
AGAGTTGCCCTCTGCAGTGCTCGCTCCCCAGGGTGCGCTCAGAAGCTGCACACTGACATTTCTCACAAGGTGCTTTCCAA
ATAACATGGTGGATTTTACTGCTGTTCCTTCTGTGAAGGTTAAAGGGTGGAAGCTCAGCCTCTCGGCTCAGGAAGGCAGA
CCTAGAACAGGATTATCTACCCAGGATGGACAAGACAGAAGCAAAACTTTTCTTGTCTGTGCCTAGAGCTTTTCTCTGAC
AAGTGTTCTCTCCATTCCTTTCCCTTCCCGAGCTGCTTTGATTGAGCTGTTTTGCCTCCACCCTTCCGTACTTCTGTGGG
AAGTACTTGCAGCATGGCTGCCTCCATCAGTGGGGAAGAAACGGTAGAGGGTGGAAGCCCCTGTATTCCGCAGGCTCCTA
GAGGTTGTCATGTGTCAGAGACAGACACACATGACATGTTTTGATGCCCTGCCTAGAATCAATCTTGGAATTACTTTCTT
TTGACTAAACCCAGAAACAATGTCATTTCATAGAGACAGCAATCTCTTTGTGTTTGGAGAGAGTCCAGAATAGGTAATTA
GTGGTCAGGAGCCTTGACCAACTCATCCAGATTTTAAATTTGTCAGTAGACTGCATAAATTATGAAATGTGAAAATGTGA
AAGTATAGGGTAAAGAACAATGTATCAAAATATATGTCATGAAAGTAAAGCCAGTTGAAGCTGCATGTCTGTACTGGGTA
AGAGGACAAAAATGTCTGCACGCCATAGCGCTGCACTTTTCTAGTATTAGTAACCCTTGGCGCTTTAGGGGTGTTTGTCA
TAGTTGGAGGCTTCAATTATGCTAATTTTTTCAAGTACTGGGAATTGAATTCACAGTCTTTAGCATATTAGGCAAGTACT
CTATTACAGAAATACAGTCCTGTGTCCCTACCAGCTGCATTTTTAATAAGTTCCCTAAGATATTTATTGTTTTGTTTTAA
GGTTTGTTTATTATAAATAAGTATACTATTACTGTCTTCAGACACACCAGAAGAGGGCGTCAGATCTCAATACGGGTGGT
TGTGAGCCACTATGTGGTTGCTGGGAATTGAACTCAGGACCTTTGGAAGAGCAGTCAGTGCTCCTACCCGCTGAGCCATC
TCGCCAGCCCATATTTATTGTTTTTAATTTTATTTTTTGTGTGGGATGTGTATATATGTGCACATGGGTATATATGCATG
TGTGCTTATGCAGGTAAAGGCCAGAAGTTGATGCTGAGTGTCTTTTTAACCCTCTCTACATATTTATTTATACATTTTTA
GATAAGGTCATCACTATATAGCCTGGAAATCACTATGTGGACCAGGAGTACAAACTCACAGAGATCTGCTCCCTCTGCCT
CCTGAGTGCGACCACGCCTGGCCTTACCTATGTTTTGTGAGAATGAAACTTTCACTAAACCAGAACATGAGTTAGTTAGA
CCAGGCGGGCTGGCCAGAGAGCTTCAGGGATGCTCATGACTCTCTACCAGCCCCCCCTTCAGACCTGGGGTTCCAGGCCC
AGCTACTGCCCCTGGCTTTTCTCATGGGGCTCTGAACTCAGGTCTTCAGGCTTGTGCAGTAGGCATCTTACCAAGTGAGC
TACCCTTCCAGCCTTCTTTAAGATATGCCATCCAGATAGTGACAACCAATAGCTAGGCGTTATTACATACTGTAAATACT
TTTCAGGTCAATAGATACTATACCAGGCTAAAATCAACCTAGTTCCTACCATTAGAGTTCACAGTATGGAGCAGGGAAGA
GGGAGAAAGGATGGACACATGACACAGTCTAAGATGTGCCATGGGAGCACAAAGAATAGGGCAGAGAGGAGCCCAGCCCT
CTCCATCGCAGGCGGCTGGTGAGACTCGGGCTATTTTGATTCCTTTGAACCCCCCTCTCCTGGATTCCTCTGAAGTGGTT
TCAGTCTGCCCGGCTCAGATTTTCACTTCTTTATGTCAGAGGAAGCTATGGAGGGAGAATACTGCAGCTCTGTAGCGTCT
AGAGAGTCAGAGCCCTGAGAACATTATTTTTGTACAGATACAGATTGGCTTTGATTTAATTTAAATAAACTGGCTCTCAG
CAGTTCTAAGAATACTAACTACTCACACGGCTCCGCTTTCATTTACACACAGATGAGGAAGCATCTGCAGCCCTCCGTTT
TATTTGCTATAAGCAAAAAAGTGCTTTGAGATATTTAAGTTTTGGAAGCTCAGTTGTGTCGAGTCCTCATATGTCCCAGT
TCAGCCTGCTGCAGATGTTTTTTTTTTTTTTAATTATTTTTTTATGACACTTACATAATGCTACAGAAGGGAGGCTTTCA
ATGGATAAAGTGACAAACTTTTCCTCTATTTGCCATATCTGCTGAAATAACGTTTTACAGCTAGCTGTATTTTTCTTTGT
TTCCTTTCATGCTCATTGCTAATTTATTTAATCTGTACGACTTTGCTGTAGCTTTCTAAATGACCTTTTCTTTAGAAACA
AGAAAACAAACCAGGGGTGGGGGGAAAAGCCTTCTCCAAAACAAAACAGGGCTCTGATTCAAGGTTCTTTGTGTGGGTTT
CAGAAGGAGGTTGGTGTGATTGTAGTTGAATGCAAATAATTTATCAGCTCATAATAACTGCAGTCAGAGACGGCAATCAA
CTGCAGCTTCCTAACAATAACAGGGACGAGGGGGCCGCGCCGCGCAGGGACTGCTAGCTCCTGGCTTCAGAGCTAGGTAC
TTTTTATTTTTTACATTTTCTTTCCTTCCCAGAGCCCACACTTTTATATACAAATCAAAGCTTATCTGTTATCATTTGAT

ACCTGTGCTTTTGCAATACAAAGACAGCCTTCCATGGAGAGGTGTGGGCTCCTCTCACGCTGAGGTTTGGAGGCGTGCTC
TCCTTGCTGACAGCATTCTCTAGAGTCTTTTAGTCATAAGGTGGTGGGAGAAAAAGCAAATCAGGATTCTGAGTACATCA
CATGCAGCAACGTAACCCCCCTAGTTACAGGGTTGTTGGTTGTTTTTCTTTTTTTTTAAAGTACACGTTTTAATCATTTG
CCTTCAATCTGCCTTGAAATATTATAAAGGCCTTAATGACTGGATTGTTTCTGAGCAGGTGACTTTATGGTAAGAGAGCT
ATTTTCAGCCATACCAGTGATTTGATTAACACTTGGTTGTGAAAAATGCCTCTGGGCTAAACCTTGACAGATGGGCCTTT
GAAACGTCATGACAACTATATCCAATTAATGCAAACTTTTCATTTATTAGTAAGGAGCAGGCAGGAGCTGGAGGCCTCAG
AATTAAAACCCAGATAGAATGCTTTCCATGTTTTCTCATAGGTGGCCAGAGCTTTGAGATGTTTAAAATGTGTCTTTTTC
AGCCAAGGGCAGGGGAGTGGAGCAGGTATTTGCAGCAATGGGCGGGTGTGTGTGTGTGTGTGTGTGTGTGTGTGTGTG
TGTGTCTGTGTCTGTGTCTGTGTGTGTGTCTGTGTGCTCTCTCTGCCTGGATAGACTAAGAAGCTGCTCTCCACTGTGGA
CTTTGTTCAGAAGTTTCCATGGTGAAAACCTCTCTCATCTTGAAGTGAAATGGAGTGGTCTGAAATAGGCAGCTCTAGGA
TCTGAGACTTGGTTGGTCCTTTCATAAAGATTGCATTGTGCTTTGAAAGAACTTTCCAGCTTAGGGTCTTGACAGGAAAG
CCTATTTCCTAGCTGGCTCAATACTCAGTGGTCCCTTTGGCCACTGAGCATTTTCTTCAGGTTCGCTCTGCACACTCATC
ATGCTTCTGCGTGAGTGCATTCCTCAGTTCCCCTCCCTCCTCTTCCGTGTGAGGTCGGGTCTAGCCTTGGTCCTCCT
GAGTGTCAGTCTCATGAGGGCTGAGATGGCAGGCAGCCTTACCATACCTAACTTAACTGATTTCCAAGGAGACTTCTCGG
CATGGGAATCTCACTCCAATGACTAAAACGCAAGTGATTTATTTAACCATTGAATGAACTTAAAAACTAAGGGAAATCTA
CGGATGTTTACAGAGTGTCAAGCATCTTACTGAGCCCGTAAACCCAAAGCTACAAGGTTCAGGCCTAGCACTTACAGAGG
AAGGCTGCATGAGGTGGACAGAGACCATCCAGGGCAGAAATGTAGGCCTTACAATTCCAGTGGGAATTGAACCCCAGTCC
TCTGGAAGAACAGCCAGTGCTCTTAACCCTTGAGCCATCTCTCTAACTCTGAAAAGTTTTTTTCATCTTTACAGATCAGC
AAACGTTAATGTAAATAACAGCAGAGACATATGAGTTGGACAGCTGTGTCCTGGAGAGTTTGTCATAATGACCCATTGGA
ACATGGAAACGCTGCAGCCACAGGAAAGGAGTGAAAGGCCAATGACTCTTGTTTAGCAGAGTTTAGTTTCAGCAAGTTAC
CTACACCATAACATTAAACAAACTGCTCTTAACAATCTAGGCACACAGCAAAGGCAGCAAGCGCTTAGTAATTATTTTCT
TTTCAAAGCCTTGCTTTGTGAGGCAGCTGCTACCTTTAGTCCAACTTGTGCAGTTAAGAGGAAAAAAGTGCTGGCCCTTT
TGAGAAAGAGGAGGGGGGAATGGTATTACTCTGGCTTTTTTCAAACTTCATAATACCTAATTGCACCCAGTGGAAGGGTT
TTTGTTAACACCCCCCACCCCCCGGGCCTGGCCTTTCCTCTGCAGAGCATACTCTCTGCAGAGGAAAGCTGGTGTGGGGA
GGAACGTGGCACCAGTTTTGTATTTGTTCACTAGTGGGTGTATAGGCAACAGACATCCTGACAGCAAAAGAAGGGTGGGG
TGCTCTTAAGGTGGCTTTTGAGCAGTTCTAATAGTGTGCCTGTTTCCCAGTTTTCTGGGGCATTCATCATAGCTGAGACA
CAGCCTGCCTTTGATGATGGCTGGTGGAAAGTAGATGGCGTACAGCCGCAGTTCACAGGTTTAGTACCAAATCTAAGGCT
CTGCTTTACCACTGACTAATAGCTCATTAATGGGTCCAGAGGAAAACATTTGATGAATTCTATACATTGTTACTGAATTG
TGAGACTTCATAAAAATAATTTTAGCTCTGATAAATTAAAACAGTCACTAAAACGTGCAGATTTTACCAACCAACCAATG
CCCTCTTTGCGCTGTTTTCTGCAGAAAAAAAAACCCACCCCAGGGAAGAACGTATCAGCTGCTCAGGGTTTTTTCTTTTC
TGAAGCAACGCTGGTCCCTACTTCTATTTCCGCCATCACAGCCCTTCCCTTTGGATGCAGCATGGTGGATCTGGTTCAGT
TCCCGGGCGCTTTCTCGTGTGGTTTTTGAGGTAGTGGGTGTTCTGTATTTATTCCCCCATGTGGTTGCCAGCCAGTGGAG
TTTCCAAGTTTGCTCCTGAAATCAGGCTTCTTACCTGCCTGAGCTTTAAGAATGCCAGAGGCAACTGCAGTGTCTCTAAA
TATTTCCAGAGTTCTTCACGGCTTACTGAAAGCATTTAGTGAATTTCCTCCTGGCAATAATTCATTTATTCTGTAGACTT
TTTCACTCTGCTACTTGGAATTATGGAACCTGGTCTAGATTTTGTGCCAGATTTATTAGAATTCTGCTTTTTTGAGGAGT
GGTGAGAATAAGCGTTGCTAGTTCCAGGGCCTCTTGTTTTGGGGATCATCCAGGTAACACAGATGGGAGTTCTGTCTTCT
TTGCTTTGCCGTCATTATAGACAGTGATTAGCTTTGCTCGTTGCTCCCACTCTGGCTGAGATTTTTATATGTTCCTCCCA
ACAGTGAGCTCCAGCCGTTCTCAAAGGGTTTTCAGTCTCGGGTTCTACCAACTGTAAGCCCTTTTTTGTAAGCATTTAAT
ATTGCTTTGCTAAGCCCTGGGAGCAGAGCCAGCCTATGGAGGCGTGGGCAGGAAGAGGAACTGATCTAAAATTGGAGTTT
ATTTTCACCTCACCTTTTATCCACGTTCTTCTGGAATGCAATATTGACTCCCTCAGTGCCCCGCCCCCTCCTCTCACTAA
CTGTCTCCAAGAGCAGCAGCAACTGAATCTTGGAGAAGTCAAGTTATCCTTCATAGGTTACATTTCTAGTGGCTGGTGTT
CAGAGCTGAAGTTAGGGCTGGCATCTGCTTAAGATGGTTAATTACCCGGCCTGGAGGATGGCTCAGTGGTTAAGAGCATT
GGCTGTTCTTCCAGAGGACCCAGGTTCAGTTCCCAGTACTCACATGGCAGCTCACAACTGTCAGTAAATCCAGTTCCAGG
GGGTCTGACTCCCTCACACCAGTGCATAAGTGCAGTTCCGGGCGTCTGACTCCAGTGCATATTAAAAAAAAAAAACGATG
GCTAATTATCTCTTCATCATCCAAGAGGAGGGATTTTTTCTCATCCAGTGAATGGGTGGGGAAGAACTGTTTTCTAATTA
TGAAACCCCAATGGAACAGGCGTGTGATGGCTTATTCCTATGGCCACCTTGACTGGATTAGTAAGCACTTAGCCCACCAA
TGAGGCATACATTGGAGTGTATATTAAGGCGTTTTCAGGGAGGGGGTTGAACTGAAGACCCATGTTGAAAATGTGTGGCA
TCTTCACTCATGGGCTCAGGTCCCAGACTGCATAGAAAGGGGAAAGGATAAGGCCAGCTGAGCACCAGCTCCCTTCTCTC
TGTCTCCTGCTTGGTACCATAGACCAGTCCCCTCCGTGGTGGATCGTATTCTGCTGAGCTGGAGGCAAACAGAGAGGCTT
TCTGTCCTCACACTGCTTTCTCTCAGGTATTTGGTCACTAGAATGAGAAAACACCAGTAAGTAGCATTTAATAGTGATAA
AATACTGCTTTTGTTTACGTAGGTATTTTATGTAAATAATGGCTAAACTTTGTTTACTTATTTGTTTTTTAGAAACAGGA
TCTTGCTCTGTAGCCCAGGCTGGCTTGGAGATCACTGTGACCTGCCTCAGCTTCCCAAGTGGTGGGCTTACAAATGTGTA
CTACCAAAGCTGGCAGGCTCAATTTTTACGATAGGAAACTAATGTTTTATACCTCTATAAAACATTGAAAAAGAATAATA
CATTAAGAGCAATTAATGAAACACAAGTAAGCAAACAGAAGACCATAGAGGGAAAAAAATCAATAAAAATAAAATGTGGT
TTGAAAAATTAATAAACCTAATAAACTCAAACCTATCACAAGAAAAAAAGAACACTGTCACAAAATACCAAGAATGCAGA
AGAGTAGGACCAGAGAGATGGCGTAGAGGTAAGAAGCATTTGTGTGGGTCCCAGCATCCATGTCAGAAAGGCTCACAGCT
GCCTGTAACTTGATTCCAGGGACCTACACTCATCATGTGCTCTCACACTCAAAATTAAAAACGAGAAAAACGGGGCTGGT
GAGATGGCTCAGAGGTTAAGAGCACTGACTGCTCTTCTGGAGGTCCTGAGTTCAATTTCCAGCAACCACATGGTGGCTCA
CAACCATCTGTAATGGGATCTGATGCCCTTTTCTGCTGTCTGAAGACATACTATAAATAAATAAATAAATAAATAAATAA
ATAAATAAATAAATAGATAAATCTTTTTTTTTAAAAATGAGAAAAATGAGTATTTAAAAAAAGGAAAGGCGTGGAGCATAT
TGACTCGCTCTTATAGTCCTAGTATTCAAGAGGCTGAGCTAGGAGGATTGCTGTGATTTCAAGACTAGCCTGGACTATGG
AGTGAGACTATTTCTCAAAAGACAAAACAACAACAAAGTCAGAAGGTGTGTTATCAGAGACATGGTAAGCTGGGGTCTAC
AGATTACCCCCAGCAGACACTGGCTGCTCCCTGTTTTGTTGGTTTTAAAAATATTCTTGGGGCATTTTGATGACATATAA


mKLi2F1
mKLi2F2
mKLi2F3
mKLi2F4
mKLi2F5
mKLi2F6
mKLi2F7
mKLi2F8
mKLi2F9
mKLi2R1
mKLi2R2
mKLi2R3
mKLi2R4
mKLi2R5
mKLi2R6
mKLi2R7
mKLi2R8
mKLi2R9


mKLi2F10
mKLi2R10
mKLi2F11
AU040320-5'-arm
5' arm
mKLi2F12
mKLi2R11
Reporter cassette
SA-F1
FRT
SA-F2
LAR3
SA-F3
SA-R1
En-2 intron + exon = SA
SA-F4
SA-R2
IRES-R1
IRES-F2
IRES-R2
IRES-R
IRES-R3
IRES-F1
IRES
lacZ-F3
lacZ-R1
lacZRev
lacZ
lacZ-R2
lacZ-F4
lacZ-F5
lacZ-R3
lacZ-F6
lacZ-F7
lacZ-F8
lacZ-R4
lacZ-F9
lacZ-R5


lacZ-F1
lacZ-F2
RAF5
bAp-F1
bAp-F2
Neo-F1
Neo-F2
Neo-F3
Neo-F4
RAF5
PNF
R2R
mKLi2F14
mKLi2F15
mKL-3F
mKL3F1
mKL3F2
AU040320-for
mKLi3F1
mKLi3F
lacZ-R6
lacZ-R7
SV40 pA
loxP
bAp-R1
bAp-R2
Neo-R1
Neo-R2
Neo-R3
FRT
loxP
R2R-R
Target region
mKLi2R13
AU040320-3'-arm (R)
mKL-3R1
3
mKL3R3
mKL-3R2
mKLi3R1
loxP
loxP3R
loxR primer (R)
mKLi3R3
3' arm


mKLi3F4
mKLi3F5
mKLi3F6
mKLi3F7
mKLi3F8
mKLi3F9
mKLi3F10
mKLi3F11
mKLi3F12
mKLi3F13
mKLi3R4
mKLi3R5
mKLi3R6
mKLi3R7
mKLi3R8
mKLi3R9
mKLi3R10
mKLi3R11
mKLi3R12
mKLi3R15
mKLi3R13
mKLi3R16
mKLi3R14
mKLi3R17
mKLi3R18

AAATGTATATAAAGAAAATATCTAATAAAAATATTATAAAATTAAAAAATTTTTAAAAAGAAAGTCTCTTACAAATTCTG
TGCTAAAACAGCTTGGTCCTCTTTTGTTGTTGTTGTTGTTTGTTTCTTTCTTTCTTTTTTTGGTTGGGAGACTTTTA
ATGACTGCTTCTATTTCCTTAGGGGCTATAGGTCTGTGTTGTTTATCTGGTCTTGGCTTAACTTTGGTAAGTGGTATCTA
TAGAGAAACTTGTCCATTTCTTTTAGATTTTCCAATTTTGTGTAGGACAGGCTTTTGACGTATGATCTACTGATTCTTTG
GACTTTCTTGGTACCTGTTATGTCCCCTTTTTGTTTCAGATTTTGTGAATTTGGATGTTTTTTTCTCTCTGCCTTGTAGT
TAGCTTGGATAAGGGTTTGTCTGTGTTGTTGAGTTTTCTCAAAGAACCAGCTTTTTGTTTCTTTTGATTCTTTGCATTGT
TCTCTTTGTTTTTAATTGATTGATTTCAGCTTTGAGTTTGATTATTTCCTGCCATCTGCTCCTCTTGGGTGTGTTTATTG
CTTTTTCTTCTAGAGCTCTTAGGTGTGCTGTTAAGTCACTAGTATGAGGTCTCTCTAATTTCTTTATGGAGGCATTTAGT
GCTATGAACTTTTCTTTTAGCACGGCTTTCATTGTGTCCCATTAATTTTGGGTATGTTATACATTCATTTTCAGTGAATT
TTAGGAAGTCTTCAGTTTCTTCCTTCCTTTCTTTCTTTCTTCCTTTCTTCCTTCCTTTCTCTCTCTCTCTCTCTCTCT
CTCTCTCTCTCTCTCTCTCTCTCTCTTTCTTTCTTTCTTTCTTTCCCTCTCTCTTCCTTGACCCAGTGGTCATT
CAGTAGAGATTTGTTGTTTCCATGAATGTGTAGGCTTTTTGTTGTTTCATTATTGTTCAAGTCCAGCTTTAAAGTATGGT
GGTCTGATAAGATACGGGGGCATATTTCAATTTTCTTGTATCTGTTGAGACTTGCTTTGTGATAGAGTATATGGTCAGCT
TTAGAGAAGGTTCTGTGAGGTGCTGAGAATAAAGTATATTTTTTTGTATTTGGGTTCTATAGATGTCTGTTAAGTCCATT
TGATTCATAACATCTGTTTCATTATTTCTGTTTAGTTTCTGTCTGGATGACCTGTCAATTGGTGAGAGTAGGGTGTTGAA
GTATCCCACTATTAATGTGTGGGGTTCCATGCATGATTTAAACTTTAGTAATTGTTGTTGTTGTTGTTTTACAAAAG
TAGGTGCCCTTGCATTTGGAGGATACATGTTCAGAATTGAGGTGTAATCTTGGAGGATTTTTCCTTTGAGTCTGAAGTGT
CCTCACCCATCTCTTTTGATTAATTTTGGTTGGAAGTCTATTTTATTAGATACTAGAATGGCTTCACCAGGTTGTTTCTT
GAGTTCATTTGCTTGGAAAGCCTTTTTTCAACCCTTGACTCTGAAGTAATGTGTATCTTTATTTTTGAGTTTGTAAGGGT
CAAAATCACTGAAGGGCCAGGCAGTGGTGGCCCACACCTTTAATCCTAGCACTTGGGAGGCAGAGGCAGGCTGATTTCTG
AGTTCGAGGCCAGCCTGGTCTACAGAGTGAATTCCAGGATAGCCAGGGCTATACAGAGAAACCCTGTCTCAAAACAAAAA
CAAAAACAAAACAAAACAAAGCAAAAAAAACAAAATCACTGAAGAAAGACCCCAGATTCATATAATATGCAAAAAACAAG
GAATACAGAAACAACTAGCATGACTGCATTGGGGTGGGGACTCAACCATTCTTTGAAATGGTGACCTCAGACAAAGGCAC
AAAGTCCCCCCTCCCCCCTTTTTTTTTGAGACAGGGTTTCTCTGTGTAGCCCTGGCTGTCCTGAAACTCACTTTGTAGAC
CAGGCTGGCCTCAAACTCTGAAATCCACCTGCCTCTGCCTCCCGAGTGCTGGGATTAAAGGCATGTACCACCACGTCCAG
CTCCACAAAGGCCTTCTTATAGGGAACCAGGGGAACTCTCTAGAAGGATTAGGCAATCTAAAATTTCATTGTTGGGTCCT
AGGGGTTCACAGGTGGTCAGATGTCTGCATTCCTATGTCATGAACATTTAACCATCGAACGCGATAGGGCTGCCCAGTGC
AGATGGTTCTTTGGGAGAGGGTTTTATGATCTTGTTATGGATTTCATGGACTGTCTCTGGAGCTGGTGCCTTATGACCAT
TTTTTTTGAAATCAGGCCTGTCCTTAATGGAGACAAATGGGTTTATGTTGTCCTTTCAAGGTGTGCTTCTTATATGCAGC
AGAAATGATGGATTCTGTTTTCACATCTATTCTGTTAGCCTGTGTCCTTTTACTAGGGACTTGAGTTCATTGATATTAAG
AGATAATTAATGATCAATGATTGTTATTTCATAATATTTTAATGGTGGTGGTGATGTGTATGTGTGTGTGTGTGTG
TGTGTGTGTGTGTGTATGTGTGTGTGCACGCGCGCAAGAGCATGCTTCCCTTCTTTTGGTTTTGCTGAGAAATTATTTAT
TTCCTGTGCTTTCTTGGTGAGTTTTCTAGTATCTTTTGTAGGGCTGAATTTGTGGATAGATATAGTTTAAATTTGGTTTT
GACGTGGAATATCTTGTTTTTTCCATCTATGTTGATTGAAAGTTTTGCTGGATATGGTGGTCTGGGCTGACATTTGTAGT
TTCTTAGTCTCCAAGATACTGTCCAGGCCCTTCTGGCTTTTAGAGTCTCTGTTGAGAAGTCAAATGTAATTCAAATAGGT
CTGCCTTTTTATGTCAATTTTCTTGCCTTTTTCCAGAAGACACTATTTCTTTACAATTATCCACTACATCTGGCTCTTAT
ATTCTTTTTTCTCCCTTTTCTTTTGGAGGACAGGGTGTAGTATATATGTTCCATTTAAGGCTGAACATTCTACATTTCTT
ATTCTCTGCATCTAGTTGTGAATTTCAATGTTAATTATCATCTACTGCACTTAGAAACTTCTCTAATGGGGATGAGAACT
GCAGTGACTAAGGGTATAGTGTAAGTCATTAGGAGTCAGTTCAATGTTGTGTCCATGTAGCAGAAAAATACCAGTAGGTT
CTCCTCTAGAGCCTATGACCTGTCTACCTAAGGTTCTCGGGCTAACAATGGTACCAGATAGGTTTCATCTTGTGGACTTT
TCTTATTTATTTATTTATTTATTTATTTATTTATTTGTTTAGGATTGCGATGACTGGCTAGATTGGAACAGGAAAAAATA
TATAGAGCTCCATAAAGTAGGCTCTTCAGGCTAGAGAGGTGCTTTGCTATGTAAATATGTAATATGTAAAAGGTAGAGAG
AGATCAACAAGAATCCCCTAAGACGTGGGCCCCCCAGGCTTTGCCATCTGTCAGCATCACCTGAAGCCTGTGTTCAAAGC
GATCTCTAGGCCCCAGGTCCAGGGTCGAAGAGTCCACAGGTTTAGAGTGGGGCCTCAGAATTTGATTTTCTAAGTTCCCA
GAGATGACCAGTGCTCTGGTCCAGGGGCCATACGTTAGAGCCGCTGCTTTATAGGATGGGTAGGAGTGGGAGGGACATTG
GGATTGTCCTTAATCATGGGATCAGCCATGAGCAGGATCCACTCTTCATTGTAATATGGAAGAAGGATTTCATGGATATC
TAACATGGGTATTTATAAGTTTGCTAAAAGTGATTCTTAAGTCATTTCTTGGTTCTTCTGAAGTGTGGTAGATTATTTAT
AGGAAATAGAAGTAGGATGGGGACAGGTAGACAACAGACAGGCAGATTATAAGGGTTGGGGAGAGTGGTAAGGGTCTGAA
ATAGCCTTAGAGACAGATAGAAGATGGCAAACTAGGTAAGGAAATAGGAATCCTTTTAGGTAGCCTTGAGGCCGGAGACT
GTGAACATACAACAGTGTGCGCATCTCTCCAGTTACGCGAGTCTTCTCTGTAGCCCCCAGCAACCCTGCCAGGAAAAGCC
TGGTGGCTTGACTCATCCAAGTTAGGAAATTTGCTAGGTGGTTTGTGCAGAAGGAAATTGGGGCATGGAAATTAAAGTTT
TCAAGAGAGTGTATGACAGACTACAGAAGATTTGAAGGGAAGCAAAGACAGGAGGGGCTGACAGTTAAATGGAGAGACTT
GTCGTTTAGAGATTGCTGTGATCGACACAGATATCGAGGGAACAGGGTGACGATGGGAAGGGCAGGAGGCCATATGCAGA
AAGTAGGATGCTTGAATTTAGGTTGTGAGGTTGTAGTTCTGAGAGTAACAGTGTCGGAAGAATGGCTGTGGAAGACATGG
CTGAAGTAGAGTGGAGGGGTTTATTGGTGACGAGGAGGTGAAAGAGCTCAGGAAGCCGTGAAGGACTGTTAGTGAGTTGT
CCTTGTGGGAGCCGAAATGGTCTTTAACATGGTGGCGTCAACAGCAACAGCCAAGGGTAACTGAACAAGTCTATACAGTA
CTGCCAGTATCCCTGTTAGAGAAGAAACAAAGGGGGAAGACTAGACACCCAGCTAGTCTAGGACCAGTGTGTATTCCATC
TGTAGTCTCTTCTTGAAACCCTCTTACTCCTTAGGTGGGACTTGGGATGAGAAGGGAGTTTGAGAGCCAGCCATTGTAGA
GAGGAGGAGTGCTGAGTGCACCGGGATAGGATGGAAATGAGTCCAGCACGTTGGTGGGGACGTGTGCTTACAGGAATGTG
TCAGCTGGAGGCTTCTTCTCCTTGTTTACCTGTGGCAGAGGCACACAGTTTGCTGGTACTGCACAGGATTCCAGAGCTCT
GGAGGAGGACTGCTGCACATGAACTTGGGAGTAGGAATAGGGCTTTGCTGCAGGTACTGCAAGCAGTCTTCCCAGCCATG
AAGCTGTTAGACCCTCCCTCCACGCTGTTCTTAGGGGCTTAATGCTCACCCCTCAGGCCATGGGAAGCTCTGCGAGTTGG
TAAGTTGTGCATTTCAAGTATTTAACCAGCAGGCGTTTCTTTGAGGAGACAATTTCAGAGTTCAAACTCCTGTGTAATCA

ACAGGGAAAGGTAGAAGACTATATCTGCACTAAGTAGTTCTCATCCTCGTCAGTGAGGACTGGCCAGCGCCACTGTTTCT
CGTTTATTCTGTTTTCTCGGGTAGGCCAAGTAACTCTGCATCCGAAGTTGGGCAGAGCTGTAGCCTGCATTACTCTGCTC
TTTCCTGAAATGTCTGCAGCACTGTACAGTCCCTGTCTTGTCACAGTGAATTGTTCTTTCTTTTGGATACACAGATCATG
ATCCCCAGAGCAGTTTGCATTTGAAGTGGGGAGTGTCTTTATTCCCTTCCCACTACTTAAAAGAGGGAAAAGTTAGTCTT
GTTTGGCTTGAGCACTGTACTTTTTGTGTCAAGAGCCTTTGAATTGCTGCTGAAGGGACAAGGAGGCTGGTTAATTGGGT
CCTGGAACAGGCACTGGGCATGTGGTTTAGCCCCAGGCAATGAGCTGCTGCCAGTCTGCTTTGTGCAGGAGGCCAGGAAG
GAAGGCCCACATGGATGACAGTGGCTCAGGTGCTGTCTCCACCAGGAGCATCCCCATTCCAGCCACTGACCGCAGCTTCC
ACCGCCTTTCCTCTGCACAGCTGACTGCAGCTTGCTTTCCCGAGAACTCCTGTGCTGACTCTGTAGAGCCTGAGCTCACC
TCTTATCAGAAGATAAGGCATGGGGTGTGGGCAGCGGGGAGGAGCTTACATAACAGCCAAGGACGCGCTCAGCTCCAGCA
ATTGAGGTGTTCTTTGTTGTTAGCCATGCCCCGCCCCAGCTCACCAGGCTTCTCTGCCTGCTTGCTTTTGGTTTGTATTT
TTAAATTTCCTCTAAACCCTTCCGGCATGTGAAACTATTGCCAAGAGTTCATTTGTTCTTCTGGTTATTACTCTGACAAA
TTTGGAATCCCTTGGGGCCTAGCTTTTTTTTCAAATTCTAATTCTTAGTTACCTAACAGACAAGCTAACAGTCTTTGCCA
TTTTTTTTCTTTTATAGCCCTAGGTCTGCTTCCAGGCATCTGCCTTGGATAGTTTGTGTGGGTCTCTCGCTCCTTCTGAC
TTTGACTCTCCTTGTACTTAGCATATATACCACTAAGCATCTCCTGTCTCCATTGTAATCTTACACAAATGGCTTATTAC
ATCATGAGAAAAATTGGGCAGCCTGTTCTCTTGTTTTGTGGCATGACAGAAGTCCCTGAAGCCCAGCTTCCTTTCTCAAA
GCCTTAATTTCTGAGCTATAACACCTTCCATTTCCCTTTATCTCACAACTGCCCAGTTGCCCATGTATTGTCGTAAGTAC
ATCTTTAATAGTCTGCTTTACCGTATGCAGCCAGTGAGACCGTGGTAGCCTCTTTGTCTTGGTTCGTTTGGACTGCCATA
ACAATACACCATGAGCAAGGAGACGTAGGAACAACAGAATCCTCCTCCTCACAGTTGCAGAGGTGGGGAAGTTCAAGACG
AAGGCTTCTGCAGAGATGCAGGGAGGAGCTGCACCTGCTCCCCTCACATGGTGGGAAAGATAAACAGACTCCGCCAGCCT
GTTTTAGAGGGGTAGCCCTCACCCCCAACGGCCTCATGTCCTCAGTACCATCCTGGAGGGTTAGAATTTCAGTATACAGT
TGGGAGTGCACAGCATCCATACAGTTGGGAGTGCACAGCACCTATACAGTTGGGTGTGCACAGCATCCATACAGTTGGGA
GTGCACAGCATCCATACAGTTGGGAGTGCACAGCATCCATACAGTTGGGTGTGCACAGCATCCATACAGTTGGGTGTGCA
CAGAATCCATACAGTTGGGAGTGTGCACAGCATCCATACAGTTGGGTGTGCACAGCATCCATACAGTTGGGTGTGCACAG
CATCCATACAGTTGGGAGTGTGCACAGCATCCATACAGTTGGGTGTGCACAGAATCCATACAGTTGGGAGTGTGCACAGC
ATCCATACAGTTGGGTGTGCACAGCATCCATACAGTTGGGAGTGCACAGCATCCATACAGTTGGGAGTACACAGCATCCA
TACAGTTGGGAGTGCACAGCATCCATACAGTTGGGAGTGCACAGCATCCATACAGTTGGGAGTGCACAGCATCCATACAG
TTGGGAGTGTGCACAGCATCCATTCCCTAGAGTTTCTGAATGAACTTTGTTCAGATTGGGGTCCTTCTAAAATAACTTCC
GCCACCCTGCCCCAATTTCAGTATTGTTTCATAGTTTTTTGAAGTAAAATACTTTGTTTCAAGTTTCCTTCTCTCATTTC
CTTATAAATAAGGACACAAATAAATGATAAGCTGTTTCTTTTTAAAACTAAAATTCTAACTTTAAAAAGCTTCCAGTTTT
CTACTTCTGGGAAGCTAATCTTGTGCGGTGATTCCTGAAGCATAATGATAGGATACTGTTTGTGTTGTACTAACTCATTC
TCTCTGCATAGCGTCTGCCTGTGTAACCCTGCCCTGGAATTCACTCCGAGCTAGGCTGGCTTGGATTTACATTCGCCCTC
TTGCCTCTGCCTTCCAAGTGTTGGTATTATAGGTAGAAGCCACCTTGCCCCGTAACATTGCCATGCCTGTATCTTTCCTT
CTCAGTATTAGCCATCCTTCAAGCTTAGTAGCTCCTAGCTCCAAGTCTTCCCTGGAGCTTGCTATGTAAACTCACCACAA
CCCACCTGCCTCTGCCTCCACCTGAGGACTGGGCAGAGAGGCATGCCCAAATATACTTCGTTCTTGCTGTCCCTCCTGGC
TTCCTGATACATCTAACCCCACTGTTTCCTTCTTTCCTCTCCCCTCTGTCTTCCCTTCCTGCTTTTCTTGTTTTCTTTCT
TAAATCATGTTCCATGCTGGCCTTGACTAATGTAGCTGAGGATGACCTTGAATTTGTAGTGCTCTTGCATCTATTTTATG
GTTCTGAGATCACAGGCATGCATCCCTGCAGCCGTTTATGTGGTGCTGGGATTACCCAGGGCCTCCTGCTAGGCAGGCAC
TCGAGAAACTGAGTTCTGTCACCAGCGTCTCACCAAGCCTATCTAAGGGACGGAGAGCCTGAACAGTGACTATGCCAGAG
AGGACAGAGAAGATCAAGGGCAGCAGGGATTCCTCTGTGATGTAATCAGGAGTAAGGAAAGCCACCAGAAGGAAAAAGAA
TGCTCTTCCAGAGGTCCTGAGTTCAAATCCCAGCAATTACATGGTGGCTCACAGCCATCTGTAACAGGGTCCGATGCCCT
CATCTGGTGAGGCATCAGATGTACATGCAGCAGAGAACTTTCATATTAAAAAAACAGTCTCATGCCTCAAGTTTGTTCTG
TAGCAGGGATGACCTTGGAGTCTCCTTTCTCTGCCTCCCTTTGGAATCTTTATCTGGTTTTACTGTCAGTGTAATACTGG
CCTCTTACAAATAGTGACAGTTTTTACTCTTCAGGATTTTTTGTTTTTTGTTTTTTAAGATTTATTTATTATATGTAAAT
ACACTGTAGCTGTCTTCAGACAGCCCAGAAGAGGGCATCAGATCTCTTCAGGGGTGGTTGTGAGCCACCATGTGGTTGCT
GGGAATTGCACTCAGGACCTTCAGAAGAGCAGTCAGTGTTCTTGACCTCTGAGCCATCTCTCCAGCCCACTTTCTACTTC
TTTTTATTTTTTATTTTTTCACTTCCTACTTGTTAAAGGTTTTATTGGTAAACCAAACCATCAATACTTGGATCTTTGGA
GAACGTGTCAGACCCAAACTAAAGCAGAGACTAACATATAAATAACTGATAATGGAATAGAAAAACGTATATATTTAGTA
AATTAAGGGTTACTTGAACATGTGCACTGTGTTACAATGACAGTTGAGCTGATAACCAAGATAGCAAATGCTATGTGGAT
TCACTGCAAAGGAGTGATTCAGGTTCCAGGAAGGAGAGACTCAGATGGTGTGGGATTTTATCATGTGACAAAGAATGGCG
TGCACTCATAACTTGTGTGTTGTTTAGCTCTGGAAATTTCCATTTAGTATTTTCAGACTGCATTGGTCTCTAGTAACTGA
AACCACAGCCAGCTAAATTATGGTTTAGAAGAAGTTATTGTATGTTTACCTTCTCCTACAGCTTCTTGGATGTGTATGAA
ATAGAATGATTATGTGTTTTGTGGTGCTCGGAGACCACACCTAGGGCCTCTGCACTGCAGGCAACTGCCTTATCTCTGCC
TCTTGGTACCTTTGAGACAGGGCCCTTTACGTAGGCAGACTATTACATAGCCCGAATGGTTTTCAGGCTCCCATGGTCCT
CCCGTGTCAGCCTTCCAAGTGCTGCAATGAAAGGTGTTCCTTACCATATTTAGCTCTTTCCCTTTCTTCTCTTTTCCATG
AAAGGCCCAGTGCTAGGGCTGGAAATCTAGTGCCTCTCACATGCTAGATTAGGTCTCCACCACTGAATTATAGCACCAGA
CTAGATTGTGTTTTTAAAAAGTTTAATTAATTTTTGAAAATCAACATTATTATTAATGTGTATGTATGTGTGGTATGCAT
GCATGCATATGTGTGTGCATGTATGTGATGTGGAGTAGGGGGCACCCATATACCAGTGTAGGTGGTATGCAGAGAACAAC
CTCATGGAGCTGGTTCTGGGAGCTGAGTTCACTTTACTCATTTCTGCCCAGGGCCCGTGTAAAGTGAATGAGATCTCGCT
GTGCCGGGAC

A.3 Primary cilia in double KO cortical neurons

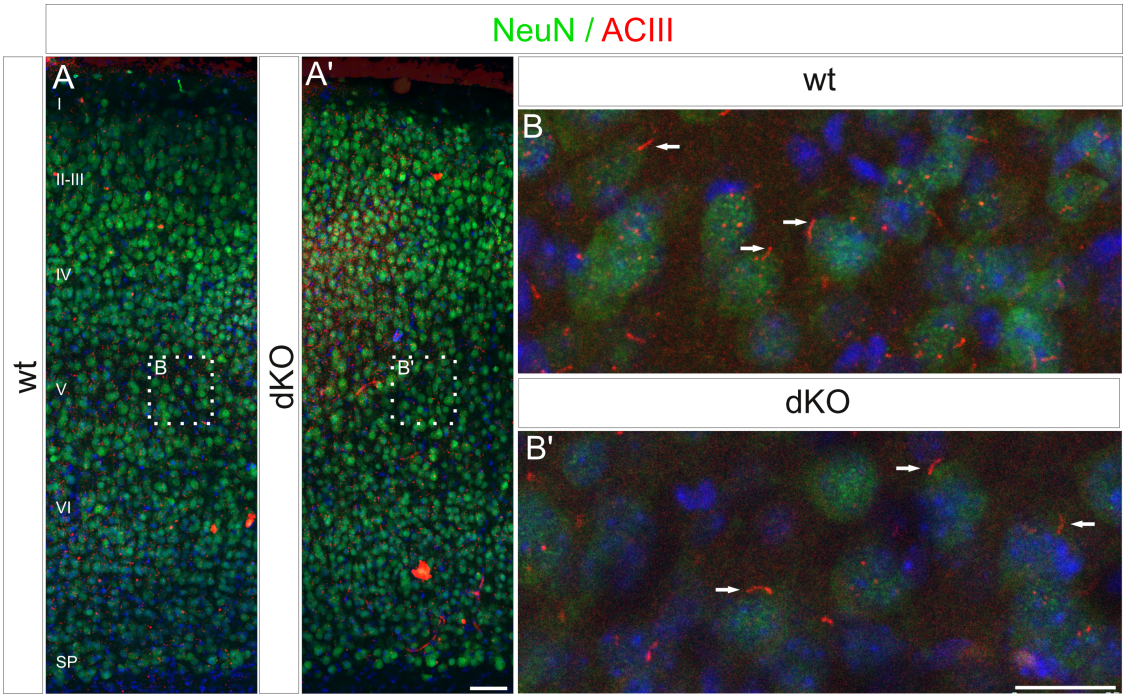


Figure A.1: Cilia morphology unaffected by absence of KIAA0319 and AU040320. Staining of cortical neurons (NeuN, green) in somatosensory cortex showing normal ciliary axoneme (ACIII, red) in dKOs (B). High-magnification of layer V neurons (highlighted in A-A') show detail of primary cilium (arrows) present in dKOs and wildtype brains. Scale bar: 50 μm (A,B).

B

Appendix 2

Contents

B.1 ABR comparisons by gender for each cohort 232
B.2 ABR comparisons by age for each cohort 234
B.3 Tables with statistical values for each experimental condition tested 236

B.1 ABR comparisons by gender for each cohort

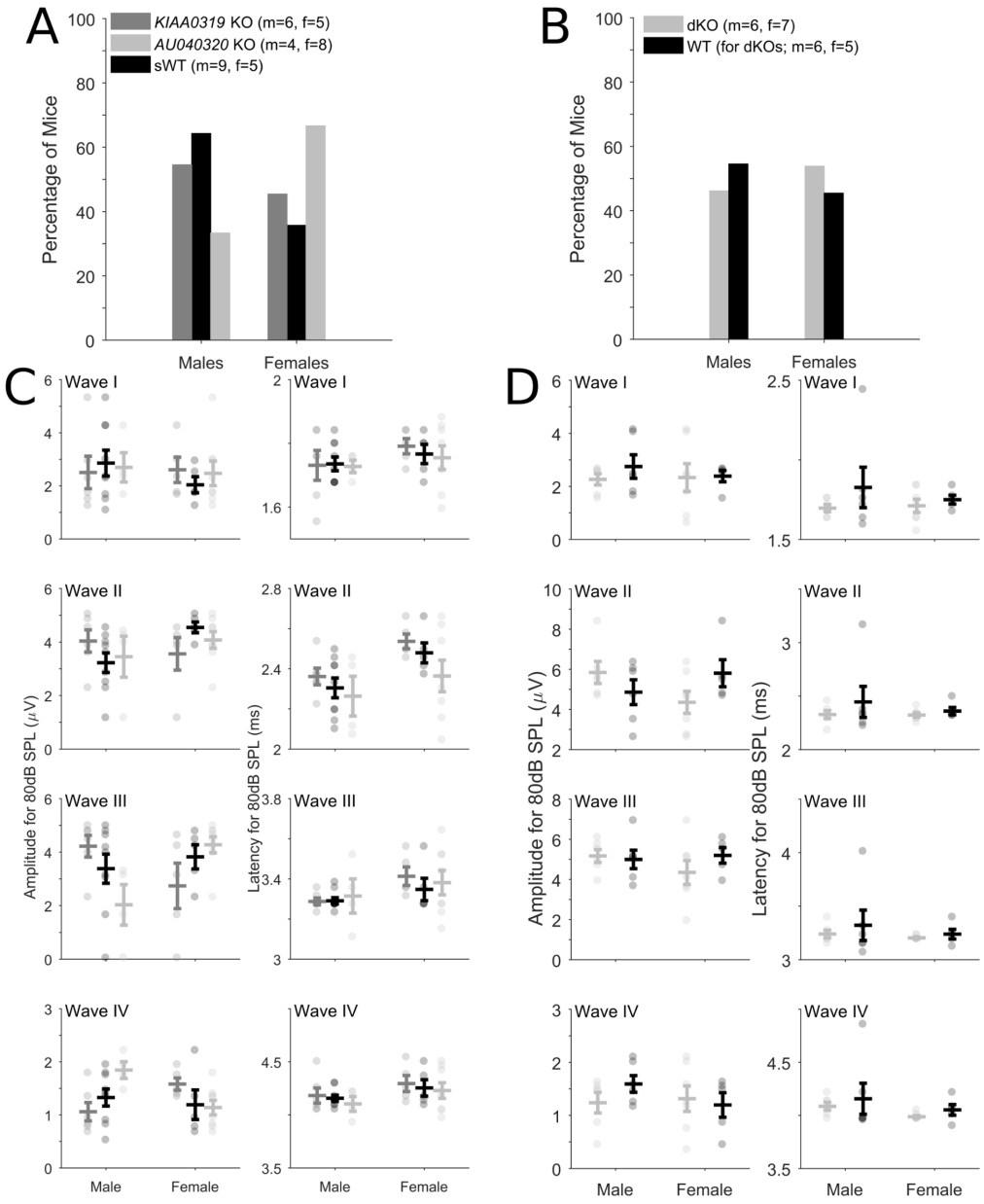


Figure B.1: Click-evoked ABR wave amplitudes and latencies by gender. ABR wave amplitudes and latencies for an 80 dB SPL click (10 clicks/sec), for males and females of each group. (A, B) Percentage of males and females in each group. (C, D) Click-evoked ABR wave amplitudes and latencies for double KO and dWT mice (C) and for single KO and sWT mice (D) for waves I-IV. For display purposes only 80dB SPL condition is shown; however, analysis was performed across sound levels (RM-ANOVA). Significant difference between dKO and dWT for wave III latency (RM-ANOVA (group x sound level x gender) $p = 0.0001$; $F = 7.971$). There were no other significant differences in wave amplitude or latency between mutants and wild-types due to gender for any wave (RM-ANOVA all $p > 0.05$). Data shown as mean ±SEM.

B.2 ABR comparisons by age for each cohort

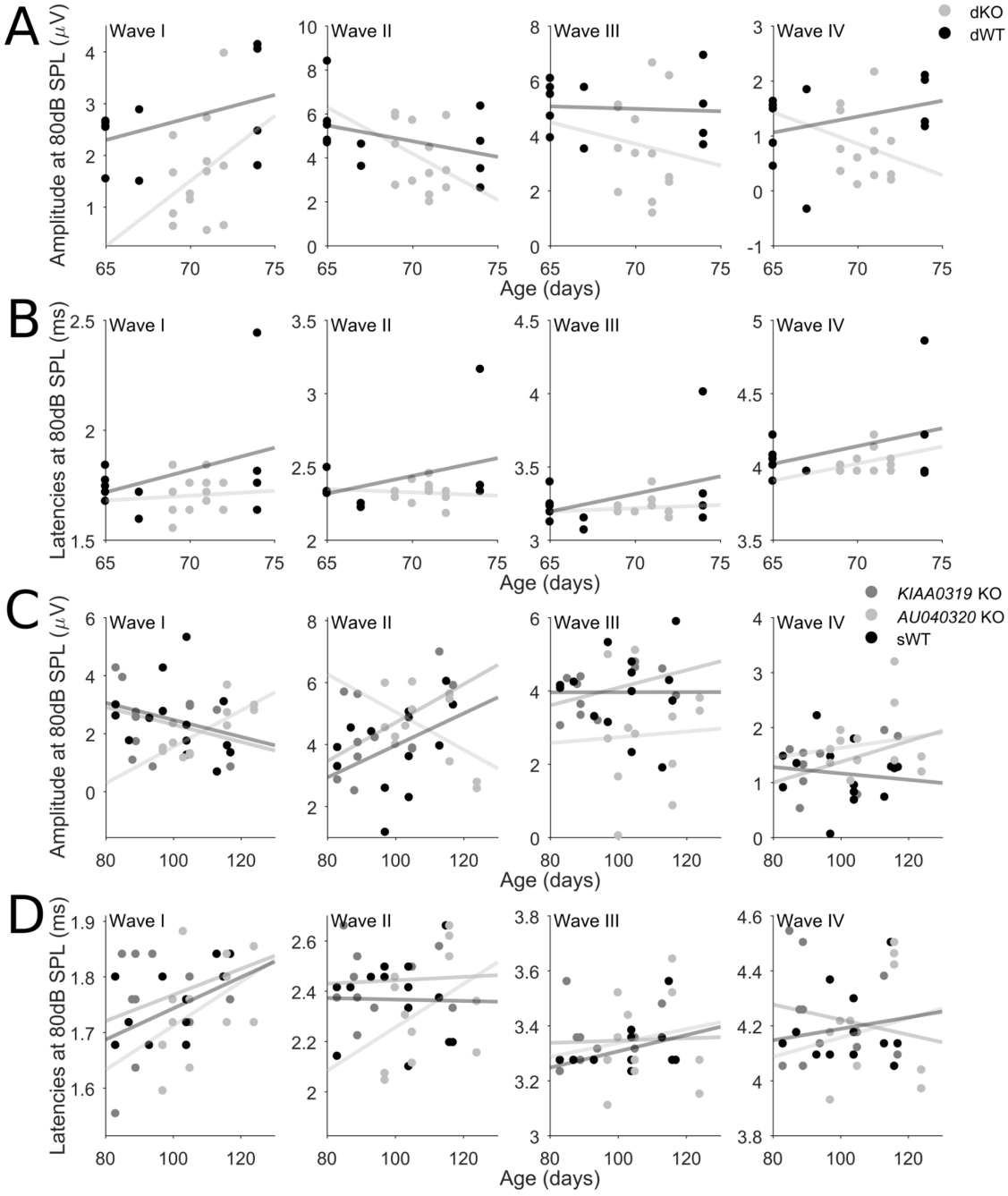


Figure B.2: Click-evoked ABR wave amplitudes and latencies by age. Scatter plots for ABR wave amplitudes and latencies evoked by an 80 dB SPL click (10 clicks/sec) as a function of age for the two cohorts. Lines show linear regression and data points indicate individual mice. (A, B) Click ABR amplitudes (A) and latencies (B) by age for ABR waves for dKO and dWT mice. (C, D) Click ABR amplitudes (C) and latencies (D) by age for ABR waves I-IV for single KO and sWT mice. Significant correlation was only found between age and wave I amplitude for AU040320 KO mice (C, $p = 0.004$).

B.3 Tables with statistical values for each experimental condition tested

Table 1. Results of RM-ANOVA tests for click (10 clicks/sec) ABR amplitudes in dKO versus dWT mice, and *AU040320*-KO or *Kiaa0319*-KO vs sWT.

Amplitudes, 10 clicks/sec	RM-ANOVA (sound level x group)	RM-ANOVA (group)	*Post-hoc* Tukey test (where applicable) [a]			
			50dB SPL	60dB SPL	70dB SPL	80dB SPL
dKO vs dWT						
Wave I	**p=0.002; F=5.536**	p=0.079; F=3.401	0.132	0.251	0.208	**0.016**
Wave II	**p=0.044; F=2.855**	p=0.336; F=0.968	0.632	0.530	0.394	0.140
Wave III	p=0.317; F=1.200	**p=0.014; F=7.132**	**0.010**	**0.009**	**0.019**	**0.036**
Wave IV	p=0.258; F=1.375	p=0.053; F=4.190	0.562	0.210	0.055	0.101
***AU040320*-KO vs sWT**						
Wave I	p=0.209; F=1.550	p=0.896; F=0.018	0.149	0.794	0.745	0.408
Wave II	p=0.061; F=2.563	p=0.679; F=0.176	0.114	0.334	0.771	0.343
Wave III	p=0.339; F=1.141	**p=0.029; F=5.405**	**0.036**	**0.024**	0.109	**0.031**
Wave IV	p=0.426; F=0.940	p=0.240; F=1.451	0.481	0.261	0.895	0.020
***Kiaa0319*-KO vs sWT**						
Wave I	p=0.853; F=0.261	p=0.695; F=0.158	0.244	0.657	0.742	0.984
Wave II	p=0.366; F=1.075	p=0.923; F=0.010	0.522	0.742	0.839	0.448
Wave III	p=0.517; F=0.766	p=0.651; F=0.210	0.534	0.347	0.927	0.938
Wave IV	p=0.633; F=0.576	p=0.717; F=0.135	0.574	0.423	0.985	0.474

a**:** *post-hoc* Tukey test results shown where RM-ANOVA result was significant. RM-ANOVA tests were conducted only on suprathreshold data (50-80 dB SPL clicks). P-values deemed significant (using an alpha value of 0.05) are in bold.

Table 2. Results of RM-ANOVA tests for click (10 clicks/sec) ABR latencies in dKO versus dWT mice, and *AU040320*-KO or *Kiaa0319*-KO vs sWT.

Latencies, 10 clicks/sec	RM-ANOVA (sound level x group)	RM-ANOVA (group)	*Post-hoc* Tukey test (where applicable)			
			50dB SPL	60dB SPL	70dB SPL	80dB SPL
dKO vs dWT						
Wave I	p=0.594 F=0.637	p=0227 F=1.546	0.481	0.134	0.218	0.213
Wave II	p=0.229 F=1.477	p=0.318 F=1.046	0.589	0.259	0.204	0.287
Wave III	p=0.211 F=1.546	p=0.447 F=0.599	0.630	0.467	0.322	0.398
Wave IV	p=0.213 F=1.539	p=0.483 F=0.509	0.700	0.531	0.408	0.341
***AU040320*-KO vs sWT**						
Wave I	p=0.537 F=0.732	p=0.288 F=1.183	0.458	0.262	0.116	0.979
Wave II	**p=0.027 F=3.241**	p=0.804 F=0.063	0.143	0.702	0.926	0.622
Wave III	p=0.239 F=1.438	p=0.216 F=1.613	0.159	0.159	0.300	0.350
Wave IV	p=0.251 F=1.398	p=0.681 F=0.173	0.434	0.766	0.636	0.949
***Kiaa0319*-KO vs sWT**						
Wave I	p=0.804 F=0.330	p=0.264 F=1.309	0.625	0.154	0.163	0.715
Wave II	p=0.410 F=0.975	p=0.400 F=0.736	0.689	0.642	0.397	0.218
Wave III	p=0.552 F=0.706	p=0.241 F=1.446	0.202	0.263	0.287	0.360
Wave IV	p=0.936 F=0.140	p=0.589 F=0.300	0.729	0.526	0.656	0.496

Conventions as in Table S5.

Table 3. Results of RM-ANOVA tests for slow-click rate (2 clicks/sec) ABR amplitudes and latencies in *AU040320*-KO or *Kiaa0319*-KO vs sWT.

2 clicks/sec	RM-ANOVA (sound level x group)	RM-ANOVA (group)	*Post-hoc* Tukey test (where applicable)			
			50dB SPL	60dB SPL	70dB SPL	80dB SPL
***AU040320*-KO vs sWT; Amplitudes**						
Wave I	p=0.704; F=0.470	p=0.849; F=0.037	0.746	0.884	0.770	0.696
Wave II	p=0.301; F=1.242	p=0.297; F=1.137	0.051	0.335	0.175	0.956
Wave III	p=0.056; F=2.640	**p=0.005; F=9.347**	**0.024**	**0.002**	**0.010**	**0.012**
Wave IV	p=0.204; F=1.569	p=0.233; F=1.496	0.234	0.165	0.200	0.932
***AU040320*-KO vs sWT; Latencies**						
Wave I	p=0.335 F=1.149	p=0.578 F=0.317	0.708	0.217	0.636	0.815
Wave II	**p=0.048 F=2.759**	p=0.951 F=0.004	0.403	0.921	0.955	0.479
Wave III	**p=0.048 F=2.759**	p=0.336 F=0.965	0.250	0.220	0.439	0.600
Wave IV	p=0.818 F=0.310	p=0.898 F=0.017	0.861	0.980	0.987	0.720
***Kiaa0319*-KO vs sWT; Amplitudes**						
Wave I	p=0.677 F=0.510	p=0.879 F=0.024	0.936	0.892	0.784	0.718
Wave II	**p=0.009 F=4.186**	p=0.918 F=0.011	0.401	0.303	0.754	0.247
Wave III	p=0.394 F=1.009	p=0.692 F=0.161	0.752	0.558	0.316	0.668
Wave IV	p=0.127 F=1.968	p=0.824 F=0.051	0.927	0.487	0.768	0.031
***Kiaa0319*-KO vs sWT; Latencies**						
Wave I	p=0.767 F=0.381	p=0.101 F=2.920	0.089	0.130	0.175	0.220
Wave II	p=0.877 F=0.228	p=0.382 F=7.94	0.429	0.464	0.511	0.284
Wave III	p=0.913 F=0.176	p=0.262 F=1.322	0.329	0.243	0.222	0.349
Wave IV	p=0.428 F=0.936	p=0.519 F=0.428	0.888	0.611	0.313	0.384

Conventions as in Table S5.

Tables for comparisons between gender and age for each experimental condition.

Double KO Amplitudes	RNOVA (sound level x group)	RANOVA (sound level x group x gender)	RANOVA (group)	RNOVA (gender)	RNOVA (group x gender)	*Post*-hoc Tukey test (group x gender)	
						Females	Males
Wave I	**P=0.003 F=5.345**	P=0.597 F=0.633	P=0.100 F=2.970	P=0.171 F=2.021	P=0.883 F=0.022	P=0.204	P=0.276
Wave II	**P=0.020 F=3.538**	P=0.463 F=0.867	P=0.284 F=1.213	P=0.188 F=1.858	P=0.547 F=0.376	P=0.243	P=0.732
Wave III	P=0.309 F=1.223	P=0.977 F=0.067	**P=0.019 F=6.544**	P=0.947 F=0.005	P=0.565 F=0.343	**P=0.039**	P=0.175
Wave IV	P=0.221 F=1.509	P=0.568 F=0.679	P=0.058 F=4.031	P=0.906 F=0.014	P=0.282 F=1.221	P=0.533	**P=0.038**

Double KO Latencies	RNOVA (sound level x group)	RANOVA (sound level x group x gender)	RANOVA (group)	RNOVA (gender)	RNOVA (group x gender)	*Post*-hoc Tukey test (group x gender)	
						Females	Males
Wave I	P=0.555 F=0.702	P=0.837 F=0.284	P=0.266 F=1.309	P=0.576 F=0.324	P=0.679 F=0.176	P=0.617	P=0.279
Wave II	P=0.254 F=1.393	P=0.186 F=1.656	P=0.355 F=0.898	P=0.639 F=0.227	P=0.396 F=0.752	P=0.955	P=0.211
Wave III	P=0.131 F=1.949	**P=0.0001 F=7.971**	P=0.502 F=0.467	P=0.455 F=0.579	P=0.515 F=0.439	P=0.989	P=0.349
Wave IV	P=0.210 F=1.554	P=0.438 F=0.917	P=0.557 F=0.358	P=0.228 F=1.550	P=0.782 F=0.079	P=0.826	P=0.539

KIAA-Like KO Amplitudes Fast click	RNOVA (sound level x group)	RANOVA (sound level x group x gender)	RANOVA (group)	RNOVA (gender)	RNOVA (group x gender)	*Post*-hoc Tukey test	
						Females	Males
Wave I	P=0.175 F=1.702	P=0.199 F=1.594	P=0.847 F=0.038	P=0.794 F=0.070	P=0.776 F=0.083	P=0.728	P=0.950
Wave II	P=0.185 F=1.656	P=0.422 F=0.950	P=0.711 F=0.141	P=0.939 F=0.006	P=0.541 F=0.385	P=0.860	P=0.500
Wave III	P=0.158 F=1.791	P=0.630 F=0.581	**P=0.043 F=4.615**	P=0.888 F=0.021	P=0.312 F=1.072	P=0.428	**P=0.039**
Wave IV	P=0.305 F=1.233	P=0.569 F=0.677	P=0.278 F=1.236	P=0.955 F=0.003	P=0.446 F=0.603	P=0.810	P=0.207

KIAA0319 KO Amplitudes Fast click	RNOVA (sound level x group)	RANOVA (sound level x group x gender)	RANOVA (group)	RNOVA (gender)	RNOVA (group x gender)	*Post*-hoc Tukey test	
						Females	Males
Wave I	P=0.943 F=0.129	P=0.517 F=0.766	P=0.634 F=0.234	P=0.863 F=0.031	P=0.513 F=0.443	P=0.463	P=0.889
Wave II	P=0.600 F=0.628	P=0.497 F=0.803	P=0.829 F=0.048	P=0.972 F=0.001	P=0.497 F=0.478	P=0.560	P=0.716
Wave III	P=0.403 F=0.990	P=0.504 F=0.790	P=0.913 F=0.012	P=0.704 F=0.149	P=0.045 F=4.530	P=0.203	P=0.095
Wave IV	P=0.554 F=0.703	P=0.358 F=1.095	P=0.613 F=0.264	P=0.727 F=0.126	P=0.497 F=0.479	P=0.441	P=0.891

KIAA-Like KO Amplitudes Slow click	RNOVA (sound level x group)	RANOVA (sound level x group x gender)	RANOVA (group)	RNOVA (gender)	RNOVA (group x gender)	*Post*-hoc Tukey test	
						Females	Males
Wave I	P=0.450 F=0.892	P=0.612 F=0.608	P=0.730 F=0.122	P=0.569 F=0.335	P=0.797 F=0.068	P=0.662	P=0.952
Wave II	P=0.500 F=0.797	P=0.727 F=0.437	P=0.253 F=1.380	P=0.571 F=0331	P=0.574 F=0.325	P=0.665	P=0.242
Wave III	P=0.092 F=2.241	P=0.818 F=0.310	**P=0.011** **F=7.714**	P=0.542 F=0.384	P=0.175 F=1.963	P=0.328	**P=0.009**
Wave IV	P=0.071 F=2.452	P=0.301 F=1.245	P=0.187 F=1.852	P=0.463 F=0.558	P=0.897 F=0.017	P=0.381	P=0.315

KIAA0319 KO Amplitudes Slow click	RNOVA (sound level x group)	RANOVA (sound level x group x gender)	RANOVA (group)	RNOVA (gender)	RNOVA (group x gender)	*Post*-hoc Tukey test	
						Females	Males
Wave I	P=0.556 F=0.700	P=0.051 F=2.733	P=0.914 F=0.012	P=0.280 F=1.228	P=0.720 F=0.132	P=0.761	P=0.844
Wave II	**P=0.030** **F=3.190**	P=0.557 F=0.698	P=0.897 F=0.017	P=0.709 F=0.143	P=0.713 F=0.139	P=0.746	P=0.852
Wave III	P=0.500 F=0.798	P=0.853 F=0.261	P=0.908 F=0.014	P=0.561 F=0.348	**P=0.015** **F=7.021**	P=0.086	P=0.061
Wave IV	P=0.125 F=1.988	P=0.429 F=0.936	P=0.897 F=0.017	P=0.215 F=1.634	P=0.848 F=0.038	P=0.835	P=0.961

KIAA-Like KO Latencies Fast click	RNOVA (sound level x group)	RANOVA (sound level x group x gender)	RANOVA (group)	RNOVA (gender)	RNOVA (group x gender)	*Post*-hoc Tukey test	
						Females	Males
Wave I	P=0.738 F=0.421	P=0.652 F=0.547	P=0.649 F=0.213	P=0.059 F=3.977	P=0.919 F=0.011	P=0.796	P=0.701
Wave II	P=0.051 F=2.729	P=0.475 F=0.843	P=0.615 F=0.261	**P=0.021** **F=6.179**	P=0.980 F=0	P=0.701	P=0.741
Wave III	P=0.352 F=1.109	P=0.422 F=0.950	P=0.418 F=0.680	P=0.249 F=1.405	P=0.998 F=0	P=0.554	P=0.577
Wave IV	P=0.282 F=1.299	P=0.291 F=1.272	P=0.935 F=0.007	P=0.143 F=2.308	P=0.663 F=0.196	P=0.796	P=0.721

KIAA0319 KO Latencies Fast click	RNOVA (sound level x group)	RANOVA (sound level x group x gender)	RANOVA (group)	RNOVA (gender)	RNOVA (group x gender)	*Post*-hoc Tukey test	
						Females	Males
Wave I	P=0.877 F=0.129	P=0.560 F=0.766	P=0.372 F=0.234	P=0.084 F=0.031	P=0.721 F=0.443	P=0.724	P=0.331
Wave II	P=0.555 F=0.628	P=0.967 F=0.803	P=0.479 F=0.048	**P=0.001** **F=0.001**	P=0.791 F=0.478	P=0.527	P=0.727
Wave III	P=0.724 F=0.990	P=0.205 F=0.790	P=0.258 F=0.012	**P=0.023** **F=0.149**	P=0.528 F=4.530	P=0.254	P=0.688
Wave IV	P=0.993 F=0.703	P=0.138 F=1.095	P=0.647 F=0.264	P=0.127 F=0.126	P=0.687 F=0.479	P=0.576	P=0.965

KIAA-Like KO Latencies Slow click	RNOVA (sound level x group)	RANOVA (sound level x group x gender)	RANOVA (group)	RNOVA (gender)	RNOVA (group x gender)	*Post*-hoc Tukey test	
						Females	Males
Wave I	P=0.394 F=1.011	P=0.948 F=0.120	P=0.918 F=0.011	**P=0.047** **F=4.440**	P=0.528 F=0.411	P=0.700	P=0.613
Wave II	P=0.072 F=2.438	P=0.534 F=0.736	P=0.335 F=0.973	**P=0.003** **F=11.272**	P=0.483 F=0.510	P=0.845	P=0.254
Wave III	**P=0.031** **F=3.152**	P=0.402 F=0.993	P=0.733 F=0.120	P=0.057 F=4.037	P=0.862 F=0.031	P=0.708	P=0.908
Wave IV	P=0.983 F=0.054	P=0.761 F=0.390	P=0.314 F=1.062	**P=0.010** **F=7.941**	P=0.412 F=0.699	P=0.889	P=0.212

KIAA0319 KO Latencies Slow click	RNOVA (sound level x group)	RANOVA (sound level x group x gender)	RANOVA (group)	RNOVA (gender)	RNOVA (group x gender)	*Post*-hoc Tukey test	
						Females	Males
Wave I	P=0.753 F=0.700	P=0.222 F=2.733	P=0.122 F=0.012	P=0.082 F=1.228	P=0.725 F=0.132	P=0.214	P=0.338
Wave II	P=0.954 F=3.190	P=0.601 F=0.698	P=0.467 F=0.017	**P=0.004** **F=0.143**	P=0.845 F=0.139	P=0.548	P=0.675
Wave III	P=0.927 F=0.798	P=0.122 F=0.261	P=0.307 F=0.014	**P=0.006** **F=0.348**	P=0.782 F=7.021	P=0.397	P=0.555
Wave IV	P=0.515 F=1.988	P=0.362 F=0.936	P=0.663 F=0.017	P=0.073 F=1.634	P=0.846 F=0.038	P=0.874	P=0.623

All Single KO/WT Click ABR Amplitudes by age – Regression (fast-click)	Wave I	Wave II	Wave III	Wave IV
R^2	0.012	0.047	0.009	0.058
F	0.426	1.716	0.309	2.168
P	0.518	0.199	0.582	0.150
Error	1.190	0.582	0.150	0.313

Single WT Click ABR Amplitudes by age – Regression (fast-click)	Wave I	Wave II	Wave III	Wave IV
R^2	0.077	0.197	0	0.016
F	1	2.952	0	0.2
P	0.337	0.111	0.996	0.663
Error	1.533	1.626	1.241	0.297

KIAA-Like KO Click ABR Amplitudes by age – Regression (fast-click)	Wave I	Wave II	Wave III	Wave IV
R^2	0.584	0.272	0.003	0.023
F	14.048	3.742	0.028	0.237
P	**0.004**	0.082	0.871	0.637
Error	0.311	1.103	2.503	0.385

KIAA KO Click ABR Amplitudes by age – Regression (fast-click)	Wave I	Wave II	Wave III	Wave IV
R^2	0.090	0.278	0.210	0.246
F	0.892	3.471	2.395	2.930
P	0.369	0.095	0.156	0.121
Error	1.394	1.551	0.337	0.169

All Single KO/WT Click ABR Latencies by age – Regression (fast-click)	Wave I	Wave II	Wave III	Wave IV
R^2	0.119	0.001	0.04	0
F	4.709	0.034	1.453	0.004
P	**0.037**	0.855	0.236	0.95
Error	0.006	0.03	0.014	0.027

Single WT Click ABR Latencies by age – Regression (fast-click)	Wave I	Wave II	Wave III	Wave IV
R^2	0.077	0.197	2.0659e-6	0.016
F	1	2.952	2.4791e-05	0.200
P	0.337	0.111	0.996	0.663
Error	1.5326	1.626	1.241	0.297

KIAA-Like KO Click ABR Latencies by age – Regression (fast-click)	Wave I	Wave II	Wave III	Wave IV
R^2	0.206	0.168	0.023	0.034
F	2.598	2.024	0.235	0.352
P	0.138	0.185	0.063	0.566
Error	0.007	0.041	0.030	0.039

KIAA KO Click ABR Latencies by age – Regression (fast-click)	Wave I	Wave II	Wave III	Wave IV
R^2	0.088	0.004	0.003	0.035
F	0.870	0.035	0.023	0.323
P	0.375	0.855	0.882	0.584
Error	0.009	0.018	0.010	0.033

All Single KO/WT Click ABR Amplitudes by age – Regression (slow-click)	Wave I	Wave II	Wave III	Wave IV
R^2	0.03	0.047	0.009	0.035
F	1.062	1.741	0.329	1.28
P	0.31	0.196	0.57	0.266
Error	1.887	2.003	1.845	0.384

Single WT Click ABR Amplitudes by age – Regression (slow-click)	Wave I	Wave II	Wave III	Wave IV
R^2	0.059	0.278	0	0.179
F	0.746	4.618	0.004	2.619
P	0.405	0.053	0.949	0.132
Error	2.842	1.71	0.825	0.13

KIAA-Like KO Click ABR Amplitudes by age – Regression (slow-click)	Wave I	Wave II	Wave III	Wave IV
R^2	0.157	0.02	0.01	0.001
F	1.861	0.203	0.098	0.009
P	0.202	0.662	0.761	0.926
Error	0.815	1.479	2.804	0.771

KIAA KO Click ABR Amplitudes by age – Regression (slow-click)	Wave I	Wave II	Wave III	Wave IV
R^2	0.084	0.2	0.391	0.01
F	0.821	2.249	5.773	0.091
P	0.389	0.168	**0.04**	0.77
Error	2.138	2.288	0.699	0.315

All Single KO/WT Click ABR Latencies by age – Regression (slow-click)	Wave I	Wave II	Wave III	Wave IV
R^2	0.057	0.022	0.054	0.012
F	2.122	0.774	1.993	0.417
P	0.154	0.385	0.167	0.523
Error	0.005	0.0234	0.015	0.025

Single WT Click ABR Latencies by age – Regression (slow-click)	Wave I	Wave II	Wave III	Wave IV
R^2	0.103	0.002	0.035	0.03
F	1.37	0.024	0.432	0.371
P	0.265	0.881	0.523	0.554
Error	0.004	0.019	0.013	0.03

KIAA-Like KO Click ABR Latencies by age – Regression (slow-click)	Wave I	Wave II	Wave III	Wave IV
R^2	0.474	0.501	0.334	0.426
F	9.003	10.046	5.018	7.422
P	**0.013**	**0.01**	**0.049**	**0.021**
Error	0.004	0.021	0.021	0.016

KIAA KO Click ABR Latencies by age – Regression (slow-click)	Wave I	Wave II	Wave III	Wave IV
R^2	0.03	0.003	0.002	0.033
F	0.282	0.029	0.014	0.309
P	0.609	0.868	0.908	0.592
Error	0.008	0.015	0.011	0.021

Double WT Click ABR Amplitudes by age – Regression	Wave I	Wave II	Wave III	Wave IV
R^2	0.188	0.157	0.005	0.119
F	2.085	1.671	0.043	1.215
P	0.183	0.228	0.84	0.299
Error	0.68	2.261	1.365	0.513

Double KO Click ABR Amplitudes by age – Regression	Wave I	Wave II	Wave III	Wave IV
R^2	0.095	0.112	0.012	0.049
F	1.158	1.391	0.129	0.567
P	0.305	0.263	0.726	0.467
Error	0.943	2.19	3.323	0.398

All Double KO/WT Click ABR Amplitudes by age – Regression	Wave I	Wave II	Wave III	Wave IV
R^2	0.018	0.154	0.032	0.006
F	0.392	4.007	0.739	0.122
P	0.538	0.059	0.4	0.73
Error	1.109	2.181	2.663	0.504

Double WT Click ABR Latencies by age – Regression	Wave I	Wave II	Wave III	Wave IV
R^2	0.149	0.16	0.162	0.152
F	1.569	1.712	1.735	1.608
P	0.242	0.223	0.22	0.237
Error	0.049	0.064	0.062	0.068

Double KO Click ABR Latencies by age – Regression	Wave I	Wave II	Wave III	Wave IV
R^2	0.004	0.006	0.007	0.117
F	0.041	0.07	0.082	1.461
P	0.843	0.797	0.78	0.252
Error	0.008	0.005	0.004	0.006

All Double KO/WT Click ABR Latencies by age – Regression	Wave I	Wave II	Wave III	Wave IV
R^2	0.058	0.072	0.091	0.09
F	1.36	1.704	2.2	2.165
P	0.256	0.205	0.152	0.155
Error	0.028	0.033	0.03	0.035

References

Abbas, PJ & Gorga, MP (1981). AP responses in forward-masking paradigms and their relationship to responses of auditory-nerve fibers. *J Acoust Soc Am* 69:492.

Ables, JL, Breunig, JJ, Eisch, AJ, & Rakic, P (2011). Not(ch) just development: Notch signalling in the adult brain. *Nat Rev Neurosci* 12:269–83.

Abou-Haila, A & Tulsiani, DR (2000). Mammalian Sperm Acrosome: Formation, Contents, and Function. *Arch Biochem Biophys* 379:173–182.

Adler, WT, Platt, MP, Mehlhorn, AJ, Haight, JL, Currier, TA, Etchegaray, MA, Galaburda, AM, & Rosen, GD (2013). Position of neocortical neurons transfected at different gestational ages with shRNA targeted against candidate dyslexia susceptibility genes. *PLoS One* 8:e65179.

Agarwal, A, Mulgund, A, Hamada, A, & Chyatte, MR (2015). A unique view on male infertility around the globe. *Reprod Biol Endocrinol* 13:37.

Aguas, AP & da Silva, PP (1985). The acrosomal membrane of boar sperm: a Golgi-derived membrane poor in glycoconjugates. *J Cell Biol* 100:528–534.

Allison, AC & Hartree, EF (1970). Lysosomal enzymes in the acrosome and their possible role in fertilization. *J Reprod Fertil* 21:501–15.

Altarelli, I, Leroy, F, Monzalvo, K, Fluss, J, Billard, C, Dehaene-Lambertz, G, Galaburda, AM, & Ramus, F (2014). Planum temporale asymmetry in developmental dyslexia: Revisiting an old question. *Hum Brain Mapp* 35:5717–35.

Altarelli, I, Monzalvo, K, Iannuzzi, S, Fluss, J, Billard, C, Ramus, F, & Dehaene-Lambertz, G (2013). A functionally guided approach to the morphometry of occipitotemporal regions in developmental dyslexia: evidence for differential effects in boys and girls. *J Neurosci* 33:11296–301.

Altman, J & Bayer, SA (1990a). Migration and distribution of two populations of hippocampal granule cell precursors during the perinatal and postnatal periods. *J Comp Neurol* 301:365–381.

— (1990b). Prolonged sojourn of developing pyramidal cells in the intermediate zone of the hippocampus and their settling in the stratum pyramidale. *J Comp Neurol* 301:343–64.

Alvarez, Va, Ridenour, Da, & Sabatini, BL (2006). Retraction of synapses and dendritic spines induced by off-target effects of RNA interference. *J Neurosci* 26:7820–5.

American Psychiatric Association (2013). *Diagnostic and Statistical Manual of Mental Disorders*. American Psychiatric Association.

Anastasiades, PG & Butt, SJB (2011). Decoding the transcriptional basis for GABAergic interneuron diversity in the mouse neocortex. *Eur J Neurosci* 34:1542–52.

Anderson, LA & Linden, JF (2016). Mind the Gap: Two Dissociable Mechanisms of Temporal Processing in the Auditory System. *J Neurosci* 36:1977–1995.

Angevine, JB & Sidman, RL (1961). Autoradiographic study of cell migration during histogenesis of cerebral cortex in the mouse. *Nature* 192:766–768.

Anggono, V & Huganir, RL (2012). Regulation of AMPA receptor trafficking and synaptic plasticity. *Curr Opin Neurobiol* 22:461–469.

Anthoni, H, Sucheston, LE, Lewis, Ba, Tapia-Páez, I, Fan, X, Zucchelli, M, et al. (2012). The aromatase gene CYP19A1: several genetic and functional lines of evidence supporting a role in reading, speech and language. *Behav Genet* 42:509–527.

Anthoni, H, Zucchelli, M, Matsson, H, Müller-Myhsok, B, Fransson, I, Schumacher, J, et al. (2007). A locus on 2p12 containing the co-regulated MRPL19 and C2ORF3 genes is associated to dyslexia. *Hum Mol Genet* 16:667–77.

Aston, KI, Uren, PJ, Jenkins, TG, Horsager, A, Cairns, BR, Smith, AD, & Carrell, DT (2015). Aberrant sperm DNA methylation predicts male fertility status and embryo quality. *Fertil Steril* 104:1388–97.e1–5.

Audouard, C, Le Masson, F, Charry, C, Li, Z, & Christians, ES (2011). Oocyte-targeted deletion reveals that hsp90b1 is needed for the completion of first mitosis in mouse zygotes. *PLoS One* 6:e17109.

Ayala, R, Shu, T, & Tsai, LH (2007). Trekking across the brain: the journey of neuronal migration. *Cell* 128:29–43.

Azevedo, FAC, Carvalho, LRB, Grinberg, LT, Farfel, JM, Ferretti, REL, Leite, REP, Jacob Filho, W, Lent, R, & Herculano-Houzel, S (2009). Equal numbers of neuronal and nonneuronal cells make the human brain an isometrically scaled-up primate brain. *J Comp Neurol* 513:532–41.

Baccetti, B, Renieri, T, Rosati, F, Selmi, MG, & Casanova, S (1977). Further observations on the morphogenesis of the round headed human spermatozoa. *Andrologia* 9:255–64.

Bache, I, Assche, EV, Cingoz, S, Bugge, M, Tümer, Z, Hjorth, M, et al. (2004). An excess of chromosome 1 breakpoints in male infertility. *Eur J Hum Genet* 12:993–1000.

Baek, ST, Kerjan, G, Bielas, SL, Lee, JE, Fenstermaker, AG, Novarino, G, & Gleeson, JG (2014). Off-target effect of doublecortin family shRNA on neuronal migration associated with endogenous microRNA dysregulation. *Neuron* 82:1255–62.

Bai, J, Ramos, RL, Ackman, JB, Thomas, AM, Lee, RV, LoTurco, JJ, & Other (2003). RNAi reveals doublecortin is required for radial migration in rat neocortex. *Nat Neurosci* 6:1277–1283.

Bakker, DJ (1992). Neuropsychological Classification and Treatment of Dyslexia. *J Learn Disabil* 25:102–109.

Basu, M, Krishnan, A, & Weber-Fox, C (2010). Brainstem correlates of temporal auditory processing in children with specific language impairment. *Dev Sci* 13:77–91.

Bates, TC, Lind, PA, Luciano, M, Montgomery, GW, Martin, NG, & Wright, MJ (2010). Dyslexia and DYX1C1: deficits in reading and spelling associated with a missense mutation. *Mol Psychiatry* 15:1190–6.

Bates, TC, Luciano, M, Castles, A, Coltheart, M, Wright, MJ, & Martin, NG (2007). Replication of reported linkages for dyslexia and spelling and suggestive evidence for novel regions on chromosomes 4 and 17. *Eur J Hum Genet* 15:194–203.

Bates, TC, Luciano, M, Medland, SE, Montgomery, GW, Wright, MJ, & Martin, NG (2011). Genetic Variance in a Component of the Language Acquisition Device: ROBO1 Polymorphisms Associated with Phonological Buffer Deficits. *Behav Genet* 41:50–57.

Baudoin, JP, Viou, L, Launay, PS, Luccardini, C, Espeso Gil, S, Kiyasova, V, Irinopoulou, T, Alvarez, C, Rio, JP, Boudier, T, Lechaire, JP, Kessaris, N,

Spassky, N, & Métin, C (2012). Tangentially migrating neurons assemble a primary cilium that promotes their reorientation to the cortical plate. *Neuron* 76:1108–22.

Beaton, AA (1997). The relation of planum temporale asymmetry and morphology of the corpus callosum to handedness, gender, and dyslexia: a review of the evidence. *Brain Lang* 60:255–322.

Beaton, AA (2002). Dyslexia and the cerebellar deficit hypothesis. *Cortex* 38:479–90.

Beaulieu, C, Plewes, C, Paulson, LA, Roy, D, Snook, L, Concha, L, & Phillips, L (2005). Imaging brain connectivity in children with diverse reading ability. *Neuroimage* 25:1266–71.

Becker, J, Czamara, D, Hoffmann, P, Landerl, K, Blomert, L, Brandeis, D, Vaessen, A, Maurer, U, Moll, K, Ludwig, KU, Müller-Myhsok, B, Nöthen, MM, Schulte-Körne, G, & Schumacher, J (2012). Evidence for the involvement of ZNF804A in cognitive processes of relevance to reading and spelling. *Transl Psychiatry* 2:e136.

Becker, J, Czamara, D, Scerri, TS, Ramus, F, Csepe, V, Talcott, JB, et al. (2014). Genetic analysis of dyslexia candidate genes in the European cross-linguistic NeuroDys cohort. *Eur J Hum Genet* 22:675–80.

Belgard, TG, Marques, AC, Oliver, PL, Abaan, HO, Sirey, TM, Hoerder-Suabedissen, A, García-Moreno, F, Molnár, Z, Margulies, EH, & Ponting, CP (2011). A transcriptomic atlas of mouse neocortical layers. *Neuron* 71:605–16.

Bellini, G, Bravaccio, C, Calamoneri, F, Donatella Cocuzza, M, Fiorillo, P, Gagliano, A, Mazzone, D, del Giudice, EM, Scuccimarra, G, Militerni, R, & Pascotto, A (2005). No Evidence for Association Between Dyslexia and <I>DYX1C1</I> Functional Variants in a Group of Children and Adolescents From Southern Italy. *J Mol Neurosci* 27:311–314.

Berruti, G (2016). Towards defining an 'origin'—The case for the mammalian acrosome. *Semin Cell Dev Biol*.

Berruti, G & Paiardi, C (2011). Acrosome biogenesis: Revisiting old questions to yield new insights. *Spermatogenesis* 1:95–98.

Berruti, G, Ripolone, M, & Ceriani, M (2010). USP8, a regulator of endosomal sorting, is involved in mouse acrosome biogenesis through interaction with the spermatid ESCRT-0 complex and microtubules. *Biol Reprod* 82:930–9.

Berry, M & Rogers, AW (1965). The migration of neuroblasts in the developing cerebral cortex. *J Anat* 99:691–709.

Betizeau, M, Cortay, V, Patti, D, Pfister, S, Gautier, E, Bellemin-Ménard, A, Afanassieff, M, Huissoud, C, Douglas, RJ, Kennedy, H, & Dehay, C (2013). Precursor diversity and complexity of lineage relationships in the outer subventricular zone of the primate. *Neuron* 80:442–57.

Bielle, F, Griveau, A, Narboux-Nême, N, Vigneau, S, Sigrist, M, Arber, S, Wassef, M, & Pierani, A (2005). Multiple origins of Cajal-Retzius cells at the borders of the developing pallium. *Nat Neurosci* 8:1002–12.

Bisgaard, ML, Eiberg, H, Møller, N, Niebuhr, E, & Mohr, J (1987). Dyslexia and chromosome 15 heteromorphism: negative lod score in a Danish material. *Clin Genet* 32:118–9.

Bishop, DVM (2015). The interface between genetics and psychology: lessons from developmental dyslexia. *Proc Biol Sci* 282:20143139.

Bishop, DVM (2012). *Neuronal migration in language learning impairments: a suggestion.*

Bishop, DVM (2013). Cerebral asymmetry and language development: cause, correlate, or consequence? *Science* 340:1230531.

Bishop, DVM & Snowling, MJ (2004). Developmental dyslexia and specific language impairment: same or different? *Psychol Bull* 130:858–86.

Bloom, JS, Garcia-Barrera, MA, Miller, CJ, Miller, SR, & Hynd, GW (2013). Planum temporale morphology in children with developmental dyslexia. en. *Neuropsychologia* 51:1684–92.

Bloomfield, L (1933). *Language*. University of Chicago Press. 564.

Blümcke, I, Thom, M, Aronica, E, Armstrong, DD, Vinters, HV, Palmini, A, et al. (2011). The clinicopathologic spectrum of focal cortical dysplasias: a consensus classification proposed by an ad hoc Task Force of the ILAE Diagnostic Methods Commission. *Epilepsia* 52:158–174.

Boets, B, Op de Beeck, HP, Vandermosten, M, Scott, SK, Gillebert, CR, Mantini, D, Bulthé, J, Sunaert, S, Wouters, J, & Ghesquière, P (2013). Intact but less accessible phonetic representations in adults with dyslexia. *Science* 342:1251–4.

Bonifacino, JS & Glick, BS (2004). The mechanisms of vesicle budding and fusion. *Cell* 116:153–66.

Borg, CL, Wolski, KM, Gibbs, GM, & O'Bryan, MK (2010). Phenotyping male infertility in the mouse: how to get the most out of a 'non-performer'. *Hum Reprod Update* 16:205–24.

Boscariol, M, Garcia, VL, Guimarães, CA, Montenegro, MA, Hage, SRV, Cendes, F, et al. (2010). Auditory processing disorder in perisylvian syndrome. *Brain Dev* 32:299–304.

Boscariol, M, Guimarães, CA, Hage, SRdV, Garcia, VL, Schmutzler, KMR, Cendes, F, & Guerreiro, MM (2011). Auditory processing disorder in patients with language-learning impairment and correlation with malformation of cortical development. *Brain Dev* 33:824–831.

Bourgeron, T (2015). From the genetic architecture to synaptic plasticity in autism spectrum disorder. en. *Nat Rev Neurosci* 16:551–563.

Bowen, RH (1924). On the acrosome of the animal sperm. *Anat Rec* 28:1–13.

Brameier, M, Krings, A, & MacCallum, RM (2007). NucPred–predicting nuclear localization of proteins. *Bioinformatics* 23:1159–60.

Brandler, WM & Paracchini, S (2014). The genetic relationship between handedness and neurodevelopmental disorders. *Trends Mol Med* 20:83–90.

Brandon, NJ, Millar, JK, Korth, C, Sive, H, Singh, KK, & Sawa, A (2009). Understanding the role of DISC1 in psychiatric disease and during normal development. *J Neurosci* 29:12768–75.

Bras, J, Guerreiro, R, & Hardy, J (2012). Use of next-generation sequencing and other whole-genome strategies to dissect neurological disease. *Nat Rev Neurosci* 13:453–64.

Breier, JI, Fletcher, JM, Foorman, BR, Klaas, P, & Gray, LC (2003). Auditory Temporal Processing in Children With Specific Reading Disability With and Without Attention Deficit/ Hyperactivity Disorder. *J Speech Lang Hear Res* 46:31.

Brkanac, Z, Chapman, NH, Matsushita, MM, Chun, L, Nielsen, K, Cochrane, E, Berninger, VW, Wijsman, EM, & Raskind, WH (2007). Evaluation of candidate genes for DYX1 and DYX2 in families with dyslexia. *Am J Med Genet B Neuropsychiatr Genet* 144B:556–60.

Brodmann, K (1909). *Vergleichende Lokalisationslehre der Großhirnrinde in ihren Prinzipien dargestellt auf Grund des Zellenbaues*. Leipzig: Barth.

Brogna, S & Wen, J (2009). Nonsense-mediated mRNA decay (NMD) mechanisms. *Nat Struct Mol Biol* 16:107–113.

Brown, MT, Andrade, J, Radhakrishna, H, Donaldson, JG, Cooper, JA, & Randazzo, PA (1998). ASAP1, a phospholipid-dependent arf GTPase-activating protein that associates with and is phosphorylated by Src. *Mol Cell Biol* 18:7038–51.

Brugo-Olmedo, S, Chillik, C, & Kopelman, S (2001). Definition and causes of infertility. *Reprod Biomed Online* 2:41–53.

Burbridge, TJ, Wang, Y, Volz, AJ, Peschansky, VJ, Lisann, L, Galaburda, AM, Lo Turco, JJ, & Rosen, GD (2008). Postnatal analysis of the effect of embryonic knockdown and overexpression of candidate dyslexia susceptibility gene homolog Dcdc2 in the rat. *Neuroscience* 152:723–733.

Burkhardt, J, Kirsten, H, Holland, H, Krupp, W, Ligges, C, Quente, E, Boltze, J, Ahnert, P, & Wilcke, A (2012). Association of rs2069459 in the CDK5 gene with dyslexia in a German cohort. *Psychiatr Genet* 22:307–8.

Bustin, SA (2014). The reproducibility of biomedical research: Sleepers awake! *Biomol Detect Quantif* 2:35–42.

Caffrey, DR, Zhao, J, Song, Z, Schaffer, ME, Haney, SA, Subramanian, RR, Seymour, AB, & Hughes, JD (2011). siRNA Off-Target Effects Can Be Reduced at Concentrations That Match Their Individual Potency. *PLoS One* 6. Ed. by T Preiss:e21503.

Cai, H, Reinisch, K, & Ferro-Novick, S (2007). Coats, tethers, Rabs, and SNAREs work together to mediate the intracellular destination of a transport vesicle. *Dev Cell* 12:671–82.

Cantwell, DP & Baker, L (1987). The prevalence of anxiety in children with communication disorders. *J Anxiety Disord* 1:239–248.

Cao, C, Rioult-Pedotti, MS, Migani, P, Yu, CJ, Tiwari, R, Parang, K, et al. (2013). Impairment of TrkB-PSD-95 signaling in Angelman syndrome. *PLoS Biol* 11. Ed. by M Dalva:e1001478.

Cardon, LR, Smith, SD, Fulker, DW, Kimberling, WJ, Pennington, BF, & DeFries, JC (1994). Quantitative trait locus for reading disability on chromosome 6. *Science* 266:276–9.

Cardon, L, Smith, S, Fulker, D, Kimberling, W, Pennington, B, & DeFries, J (1995). Quantitative trait locus for reading disability: correction. *Science* 268.

Carreiras, M, Armstrong, BC, Perea, M, & Frost, R (2014). The what, when, where, and how of visual word recognition. *Trends Cogn Sci* 18:90–8.

Carrion-Castillo, A, van Bergen, E, Vino, A, van Zuijen, T, de Jong, PF, Francks, C, & Fisher, SE (2016). Evaluation of results from genome-wide studies of language and reading in a novel independent dataset. *Genes, Brain Behav* 15:531–541.

Carrion-Castillo, A, Franke, B, Fisher, SE, & Other (2013). Molecular genetics of dyslexia: an overview. *Dyslexia* 19:214–240.

Carrion-Castillo, A, Maassen, B, Franke, B, Heister, A, Naber, M, van der Leij, A, Francks, C, & Fisher, SE (2017). Association analysis of dyslexia candidate genes in a Dutch longitudinal sample. *Eur J Hum Genet*.

Castles, A & Coltheart, M (1993). Varieties of developmental dyslexia. *Cognition* 47:149–80.

Caviness, VS & Sidman, RL (1973). Time of origin or corresponding cell classes in the cerebral cortex of normal and reeler mutant mice: an autoradiographic analysis. *J Comp Neurol* 148:141–51.

Centanni, TM, Booker, AB, Sloan, AM, Chen, F, Maher, BJ, Carraway, RS, Khodaparast, N, Rennaker, R, LoTurco, JJ, & Kilgard, MP (2014a). Knockdown of the dyslexia-associated gene Kiaa0319 impairs temporal responses to speech stimuli in rat primary auditory cortex. *Cereb Cortex* 24:1753–66.

Centanni, TM, Chen, F, Booker, AM, Engineer, CT, Sloan, AM, Rennaker, RL, LoTurco, JJ, & Kilgard, MP (2014b). Speech sound processing deficits and training-induced neural plasticity in rats with dyslexia gene knockdown. *PLoS One* 9:e98439.

Centanni, TM, Booker, AB, Chen, F, Sloan, AM, Carraway, RS, Rennaker, RL, LoTurco, JJ, & Kilgard, MP (2016). Knockdown of Dyslexia-Gene Dcdc2 Interferes with Speech Sound Discrimination in Continuous Streams. *J Neurosci* 36:4895–4906.

Chaineau, M, Danglot, L, Proux-Gillardeaux, V, & Galli, T (2008). Role of HRB in clathrin-dependent endocytosis. *J Biol Chem* 283:34365–73.

Chan, DW, Ho, CS, Tsang, S, Lee, S, & Chung, KKH (2007). Prevalence, gender ratio and gender differences in reading-related cognitive abilities among Chinese children with dyslexia in Hong Kong. en. *Educ Stud* 33:249–265.

Chandrasekaran, B, Hornickel, J, Skoe, E, Nicol, T, & Kraus, N (2009). Context-dependent encoding in the human auditory brainstem relates to hearing speech in noise: implications for developmental dyslexia. *Neuron* 64:311–9.

Chang, BS, Katzir, T, Liu, T, Corriveau, K, Barzillai, M, Apse, Ka, Bodell, a, Hackney, D, Alsop, D, Wong, ST, Wong, S, & Walsh, Ca (2007). A structural basis for reading fluency: white matter defects in a genetic brain malformation. *Neurology* 69:2146–54.

Chang, BS, Ly, J, Appignani, B, Bodell, A, Apse, KA, Ravenscroft, RS, Sheen, VL, Doherty, MJ, Hackney, DB, O'Connor, M, Galaburda, AM, & Walsh, CA (2005). Reading impairment in the neuronal migration disorder of periventricular nodular heterotopia. *Neurology* 64:799–803.

Chapman, NH, Igo, RP, Thomson, JB, Matsushita, M, Brkanac, Z, Holzman, T, Berninger, VW, Wijsman, EM, & Raskind, WH (2004). Linkage analyses of four regions previously implicated in dyslexia: Confirmation of a locus on chromosome 15q. *Am J Med Genet* 131B:67–75.

Chen, WH, Zhao, XM, van Noort, V, & Bork, P (2013). Human monogenic disease genes have frequently functionally redundant paralogs. *PLoS Comput Biol* 9:e1003073.

Chen, Y & Ghosh, A (2005). Regulation of dendritic development by neuronal activity. *J Neurobiol* 64:4–10.

Chen, Y, Zhao, H, Zhang, Yx, & Zuo, Px (2017). DCDC2 gene polymorphisms are associated with developmental dyslexia in Chinese Uyghur children. *Neural Regen Res* 12:259.

Cheung, AFP, Kondo, S, Abdel-Mannan, O, Chodroff, RA, Sirey, TM, Bluy, LE, Webber, N, DeProto, J, Karlen, SJ, Krubitzer, L, Stolp, HB, Saunders, NR, & Molnár, Z (2010). The subventricular zone is the developmental milestone of a

6-layered neocortex: comparisons in metatherian and eutherian mammals. *Cereb Cortex* 20:1071–81.

Choudhury, N & Other (2007). Infant information processing and family history of specific language impairment: converging evidence for RAP deficits from two paradigms. *Dev Sci* 10:213–36.

Christiansen, MH & Chater, N (2008). Language as shaped by the brain. *Behav Brain Sci* 31:489–508.

Christopherson, KS, Ullian, EM, Stokes, CC, Mullowney, CE, Hell, JW, Agah, A, et al. (2005). Thrombospondins Are Astrocyte-Secreted Proteins that Promote CNS Synaptogenesis. *Cell* 120:421–433.

Churchward, MA, Rogasevskaia, T, Höfgen, J, Bau, J, & Coorssen, JR (2005). Cholesterol facilitates the native mechanism of Ca2+-triggered membrane fusion. *J Cell Sci* 118:4833–48.

Clark, MG, Rosen, GD, Tallal, P, & Fitch, RH (2000). Impaired processing of complex auditory stimuli in rats with induced cerebrocortical microgyria: An animal model of developmental language disabilities. *J Cogn Neurosci* 12:828–39.

Cohen, L, Lehéricy, S, Chochon, F, Lemer, C, Rivaud, S, & Dehaene, S (2002). Language-specific tuning of visual cortex? Functional properties of the Visual Word Form Area. *Brain* 125:1054–69.

Cohen, M, Campbell, R, & Yaghmai, F (1989). Neuropathological abnormalities in developmental dysphasia. *Ann Neurol* 25:567–70.

Coltheart, M (2006). The genetics of learning to read. *J Res Read* 29:124–132.

Coltheart, M, Rastle, K, Perry, C, Langdon, R, & Ziegler, J (2001). DRC: A dual route cascaded model of visual word recognition and reading aloud. English. *Psychol Rev* 108:204–256.

Cooke, HJ & Saunders, PTK (2002). Mouse models of male infertility. *Nat Rev Genet* 3:790–801.

Cope, NA, Hill, G, van den Bree, M, Harold, D, Moskvina, V, Green, EK, Owen, MJ, Williams, J, & O'Donovan, MC (2005a). No support for association between Dyslexia Susceptibility 1 Candidate 1 and developmental dyslexia. *Mol Psychiatry* 10:237–238.

Cope, N, Eicher, JD, Meng, H, Gibson, CJ, Hager, K, Lacadie, C, Fulbright, RK, Constable, RT, Page, GP, & Gruen, JR (2012). Variants in the DYX2 locus are associated with altered brain activation in reading-related brain regions in subjects with reading disability. *Neuroimage* 63:148–56.

Cope, N, Harold, D, Hill, G, Moskvina, V, Stevenson, J, Holmans, P, Owen, MJ, O'Donovan, MC, & Williams, J (2005b). Strong evidence that KIAA0319 on chromosome 6p is a susceptibility gene for developmental dyslexia. *Am J Hum Genet* 76:581–591.

Corbo, JC, Deuel, Ta, Long, JM, LaPorte, P, Tsai, E, Wynshaw-Boris, A, & Walsh, Ca (2002). Doublecortin is required in mice for lamination of the hippocampus but not the neocortex. *J Neurosci* 22:7548–7557.

Cosker, KE, Courchesne, SL, & Segal, RA (2008). Action in the axon: generation and transport of signaling endosomes. *Curr Opin Neurobiol* 18:270–5.

Couto, JM, Gomez, L, Wigg, K, Cate-Carter, T, Archibald, J, Anderson, B, Tannock, R, Kerr, EN, Lovett, MW, Humphries, T, & Barr, CL (2008). The KIAA0319-like

(KIAA0319L) gene on chromosome 1p34 as a candidate for reading disabilities. *J Neurogenet* 22:295–313.

Couto, JM, Gomez, L, Wigg, K, Ickowicz, A, Pathare, T, Malone, M, Kennedy, JL, Schachar, R, & Barr, CL (2009). Association of attention-deficit/hyperactivity disorder with a candidate region for reading disabilities on chromosome 6p. *Biol Psychiatry* 66:368–75.

Couto, JM, Livne-Bar, I, Huang, K, Xu, Z, Cate-Carter, T, Feng, Y, Wigg, K, Humphries, T, Tannock, R, Kerr, EN, Lovett, MW, Bremner, R, & Barr, CL (2010). Association of reading disabilities with regions marked by acetylated H3 histones in KIAA0319. *Am J Med Genet B Neuropsychiatr Genet* 153B:447–62.

Coutton, C, Arnoult, C, & Ray, PF (2015a). Comprehensive investigation in patients affected by globozoospermia. *Andrology* 3:1183.

Coutton, C, Abada, F, Karaouzene, T, Sanlaville, D, Satre, V, Lunardi, J, Jouk, PS, Arnoult, C, Thierry-Mieg, N, & Ray, PF (2013). Fine characterisation of a recombination hotspot at the DPY19L2 locus and resolution of the paradoxical excess of duplications over deletions in the general population. *PLoS Genet* 9:e1003363.

Coutton, C, Escoffier, J, Martinez, G, Arnoult, C, & Ray, PF (2015b). Teratozoospermia: spotlight on the main genetic actors in the human. *Hum Reprod Update* 21:455–85.

Coutton, C, Zouari, R, Abada, F, Ben Khelifa, M, Merdassi, G, Triki, C, et al. (2012). MLPA and sequence analysis of DPY19L2 reveals point mutations causing globozoospermia. *Hum Reprod* 27:2549–58.

Cradick, TJ, Fine, EJ, Antico, CJ, & Bao, G (2013). CRISPR/Cas9 systems targeting β-globin and CCR5 genes have substantial off-target activity. *Nucleic Acids Res* 41:9584–9592.

Currier, TA, Etchegaray, MA, Haight, JL, Galaburda, AM, & Rosen, GD (2011). The effects of embryonic knockdown of the candidate dyslexia susceptibility gene homologue Dyx1c1 on the distribution of GABAergic neurons in the cerebral cortex. *Neuroscience* 172:535–46.

Dahdouh, F, Anthoni, H, Tapia-Páez, I, Peyrard-Janvid, M, Schulte-Körne, G, Warnke, A, Remschmidt, H, Ziegler, A, Kere, J, Müller-Myhsok, B, Nöthen, MM, Schumacher, J, & Zucchelli, M (2009). Further evidence for DYX1C1 as a susceptibility factor for dyslexia. *Psychiatr Genet* 19:59–63.

Dalva, MB, McClelland, AC, & Kayser, MS (2007). Cell adhesion molecules: signalling functions at the synapse. *Nat Rev Neurosci* 8:206–220.

Dam, AHDM, Feenstra, I, Westphal, JR, Ramos, L, van Golde, RJT, & Kremer, JAM (2007a). Globozoospermia revisited. *Hum Reprod Update* 13:63–75.

Dam, AHDM, Koscinski, I, Kremer, JAM, Moutou, C, Jaeger, AS, Oudakker, AR, Tournaye, H, Charlet, N, Lagier-Tourenne, C, van Bokhoven, H, & Viville, S (2007b). Homozygous mutation in SPATA16 is associated with male infertility in human globozoospermia. *Am J Hum Genet* 81:813–820.

Darki, F, Peyrard-Janvid, M, Matsson, H, Kere, J, & Klingberg, T (2012). Three dyslexia susceptibility genes, DYX1C1, DCDC2, and KIAA0319, affect temporo-parietal white matter structure. *Biol Psychiatry* 72:671–6.

Davis, OSP, Band, G, Pirinen, M, Haworth, CMA, Meaburn, EL, Kovas, Y, et al. (2014). The correlation between reading and mathematics ability at age twelve has a substantial genetic component. *Nat Commun* 5:4204.

De Boer, B (2016). Evolution of speech and evolution of language. *Psychon Bull {&} Rev*, 1–5.

De Boer, P, de Vries, M, & Ramos, L (2014). A mutation study of sperm head shape and motility in the mouse: lessons for the clinic. *Andrology*, 1–29.

De Groot, BJA, van den Bos, KP, van der Meulen, BF, & Minnaert, AEMG (2015). Rapid Naming and Phonemic Awareness in Children with Reading Disabilities and/or Specific Language Impairment: Differentiating Processes? *J Speech Lang Hear Res*.

De Kovel, CGF, Hol, FA, Heister, JGAM, Willemen, JJHT, Sandkuijl, LA, Franke, B, & Padberg, GW (2004). Genomewide scan identifies susceptibility locus for dyslexia on Xq27 in an extended Dutch family. *J Med Genet* 41:652–657.

De Kovel, CGF, Franke, B, Hol, FA, Lebrec, JJP, Maassen, B, Brunner, H, Padberg, GW, Platko, J, & Pauls, D (2008). Confirmation of dyslexia susceptibility loci on chromosomes 1p and 2p, but not 6p in a Dutch sib-pair collection. *Am J Med Genet B Neuropsychiatr Genet* 147:294–300.

Decaen, PG, Delling, M, Vien, TN, & Clapham, DE (2013). Direct recording and molecular identification of the calcium channel of primary cilia. *Nature* 504:315–318.

Dediu, D & Levinson, SC (2013). On the antiquity of language: the reinterpretation of Neandertal linguistic capacities and its consequences. *Front Psychol* 4:397.

Deffenbacher, K, Kenyon, J, Hoover, D, Olson, R, Pennington, B, DeFries, J, & Smith, S (2004). Refinement of the 6p21.3 quantitative trait locus influencing dyslexia: linkage and association analyses. *Hum Genet* 115:128–38.

DeFries, JC & Alarcón, M (1996). Genetics of specific reading disability. *Ment Retard Dev Disabil Res Rev* 2:39–47.

DeFries, JC, Fulker, DW, & LaBuda, MC (1987). Evidence for a genetic aetiology in reading disability of twins. *Nature* 329:537–9.

DeFries, JC, Singer, SM, Foch, TT, & Lewitter, FI (1978). Familial nature of reading disability. *Br J Psychiatry* 132:361–367.

Dehaene, S (2009). *Reading in the Brain*. New York: Penguin.

Dehaene, S (2005). *From monkey brain to human brain : a Fyssen Foundation symposium*. St. Germain-en-Laye, France: MIT Press. 400.

— (2010). *Reading in the brain : the new science of how we read*. Penguin Books. 388.

Dehaene, S, Cohen, L, Sigman, M, & Vinckier, F (2005). The neural code for written words: a proposal. *Trends Cogn Sci* 9:335–41.

Del Río, JA, Martínez, A, Auladell, C, & Soriano, E (2000). Developmental history of the subplate and developing white matter in the murine neocortex. Neuronal organization and relationship with the main afferent systems at embryonic and perinatal stages. *Cereb Cortex* 10:784–801.

Delevoye, C, Hurbain, I, Tenza, D, Sibarita, JB, Uzan-Gafsou, S, Ohno, H, Geerts, WJ, Verkleij, AJ, Salamero, J, Marks, MS, & Raposo, G (2009). AP-1 and KIF13A coordinate endosomal sorting and positioning during melanosome biogenesis. *J Cell Biol* 187:247–264.

Dennis, MY, Paracchini, S, Scerri, TS, Prokunina-Olsson, L, Knight, JC, Wade-Martins, R, Coggill, P, Beck, S, Green, ED, & Monaco, AP (2009). A common variant associated with dyslexia reduces expression of the KIAA0319 gene. *PLoS Genet* 5:e1000436.

Deretic, D & Wang, J (2012). Molecular assemblies that control rhodopsin transport to the cilia. *Vision Res* 75:5–10.

Deuel, TAS, Liu, JS, Corbo, JC, Yoo, SY, Rorke-Adams, LB, & Walsh, CA (2006). Genetic interactions between doublecortin and doublecortin-like kinase in neuronal migration and axon outgrowth. *Neuron* 49:41–53.

Diamond, J (1997). *Guns, germs, and steel*. London: New York: W. W. Norton.

Díaz, B, Hintz, F, Kiebel, SJ, & von Kriegstein, K (2012). Dysfunction of the auditory thalamus in developmental dyslexia. *Proc Natl Acad Sci* 109:13841–6.

Dickerson, JE & Robertson, DL (2012). On the origins of Mendelian disease genes in man: the impact of gene duplication. *Mol Biol Evol* 29:61–9.

Diez-Roux, G, Banfi, S, Sultan, M, Geffers, L, Anand, S, Rozado, D, et al. (2011). A high-resolution anatomical atlas of the transcriptome in the mouse embryo. *PLoS Biol* 9:e1000582.

Don, M, Ponton, CW, Eggermont, JJ, & Masuda, A (1994). Auditory brainstem response (ABR) peak amplitude variability reflects individual differences in cochlear response times. *J Acoust Soc Am* 96:3476–91.

Doran, J, Walters, C, Kyle, V, Wooding, P, Hammett-Burke, R, & Colledge, WH (2016). Mfsd14a (Hiat1) gene disruption causes globozoospermia and infertility in male mice. *Reproduction*.

Doria, M, Salcini, AE, Colombo, E, Parslow, TG, Pelicci, PG, & Di Fiore, PP (1999). The eps15 homology (EH) domain-based interaction between eps15 and hrb connects the molecular machinery of endocytosis to that of nucleocytosolic transport. *J Cell Biol* 147:1379–84.

Douglas, RJ & Martin, KA (2004). Neuronal circuits of the neocortex. *Annu Rev Neurosci* 27:419–451.

Drake, WE (1968). Clinical and Pathological Findings in a Child with a Developmental Learning Disability. *J Learn Disabil* 1:486–502.

D'Souza, S, Backhouse-Smith, A, Thompson, JMD, Slykerman, R, Marlow, G, Wall, C, Murphy, R, Ferguson, LR, Mitchell, EA, & Waldie, KE (2016). Associations Between the KIAA0319 Dyslexia Susceptibility Gene Variants, Antenatal Maternal Stress, and Reading Ability in a Longitudinal Birth Cohort. *Dyslexia*.

Dunlop, DB (1972). The binocular basis of dyslexic confusion. *Aust Orthopt J* 12:16–20.

Eckert, M (2004). Neuroanatomical markers for dyslexia. *Neurosci.* 10:362–371.

Edelman, GM & Gally, JA (2001). Degeneracy and complexity in biological systems. *Proc Natl Acad Sci* 98:13763–13768.

Eicher, JD, Other, Powers, NR, Miller, LL, Akshoomoff, N, Amaral, DG, et al. (2013). Genome-wide association study of shared components of reading disability and language impairment. *Genes. Brain. Behav.* 12:792–801.

Eicher, JD & Gruen, JR (2014). Language Impairment and Dyslexia Genes Influence Language Skills in Children With Autism Spectrum Disorders. *Autism Res*, 1–6.

Eicher, JD, Montgomery, AM, Akshoomoff, N, Amaral, DG, Bloss, CS, Libiger, O, et al. (2016). Dyslexia and language impairment associated genetic markers influence cortical thickness and white matter in typically developing children. *Brain Imaging Behav* 10:272–82.

Eicher, JD, Powers, NR, Miller, LL, Mueller, KL, Mascheretti, S, Marino, C, Willcutt, EG, Defries, JC, Olson, RK, Smith, SD, Pennington, BF, Tomblin, JB,

Ring, SM, & Gruen, JR (2014). Characterization of the DYX2 locus on chromosome 6p22 with reading disability, language impairment, and IQ. *Hum Genet* 133:869–81.

Eicher, JD, Stein, CM, Deng, F, Avrich Ciesla, A, Powers, NR, Boada, R, Smith, SD, Pennington, BF, Iyengar, SK, Lewis, BA, & Gruen, JR (2015). The DYX2 locus and neurochemical signaling genes contribute to speech sound disorder and related neurocognitive domains. *Genes Brain Behav*.

Einarsdottir, E, Svensson, I, Darki, F, Peyrard-Janvid, M, Lindvall, JM, Ameur, A, Jacobsson, C, Klingberg, T, Kere, J, & Matsson, H (2015). Mutation in CEP63 co-segregating with developmental dyslexia in a Swedish family. *Hum Genet* 134:1239–48.

Elbert, A, Lovett, MW, Cate-Carter, T, Pitch, A, Kerr, EN, & Barr, CL (2011). Genetic variation in the KIAA0319 5' region as a possible contributor to dyslexia. *Behav Genet* 41:77–89.

ElInati, E, Fossard, C, Okutman, O, Ghédir, H, Ibala-Romdhane, S, Ray, PF, Saad, A, Hennebicq, S, & Viville, S (2016). A new mutation identified in SPATA16 in two globozoospermic patients. *J Assist Reprod Genet* 33:815–20.

Elinati, E, Kuentz, P, Redin, C, Jaber, S, Vanden Meerschaut, F, Makarian, J, et al. (2012). Globozoospermia is mainly due to DPY19L2 deletion via non-allelic homologous recombination involving two recombination hotspots. *Hum Mol Genet* 21:3695–3702.

Englund, C, Fink, A, Lau, C, Pham, D, Daza, RAM, Bulfone, A, Kowalczyk, T, & Hevner, RF (2005). Pax6, Tbr2, and Tbr1 are expressed sequentially by radial glia, intermediate progenitor cells, and postmitotic neurons in developing neocortex. *J Neurosci* 25:247–251.

Eroglu, Ç, Allen, NJ, Susman, MW, O'Rourke, NA, Park, CY, Özkan, E, et al. (2009). Gabapentin Receptor $\alpha 2\delta$-1 Is a Neuronal Thrombospondin Receptor Responsible for Excitatory CNS Synaptogenesis. *Cell* 139:380–392.

Evans, TM, Flowers, DL, Napoliello, EM, & Eden, GF (2014). Sex-specific gray matter volume differences in females with developmental dyslexia. *Brain Struct Funct* 219:1041–54.

Facoetti, A, Paganoni, P, Turatto, M, Marzola, V, & Mascetti, GG (2000). Visual-spatial attention in developmental dyslexia. *Cortex* 36:109–23.

Fagerheim, T, Raeymaekers, P, & Toenessen, F (2000). A genome wide search for dyslexia loci in a large Norwegian family. *Am J Hum Genet* 67:310.

Fagerheim, T, Toenessen, F, & Lubs, H (2002). Refinement of the dyslexia 3 locus (DYX3) on chromosome 2p15–p16 and mutation screening of candidate genes. *Am J Hum Genet* 71:461.

Fagerheim, T, Raeymaekers, P, Tønnessen, FE, Pedersen, M, Tranebjærg, L, & Lubs, HA (1999). A new gene (DYX3) for dyslexia is located on chromosome 2. *J Med Genet* 36:664–669.

Farrag, AF, El-Behary, AA, & Kandil, MR (1988). Prevalence of specific reading disability in Egypt. *Lancet (London, England)* 2:837–9.

Faux, C, Rakic, S, Andrews, W, & Britto, JM (2012). Neurons on the move: migration and lamination of cortical interneurons. *Neurosignals* 20:168–89.

Fertuzinhos, S, Li, M, Kawasawa, YI, Ivic, V, Franjic, D, Singh, D, Crair, M, & Sestan, N (2014). Laminar and temporal expression dynamics of coding and noncoding RNAs in the mouse neocortex. *Cell Rep* 6:938–50.

Field, LL, Kaplan, BJ, Kloboukova, E, Zoghbi, H, Smith, S, Alexander, A, Andersen, H, & Al., E (1998). Absence of linkage of phonological coding dyslexia to chromosome 6p23-p21.3 in a large family data set. *Am J Hum Genet* 63:1448–56.

Field, LL, Shumansky, K, Ryan, J, Truong, D, Swiergala, E, & Kaplan, BJ (2013). Dense-map genome scan for dyslexia supports loci at 4q13, 16p12, 17q22; suggests novel locus at 7q36. *Genes Brain Behav* 12:56–69.

Fietz, SA, Kelava, I, Vogt, J, Wilsch-Bräuninger, M, Stenzel, D, Fish, JL, Corbeil, D, Riehn, A, Distler, W, Nitsch, R, & Huttner, WB (2010). OSVZ progenitors of human and ferret neocortex are epithelial-like and expand by integrin signaling. *Nat Neurosci* 13:690–9.

Fischer, ER, Hansen, BT, Nair, V, Hoyt, FH, & Dorward, DW (2012). Scanning electron microscopy. *Curr Protoc Microbiol* Chapter 2:Unit 2B.2.

Fisher, JH (1905). Case of congenital word-blindness. *Ophthalmic Rev* 24:314.

Fisher, SE, Marlow, AJ, Lamb, J, Maestrini, E, Williams, DF, Richardson, AJ, Weeks, DE, Stein, JF, & Monaco, AP (1999). A quantitative-trait locus on chromosome 6p influences different aspects of developmental dyslexia. *Am J Hum Genet* 64:146–56.

Fisher, SE (2007). Molecular windows into speech and language disorders. *Folia Phoniatr Logop* 59:130–40.

Fisher, SE & DeFries, JC (2002). Developmental dyslexia: genetic dissection of a complex cognitive trait. *Nat Rev Neurosci* 3:767–780.

Fisher, SE, Francks, C, Marlow, AJ, MacPhie, IL, Newbury, DF, Cardon, LR, et al. (2002). Independent genome-wide scans identify a chromosome 18 quantitative-trait locus influencing dyslexia. *Nat Genet* 30:86–91.

Fisher, SE & Marcus, GF (2006). The eloquent ape: genes, brains and the evolution of language. *Nat Rev Genet* 7:9–20.

Fisher, SE & Scharff, C (2009). FOXP2 as a molecular window into speech and language. *Trends Genet* 25:166–177.

Fitch, RH, Tallal, P, Brown, CP, Galaburda, AM, & Rosen, GD (1994). Induced microgyria and auditory temporal processing in rats: a model for language impairment? *Cereb Cortex* 4:260–70.

Fitch, RH, Alexander, ML, & Threlkeld, SW (2013). Early neural disruption and auditory processing outcomes in rodent models: implications for developmental language disability. *Front Syst Neurosci* 7:58.

Fitch, RH, Threlkeld, SW, McClure, MM, & Peiffer, AM (2008). Use of a modified prepulse inhibition paradigm to assess complex auditory discrimination in rodents. *Brain Res Bull* 76:1–7.

Fitch, WT (2010). *The Evolution of Language*. Ed. by M Gazzaniga. 3rd Editio. Cambridge: Cambridge University Press.

Flannery, KA, Liederman, J, Daly, L, & Schultz, J (2000). Male prevalence for reading disability is found in a large sample of black and white children free from ascertainment bias. *J Int Neuropsychol Soc* 6:433–42.

Fliegauf, M, Benzing, T, & Omran, H (2007). When cilia go bad : cilia defects and ciliopathies. *Nat Rev Mol Cell Biol* 8:880–893.

Florio, M & Huttner, WB (2014). Neural progenitors, neurogenesis and the evolution of the neocortex. *Development* 141:2182–94.

Fournier, P & Hébert, S (2013). Gap detection deficits in humans with tinnitus as assessed with the acoustic startle paradigm: Does tinnitus fill in the gap? *Hear Res* 295:16–23.

Franceschini, S, Gori, S, Ruffino, M, Pedrolli, K, & Facoetti, A (2012). A causal link between visual spatial attention and reading acquisition. *Curr Biol* 22:814–9.

Francks, C, Fisher, SE, Olson, RK, Pennington, BF, Smith, SD, DeFries, JC, & Monaco, AP (2002). Fine mapping of the chromosome 2p12-16 dyslexia susceptibility locus: quantitative association analysis and positional candidate genes SEMA4F and OTX1. *Psychiatr Genet* 12:35–41.

Francks, C, Paracchini, S, Other, Smith, SD, Richardson, AJ, Scerri, TS, et al. (2004). A 77-kilobase region of chromosome 6p22.2 is associated with dyslexia in families from the United Kingdom and from the United States. *Am J Hum Genet* 75:1046–1058.

Franco, SJ, Gil-Sanz, C, Martinez-Garay, I, Espinosa, A, Harkins-Perry, SR, Ramos, C, & Müller, U (2012). Fate-restricted neural progenitors in the mammalian cerebral cortex. *Science* 337:746–9.

Franquinho, F, Nogueira-Rodrigues, J, Duarte, JM, Esteves, SS, Carter-Su, C, Monaco, AP, Moln?r, Z, Velayos-Baeza, A, Brites, P, & Sousa, MM (2017). The Dyslexia-susceptibility Protein KIAA0319 Inhibits Axon Growth Through Smad2 Signaling. *Cereb Cortex* 27:1732–1747.

Freedman, LPL, Cockburn, IM, Simcoe, TS, Collins, F, Tabak, L, Begley, C, et al. (2015). The Economics of Reproducibility in Preclinical Research. 13:e1002165.

French, CA, Groszer, M, Preece, C, Coupe, AM, Rajewsky, K, & Fisher, SE (2007). Generation of mice with a conditional Foxp2 null allele. *Genesis* 45:440–6.

Frenkel, M, Sherman, GF, Bashan, KA, Galaburda, AM, LoTurco, JJ, Ca, JJL, & LoTurco, JJ (2000). Neocortical ectopias are associated with attenuated neurophysiological responses to rapidly changing auditory stimuli. *Neuroreport* 11:575–9.

Friederici, AD (2016). Evolution of the neural language network. *Psychon Bull Rev*, 1–7.

Friederici, AD & Gierhan, SME (2013). The language network. *Curr Opin Neurobiol* 23:250–4.

Friedman, JT, Peiffer, AM, Clark, MG, Benasich, Aa, & Fitch, RH (2004). Age and experience-related improvements in gap detection in the rat. *Brain Res Dev Brain Res* 152:83–91.

Froster, U, Schulte-Körne, G, Hebebrand, J, & Remschmidt, H (1993). Cosegregation of balanced translocation (1;2) with retarded speech development and dyslexia. *Lancet (London, England)* 342:178–9.

Frye, RE, Liederman, J, Malmberg, B, McLean, J, Strickland, D, & Beauchamp, MS (2010). Surface area accounts for the relation of gray matter volume to reading-related skills and history of dyslexia. *Cereb Cortex* 20:2625–35.

Fu, Y, Foden, JA, Khayter, C, Maeder, ML, Reyon, D, Joung, JK, & Sander, JD (2013). High-frequency off-target mutagenesis induced by CRISPR-Cas nucleases in human cells. *Nat Biotechnol* 31:822–6.

Fujihara, Y, Satouh, Y, Inoue, N, Isotani, A, Ikawa, M, & Okabe, M (2012). SPACA1-deficient male mice are infertile with abnormally shaped sperm heads reminiscent of globozoospermia. *Development* 139:3583–9.

Fulker, DW, Cardon, LR, Defries, JC, Kimberling, WJ, Pennington, BF, & Smith, SD (1991). Multiple regression analysis of sib-pair data on reading to detect quantitative trait loci. *Read Writ* 3:299–313.

Funaki, T, Kon, S, Tanabe, K, Natsume, W, Sato, S, Shimizu, T, et al. (2013). The Arf GAP SMAP2 is necessary for organized vesicle budding from the trans-Golgi network and subsequent acrosome formation in spermiogenesis. *Mol Biol Cell* 24:2633–44.

Gabel, LA, Gibson, CJ, Gruen, JR, & LoTurco, JJ (2010). Progress towards a cellular neurobiology of reading disability. *Neurobiol Dis* 38:173–80.

Galaburda, AM (1989). Ordinary and extraordinary brain development: Anatomical variation in developmental dyslexia. *Ann Dyslexia* 39:65–80.

Galaburda, aM & Kemper, TL (1979). Cytoarchitectonic abnormalities in developmental dyslexia: a case study. *Ann Neurol* 6:94–100.

Galaburda, AM, Menard, MT, & Rosen, GD (1994). Evidence for aberrant auditory anatomy in developmental dyslexia. *Proc Natl Acad Sci* 91:8010–8013.

Galaburda, A & Livingstone, M (1993). Evidence for a magnocellular defect in developmental dyslexia. *Ann N Y Acad Sci* 682. Ed. by P Tallal, AM Galaburda, RR Llins, & C Von Euler:70–82.

Galaburda, AM, LoTurco, J, Ramus, F, Fitch, RH, & Rosen, GD (2006). From genes to behavior in developmental dyslexia. *Nat Neurosci* 9:1213–7.

Galaburda, AM, Sherman, GF, Rosen, GD, Aboitiz, F, & Geschwind, N (1985). Developmental Dyslexia : Four Consecutive Patients with Cortical Anomahes.

García-Moreno, F, López-Mascaraque, L, & de Carlos, JA (2008a). Early telencephalic migration topographically converging in the olfactory cortex. *Cereb Cortex* 18:1239–52.

— (2008b). Early telencephalic migration topographically converging in the olfactory cortex. *Cereb Cortex* 18:1239–52.

García-Moreno, F & Molnár, Z (2015). Subset of early radial glial progenitors that contribute to the development of callosal neurons is absent from avian brain. *Proc Natl Acad Sci* 112:E5058–E5067.

García-Moreno, F, Vasistha, NA, Trevia, N, Bourne, JA, & Molnár, Z (2012). Compartmentalization of cerebral cortical germinal zones in a lissencephalic primate and gyrencephalic rodent. *Cereb Cortex* 22:482–92.

Gayán, J, Smith, SD, Cherny, SS, Cardon, LR, Fulker, DW, Brower, AM, Olson, RK, Pennington, BF, & DeFries, JC (1999). Quantitative-trait locus for specific language and reading deficits on chromosome 6p. *Am J Hum Genet* 64:157–64.

Geiger, G, Lettvin, JY, & Fahle, M (1994). Dyslexic children learn a new visual strategy for reading: a controlled experiment. *Vision Res* 34:1223–1233.

Georgiou, GK, Protopapas, A, Papadopoulos, TC, Skaloumbakas, C, & Parrila, R (2010). Auditory temporal processing and dyslexia in an orthographically consistent language. *Cortex* 46:1330–44.

Germanò, E, Gagliano, A, & Curatolo, P (2010). Comorbidity of ADHD and dyslexia. *Dev Neuropsychol* 35:475–93.

Gerrow, K & El-Husseini, A (2006). Cell adhesion molecules at the synapse. *Front Biosci* 11:2400–19.

Geschwind, N & Galaburda, AM (1985). Cerebral lateralization. Biological mechanisms, associations, and pathology: I. A hypothesis and a program for research. *Arch Neurol* 42:428–59.

Geschwind, N & Levitsky, W (1968). Human brain: left-right asymmetries in temporal speech region. *Science* 161:186–7.

Ghédir, H, Ibala-Romdhane, S, Okutman, O, Viot, G, Saad, A, & Viville, S (2016). Identification of a new DPY19L2 mutation and a better definition of DPY19L2 deletion breakpoints leading to globozoospermia. *Mol Hum Reprod* 22:35–45.

Gialluisi, A, Newbury, DF, Wilcutt, EG, Olson, RK, DeFries, JC, Brandler, WM, et al. (2014). Genome-wide screening for DNA variants associated with reading and language traits. *Genes Brain Behav* 13:686–701.

Gialluisi, A, Visconti, A, Willcutt, EG, Smith, SD, Pennington, BF, Falchi, M, DeFries, JC, Olson, RK, Francks, C, & Fisher, SE (2016). Investigating the effects of copy number variants on reading and language performance. *J Neurodev Disord* 8:17.

Gilbert, CD & Kelly, JP (1975). The projections of cells in different layers of the cat's visual cortex. *J Comp Neurol* 163:81–105.

Gilbert, SF (2010). *Developmental biology*. Sinauer Associates.

Gilger, JW, Borecki, IB, DeFries, JC, & Pennington, BF (1994). Commingling and segregation analysis of reading performance in families of normal reading probands. *Behav Genet* 24:345–55.

Gilger, JW & Kaplan, BJ (2001). Atypical brain development: a conceptual framework for understanding developmental learning disabilities. *Dev Neuropsychol* 20:465–81.

Gilger, JW (1992). Using self-report and parental- report survey data to assess past and present academic achievement of adults and children. *J Appl Dev Psychol* 13:235–256.

Giraud, AL & Poeppel, D (2012). Cortical oscillations and speech processing: emerging computational principles and operations. *Nat Neurosci* 15:511–517.

Giraud, AL & Ramus, F (2013). Neurogenetics and auditory processing in developmental dyslexia. *Curr. Opin. Neurobiol.* 23:37–42.

Girirajan, S, Brkanac, Z, Coe, BP, Baker, C, Vives, L, Vu, TH, et al. (2011). Relative Burden of Large CNVs on a Range of Neurodevelopmental Phenotypes. *PLoS Genet* 7. Ed. by HT Orr:e1002334.

Girirajan, S, Rosenfeld, JA, Cooper, GM, Antonacci, F, Siswara, P, Itsara, A, et al. (2010). A recurrent 16p12.1 microdeletion supports a two-hit model for severe developmental delay. *Nat Genet* 42:203–9.

Gleeson, JG & Walsh, Ca (2000). Neuronal migration disorders: from genetic diseases to developmental mechanisms. *Trends Neurosci.* 23:352–359.

Gonda, Y, Andrews, WD, Tabata, H, Namba, T, Parnavelas, JG, Nakajima, K, Kohsaka, S, Hanashima, C, & Uchino, S (2013). Robo1 Regulates the Migration and Laminar Distribution of Upper-Layer Pyramidal Neurons of the Cerebral Cortex. *Cereb Cortex* 23:1495–1508.

Gori, S, Facoetti, A, L., B, H., B, H., B, T., CS, et al. (2015). How the visual aspects can be crucial in reading acquisition? The intriguing case of crowding and developmental dyslexia. *J Vis* 15:8–8.

Goswami, U (2000). Phonological representations, reading development and dyslexia: towards a cross-linguistic theoretical framework. *Dyslexia* 6:133–151.

— (2014). Sensory theories of developmental dyslexia: three challenges for research. *Nat Rev Neurosci* 8.

Gould, SJ (1991). Exaptation: A Crucial Tool for an Evolutionary Psychology. *J Soc Issues* 47:43–65.

Graham, L & Orenstein, JM (2007). Processing tissue and cells for transmission electron microscopy in diagnostic pathology and research. *Nat Protoc* 2:2439–2450.

Graham, SA & Fisher, SE (2015). Understanding Language from a Genomic Perspective. *Annu Rev Genet* 49:131–160.

Granseth, B, Odermatt, B, Royle, SJ, & Lagnado, L (2006). Clathrin-Mediated Endocytosis Is the Dominant Mechanism of Vesicle Retrieval at Hippocampal Synapses. *Neuron* 51:773–786.

Grati, M, Chakchouk, I, Ma, Q, Bensaid, M, Desmidt, A, Turki, N, Yan, D, Baanannou, A, Mittal, R, Driss, N, Blanton, S, Farooq, A, Lu, Z, Liu, XZ, & Masmoudi, S (2015). A missense mutation in DCDC2 causes human recessive deafness DFNB66, likely by interfering with sensory hair cell and supporting cell cilia length regulation. *Hum Mol Genet* 24:2482–91.

Gratten, J, Wray, NR, Keller, MC, & Visscher, PM (2014). Large-scale genomics unveils the genetic architecture of psychiatric disorders. *Nat Neurosci* 17:782–90.

Greenham, SL (1999). Learning Disabilities and Psychosocial Adjustment: A Critical Review. *Child Neuropsychol (Neuropsychology, Dev Cogn Sect C)* 5:171–196.

Greig, LC, Woodworth, MB, Galazo, MJ, Padmanabhan, H, & Macklis, JD (2013). Molecular logic of neocortical projection neuron specification, development and diversity. *Nat Rev Neurosci* 14:755–69.

Griffiths, G, Warren, G, Stuhlfauth, I, & Jockusch, BM (1981). The role of clathrin-coated vesicles in acrosome formation. *Eur J Cell Biol* 26:52–60.

Grigorenko, EL, Wood, FB, Meyer, MS, Hart, LA, Speed, WC, Shuster, A, & Pauls, DL (1997). Susceptibility loci for distinct components of developmental dyslexia on chromosomes 6 and 15. *Am J Hum Genet* 60:27–39.

Grigorenko, EL, Wood, FB, Meyer, MS, & Pauls, DL (2000). Chromosome 6p influences on different dyslexia-related cognitive processes: further confirmation. *Am J Hum Genet* 66:715–23.

Grigorenko, EL, Wood, FB, Meyer, MS, Pauls, JE, Hart, LA, & Pauls, DL (2001). Linkage studies suggest a possible locus for developmental dyslexia on chromosome 1p. *Am J Med Genet* 105:120–9.

Grigorenko, EL, Wood, FB, Golovyan, L, Meyer, M, Romano, C, & Pauls, D (2003). Continuing the search for dyslexia genes on 6p. *Am J Med Genet B Neuropsychiatr Genet* 118B:89–98.

Grobler, JA & Hurley, JH (1997). Similarity between C2 domain jaws and immunoglobulin CDRs. *Nat Struct Biol* 4:261–262.

Grootegoed, J, Baarends, WM, Hendriksen, PJ, Hoogerbrugge, JW, Slegtenhorst-Eegdeman, KE, & Themmen, AP (1995). Molecular and cellular events in spermatogenesis. *Hum Reprod* 10:10–14.

Gu, X (2003). Evolution of duplicate genes versus genetic robustness against null mutations. *Trends Genet* 19:354–356.

Guadalupe, T, Zwiers, MP, Wittfeld, K, Teumer, A, Vasquez, AA, Hoogman, M, et al. (2015). Asymmetry within and around the human planum temporale is sexually dimorphic and influenced by genes involved in steroid hormone receptor activity. *Cortex* 62:41–55.

Guerreiro, MM, Hage, SRV, Guimarães, CA, Abramides, DV, Fernandes, W, Pacheco, PS, Piovesana, AMSG, Montenegro, MA, & Cendes, F (2002). Developmental language disorder associated with polymicrogyria. *Neurology* 59:245–50.

Guerrini, R & Dobyns, WB (2014). Malformations of cortical development: clinical features and genetic causes. *Lancet Neurol* 13:710–26.

Guerrini, R & Parrini, E (2010). Neuronal migration disorders. *Neurobiol Dis* 38:154–166.

Guinan, JJ (2006). Olivocochlear Efferents: Anatomy, Physiology, Function, and the Measurement of Efferent Effects in Humans. *Ear Hear* 27:589–607.

Guo, C, Eckler, MJ, McKenna, WL, McKinsey, GL, Rubenstein, JLR, & Chen, B (2013). Fezf2 expression identifies a multipotent progenitor for neocortical projection neurons, astrocytes, and oligodendrocytes. *Neuron* 80:1167–74.

Guo, J & Anton, ES (2014). Decision making during interneuron migration in the developing cerebral cortex. *Trends Cell Biol* 24:342–51.

Gupta, SK, Bhandari, B, Shrestha, A, Biswal, BK, Palaniappan, C, Malhotra, SS, & Gupta, N (2012). Mammalian zona pellucida glycoproteins: structure and function during fertilization. *Cell Tissue Res* 349:665–678.

Guttman, JA, Takai, Y, & Vogl, AW (2004). Evidence that tubulobulbar complexes in the seminiferous epithelium are involved with internalization of adhesion junctions. *Biol Reprod* 71:548–59.

Habib, M (2000). The neurological basis of developmental dyslexia: an overview and working hypothesis. *Brain* 123 Pt 12:2373–2399.

Hage, SRV, Joaquim, RSS, Carvalho, KG, Padovani, CR, & Guerreiro, MM (2005). [Diagnosis of children with specific language impairment using a developmental scale]. *Arq Neuropsiquiatr* 62:649–53.

Hagoort, P (2014). Nodes and networks in the neural architecture for language: Broca's region and beyond. *Curr Opin Neurobiol* 28:136–41.

Hallgren, B (1950). Specific dyslexia (congenital word-blindness); a clinical and genetic study. *Acta Psychiatr Neurol Suppl* 65:1–287.

Hannula-Jouppi, K, Kaminen-Ahola, N, Taipale, M, Eklund, R, Nopola-Hemmi, J, Kääriäinen, H, & Kere, J (2005). The axon guidance receptor gene ROBO1 is a candidate gene for developmental dyslexia. *PLoS Genet* 1:e50.

Hansen, DV, Lui, JH, Parker, PRL, & Kriegstein, AR (2010). Neurogenic radial glia in the outer subventricular zone of human neocortex. *Nature* 464:554–561.

Harbuz, R, Zouari, R, Pierre, V, Ben Khelifa, M, Kharouf, M, Coutton, C, et al. (2011). A recurrent deletion of DPY19L2 causes infertility in man by blocking sperm head elongation and acrosome formation. *Am J Hum Genet* 88:351–61.

Harlaar, N, Meaburn, EL, Hayiou-Thomas, ME, Davis, OSP, Docherty, S, Hanscombe, KB, Haworth, CMA, Price, TS, Trzaskowski, M, Dale, PS, & Plomin, R (2014). Genome-wide association study of receptive language ability of 12-year-olds. *J Speech Lang Hear Res* 57:96–105.

Harold, D, Other, Paracchini, S, Scerri, T, Dennis, M, Cope, N, et al. (2006). Further evidence that the KIAA0319 gene confers susceptibility to developmental dyslexia. *Mol Psychiatry* 11:1085–1091.

Harrison, C (2013). RNA interference: Reducing off-target effects of shRNA. *Nat Rev Drug Discov* 12:24–24.

Hartree, EF (1975). The acrosome-lysosome relationship. *J Reprod Fertil* 44:125–6.

Haubensak, W, Attardo, A, Denk, W, & Huttner, WB (2004). Neurons arise in the basal neuroepithelium of the early mammalian telencephalon: a major site of neurogenesis. *Proc Natl Acad Sci* 101:3196–201.

Hauser, MD, Chomsky, N, Fitch, TW, & Fitch, WT (2002). The faculty of language: What is it, who has it, and how did it evolve? *Science* 298:1569–1579.

Hawrylycz, MJ, Lein, ES, Guillozet-Bongaarts, AL, Shen, EH, Ng, L, Miller, JA, et al. (2012). An anatomically comprehensive atlas of the adult human brain transcriptome. *Nature* 489:391–9.

Hayashi, S, Lewis, P, Pevny, L, & McMahon, AP (2002). Efficient gene modulation in mouse epiblast using a Sox2Cre transgenic mouse strain. *Gene Expr Patterns* 2:93–7.

He, J, Xia, M, Tsang, WH, Chow, KL, & Xia, J (2015). ICA1L forms BAR-domain complexes with PICK1 and is crucial for acrosome formation in spermiogenesis. *J Cell Sci* 128:3822–36.

Heim, S, Tschierse, J, Amunts, K, Wilms, M, Vossel, S, Willmes, K, Grabowska, A, & Huber, W (2008). Cognitive subtypes of dyslexia. *Acta Neurobiol Exp (Wars)* 68:73–82.

Hendry, SH, Jones, EG, Emson, PC, Lawson, DE, Heizmann, CW, & Streit, P (1989). Two classes of cortical GABA neurons defined by differential calcium binding protein immunoreactivities. *Exp brain Res* 76:467–72.

Henry, KR (1979). Auditory brainstem volume-conducted responses: origins in the laboratory mouse. *J Am Aud Soc* 4:173–8.

Heuser, JE & Reese, TS (1973). Evidence for recycling of synaptic vesicle membrane during transmitter release at the frog neuromuscular junction. *J Cell Biol* 57:315–44.

Hickok, G & Poeppel, D (2007). The cortical organization of speech processing. *Nat Rev Neurosci* 8:393–402.

Higgins, N, Escabí, M, Rosen, G, Galaburda, A, & Read, H (2008). Spectral processing deficits in belt auditory cortex following early postnatal lesions of somatosensory cortex. *Neuroscience* 153:535–549.

Hinshelwood, J (1911). Two Cases of Hereditary Congenital Word-Blindness. *Br Med J* 1:608–9.

Hirst, J, Borner, GHH, Antrobus, R, Peden, Aa, Hodson, Na, Sahlender, Da, & Robinson, MS (2012). Distinct and overlapping roles for AP-1 and GGAs revealed by the "knocksideways" system. *Curr Biol* 22:1711–6.

Hoeft, F, Meyler, A, Hernandez, A, Juel, C, Taylor-Hill, H, Martindale, JL, McMillon, G, Kolchugina, G, Black, JM, Faizi, A, Deutsch, GK, Siok, WT, Reiss, AL, Whitfield-Gabrieli, S, & Gabrieli, JDE (2007). Functional and morphometric brain dissociation between dyslexia and reading ability. *Proc Natl Acad Sci* 104:4234–9.

Hoerder-Suabedissen, A & Molnár, Z (2015). Development, evolution and pathology of neocortical subplate neurons. *Nat Rev Neurosci* 16:133–46.

Hofmeister, W, Nilsson, D, Topa, A, Anderlid, BM, Darki, F, Matsson, H, Tapia Páez, I, Klingberg, T, Samuelsson, L, Wirta, V, Vezzi, F, Kere, J, Nordenskjöld, M, Syk Lundberg, E, & Lindstrand, A (2015). CTNND2-a candidate gene for reading problems and mild intellectual disability. *J Med Genet* 52:111–22.

Holt, R, Sykes, NH, Conceição, IC, Cazier, JB, Anney, RJL, Oliveira, G, Gallagher, L, Vicente, A, Monaco, AP, & Pagnamenta, AT (2012). CNVs leading to fusion transcripts in individuals with autism spectrum disorder. *Eur J Hum Genet* 20:1141–7.

Hong, SJ, Kim, H, Schrader, D, Bernasconi, N, Bernhardt, BC, & Bernasconi, A (2014). Automated detection of cortical dysplasia type II in MRI-negative epilepsy. *Neurology* 83:48–55.

Hornickel, J & Kraus, N (2013). Unstable representation of sound: a biological marker of dyslexia. *J Neurosci* 33:3500–4.

Hsiung, GYR, Kaplan, BJ, Petryshen, TL, Lu, S, & Field, LL (2004). A dyslexia susceptibility locus (DYX7) linked to dopamine D4 receptor (DRD4) region on chromosome 11p15.5. *Am J Med Genet B Neuropsychiatr Genet* 125B:112–9.

Hsu, PD, Scott, DA, Weinstein, JA, Ran, FA, Konermann, S, Agarwala, V, Li, Y, Fine, EJ, Wu, X, Shalem, O, Cradick, TJ, Marraffini, LA, Bao, G, & Zhang, F (2013). DNA targeting specificity of RNA-guided Cas9 nucleases. *Nat Biotechnol* 31:827–32.

Huc-Chabrolle, M, Charon, C, Guilmatre, A, Vourc'h, P, Tripi, G, Barthez, MA, et al. (2013). Xq27 FRAXA locus is a strong candidate for dyslexia: evidence from a genome-wide scan in French families. *Behav Genet* 43:132–40.

Hughes, J, Ward, CJ, Peral, B, Aspinwall, R, Clark, K, San Millán, JL, Gamble, V, & Harris, PC (1995). The polycystic kidney disease 1 (PKD1) gene encodes a novel protein with multiple cell recognition domains. eng. *Nat Genet* 10:151–60.

Humphreys, P, Kaufmann, WE, & Galaburda, aM (1990). Developmental dyslexia in women: neuropathological findings in three patients. *Ann Neurol* 28:727–738.

Hunter, KP & Willott, JF (1987). Aging and the auditory brainstem response in mice with severe or minimal presbycusis. *Hear Res* 30:207–218.

Ibraghimov-Beskrovnaya, O, Bukanov, NO, Donohue, LC, Dackowski, WR, Klinger, KW, & Landes, GM (2000). Strong homophilic interactions of the Ig-like domains of polycystin-1, the protein product of an autosomal dominant polycystic kidney disease gene, PKD1. *Hum Mol Genet* 9:1641–1649.

Igo, RP, Chapman, NH, Berninger, VW, Matsushita, M, Brkanac, Z, Rothstein, JH, Holzman, T, Nielsen, K, Raskind, WH, & Wijsman, EM (2006). Genomewide scan for real-word reading subphenotypes of dyslexia: Novel chromosome 13 locus and genetic complexity. *Am J Med Genet Part B Neuropsychiatr Genet* 141B:15–27.

Ioannidis, JPA (2005). Why Most Published Research Findings Are False. *PLoS Med* 2:e124.

Ippolito, DM & Eroglu, C (2010). Quantifying synapses: an immunocytochemistry-based assay to quantify synapse number. *J Vis Exp.*

Ison, JR, O'Connor, K, Bowen, GP, & Bocirnea, A (1991). Temporal resolution of gaps in noise by the rat is lost with functional decortication. *Behav Neurosci* 105:33–40.

Ison, JR, Allen, PD, O'Neill, WE, & O'Neill, WE (2007). Age-Related Hearing Loss in C57BL/6J Mice has both Frequency-Specific and Non-Frequency-Specific

Components that Produce a Hyperacusis-Like Exaggeration of the Acoustic Startle Reflex. *J Assoc Res Otolaryngol* 8:539–550.

Ivliev, AE, 't Hoen, PaC, van Roon-Mom, WMC, Peters, DJM, Sergeeva, MG, & Other (2012). Exploring the transcriptome of ciliated cells using in silico dissection of human tissues. *PLoS One* 7:e35618.

Jackson, AL & Linsley, PS (2010). Recognizing and avoiding siRNA off-target effects for target identification and therapeutic application. *Nat Rev Drug Discov* 9:57–67.

Jamadar, S, Powers, NR, Meda, SA, Calhoun, VD, Gelernter, J, Gruen, JR, & Pearlson, GD (2013). Genetic influences of resting state fMRI activity in language-related brain regions in healthy controls and schizophrenia patients: a pilot study. *Brain Imaging Behav* 7:15–27.

Jan, SZ, Hamer, G, Repping, S, de Rooij, DG, van Pelt, AMM, & Vormer, TL (2012). Molecular control of rodent spermatogenesis. *Biochim Biophys Acta* 1822:1838–50.

Jansen, AC, Robitaille, Y, Honavar, M, Mullatti, N, Leventer, RJ, Andermann, E, Andermann, F, & Squier, W (2016). The histopathology of polymicrogyria: a series of 71 brain autopsy studies. *Dev Med Child Neurol* 58:39–48.

Jednoróg, K, Marchewka, A, Altarelli, I, Monzalvo Lopez, AK, van Ermingen-Marbach, M, Grande, M, Grabowska, A, Heim, S, & Ramus, F (2015). How reliable are gray matter disruptions in specific reading disability across multiple countries and languages? insights from a large-scale voxel-based morphometry study. *Hum Brain Mapp* 36:1741–1754.

Jenkins, TG, Aston, KI, Hotaling, JM, Shamsi, MB, Simon, L, & Carrell, DT (2016). Teratozoospermia and asthenozoospermia are associated with specific epigenetic signatures. *Andrology* 4:843–849.

Jin, W, Ge, WP, Xu, J, Cao, M, Peng, L, Yung, W, Liao, D, Duan, S, Zhang, M, & Xia, J (2006). *Lipid binding regulates synaptic targeting of PICK1, AMPA receptor trafficking, and synaptic plasticity.*

Jones, BJ & Roberts, DJ (1968). The quantitative measurement of motor inco-ordination in naive mice using an accelerating rotarod. *J Pharm Pharmacol* 20:302–304.

Jones, EG (1985). The Thalamus. Ed. by EG Jones, 935.

Kaas, JH (2012). Evolution of columns, modules, and domains in the neocortex of primates. *Proc Natl Acad Sci*, 10655–60.

Kabat, J & Król, P (2012). Focal cortical dysplasia - review. *Pol J Radiol* 77:35–43.

Kafri, R, Springer, M, & Pilpel, Y (2009). Genetic redundancy: new tricks for old genes. *Cell* 136:389–392.

Kalebic, N, Taverna, E, Tavano, S, Wong, FK, Suchold, D, Winkler, S, Huttner, WB, & Sarov, M (2016). CRISPR/Cas9-induced disruption of gene expression in mouse embryonic brain and single neural stem cells in vivo. *EMBO Rep* 17:338–48.

Kaminen, N, Hannula-Jouppi, K, Kestilä, M, Lahermo, P, Muller, K, Kaaranen, M, Myllyluoma, B, Voutilainen, A, Lyytinen, H, Nopola-Hemmi, J, & Kere, J (2003). A genome scan for developmental dyslexia confirms linkage to chromosome 2p11 and suggests a new locus on 7q32. *J Med Genet* 40:340–5.

Kamiya, A, Kubo, Ki, Tomoda, T, Takaki, M, Youn, R, Ozeki, Y, Sawamura, N, Park, U, Kudo, C, Okawa, M, Ross, CA, Hatten, ME, Nakajima, K, & Sawa, A (2005). A schizophrenia-associated mutation of DISC1 perturbs cerebral cortex development. *Nat Cell Biol* 7:1167–78.

Kang, C & Drayna, D (2011). Genetics of speech and language disorders. *Annu Rev Genomics Hum Genet* 12:145–164.

Kang-Decker, N, Mantchev, GT, Juneja, SC, McNiven, MA, & van Deursen, JM (2001). Lack of acrosome formation in Hrb-deficient mice. *Science* 294:1531–3.

Kaplan, DE, Gayán, J, Ahn, J, Won, TW, Pauls, D, Olson, RK, DeFries, JC, Wood, F, Pennington, BF, Page, GP, Smith, SD, & Gruen, JR (2002). Evidence for linkage and association with reading disability on 6p21.3-22. *Am J Hum Genet* 70:1287–98.

Karaca, N, Yilmaz, R, Kanten, GE, Kervancioglu, E, Solakoglu, S, & Kervancioglu, ME (2014). First successful pregnancy in a globozoospermic patient having homozygous mutation in SPATA16. *Fertil Steril* 102:103–7.

Katidou, M, Vidaki, M, Strigini, M, & Karagogeos, D (2008). The immunoglobulin superfamily of neuronal cell adhesion molecules: Lessons from animal models and correlation with human disease. *Biotechnol J* 4:416–416.

Katusic, SK, Colligan, RC, Barbaresi, WJ, Schaid, DJ, & Jacobsen, SJ (2001). Incidence of reading disability in a population-based birth cohort, 1976-1982, Rochester, Minn. *Mayo Clin Proc* 76:1081–92.

Kaufmann, WE & Galaburda, AM (1989). Cerebrocortical microdysgenesis in neurologically normal subjects: a histopathologic study. *Neurology* 39:238–244.

Keays, Da (2007). Neuronal migration: unraveling the molecular pathway with humans, mice, and a fungus. *Mamm Genome* 18:425–430.

Kelava, I, Reillo, I, Murayama, AY, Kalinka, AT, Stenzel, D, Tomancak, P, Matsuzaki, F, Lebrand, C, Sasaki, E, Schwamborn, JC, Okano, H, Huttner, WB, & Borrell, V (2012). Abundant occurrence of basal radial glia in the subventricular zone of embryonic neocortex of a lissencephalic primate, the common marmoset Callithrix jacchus. *Cereb Cortex* 22:469–81.

Kent, WJ, Sugnet, CW, Furey, TS, Roskin, KM, Pringle, TH, Zahler, AM, & Haussler, D (2002). The human genome browser at UCSC. *Genome Res* 12:996–1006.

Kere, J (2014). The molecular genetics and neurobiology of developmental dyslexia as model of a complex phenotype. *Biochem Biophys Res Commun* 452:236–243.

Kierszenbaum, AL (2004). Polycystins: what polycystic kidney disease tells us about sperm. *Mol Reprod Dev* 67:385–8.

Kierszenbaum, AL, Rivkin, E, & Tres, LL (2003). Acroplaxome, an F-actin-keratin-containing plate, anchors the acrosome to the nucleus during shaping of the spermatid head. *Mol Biol Cell* 14:4628–4640.

Kierszenbaum, AL, Rivkin, E, Tres, LL, Yoder, BK, Haycraft, CJ, Bornens, M, & Rios, RM (2011). GMAP210 and IFT88 are present in the spermatid golgi apparatus and participate in the development of the acrosome-acroplaxome complex, head-tail coupling apparatus and tail. *Dev Dyn* 240:723–36.

Kirsten, H & Other (2012). Association study of a functional genetic variant in KIAA0319 in German dyslexics. *Psychiatr Genet* 22:216–7.

Kitano, H (2004). Biological robustness. *Nat Rev Genet* 5:826–837.

Klingberg, T, Hedehus, M, Temple, E, Salz, T, Gabrieli, JDE, Moseley, ME, & Poldrack, RA (2000). Microstructure of Temporo-Parietal White Matter as a Basis for Reading Ability : Evidence from Diffusion Tensor Magnetic Resonance Imaging. *Neuron* 25:493–500.

Koizumi, H, Tanaka, T, & Gleeson, JG (2006). Doublecortin-like kinase functions with doublecortin to mediate fiber tract decussation and neuronal migration. *Neuron* 49:55–66.

Kok, FO, Shin, M, Ni, CW, Gupta, A, Grosse, AS, van Impel, A, et al. (2015). Reverse genetic screening reveals poor correlation between morpholino-induced and mutant phenotypes in zebrafish. *Dev Cell* 32:97–108.

Kong, R, Shao, S, Wang, J, Zhang, X, Guo, S, Zou, L, Zhong, R, Lou, J, Zhou, J, Zhang, J, & Song, R (2016). Genetic variant in DIP2A gene is associated with developmental dyslexia in Chinese population. *Am J Med Genet B Neuropsychiatr Genet* 171:203–8.

Kornilov, SA, Rakhlin, N, Koposov, R, Lee, M, Yrigollen, C, Caglayan, AO, et al. (2016). Genome-Wide Association and Exome Sequencing Study of Language Disorder in an Isolated Population. *Pediatrics* 137:165–188.

Koscinski, I, ElInati, E, Fossard, C, Redin, C, Muller, J, Velez de la Calle, J, et al. (2011). DPY19L2 Deletion as a Major Cause of Globozoospermia. *Am J Hum Genet* 88:344–350.

Kotaja, N, Kimmins, S, Brancorsini, S, Hentsch, D, Vonesch, JL, Davidson, I, Parvinen, M, & Sassone-Corsi, P (2004). Preparation, isolation and characterization of stage-specific spermatogenic cells for cellular and molecular analysis. *Nat Methods* 1:249–254.

Kowalczyk, T, Pontious, A, Englund, C, Daza, RAM, Bedogni, F, Hodge, R, Attardo, A, Bell, C, Huttner, WB, & Hevner, RF (2009). Intermediate neuronal progenitors (basal progenitors) produce pyramidal-projection neurons for all layers of cerebral cortex. *Cereb Cortex* 19:2439–50.

Krafnick, AJ, Flowers, DL, Luetje, MM, Napoliello, EM, & Eden, GF (2014). An investigation into the origin of anatomical differences in dyslexia. *J Neurosci* 34:901–908.

Kriegstein, AR & Noctor, SC (2004). Patterns of neuronal migration in the embryonic cortex. *Trends Neurosci.* 27:392–399.

Krishnan, S, Watkins, KE, & Bishop, DV (2016). Neurobiological Basis of Language Learning Difficulties. *Trends Cogn Sci* 20:701–704.

Ku, CS, Polychronakos, C, Tan, EK, Naidoo, N, Pawitan, Y, Roukos, DH, Mort, M, & Cooper, DN (2013). A new paradigm emerges from the study of de novo mutations in the context of neurodevelopmental disease. *Mol Psychiatry* 18:141–53.

Kubo, Ki, Tomita, K, Uto, A, Kuroda, K, Seshadri, S, Cohen, J, Kaibuchi, K, Kamiya, A, & Nakajima, K (2010). "Migration defects by DISC1 knockdown in C57BL/6, 129X1/SvJ, and ICR strains via in utero gene transfer and virus-mediated RNAi".

Kuhlmann, K, Other, Tschapek, A, Wiese, H, Eisenacher, M, Meyer, HE, Hatt, HH, Oeljeklaus, S, & Warscheid, B (2014). The membrane proteome of sensory cilia to the depth of olfactory receptors. *Mol Cell Proteomics* 13:1828–43.

Kumar, A & Purohit, R (2012). Computational investigation of pathogenic nsSNPs in CEP63 protein. *Gene* 503:75–82.

Kurt, S, Groszer, M, Fisher, SE, & Ehret, G (2009). Modified sound-evoked brainstem potentials in Foxp2 mutant mice. *Brain Res* 1289:30–36.

Kvajo, M, McKellar, H, & Gogos, JA (2012). Avoiding mouse traps in schizophrenia genetics: lessons and promises from current and emerging mouse models. *Neuroscience* 211:136–64.

Kwan, KY, Shen, J, & Corey, DP (2015). Stem Cell Reports Ar ticle C-MYC Transcriptionally Amplifies SOX2 Target Genes to Regulate Self-Renewal in Multipotent Otic Progenitor Cells. *Stem Cell Reports* 4:47–60.

Lai, CS, Fisher, SE, Hurst, JA, Vargha-Khadem, F, & Monaco, AP (2001). A forkhead-domain gene is mutated in a severe speech and language disorder. *Nature* 413:519–523.

Laiho, A, Kotaja, N, Gyenesei, A, & Sironen, A (2013). Transcriptome profiling of the murine testis during the first wave of spermatogenesis. *PLoS One* 8:e61558.

Lancaster, MA, Renner, M, Martin, CA, Wenzel, D, Bicknell, LS, Hurles, ME, Homfray, T, Penninger, JM, Jackson, AP, & Knoblich, JA (2013). Cerebral organoids model human brain development and microcephaly. *Nature* 501:373–9.

Landerl, K & Moll, K (2010). Comorbidity of learning disorders: prevalence and familial transmission. *J Child Psychol Psychiatry* 51:287–94.

Lang, T, Bruns, D, Wenzel, D, Riedel, D, Holroyd, P, Thiele, C, & Jahn, R (2001). SNAREs are concentrated in cholesterol-dependent clusters that define docking and fusion sites for exocytosis. *EMBO J* 20:2202–13.

Larsen, JP, Høien, T, Lundberg, I, & Odegaard, H (1990). MRI evaluation of the size and symmetry of the planum temporale in adolescents with developmental dyslexia. *Brain Lang* 39:289–301.

Lasky, RE (1991). The effects of rate and forward masking on human adult and newborn auditory evoked brainstem response thresholds. *Dev Psychobiol* 24:51–64.

Lavdas, AA, Grigoriou, M, Pachnis, V, & Parnavelas, JG (1999). The medial ganglionic eminence gives rise to a population of early neurons in the developing cerebral cortex. *J Neurosci* 19:7881–7888.

Lawler, A (2001). Archaeology. Writing gets a rewrite. *Science* 292:2418–2420.

Leblond, CS, Heinrich, J, Delorme, R, Proepper, C, Betancur, C, Huguet, G, et al. (2012). Genetic and functional analyses of SHANK2 mutations suggest a multiple hit model of autism spectrum disorders. *PLoS Genet* 8:e1002521.

Levecque, C, Velayos-Baeza, A, Holloway, ZG, Monaco, AP, & Other (2009). The dyslexia-associated protein KIAA0319 interacts with adaptor protein 2 and follows the classical clathrin-mediated endocytosis pathway. *Am J Physiol* 297:C160–8.

Leventer, RJ, Jansen, A, Pilz, DT, Stoodley, N, Marini, C, Dubeau, F, Malone, J, Mitchell, LA, Mandelstam, S, Scheffer, IE, Berkovic, SF, Andermann, F, Andermann, E, Guerrini, R, & Dobyns, WB (2010). Clinical and imaging heterogeneity of polymicrogyria: a study of 328 patients. *Brain* 133:1415–1427.

Levine, DN, Fisher, MA, & Caviness, VS (1974). Porencephaly with microgyria: a pathologic study. *Acta Neuropathol* 29:99–113.

Levine, DN, Hier, DB, & Calvanio, R (1981). Acquired learning disability for reading after left temporal lobe damage in childhood. *Neurology* 31:257–64.

Lewitter, FI, DeFries, JC, & Elston, RC (1980). Genetic models of reading disability. *Behav Genet* 10:9–30.

Li, S, Kalappa, BI, Tzounopoulos, T, Amendola, J, Woodhouse, A, Martin-Eauclaire, M, et al. (2015). Noise-induced plasticity of KCNQ2/3 and HCN channels underlies vulnerability and resilience to tinnitus. *Elife* 4.

Li, S, Qiao, Y, Di, Q, Le, X, Zhang, L, Zhang, X, Zhang, C, Cheng, J, Zong, S, Koide, SS, Miao, S, & Wang, L (2009). Interaction of SH3P13 and DYDC1 protein: a germ cell component that regulates acrosome biogenesis during spermiogenesis. *Eur J Cell Biol* 88:509–520.

Li, YC, Hu, XQ, Zhang, KY, Guo, J, Hu, ZY, Tao, SX, Xiao, LJ, Wang, QZ, Han, CS, & Liu, YX (2006). Afaf, a novel vesicle membrane protein, is related to acrosome formation in murine testis. *FEBS Lett* 580:4266–73.

Liberman, AM & Mattingly, IG (1985). The motor theory of speech perception revised. *Cognition* 21:1–36.

Liberman, IY (1973). 1. Segmentation of the spoken word and reading acquisition. *Bull Ort Soc* 23:64–77.

Lim, CKP, Wong, AMB, Ho, CSH, & Waye, MMY (2014). A common haplotype of KIAA0319 contributes to the phonological awareness skill in Chinese children. *Behav. Brain Funct.* 10:23.

Lim, CK, Ho, CS, Chou, CH, & Waye, MM (2011). Association of the rs3743205 variant of DYX1C1 with dyslexia in Chinese children. *Behav Brain Funct* 7:16.

Lin, YN, Roy, A, Yan, W, Burns, KH, & Matzuk, MM (2007). Loss of zona pellucida binding proteins in the acrosomal matrix disrupts acrosome biogenesis and sperm morphogenesis. *Mol Cell Biol* 27:6794–805.

Lin, Y, Cradick, TJ, Brown, MT, Deshmukh, H, Ranjan, P, Sarode, N, Wile, BM, Vertino, PM, Stewart, FJ, & Bao, G (2014). CRISPR/Cas9 systems have off-target activity with insertions or deletions between target DNA and guide RNA sequences. *Nucleic Acids Res* 42:7473–85.

Lind, PA, Luciano, M, Wright, MJ, Montgomery, GW, Martin, NG, & Bates, TC (2010). Dyslexia and DCDC2: normal variation in reading and spelling is associated with DCDC2 polymorphisms in an Australian population sample. *Eur J Hum Genet* 18:668–673.

Liu, G, Shi, QW, & Lu, GX (2010). A newly discovered mutation in PICK1 in a human with globozoospermia. *Asian J Androl* 12:556–560.

Liu, H, Pecka, JL, Zhang, Q, Soukup, GA, Beisel, KW, He, DZZ, David, X, & He, ZZ (2014). Characterization of Transcriptomes of Cochlear Inner and Outer Hair Cells. *J Neurosci* 34:11085–95.

Liu, Y, Loijens, JC, Martin, KH, Karginov, AV, & Parsons, JT (2002). The association of ASAP1, an ADP ribosylation factor-GTPase activating protein, with focal adhesion kinase contributes to the process of focal adhesion assembly. *Mol Biol Cell* 13:2147–56.

Livingstone, MS, Rosen, GD, Drislane, FW, & Galaburda, AM (1991). Physiological and anatomical evidence for a magnocellular defect in developmental dyslexia. *Proc Natl Acad Sci* 88:7943–7947.

Lodato, S, Rouaux, C, Quast, KB, Jantrachotechatchawan, C, Studer, M, Hensch, TK, & Arlotta, P (2011). Excitatory projection neuron subtypes control the distribution of local inhibitory interneurons in the cerebral cortex. *Neuron* 69:763–79.

Logothetis, NK & Sheinberg, DL (1996). Visual object recognition. en. *Annu Rev Neurosci* 19:577–621.

Lou, X, Paradise, S, Ferguson, SM, & De Camilli, P (2008). Selective saturation of slow endocytosis at a giant glutamatergic central synapse lacking dynamin 1. *Proc Natl Acad Sci* 105:17555–17560.

Lovegrove, WJ, Bowling, A, Badcock, D, & Blackwood, M (1980). Specific reading disability: differences in contrast sensitivity as a function of spatial frequency. *Science* 210:439–40.

Lu, R, Stewart, L, & Wilson, JM (2015). Scaffolding protein GOPC regulates tight junction structure. *Cell Tissue Res* 360:321–32.

Luciano, M, Evans, DM, Hansell, NK, Medland, SE, Montgomery, GW, Martin, NG, Wright, MJ, & Bates, TC (2013). A genome-wide association study for reading and language abilities in two population cohorts. *Genes Brain Behav* 12:645–52.

Luciano, M, Lind, PA, Duffy, DL, Castles, A, Wright, MJ, Montgomery, GW, Martin, NG, & Bates, TC (2007). A haplotype spanning KIAA0319 and TTRAP is associated with normal variation in reading and spelling ability. *Biol Psychiatry* 62:811–7.

Ludwig, KU, Roeske, D, Herms, S, Schumacher, J, Warnke, A, Plume, E, Neuhoff, N, Bruder, J, Remschmidt, H, Schulte-Körne, G, Müller-Myhsok, B, Nöthen, MM, & Hoffmann, P (2010). Variation in GRIN2B contributes to weak performance in verbal short-term memory in children with dyslexia. *Am J Med Genet B Neuropsychiatr Genet* 153B:503–11.

Ludwig, KU, Roeske, D, Schumacher, J, Schulte-Körne, G, König, IR, Warnke, A, Plume, E, Ziegler, A, Remschmidt, H, Müller-Myhsok, B, Nöthen, MM, & Hoffmann, P (2008). Investigation of interaction between DCDC2 and KIAA0319 in a large German dyslexia sample. *J Neural Transm* 115:1587–9.

Lui, JH, Hansen, DV, & Kriegstein, AR (2011). Development and evolution of the human neocortex. *Cell* 146:18–36.

Lum, JAG, Ullman, MT, & Conti-Ramsden, G (2013). Procedural learning is impaired in dyslexia: evidence from a meta-analysis of serial reaction time studies. *Res Dev Disabil* 34:3460–76.

Luskin, MB & Shatz, CJ (1985). Studies of the earliest generated cells of the cat's visual cortex: cogeneration of subplate and marginal zones. *J Neurosci* 5:1062–75.

Lyon, GR, Shaywitz, SE, & Shaywitz, BA (2003). A definition of dyslexia. *Ann Dyslexia* 53:1–14.

MacArthur, DG, Manolio, TA, Dimmock, DP, Rehm, HL, Shendure, J, Abecasis, GR, et al. (2014). Guidelines for investigating causality of sequence variants in human disease. *Nature* 508:469–476. arXiv: `NIHMS150003`.

Madasu, Y, Yang, C, Boczkowska, M, Bethoney, KA, Zwolak, A, Rebowski, G, Svitkina, T, & Dominguez, R (2015). PICK1 is implicated in organelle motility in an Arp2/3 complex-independent manner. *Mol Biol Cell* 26:1308–22.

Mai, X, Tardif, T, Xu, L, Li, M, Kileny, PR, Shao, J, & Lozoff, B (2015). Temporal processing in the auditory brainstem response by full-term 6-week- and 9-month-old infants. *Sci Rep* 5.

Maisog, JM, Einbinder, ER, Flowers, DL, Turkeltaub, PE, & Eden, GF (2008). A meta-analysis of functional neuroimaging studies of dyslexia. *Ann N Y Acad Sci* 1145:237–59.

Malatesta, P, Hartfuss, E, & Götz, M (2000). Isolation of radial glial cells by fluorescent-activated cell sorting reveals a neuronal lineage. *Development* 127:5253–63.

Malhotra, D & Sebat, J (2012). CNVs: harbingers of a rare variant revolution in psychiatric genetics. *Cell* 148:1223–41.

Manolio, TA, Collins, FS, Cox, NJ, Goldstein, DB, Hindorff, LA, Hunter, DJ, et al. (2009). Finding the missing heritability of complex diseases. *Nature* 461:747–53.

Marín, O (2012). Interneuron dysfunction in psychiatric disorders. *Nat Rev Neurosci* 13:107–20.

— (2013). Cellular and molecular mechanisms controlling the migration of neocortical interneurons. en. *Eur J Neurosci* 38:2019–29.

Marín, O & Müller, U (2014). Lineage origins of GABAergic versus glutamatergic neurons in the neocortex. *Curr Opin Neurobiol* 26:132–41.

Marín, O, Other, Valiente, M, Ge, X, Tsai, LH, Other, Valiente, M, Ge, X, & Tsai, LH (2010). Guiding neuronal cell migrations. *Cold Spring Harb Perspect Biol* 2:a001834.

Marino, C, Citterio, A, Giorda, R, Facoetti, A, Menozzi, G, Vanzin, L, Lorusso, ML, Nobile, M, & Molteni, M (2007). Association of short-term memory with a variant within DYX1C1 in developmental dyslexia. *Genes, Brain Behav* 6:640–646.

Marino, C, Giorda, R, Vanzin, L, Nobile, M, Lorusso, ML, Baschirotto, C, Riva, L, Molteni, M, & Battaglia, M (2004). A locus on 15q15-15qter influences dyslexia: further support from a transmission/disequilibrium study in an Italian speaking population. *J Med Genet* 41:42–46.

Marino, C, Giorda, R, Luisa Lorusso, M, Vanzin, L, Salandi, N, Nobile, M, Citterio, A, Beri, S, Crespi, V, Battaglia, M, & Molteni, M (2005). A family-based association study does not support DYX1C1 on 15q21.3 as a candidate gene in developmental dyslexia. *Eur J Hum Genet* 13:491–499.

Marin-Padilla, M (1971). Early prenatal ontogenesis of the cerebral cortex (neocortex) of the cat (Felis domestica). A Golgi study. I. The primordial neocortical organization. *Zeitschrift für Anat und Entwicklungsgeschichte* 134:117–45.

Markram, H, Toledo-Rodriguez, M, Wang, Y, Gupta, A, Silberberg, G, & Wu, C (2004). Interneurons of the neocortical inhibitory system. *Nat Rev Neurosci* 5:793–807.

Marland, JRK, Smillie, KJ, Cousin, MA, Blank, M, Wetmore, D, & Buckmaster, P (2016). Synaptic Vesicle Recycling Is Unaffected in the Ts65Dn Mouse Model of Down Syndrome. *PLoS One* 11. Ed. by DJ Keating:e0147974.

Marlow, AJ, Fisher, SE, Francks, C, MacPhie, IL, Cherny, SS, Richardson, AJ, Talcott, JB, Stein, JF, Monaco, AP, & Cardon, LR (2003). Use of Multivariate Linkage Analysis for Dissection of a Complex Cognitive Trait. *Am J Hum Genet* 72:561–570.

Martens, S & McMahon, HT (2008). Mechanisms of membrane fusion: disparate players and common principles. *Nat Rev Mol Cell Biol* 9:543–56.

Martin, SJ & Clark, RE (2007). The rodent hippocampus and spatial memory: from synapses to systems. *Cell Mol Life Sci* 64:401–31.

Martinez-Garay, I, Guidi, LG, Holloway, ZG, Bailey, MAG, Lyngholm, D, Schneider, T, Donnison, T, Butt, SJB, Velayos-Baeza, A, Molnár, Z, & Monaco, AP (2017).

Normal radial migration and lamination are maintained in dyslexia-susceptibility candidate gene homolog Kiaa0319 knockout mice. *Brain Struct Funct* 222:1367–1384.

Martini, FJ, Valiente, M, López Bendito, G, Szabó, G, Moya, F, Valdeolmillos, M, & Marín, O (2009). Biased selection of leading process branches mediates chemotaxis during tangential neuronal migration. *Development* 136:41–50.

Mascheretti, S, Facoetti, A, Giorda, R, Beri, S, Riva, V, Trezzi, V, Cellino, MR, & Marino, C (2015). GRIN2B mediates susceptibility to intelligence quotient and cognitive impairments in developmental dyslexia. *Psychiatr Genet* 25:9–20.

Mascheretti, S, Riva, V, Giorda, R, Beri, S, Lanzoni, LFE, Cellino, MR, & Marino, C (2014). KIAA0319 and ROBO1: evidence on association with reading and pleiotropic effects on language and mathematics abilities in developmental dyslexia. *J Hum Genet* 59:189–97.

Massinen, S, Hokkanen, ME, Matsson, H, Tammimies, K, Tapia-Páez, I, Dahlström-Heuser, V, Kuja-Panula, J, Burghoorn, J, Jeppsson, KE, Swoboda, P, Peyrard-Janvid, M, Toftgård, R, Castrén, E, Kere, J, & Other (2011). Increased Expression of the Dyslexia Candidate Gene DCDC2 Affects Length and Signaling of Primary Cilia in Neurons. *PLoS One* 6:e20580.

Matsson, H, Huss, M, Persson, H, Einarsdottir, E, Tiraboschi, E, Nopola-Hemmi, J, Schumacher, J, Neuhoff, N, Warnke, A, Lyytinen, H, Schulte-Körne, G, Nöthen, MM, Leppänen, PHT, Peyrard-Janvid, M, & Kere, J (2015). Polymorphisms in DCDC2 and S100B associate with developmental dyslexia. *J Hum Genet* 60:399–401.

Matsson, H, Tammimies, K, Zucchelli, M, Anthoni, H, Onkamo, P, Nopola-Hemmi, J, Lyytinen, H, Leppanen, PHT, Neuhoff, N, Warnke, A, Schulte-Körne, G, Schumacher, J, Nöthen, MM, Kere, J, & Peyrard-Janvid, M (2011). SNP Variations in the 7q33 Region Containing DGKI are Associated with Dyslexia in the Finnish and German Populations. *Behav Genet* 41:134–140.

Maycox, PR, Link, E, Reetz, A, Morris, SA, & Jahn, R (1992). Clathrin-coated vesicles in nervous tissue are involved primarily in synaptic vesicle recycling. *J Cell Biol* 118:1379–88.

McAnally, KI & Stein, JF (1996). Auditory temporal coding in dyslexia. *Proc Biol Sci* 263:961–5.

McBride, JL, Boudreau, RL, Harper, SQ, Staber, PD, Monteys, AM, Martins, I, Gilmore, BL, Burstein, H, Peluso, RW, Polisky, B, Carter, BJ, & Davidson, BL (2008). Artificial miRNAs mitigate shRNA-mediated toxicity in the brain: implications for the therapeutic development of RNAi. *Proc Natl Acad Sci* 105:5868–73.

McDonald, CL, Bandtlow, C, & Reindl, M (2011). Targeting the Nogo receptor complex in diseases of the central nervous system. *Curr Med Chem* 18:234–44.

McGee, AW & Strittmatter, SM (2003). *The Nogo-66 receptor: Focusing myelin inhibition of axon regeneration.*

McNutt, M (2014). Reproducibility. *Science* 343:229.

Meaburn, EL, Harlaar, N, Craig, IW, Schalkwyk, LC, & Plomin, R (2008). Quantitative trait locus association scan of early reading disability and ability using pooled DNA and 100K SNP microarrays in a sample of 5760 children. *Mol Psychiatry* 13:729–40.

Meechan, DW, Tucker, ES, Maynard, TM, & LaMantia, AS (2012). Cxcr4 regulation of interneuron migration is disrupted in 22q11.2 deletion syndrome. *Proc Natl Acad Sci* 109:18601–6.

Meng, H, Hager, K, Held, M, Page, GP, Olson, RK, Pennington, BF, DeFries, JC, Smith, SD, & Gruen, JR (2005a). TDT-association analysis of EKN1 and dyslexia in a Colorado twin cohort. *Hum Genet* 118:87–90.

Meng, H, Smith, SD, Hager, K, Held, M, Liu, J, Olson, RK, et al. (2005b). DCDC2 is associated with reading disability and modulates neuronal development in the brain. *Proc Natl Acad Sci* 102:17053–17058.

Menghini, D, Finzi, A, Benassi, M, Bolzani, R, Facoetti, A, Giovagnoli, S, Ruffino, M, & Vicari, S (2010). Different underlying neurocognitive deficits in developmental dyslexia: a comparative study. *Neuropsychologia* 48:863–72.

Miesenbock, G, De Angelis, DA, & Rothman, JE (1998). Visualizing secretion and synaptic transmission with pH-sensitive green fluorescent proteins. *Nature* 394:192–195.

Miller, JA, Ding, SL, Sunkin, SM, Smith, KA, Ng, L, Szafer, A, et al. (2014). Transcriptional landscape of the prenatal human brain. *Nature* 508:199–206.

Missler, M, Südhof, TC, & Biederer, T (2012). Synaptic cell adhesion. *Cold Spring Harb Perspect Biol* 4:a005694.

Misson, JP, Austin, CP, Takahashi, T, Cepko, CL, & Caviness, VS (1991). The alignment of migrating neural cells in relation to the murine neopallial radial glial fiber system. *Cereb Cortex* 1:221–9.

Mitchell, KJ (2012). What is complex about complex disorders? *Genome Biol* 13:237.

— (2015). *The Genetics of Neurodevelopmental Disorders*. London: Wiley-Blackwell.

Miyata, T, Kawaguchi, A, Okano, H, & Ogawa, M (2001). Asymmetric inheritance of radial glial fibers by cortical neurons. *Neuron* 31:727–41.

Miyata, T, Kawaguchi, A, Saito, K, Kawano, M, Muto, T, & Ogawa, M (2004). Asymmetric production of surface-dividing and non-surface-dividing cortical progenitor cells. *Development* 131:3133–45.

Møller, AR, Jannetta, PJ, & Møller, MB (1981). Neural generators of brainstem evoked potentials. Results from human intracranial recordings. *Ann Otol Rhinol Laryngol* 90:591–6.

Molyneaux, BJ, Arlotta, P, Menezes, JRL, & Macklis, JD (2007). Neuronal subtype specification in the cerebral cortex. *Nat Rev Neurosci* 8:427–437.

Molyneaux, BJ, Goff, LA, Brettler, AC, Chen, HH, Brown, JR, Hrvatin, S, Rinn, JL, & Arlotta, P (2015). DeCoN: genome-wide analysis of in vivo transcriptional dynamics during pyramidal neuron fate selection in neocortex. *Neuron* 85:275–88.

Monzalvo, K, Fluss, J, Billard, C, Dehaene, S, & Dehaene-Lambertz, G (2012). Cortical networks for vision and language in dyslexic and normal children of variable socio-economic status. *Neuroimage* 61:258–74.

Morel, F & Wildi, E (1952). Dysgénesie nodulaire disseminée de l'encorce frontale. *Rev Neurol* 87:251–270.

Moreno, RD, Ramalho-Santos, J, Sutovsky, P, Chan, EK, & Schatten, G (2000). Vesicular traffic and golgi apparatus dynamics during mammalian spermatogenesis: implications for acrosome architecture. *Biol Reprod* 63:89–98.

Moreno, RD & Alvarado, CP (2006). The mammalian acrosome as a secretory lysosome: new and old evidence. *Mol Reprod Dev* 73:1430–4.

Morgan, WP (1896). A case of congenital word blindness. *Br Med J* 2:1378.

Morris, DW, Robinson, L, Turic, D, Duke, M, Webb, V, Milham, C, et al. (2000). Family-based association mapping provides evidence for a gene for reading disability on chromosome 15q. *Hum Mol Genet* 9:843–848.

Mountcastle, VB (1997). The columnar organization of the neocortex. *Brain*, 701–22.

Mozzi, A, Forni, D, Clerici, M, Pozzoli, U, Mascheretti, S, Guerini, FR, Riva, S, Bresolin, N, Cagliani, R, & Sironi, M (2016). The evolutionary history of genes involved in spoken and written language: beyond FOXP2. *Sci Rep* 6:22157.

Mueller, B, Ahnert, P, Burkhardt, J, Brauer, J, Czepezauer, I, Quente, E, Boltze, J, Wilcke, a, & Kirsten, H (2014). Genetic risk variants for dyslexia on chromosome 18 in a German cohort. *Genes Brain Behav* 13:350–6.

Müller, B, Wilcke, A, Czepezauer, I, Ahnert, P, Boltze, J, Kirsten, H, & consortium, L (2016). Association, characterisation and meta-analysis of SNPs linked to general reading ability in a German dyslexia case-control cohort. *Sci Rep* 6:27901.

Muller, T, Stein, U, Poletti, A, Garzia, L, Rothley, M, Plaumann, D, et al. (2010). ASAP1 promotes tumor cell motility and invasiveness, stimulates metastasis formation in vivo, and correlates with poor survival in colorectal cancer patients. *Oncogene* 29:2393–2403.

Nadarajah, B, Brunstrom, JE, Grutzendler, J, Wong, RO, & Pearlman, AL (2001). Two modes of radial migration in early development of the cerebral cortex. *Nat Neurosci* 4:143–150.

Nagase, T, Ishikawa, K, Nakajima, D, Ohira, M, Seki, N, Miyajima, N, Tanaka, A, Kotani, H, Nomura, N, & Ohara, O (1997). Prediction of the coding sequences of unidentified human genes. VII. The complete sequences of 100 new cDNA clones from brain which can code for large proteins in vitro. *DNA Res* 4:141–50.

Nagase, T, Kikuno, R, & Ohara, O (2001). Prediction of the coding sequences of unidentified human genes. XXII. The complete sequences of 50 new cDNA clones which code for large proteins. *DNA Res* 8:319–27.

Nakamoto, KT, Jones, SJ, & Palmer, AR (2008). Descending projections from auditory cortex modulate sensitivity in the midbrain to cues for spatial position. *J Neurophysiol* 99:2347–56.

Nakatsu, F & Ohno, H (2003). Adaptor protein complexes as the key regulators of protein sorting in the post-Golgi network. *Cell Struct Funct* 28:419–29.

Neef, N, Brauer, J, Wilcke, A, Kirsten, H, Muller, B, Skeide, M, Liebig, J, Kraft, I, Schaadt, G, Kraus, N, Emmrich, F, & Friederici, A (2015). "Speech-evoked brainstem responses relate KIAA0319 variants and phonological skills in pre-reading children: a biomarker for dyslexia?" In: *Soc Neurosci*. Chicago.

Newbury, DF, Paracchini, S, Scerri, TS, Winchester, L, Addis, L, Richardson, AJ, Walter, J, Stein, JF, Talcott, JB, & Monaco, AP (2011). Investigation of dyslexia and SLI risk variants in reading- and language-impaired subjects. *Behav Genet* 41:90–104.

Newbury, DF, Fisher, SE, & Monaco, AP (2010). Recent advances in the genetics of language impairment. *Genome Med* 2:6.

Newbury, DF, Monaco, AP, & Paracchini, S (2014). Reading and language disorders: the importance of both quantity and quality. *Genes* 5:285–309.

Newbury, DF, Winchester, L, Addis, L, Paracchini, S, Buckingham, LL, Clark, A, et al. (2009). CMIP and ATP2C2 modulate phonological short-term memory in language impairment. *Am J Hum Genet* 85:264–72.

Nicodemus, KK, Elvevåg, B, Foltz, PW, Rosenstein, M, Diaz-Asper, C, & Weinberger, DR (2014). Category fluency, latent semantic analysis and schizophrenia: a candidate gene approach. *Cortex* 55:182–91.

Nicolson, RI, Fawcett, AJ, Brookes, RL, & Needle, J (2010). Procedural learning and dyslexia. *Dyslexia* 16:194–212.

Nicolson, R, Fawcett, AJ, & Dean, P (2001). Dyslexia, development and the cerebellum. *Trends Neurosci.* 24:515–516.

Nie, Z, Hirsch, DS, Luo, R, Jian, X, Stauffer, S, Cremesti, A, Andrade, J, Lebowitz, J, Marino, M, Ahvazi, B, Hinshaw, JE, & Randazzo, PA (2006). A BAR Domain in the N Terminus of the Arf GAP ASAP1 Affects Membrane Structure and Trafficking of Epidermal Growth Factor Receptor. *Curr Biol* 16:130–139.

Nie, Z & Randazzo, PA (2006). Arf GAPs and membrane traffic. *J Cell Sci* 119:1203–11.

Nittrouer, S & Pennington, B (2010). New Approaches to the Study of Childhood Language Disorders. *Curr Dir Psychol Sci* 19:308–313.

Nóbrega-Pereira, S & Marín, O (2009). Transcriptional control of neuronal migration in the developing mouse brain. *Cereb Cortex* 19 Suppl 1:i107–13.

Noctor, SC, Flint, AC, Weissman, TA, Dammerman, RS, & Kriegstein, AR (2001). Neurons derived from radial glial cells establish radial units in neocortex. *Nature* 409:714–20.

Noctor, SC, Martínez-Cerdeño, V, Ivic, L, & Kriegstein, AR (2004). Cortical neurons arise in symmetric and asymmetric division zones and migrate through specific phases. *Nat Neurosci* 7:136–44.

Nopola-Hemmi, J, Myllyluoma, B, Haltia, T, Taipale, M, Ollikainen, V, Ahonen, T, Voutilainen, A, Kere, J, & Widén, E (2001). A dominant gene for developmental dyslexia on chromosome 3. *J Med Genet* 38:658–64.

Norris, D (2013). Models of visual word recognition. *Trends Cogn Sci* 17:517–524.

Norton, ES, Beach, SD, & Gabrieli, JDE (2015). Neurobiology of dyslexia. *Curr Opin Neurobiol* 30:73–8.

Norton, N, Heiervang, E, & Hamshere, ML (2000). Suggestive evidence of linkage with reading disability in a large Norwegian family. *Am J Hum Genet* 96:556.

Nöthen, MM, Schulte-Körne, G, Grimm, T, Cichon, S, Vogt, IR, Müller-Myhsok, B, Propping, P, & Remschmidt, H (1999). Genetic linkage analysis with dyslexia: Evidence for linkage of spelling disability to chromosome 15. *Eur Child Adolesc Psychiatry* 8:S56–S59.

Nowakowski, RS & Rakic, P (1981). The site of origin and route and rate of migration of neurons to the hippocampal region of the rhesus monkey. *J Comp Neurol* 196:129–54.

Nudel, R, Simpson, NH, Baird, G, O'Hare, A, Conti-Ramsden, G, Bolton, PF, Hennessy, ER, SLI Consortium, Ring, SM, Davey Smith, G, Francks, C, Paracchini, S, Monaco, AP, Fisher, SE, & Newbury, DF (2014). Genome-wide association analyses of child genotype effects and parent-of-origin effects in specific language impairment. *Genes Brain Behav* 13:418–29.

Ohno, S (1970). *Evolution by gene duplication.* New York: Springer-Verlag.

Oliveira, EPM, Hage, SRV, Guimarães, CA, Brandão-Almeida, I, Lopes-Cendes, I, Guerreiro, CA, Teixeira, KCS, Montenegro, MA, Cendes, F, & Guerreiro, MM (2008). *Characterization of language and reading skills in familial polymicrogyria. - PubMed - NCBI.*

Open Science Collaboration (2015). Estimating the reproducibility of psychological science. en. *Science* 349:aac4716–aac4716.

Orton, ST (1925). "Word-blindness" in school children. *Arch Neurol Psychiatry* 14:581–615.

Pagnamenta, AT, Bacchelli, E, de Jonge, MV, Mirza, G, Scerri, TS, Minopoli, F, et al. (2010). Characterization of a family with rare deletions in CNTNAP5 and DOCK4 suggests novel risk loci for autism and dyslexia. *Biol Psychiatry* 68:320–8.

Paracchini, S, Ang, QW, Stanley, FJ, Monaco, AP, Pennell, CE, & Whitehouse, AJO (2011). Analysis of dyslexia candidate genes in the Raine cohort representing the general Australian population. *Genes Brain Behav* 10:158–65.

Paracchini, S, Diaz, R, & Stein, J (2016). "Advances in Dyslexia Genetics—New Insights Into the Role of Brain Asymmetries". In: *Adv Genet*. Vol. 96. 53–97.

Paracchini, S, Scerri, T, & Monaco, AP (2007). The genetic lexicon of dyslexia. *Annu Rev Genomics Hum Genet* 8:57–79.

Paracchini, S, Steer, CD, Buckingham, LL, Morris, AP, Ring, S, Scerri, T, Stein, J, Pembrey, ME, Ragoussis, J, Golding, J, & Monaco, AP (2008). Association of the KIAA0319 dyslexia susceptibility gene with reading skills in the general population. *Am J Psychiatry* 165:1576–84.

Paracchini, S, Thomas, A, Castro, S, Lai, C, Paramasivam, M, Wang, Y, et al. (2006). The chromosome 6p22 haplotype associated with dyslexia reduces the expression of KIAA0319, a novel gene involved in neuronal migration. *Hum Mol Genet* 15:1659–1666.

Pardoe, H & Kuzniecky, R (2014). Advanced Imaging Techniques in the Diagnosis of Nonlesional Epilepsy: MRI, MRS, PET, and SPECT. *Epilepsy Curr* 14:121–4.

Parham, K, Sun, XM, & Kilgard, M (2001). "Noninvasive assessment of auditory function in mice: auditory brainstem response and distortion product otoacoustic emissions". In: *Handb Mouse Audit Res From Behav to Mol Biol*. Ed. by JF Willott. Boca Raton: CRC Press. 37–58.

Park, SY & Guo, X (2014). Adaptor protein complexes and intracellular transport. *Biosci Rep* 34:e00123.

Parnavelas, JG (2000). *The origin and migration of cortical neurones: New vistas.*

Patel, A (2015). The Primary cilium calcium channels and their role in flow sensing. *Pflügers Arch - Eur J Physiol* 467:157–165.

Paternicó, D, Manes, M, Premi, E, Cosseddu, M, Gazzina, S, Alberici, A, Archetti, S, Bonomi, E, Cotelli, MS, Cotelli, M, Turla, M, Micheli, A, Gasparotti, R, Padovani, A, & Borroni, B (2016). Frontotemporal dementia and language networks: cortical thickness reduction is driven by dyslexia susceptibility genes. *Sci Rep* 6:30848.

Pedraza, M, Hoerder-Suabedissen, A, Albert-Maestro, MA, Molnár, Z, & De Carlos, JA (2014). Extracortical origin of some murine subplate cell populations. *Proc Natl Acad Sci* 111:8613–8.

Peiffer, AM, Rosen, GD, & Fitch, R (2004). Sex differences in rapid auditory processing deficits in microgyric rats. *Dev Brain Res* 148:53–57.

Peñagarikano, O, Abrahams, BS, Herman, EI, Winden, KD, Gdalyahu, A, Dong, H, Sonnenblick, LI, Gruver, R, Almajano, J, Bragin, A, Golshani, P, Trachtenberg, JT, Peles, E, Geschwind, DH, et al. (2011). Absence of CNTNAP2 leads to epilepsy, neuronal migration abnormalities, and core autism-related deficits. *Cell* 147:235–46.

Pennington, BF, Gilger, JW, Pauls, D, Smith, SA, Smith, SD, & DeFries, JC (1991). Evidence for major gene transmission of developmental dyslexia. *JAMA* 266:1527–34.

Pennington, BF & Bishop, DVM (2009). Relations among speech, language, and reading disorders. *Annu Rev Psychol* 60:283–306.

Peschansky, VJ, Burbridge, TJ, Volz, AJ, Fiondella, C, Wissner-Gross, Z, Galaburda, AM, Lo Turco, JJ, & Rosen, GD (2010). The Effect of Variation in Expression of the Candidate Dyslexia Susceptibility Gene Homolog Kiaa0319 on Neuronal Migration and Dendritic Morphology in the Rat. *Cereb. Cortex* 20:884–897.

Peter, B, Raskind, WH, Matsushita, M, Lisowski, M, Vu, T, Berninger, VW, Wijsman, EM, & Brkanac, Z (2011). Replication of CNTNAP2 association with nonword repetition and support for FOXP2 association with timed reading and motor activities in a dyslexia family sample. *J Neurodev Disord* 3:39–49.

Peter, BJ, Kent, HM, Mills, IG, Vallis, Y, Butler, PJG, Evans, PR, & McMahon, HT (2004). BAR Domains as Sensors of Membrane Curvature: The Amphiphysin BAR Structure. *Science* 303.

Peterson, RL & Pennington, BF (2015). Developmental Dyslexia. *Annu Rev Clin Psychol*, 1–25.

Petryshen, TL, Kaplan, BJ, Fu Liu, M, de French, NS, Tobias, R, Hughes, ML, & Field, LL (2001). Evidence for a susceptibility locus on chromosome 6q influencing phonological coding dyslexia. *Am J Med Genet* 105:507–17.

Petryshen, TL, Kaplan, BJ, Hughes, ML, Tzenova, J, & Field, LL (2002). Supportive evidence for the DYX3 dyslexia susceptibility gene in Canadian families. *J Med Genet* 39:125–6.

Petryshen, TL, Kaplan, BJ, Liu, MF, Field, LL, Speed, W, Shuster, A, Pauls, D, & Al., E (2000). Absence of significant linkage between phonological coding dyslexia and chromosome 6p23-21.3, as determined by use of quantitative-trait methods: confirmation of qualitative analyses. *Am J Hum Genet* 66:708–14.

Pettitt, SJ, Liang, Q, Rairdan, XY, Moran, JL, Prosser, HM, Beier, DR, Lloyd, KC, Bradley, A, & Skarnes, WC (2009). Agouti C57BL/6N embryonic stem cells for mouse genetic resources. *Nat Methods* 6:493–495.

Peyrard-Janvid, M, Anthoni, H, Onkamo, P, Lahermo, P, Zucchelli, M, Kaminen, N, Hannula-Jouppi, K, Nopola-Hemmi, J, Voutilainen, A, Lyytinen, H, & Kere, J (2004). Fine mapping of the 2p11 dyslexia locus and exclusion of TACR1 as a candidate gene. *Hum Genet* 114:510–516.

Pierre, V, Martinez, G, Coutton, C, Delaroche, J, Yassine, S, Novella, C, Pernet-Gallay, K, Hennebicq, S, Ray, PF, & Arnoult, C (2012). Absence of Dpy19l2, a new inner nuclear membrane protein, causes globozoospermia in mice by preventing the anchoring of the acrosome to the nucleus. *Development* 139:2955–65.

Pillay, S, Meyer, NL, Puschnik, AS, Davulcu, O, Diep, J, Ishikawa, Y, Jae, LT, Wosen, JE, Nagamine, CM, Chapman, MS, & Carette, JE (2016). An essential receptor for adeno-associated virus infection. *Nature* 530:108–12. arXiv: 15334406.

Pinel, P, Fauchereau, F, Moreno, A, Barbot, A, Lathrop, M, Zelenika, D, Le Bihan, D, Poline, JB, Bourgeron, T, & Dehaene, S (2012). Genetic variants of FOXP2 and KIAA0319/TTRAP/THEM2 locus are associated with altered brain activation in distinct language-related regions. *J Neurosci* 32:817–25.

Pinker, S & Bloom, P (1990). Natural language and natural selection. *Behav Brain Sci* 13:707–727.

Pinker, S & Jackendoff, R (2005). The faculty of language: what's special about it? *Cognition* 95:201–236.

Platko, JV, Wood, FB, Pelser, I, Meyer, M, Gericke, GS, O'Rourke, J, Birns, J, Purcell, S, & Pauls, DL (2008). Association of reading disability on chromosome 6p22 in the Afrikaner population. *Am J Med Genet B Neuropsychiatr Genet* 147B:1278–87.

Platt, MP, Adler, WT, Mehlhorn, AJ, Johnson, GC, Wright, KA, Choi, RT, Tsang, WH, Poon, MW, Yeung, SY, Waye, MMY, Galaburda, AM, Rosen, GD, & Other (2013). Embryonic disruption of the candidate dyslexia susceptibility gene homolog Kiaa0319-like results in neuronal migration disorders. *Neuroscience* 248:585–593.

Plomin, R, Haworth, CMA, & Davis, OSP (2009). Common disorders are quantitative traits. *Nat Rev Genet* 10:872–8.

Poelmans, G, Buitelaar, JK, Pauls, DL, & Franke, B (2011). A theoretical molecular network for dyslexia: integrating available genetic findings. *Mol Psychiatry* 16:365–82.

Poelmans, G, Engelen, JJM, Van Lent-Albrechts, J, Smeets, HJ, Schoenmakers, E, Franke, B, Buitelaar, JK, Wuisman-Frerker, M, Erens, W, Steyaert, J, & Schrander-Stumpel, C (2009). Identification of novel dyslexia candidate genes through the analysis of a chromosomal deletion. *Am J Med Genet B Neuropsychiatr Genet* 150B:140–7.

Poeppel, D (2014). The neuroanatomic and neurophysiological infrastructure for speech and language. *Curr Opin Neurobiol* 28:142–9.

Poeppel, D, Emmorey, K, Hickok, G, & Pylkkänen, L (2012). Towards a new neurobiology of language. *J Neurosci* 32:14125–31.

Poon, MW, Other, Tsang, WH, Waye, MMY, & Chan, SO (2011a). Distribution of Kiaa0319-like immunoreactivity in the adult mouse brain–a novel protein encoded by the putative dyslexia susceptibility gene KIAA0319-like. *Histol. Histopathol.* 26:953–963.

Poon, MW, Tsang, WH, Chan, SO, Li, HM, Ng, HK, & Waye, MMY (2011b). Dyslexia-associated kiaa0319-like protein interacts with axon guidance receptor nogo receptor 1. *Cell Mol Neurobiol* 31:27–35.

Powers, NR, Eicher, JD, Butter, F, Kong, Y, Miller, LL, Ring, SM, Mann, M, & Gruen, JR (2013). Alleles of a polymorphic ETV6 binding site in DCDC2 confer risk of reading and language impairment. *Am J Hum Genet* 93:19–28.

Powers, NR, Eicher, JD, Miller, LL, Kong, Y, Smith, SD, Pennington, BF, Willcutt, EG, Olson, RK, Ring, SM, & Gruen, JR (2016). The regulatory element READ1 epistatically influences reading and language, with both deleterious and protective alleles. *J Med Genet* 53:163–71.

Price, CJ (2012). A review and synthesis of the first 20 years of PET and fMRI studies of heard speech, spoken language and reading. *Neuroimage* 62:816–47.

Price, DJ, Aslam, S, Tasker, L, & Gillies, K (1997). Fates of the earliest generated cells in the developing murine neocortex. *J Comp Neurol* 377:414–22.

Protopapas, A (2014). From temporal processing to developmental language disorders: mind the gap. *Philos Trans R Soc Lond B Biol Sci* 369:20130090.

Pryor, PR, Jackson, L, Gray, SR, Edeling, MA, Thompson, A, Sanderson, CM, Evans, PR, Owen, DJ, & Luzio, JP (2008). Molecular basis for the sorting of the SNARE VAMP7 into endocytic clathrin-coated vesicles by the ArfGAP Hrb. *Cell* 134:817–27.

Puelles, L, Harrison, M, Paxinos, G, & Watson, C (2013). A developmental ontology for the mammalian brain based on the prosomeric model. *Trends Neurosci* 36:570–578.

Pugh, KR, Landi, N, Preston, JL, Mencl, WE, Austin, AC, Sibley, D, Fulbright, RK, Seidenberg, MS, Grigorenko, EL, Constable, RT, Molfese, P, & Frost, SJ (2013). The relationship between phonological and auditory processing and brain organization in beginning readers. *Brain Lang* 125:173–83.

Rabin, M, Wen, XL, Hepburn, M, Lubs, HA, Feldman, E, & Duara, R (1993). Suggestive linkage of developmental dyslexia to chromosome 1p34-p36. *Lancet (London, England)* 342:178.

Rakic, P (1971). Guidance of neurons migrating to the fetal monkey neocortex. *Brain Res* 33:471–6.

— (1972). Mode of cell migration to the superficial layers of fetal monkey neocortex. *J Comp Neurol* 145:61–83.

— (1982). Early developmental events: cell lineages, acquisition of neuronal positions, and areal and laminar development. *Neurosci Res Progr Bull* 20:439–451.

— (1990). Principles of neural cell migration. *Experientia* 46:882–91.

Rakic, P & Nowakowski, RS (1981). The time of origin of neurons in the hippocampal region of the rhesus monkey. *J Comp Neurol* 196:99–128.

Ramalho-Santos, J, Moreno, RD, Wessel, GM, Chan, EK, & Schatten, G (2001). Membrane trafficking machinery components associated with the mammalian acrosome during spermiogenesis. *Exp Cell Res* 267:45–60.

Ramalho-Santos, J, Schatten, G, & Moreno, RD (2002). Control of membrane fusion during spermiogenesis and the acrosome reaction. *Biol Reprod* 67:1043–51.

Ramón y Cajal, S (1899). *Textura del Sistema Nervioso del Hombre y de los Vertebrados.* Madrid: Moya.

Ramos, RL, Bai, J, & LoTurco, JJ (2006). Heterotopia formation in rat but not mouse neocortex after RNA interference knockdown of DCX. *Cereb Cortex* 16:1323–31.

Ramos, RL, Smith, PT, DeCola, C, Tam, D, Corzo, O, & Brumberg, JC (2008). Cytoarchitecture and transcriptional profiles of neocortical malformations in inbred mice. *Cereb cortex* 18:2614–28.

Ramus, F (2003). Developmental dyslexia: specific phonological deficit or general sensorimotor dysfunction? *Curr. Opin. Neurobiol.* 13:212–218.

Ramus, F & Ahissar, M (2012). Developmental dyslexia: the difficulties of interpreting poor performance, and the importance of normal performance. *Cogn. Neuropsychol.* 29:104–122.

Ramus, F, Pidgeon, E, & Frith, U (2003). The relationship between motor control and phonology in dyslexic children. *J Child Psychol Psychiatry* 44:712–22.

Raposo, G, Marks, MS, & Cutler, DF (2007). Lysosome-related organelles: driving post-Golgi compartments into specialisation. *Curr Opin Cell Biol* 19:394–401.

Raschle, NM, Stering, PL, Meissner, SN, & Gaab, N (2014). Altered neuronal response during rapid auditory processing and its relation to phonological processing in prereading children at familial risk for dyslexia. *Cereb Cortex* 24:2489–501.

Raskind, WH, Igo, RP, Chapman, NH, Berninger, VW, Thomson, JB, Matsushita, M, Brkanac, Z, Holzman, T, Brown, M, & Wijsman, EM (2005). A genome scan in multigenerational families with dyslexia: Identification of a novel locus on chromosome 2q that contributes to phonological decoding efficiency. *Mol Psychiatry* 10:699–711.

Raskind, WH, Peter, B, Richards, T, Eckert, MM, & Berninger, VW (2013). The genetics of reading disabilities: from phenotypes to candidate genes. *Front Psychol* 3:601.

Redecker, P, Kreutz, MR, Bockmann, J, Gundelfinger, ED, & Boeckers, TM (2003). Brain Synaptic Junctional Proteins at the Acrosome of Rat Testicular Germ Cells. *J Histochem Cytochem* 51:809–819.

Rees, E, O'Donovan, MC, & Owen, MJ (2015). Genetics of schizophrenia. *Curr Opin Behav Sci* 2:8–14.

Reinstein, E, Chang, BS, Robertson, SP, Rimoin, DL, & Katzir, T (2012). Filamin A mutation associated with normal reading skills and dyslexia in a family with periventricular heterotopia. *Am J Med Genet A* 158A:1897–901.

Rendall, AR, Tarkar, A, Contreras-Mora, HM, LoTurco, JJ, & Fitch, RH (2015). Deficits in learning and memory in mice with a mutation of the candidate dyslexia susceptibility gene Dyx1c1. *Brain Lang*.

Rice, ML, Smith, SD, & Gayán, J (2009). Convergent genetic linkage and associations to language, speech and reading measures in families of probands with Specific Language Impairment. *J Neurodev Disord* 1:264–82.

Richardson, AJ & Ross, MA (2000). Fatty acid metabolism in neurodevelopmental disorder: a new perspective on associations between attention-deficit/hyperactivity disorder, dyslexia, dyspraxia and the autistic spectrum. *Prostaglandins Leukot Essent Fatty Acids* 63:1–9.

Richardson, FM, Seghier, ML, Leff, AP, Thomas, MSC, & Price, CJ (2011). Multiple routes from occipital to temporal cortices during reading. *J Neurosci* 31:8239–47.

Richlan, F (2012). Developmental dyslexia: dysfunction of a left hemisphere reading network. *Front Hum Neurosci* 6:120.

Richlan, F, Kronbichler, M, & Wimmer, H (2011). Meta-analyzing brain dysfunctions in dyslexic children and adults. *Neuroimage* 56:1735–42.

Risher, WC, Patel, S, Kim, IH, Uezu, A, Bhagat, S, Wilton, DK, Pilaz, LJ, Singh Alvarado, J, Calhan, OY, Silver, DL, Stevens, B, Calakos, N, Soderling, SH, & Eroglu, C (2014). Astrocytes refine cortical connectivity at dendritic spines. *Elife* 3.

Ritchie, SJ & Bates, TC (2013). Enduring links from childhood mathematics and reading achievement to adult socioeconomic status. *Psychol Sci* 24:1301–8.

Rizo, J & Rosenmund, C (2008). Synaptic vesicle fusion. *Nat Struct Mol Biol* 15:665–74.

Rodenas-Cuadrado, P, Ho, J, & Vernes, SC (2014). Shining a light on CNTNAP2: complex functions to complex disorders. *Eur J Hum Genet* 22:171–8.

Rodríguez, CI, Buchholz, F, Galloway, J, Sequerra, R, Kasper, J, Ayala, R, Stewart, AF, & Dymecki, SM (2000). High-efficiency deleter mice show that FLPe is an alternative to Cre-loxP. *Nat Genet* 25:139–140.

Roqueta-Rivera, M, Abbott, TL, Sivaguru, M, Hess, RA, & Nakamura, MT (2011). Deficiency in the Omega-3 Fatty Acid Pathway Results in Failure of Acrosome Biogenesis in Mice. *Biol Reprod* 85:721–732.

Rosen, GD, Bai, J, Wang, Y, Fiondella, CG, Threlkeld, SW, LoTurco, JJ, & Galaburda, AM (2007). Disruption of neuronal migration by RNAi of Dyx1c1 results in neocortical and hippocampal malformations. *Cereb Cortex* 17:2562–72.

Rosen, S (2003). Auditory processing in dyslexia and specific language impairment: Is there a deficit? What is its nature? Does it explain anything? *J Phon* 31:509–527.

Rossi, A, Kontarakis, Z, Gerri, C, Nolte, H, Hölper, S, Krüger, M, & Stainier, DYR (2015). Genetic compensation induced by deleterious mutations but not gene knockdowns. *Nature* 524:230–3.

Russell, L & Clermont, Y (1976). Anchoring device between Sertoli cells and late spermatids in rat seminiferous tubules. *Anat Rec* 185:259–78.

Russell, LD, Ettlin, R, Hikim, A, & Clegg, E (1990). *Histological and Histopathological Evaluation of the testis*. New York: Cache River Press. 286.

Rutter, M, Caspi, A, Fergusson, D, Horwood, LJ, Goodman, R, Maughan, B, Moffitt, TE, Meltzer, H, & Carroll, J (2004). Sex Differences in Developmental Reading Disability. *J Am Med Assoc* 291:2007–2012.

Sahara, S, Yanagawa, Y, O'Leary, DDM, & Stevens, CF (2012). The fraction of cortical GABAergic neurons is constant from near the start of cortical neurogenesis to adulthood. *J Neurosci* 4:4755–4761.

Saheki, Y & De Camilli, P (2012). Synaptic Vesicle Endocytosis. *Cold Spring Harb Perspect Biol* 4:a005645–a005645.

Sakisaka, T & Takai, Y (2005). Cell adhesion molecules in the CNS. *J Cell Sci* 118:5407–10.

Sanz, E, Evanoff, R, Quintana, A, Evans, E, Miller, JJA, Ko, C, et al. (2013). RiboTag analysis of actively translated mRNAs in Sertoli and Leydig cells in vivo. *PLoS One* 8. Ed. by S Schlatt:e66179.

Sawyer, D, Krishnamani, R, & Hannig, V (1998). Genetic analysis of phonologic core deficit dyslexia. *Am J Hum Genet* 63:307.

Scerri, TS, Fisher, SE, Francks, C, MacPhie, IL, Paracchini, S, Richardson, AJ, Stein, JF, & Monaco, AP (2004). Putative functional alleles of DYX1C1 are not associated with dyslexia susceptibility in a large sample of sibling pairs from the UK. *J Med Genet* 41:853–857.

Scerri, TS, Brandler, WM, Paracchini, S, Morris, AP, Ring, SM, Richardson, AJ, Talcott, JB, Stein, J, & Monaco, AP (2011). PCSK6 is associated with handedness in individuals with dyslexia. *Hum Mol Genet* 20:608–614.

Scerri, TS, Darki, F, Newbury, DF, Whitehouse, AJO, Peyrard-Janvid, M, Matsson, H, et al. (2012). The dyslexia candidate locus on 2p12 is associated with general cognitive ability and white matter structure. *PLoS One* 7:e50321.

Scerri, TS & Schulte-Körne, G (2010). Genetics of developmental dyslexia. *Eur Child Adolesc Psychiatry* 19:179–197.

Scheffer, DI, Shen, J, Corey, DP, & Chen, ZY (2015). Gene Expression by Mouse Inner Ear Hair Cells during Development. *J Neurosci* 35:6366–6380.

Schlaggar, BL & McCandliss, BD (2007). Development of neural systems for reading. *Annu Rev Neurosci* 30:475–503.

Schulte-Körne, G, Grimm, T, Nöthen, MM, Müller-Myhsok, B, Cichon, S, Vogt, IR, Propping, P, & Remschmidt, H (1998). Evidence for linkage of spelling disability to chromosome 15. *Am J Hum Genet* 63:279–82.

Schulte-Körne, G (2010). The prevention, diagnosis, and treatment of dyslexia. *Dtsch Ärzteblatt Int* 107:718–26, quiz 27.

Schulte-Körne, G, Ludwig, KU, el Sharkawy, J, Nöthen, MM, Müller-Myhsok, B, & Hoffmann, P (2007). Genetics and Neuroscience in Dyslexia: Perspectives for Education and Remediation. *Mind, Brain, Educ* 1:162–172.

Schumacher, J, Anthoni, H, Dahdouh, F, König, IR, Hillmer, AM, Kluck, N, et al. (2006). Strong genetic evidence of DCDC2 as a susceptibility gene for dyslexia. *Am J Hum Genet* 78:52–62.

Schumacher, J, Hoffmann, P, Schmäl, C, Schulte-Körne, G, & Nöthen, MM (2007). Genetics of dyslexia: the evolving landscape. *J Med Genet* 44:289–97.

Schumacher, J, K?nig, IR, Schr?der, T, Duell, M, Plume, E, Propping, P, Warnke, A, Libertus, C, Ziegler, A, M?ller-Myhsok, B, Schulte-K?rne, G, & N?then, MM (2008). Further evidence for a susceptibility locus contributing to reading disability on chromosome 15q15?q21. *Psychiatr Genet* 18:137–142.

Schwab, ME (2010). Functions of Nogo proteins and their receptors in the nervous system. *Nat Rev Neurosci* 11:799–811.

Sekine, K, Honda, T, Kawauchi, T, Kubo, Ki, & Nakajima, K (2011). The outermost region of the developing cortical plate is crucial for both the switch of the radial migration mode and the Dab1-dependent "inside-out" lamination in the neocortex. *J Neurosci* 31:9426–39.

Shao, S, Niu, Y, Zhang, X, Kong, R, Wang, J, Liu, L, Luo, X, Zhang, J, & Song, R (2016). Opposite Associations between Individual KIAA0319 Polymorphisms and Developmental Dyslexia Risk across Populations: A Stratified Meta-Analysis by the Study Population. *Sci Rep* 6:30454.

Shaywitz, SE, Shaywitz, BA, Fletcher, JM, & Escobar, MD (1990). Prevalence of reading disability in boys and girls. Results of the Connecticut Longitudinal Study. *JAMA* 264:998–1002.

Shaywitz, SE & Shaywitz, BA (2005). Dyslexia (specific reading disability). *Biol Psychiatry* 57:1301–9.

Shaywitz, SE & Shaywitz, BA (2008). Paying attention to reading: The neurobiology of reading and dyslexia. *Dev Psychopathol* 20:1329.

Shen, J, Scheffer, DI, Kwan, KY, & Corey, DP (2015). SHIELD: an integrative gene expression database for inner ear research. *Database (Oxford)* 2015:bav071.

Sherman, GF, Galaburda, AM, Behan, PO, & Rosen, GD (1987). Neuroanatomical anomalies in autoimmune mice. *Acta Neuropathol* 74:239–42.

Sherman, GF, Galaburda, AM, & Geschwind, N (1985). Cortical anomalies in brains of New Zealand mice: a neuropathologic model of dyslexia? *Proc Natl Acad Sci* 82:8072–4.

Sherman, SM & Guillery, RW (2002). The role of the thalamus in the flow of information to the cortex. *Philos Trans R Soc Lond B Biol Sci* 357:1695–708.

— (2006). *Exploring the thalamus and its role in cortical function*. Cambridge, MA: MIT Press.

Shima, JE, McLean, DJ, McCarrey, JR, & Griswold, MD (2004). The Murine Testicular Transcriptome: Characterizing Gene Expression in the Testis During the Progression of Spermatogenesis. *Biol Reprod* 71:319–330.

Shin, LM & Liberzon, I (2010). The neurocircuitry of fear, stress, and anxiety disorders. *Neuropsychopharmacology* 35:169–91.

Shinmyo, Y, Tanaka, S, Tsunoda, S, Hosomichi, K, Tajima, A, Kawasaki, H, et al. (2016). CRISPR/Cas9-mediated gene knockout in the mouse brain using in utero electroporation. *Sci Rep* 6:20611.

Sir, JH, Barr, AR, Nicholas, AK, Carvalho, OP, Khurshid, M, Sossick, A, Reichelt, S, D'Santos, C, Woods, CG, & Gergely, F (2011). A primary microcephaly protein complex forms a ring around parental centrioles. *Nat Genet* 43:1147–1153.

Skarnes, WC, Rosen, B, West, AP, Koutsourakis, M, Bushell, W, Iyer, V, et al. (2011). A conditional knockout resource for the genome-wide study of mouse gene function. *Nature* 474:337–342.

Smart, IHM, Dehay, C, Giroud, P, Berland, M, & Kennedy, H (2002). Unique morphological features of the proliferative zones and postmitotic compartments of the neural epithelium giving rise to striate and extrastriate cortex in the monkey. *Cereb Cortex* 12:37–53.

Smith, SD, Kimberling, WJ, Pennington, BF, & Lubs, HA (1983). Specific reading disability: identification of an inherited form through linkage analysis. *Science* 219:1345–7.

Smith, SD, Kimberling, WJ, & Pennington, BF (1991). Screening for multiple genes influencing dyslexia. *Read Writ* 3:285–298.

Snowling, MJ (1981). Phonemic deficits in developmental dyslexia. *Psychol Res* 43:219–34.

Snowling, M, Bishop, DV, & Stothard, SE (2000). Is preschool language impairment a risk factor for dyslexia in adolescence? *J Child Psychol Psychiatry* 41:587–600.

Sotelo, C & Rossi, F (2013). *Handbook of the Cerebellum and Cerebellar Disorders.* Ed. by M Manto, JD Schmahmann, F Rossi, DL Gruol, & N Koibuchi. Dordrecht: Springer Netherlands. 147–178.

Sotelo, C, Rossi, F, Komuro, Y, Fahrion, JK, Foote, KD, Fenner, KB, Kumada, T, Ohno, N, & Komuro, H (2013). "Granule Cell Migration and Differentiation". In: *Handb Cerebellum Cerebellar Disord.* Dordrecht: Springer Netherlands. 107–125.

St Pourcain, B, Cents, RAM, Whitehouse, AJO, Haworth, CMA, Davis, OSP, O'Reilly, PF, et al. (2014). Common variation near ROBO2 is associated with expressive vocabulary in infancy. *Nat Commun* 5:4831.

Stein, J (2001). The magnocellular theory of developmental dyslexia. *Dyslexia* 7:12–36.

Stein, J & Walsh, V (1997). To see but not to read: the magnocellular theory of dyslexia. *Trends Neurosci.* 20:147–152.

Stephenson, S (1907). The calmette serum reaction in ophthalmology. *Br Med J* 2:1038–9.

Su, Z, Wang, J, Gu, X, Su, Z, Wang, J, & Gu, X (2014). Effect of Duplicate Genes on Mouse Genetic Robustness: An Update. *Biomed Res Int* 2014:1–13.

Südhof, TC & Rizo, J (2011). Synaptic vesicle exocytosis. *Cold Spring Harb Perspect Biol* 3.

Südhof, TC & Rothman, JE (2009). Membrane fusion: grappling with SNARE and SM proteins. *Science* 323:474–7.

Sun, Y, Gao, Y, Zhou, Y, Chen, H, Wang, G, Xu, J, Xia, J, Huen, MSY, Siok, WT, Jiang, Y, & Tan, LH (2014). Association study of developmental dyslexia candidate genes DCDC2 and KIAA0319 in Chinese population. *Am J Med Genet B Neuropsychiatr Genet* 165B:627–34.

Sundheim, STPV & Voeller, KKS (2004). Psychiatric implications of language disorders and learning disabilities: risks and management. *J Child Neurol* 19:814–26.

Suzuki-Toyota, F, Ito, C, Toyama, Y, Maekawa, M, Yao, R, Noda, T, & Toshimori, K (2004). The coiled tail of the round-headed spermatozoa appears during epididymal passage in GOPC-deficient mice. *Arch Histol Cytol* 67:361–71.

Svidnicki, MCCM, Salgado, CA, Lima, RF, Ciasca, SM, Secolin, R, Pomilio, MCA, Junqueira, PA, Pinto, MS, Pereira, MM, & Sartorato, EL (2013). Study of candidate genes for dyslexia in Brazilian individuals. *Genet Mol Res* 12:5356–64.

Swerdlow, NR, Geyer, MA, & Braff, DL (2001). Neural circuit regulation of prepulse inhibition of startle in the rat: current knowledge and future challenges. *Psychopharmacology (Berl)* 156:194–215.

Szalkowski, CE, Hinman, JR, Threlkeld, SW, Wang, Y, LePack, A, Rosen, GD, Chrobak, JJ, LoTurco, JJ, & Fitch, RH (2011). Persistent spatial working memory deficits in rats following in utero RNAi of Dyx1c1. *Genes Brain Behav* 10:244–52.

Szalkowski, CE, Booker, AB, Truong, DT, Threlkeld, SW, Rosen, GD, & Fitch, RH (2013). Knockdown of the candidate dyslexia susceptibility gene homolog dyx1c1 in rodents: effects on auditory processing, visual attention, and cortical and thalamic anatomy. *Dev Neurosci* 35:50–68.

Szalkowski, CE, Fiondella, CG, Galaburda, AM, Rosen, GD, Loturco, JJ, & Fitch, RH (2012). Neocortical disruption and behavioral impairments in rats following in utero RNAi of candidate dyslexia risk gene Kiaa0319. *Int J Dev Neurosci* 30:293–302.

Szalontai, A & Csiszar, K (2013). Genetic insights into the functional elements of language. *Hum Genet* 132:959–86.

Taipale, M, Kaminen, N, Nopola-Hemmi, J, Haltia, T, Myllyluoma, B, Lyytinen, H, Muller, K, Kaaranen, M, Lindsberg, PJ, Hannula-Jouppi, K, & Kere, J (2003). A candidate gene for developmental dyslexia encodes a nuclear tetratricopeptide repeat domain protein dynamically regulated in brain. *Proc Natl Acad Sci* 100:11553–8.

Takeuchi, A & O'Leary, DDM (2006). Radial migration of superficial layer cortical neurons controlled by novel Ig cell adhesion molecule MDGA1. *J Neurosci* 26:4460–4.

Tallal, P (1980). Auditory temporal perception, phonics, and reading disabilities in children. *Brain Lang* 9:182–98.

Tallal, P (2004). Improving language and literacy is a matter of time. *Nat Rev Neurosci* 5:721–8.

Tan, X & Shi, SH (2013). *Neocortical neurogenesis and neuronal migration.* arXiv: `NIHMS150003`.

Tarkar, A, Loges, NT, Slagle, CE, Francis, R, Dougherty, GW, Tamayo, JV, et al. (2013). DYX1C1 is required for axonemal dynein assembly and ciliary motility. *Nat Genet* 45:995–1003.

Temple, E, Poldrack, RA, Protopapas, A, Nagarajan, S, Salz, T, Tallal, P, Merzenich, MM, & Gabrieli, JD (2000). Disruption of the neural response to rapid

acoustic stimuli in dyslexia: evidence from functional MRI. *Proc Natl Acad Sci* 97:13907–12.

Terashima, A, Pelkey, KA, Rah, JC, Suh, YH, Roche, KW, Collingridge, GL, McBain, CJ, & Isaac, JT (2008). An Essential Role for PICK1 in NMDA Receptor-Dependent Bidirectional Synaptic Plasticity. *Neuron* 57:872–882.

The Government Office for Science, L (2008). *Foresight Mental Capital and Wellbeing Project*. Tech. rep. 1–22.

Thesen, T, Quinn, BT, Carlson, C, Devinsky, O, DuBois, J, McDonald, CR, French, J, Leventer, R, Felsovalyi, O, Wang, X, Halgren, E, & Kuzniecky, R (2011). Detection of epileptogenic cortical malformations with surface-based MRI morphometry. *PLoS One* 6:e16430.

Thomas, CJ (1905). Congenital 'word-blindness' and its treatment. *Ophthalmoscope* 3:380–385.

Threlkeld, SW, Other, McClure, MM, Bai, J, Wang, Y, LoTurco, JJ, Rosen, GD, & Fitch, RH (2007). Developmental disruptions and behavioral impairments in rats following in utero RNAi of Dyx1c1. *Brain Res Bull* 71:508–14.

Threlkeld, SW, Penley, SC, Rosen, GD, & Fitch, RH (2008). Detection of silent gaps in white noise following cortical deactivation in rats. *Neuroreport* 19:893–8.

Tran, C, Gagnon, F, Wigg, K, Feng, Y, Gomez, L, Cate-Carter, T, Kerr, E, Field, L, Kaplan, B, Lovett, M, & Barr, C (2013). A family-based association analysis and meta-analysis of the reading disabilities candidate gene DYX1C1. *Am J Med Genet Part B Neuropsychiatr Genet* 162:146–156.

Tran, C, Wigg, KG, Zhang, K, Cate-Carter, TD, Kerr, E, Field, LL, Kaplan, BJ, Lovett, MW, & Barr, CL (2014). Association of the ROBO1 gene with reading disabilities in a family-based analysis. *Genes, Brain Behav* 13:430–438.

Trulioff, A, Ermakov, A, & Malashichev, Y (2017). Primary Cilia as a Possible Link between Left-Right Asymmetry and Neurodevelopmental Diseases. *Genes* 8:48.

Truong, DT, Che, A, Rendall, AR, Szalkowski, CE, LoTurco, JJ, Galaburda, AM, & Holly Fitch, R (2014). Mutation of Dcdc2 in mice leads to impairments in auditory processing and memory ability. *Genes Brain Behav* 13:802–11.

Truong, DT, Rendall, AR, Castelluccio, BC, Eigsti, IM, & Fitch, RH (2015). Auditory processing and morphological anomalies in medial geniculate nucleus of Cntnap2 mutant mice. *Behav Neurosci* 129:731–43.

Tsuboi, D, Kuroda, K, Tanaka, M, Namba, T, Iizuka, Y, Taya, S, et al. (2015). Disrupted-in-schizophrenia 1 regulates transport of ITPR1 mRNA for synaptic plasticity. *Nat Neurosci* 18:698–707.

Turic, D, Robinson, L, Duke, M, Morris, DW, Webb, V, Hamshere, M, et al. (2003). Linkage disequilibrium mapping provides further evidence of a gene for reading disability on chromosome 6p21.3–22. *Mol Psychiatry* 8:176–185.

Tzenova, J, Kaplan, BJ, Petryshen, TL, & Field, LL (2004). Confirmation of a dyslexia susceptibility locus on chromosome 1p34-p36 in a set of 100 Canadian families. *Am J Med Genet B Neuropsychiatr Genet* 127B:117–24.

Ufartes, R, Schneider, T, Mortensen, LS, de Juan Romero, C, Hentrich, K, Knoetgen, H, Beilinson, V, Moebius, W, Tarabykin, V, Alves, F, Pardo, La, Rawlins, JNP, Stuehmer, W, et al. (2013). Behavioural and functional characterization of Kv10.1 (Eag1) knockout mice. *Hum Mol Genet* 22:2247–2262.

Ullman, MT & Pierpont, EI (2005). Specific language impairment is not specific to language: the procedural deficit hypothesis. *Cortex* 41:399–433.

Vandermosten, M, Boets, B, Wouters, J, & Ghesquière, P (2012). A qualitative and quantitative review of diffusion tensor imaging studies in reading and dyslexia. *Neurosci Biobehav Rev* 36:1532–52.

Varoqueaux, F, Aramuni, G, Rawson, RL, Mohrmann, R, Missler, M, Gottmann, K, Zhang, W, Südhof, TC, & Brose, N (2006). Neuroligins Determine Synapse Maturation and Function. *Neuron* 51:741–754.

Veerappa, AM, Padakannaya, P, & Ramachandra, NB (2013a). Copy number variation-based polymorphism in a new pseudoautosomal region 3 (PAR3) of a human X-chromosome-transposed region (XTR) in the Y chromosome. *Funct. Integr. Genomics* 13:285–293.

Veerappa, AM, Saldanha, M, Padakannaya, P, & Ramachandra, NB (2013b). Family-based genome-wide copy number scan identifies five new genes of dyslexia involved in dendritic spinal plasticity. *J Hum Genet* 58:539–547.

— (2013c). Genome-wide copy number scan identifies disruption of PCDH11X in developmental dyslexia. *Am J Med Genet B Neuropsychiatr Genet* 162B:889–97.

Velayos-Baeza, A, Levecque, C, Kobayashi, K, Holloway, ZG, & Monaco, AP (2010). The dyslexia-associated KIAA0319 protein undergoes proteolytic processing with γ-secretase-independent intramembrane cleavage. *J Biol Chem* 285:40148–40162.

Velayos-Baeza, A, Toma, C, da Roza, S, Paracchini, S, & Monaco, AP (2007). Alternative splicing in the dyslexia-associated gene KIAA0319. *Mamm. Genome* 18:627–634.

Velayos-Baeza, A, Toma, C, Paracchini, S, & Monaco, AP (2008). The dyslexia-associated gene KIAA0319 encodes highly N- and O-glycosylated plasma membrane and secreted isoforms. *Hum Mol Genet* 17:859–871.

Venkatesh, SK, Siddaiah, A, Padakannaya, P, & Ramachandra, NB (2011). An Examination of Candidate Gene SNPs for Dyslexia in an Indian Sample. *Behav Genet* 41:105–109.

Venkatesh, SK, Siddaiah, A, Padakannaya, P, & Ramachandra, NB (2013a). Analysis of genetic variants of dyslexia candidate genes KIAA0319 and DCDC2 in Indian population. *J Hum Genet* 58:531–538.

— (2013b). Lack of association between genetic polymorphisms in ROBO1, MRPL19/C2ORF3 and THEM2 with developmental dyslexia. *Gene* 529:215–219.

Venkatesh, SK, Siddaiah, A, Padakannaya, P, & Ramachandra, NB (2014). Association of SNPs of DYX1C1 with developmental dyslexia in an Indian population. *Psychiatr Genet* 24:10–20.

Vidyasagar, TR & Pammer, K (2010). Dyslexia: a deficit in visuo-spatial attention, not in phonological processing. *Trends Cogn Sci* 14:57–63.

Villanueva, P, Nudel, R, Hoischen, A, Fernández, MA, Simpson, NH, Gilissen, C, et al. (2015). Exome sequencing in an admixed isolated population indicates NFXL1 variants confer a risk for specific language impairment. *PLoS Genet* 11:e1004925.

Vincent, SD & Robertson, EJ (2003). Highly efficient transgene-independent recombination directed by a maternally derived SOX2CRE transgene. *Genesis* 37:54–6.

Visscher, PM, Goddard, ME, Derks, EM, & Wray, NR (2012). Evidence-based psychiatric genetics, AKA the false dichotomy between common and rare variant hypotheses. *Mol Psychiatry* 17:474–485.

Vozdova, M, Rybar, R, Kloudova, S, Prinosilova, P, Texl, P, & Rubes, J (2014). Total globozoospermia associated with increased frequency of immature spermatozoa with chromatin defects and aneuploidy: a case report. *Andrologia* 46:831–6.

Wagner, J, Weber, B, Urbach, H, Elger, CE, & Huppertz, HJ (2011). Morphometric MRI analysis improves detection of focal cortical dysplasia type II. *Brain* 134:2844–54.

Wagner, RK & Torgesen, JK (1987). The nature of phonological processing and its causal role in the acquisition of reading skills. *Psychol Bull* 101:192–212.

Walsh, FS & Doherty, P (1997). Neural cell adhesion molecules of the immunoglobulin superfamily: role in axon growth and guidance. *Annu Rev Cell Dev Biol* 13:425–56.

Wang, ET, Kodama, G, Baldi, P, & Moyzis, RK (2006). Global landscape of recent inferred Darwinian selection for Homo sapiens. *Proc Natl Acad Sci* 103:135–140.

Wang, HZ, Qin, HD, Guo, W, Samuels, J, & Shugart, YY (2013). New insights into the genetic mechanism of IQ in autism spectrum disorders. *Front Genet* 4:195.

Wang, H, Wan, H, Li, X, Liu, W, Chen, Q, Wang, Y, Yang, L, Tang, H, Zhang, X, Duan, E, Zhao, X, Gao, F, & Li, W (2014). Atg7 is required for acrosome biogenesis during spermatogenesis in mice. *Cell Res* 24:852–69.

Wang, J, Morita, Y, Mazelova, J, & Deretic, D (2012). The Arf GAP ASAP1 provides a platform to regulate Arf4- and Rab11-Rab8-mediated ciliary receptor targeting. *EMBO J* 31:4057–71.

Wang, X, Tsai, JW, LaMonica, B, & Kriegstein, AR (2011a). A new subtype of progenitor cell in the mouse embryonic neocortex. *Nat Neurosci* 14:555–61.

Wang, Y, Yin, X, Rosen, G, Gabel, L, Guadiana, SM, Sarkisian, MR, Galaburda, aM, & Loturco, JJ (2011b). Dcdc2 knockout mice display exacerbated developmental disruptions following knockdown of doublecortin. *Neuroscience* 190:398–408.

Wang, Y, Brzozowska-Prechtl, A, & Karten, HJ (2010). Laminar and columnar auditory cortex in avian brain. *Proc Natl Acad Sci* 107:12676–12681.

Wang, ZI, Jones, SE, Jaisani, Z, Najm, IM, Prayson, RA, Burgess, RC, Krishnan, B, Ristic, A, Wong, CH, Bingaman, W, Gonzalez-Martinez, JA, & Alexopoulos, AV (2015). Voxel-based morphometric magnetic resonance imaging (MRI) postprocessing in MRI-negative epilepsies. *Ann Neurol* 77:1060–75.

Wassarman, PM (1988). Zona pellucida glycoproteins. *Annu Rev Biochem* 57:415–42.

Watanabe, S, Trimbuch, T, Camacho-Pérez, M, Rost, BR, Brokowski, B, Söhl-Kielczynski, B, Felies, A, Davis, MW, Rosenmund, C, & Jorgensen, EM (2014). Clathrin regenerates synaptic vesicles from endosomes. *Nature* 515:228–233.

Webster, RI, Erdos, C, Evans, K, Majnemer, A, Saigal, G, Kehayia, E, Thordardottir, E, Evans, A, & Shevell, MI (2008). Neurological and magnetic resonance imaging findings in children with developmental language impairment. *J Child Neurol* 23:870–7.

Weible, AP, Moore, AK, Liu, C, DeBlander, L, Wu, H, Kentros, C, & Wehr, M (2014). Perceptual gap detection is mediated by gap termination responses in auditory cortex. *Curr Biol* 24:1447–55.

Werner, LA, Folsom, RC, Mancl, LR, & Syapin, CL (2001). Human auditory brainstem response to temporal gaps in noise. *J Speech Lang Hear Res* 44:737–750.

West, AP & Willison, KR (1996). Brefeldin A and mannose 6-phosphate regulation of acrosomic related vesicular trafficking. *Eur J Cell Biol* 70:315–21.

Wigg, KG, Couto, JM, Feng, Y, Anderson, B, Cate-Carter, TD, Macciardi, F, Tannock, R, Lovett, MW, Humphries, TW, & Barr, CL (2004). Support for EKN1 as the susceptibility locus for dyslexia on 15q21. *Mol Psychiatry* 9:1111–1121.

Wigg, KG, Feng, Y, Crosbie, J, Tannock, R, Kennedy, JL, Ickowicz, A, Malone, M, Schachar, R, & Barr, CL (2008). Association of ADHD and the Protogenin gene in the chromosome 15q21.3 reading disabilities linkage region. *Genes, Brain Behav* 7:877–886.

Wigg, KG, Couto, JM, Feng, Y, Crosbie, J, Anderson, B, Cate-Carter, T, et al. (2005). Investigation of the Relationship of Attention Deficit Hyperactivity Disorder to the EKN1 Gene on Chromosome 15q21. *Sci Stud Read* 9:261–283.

Wilcke, A, Ligges, C, Burkhardt, J, Alexander, M, Wolf, C, Quente, E, Ahnert, P, Hoffmann, P, Becker, A, Müller-Myhsok, B, Cichon, S, Boltze, J, & Kirsten, H (2012). Imaging genetics of FOXP2 in dyslexia. *Eur J Hum Genet* 20:224–9.

Willcutt, EG & Pennington, BF (2000). Psychiatric comorbidity in children and adolescents with reading disability. *J Child Psychol Psychiatry* 41:1039–48.

Wills, ZP, Mandel-Brehm, C, Mardinly, AR, McCord, AE, Giger, RJ, & Greenberg, ME (2012). The nogo receptor family restricts synapse number in the developing hippocampus. *Neuron* 73:466–81.

Winer, JA (2005). Decoding the auditory corticofugal systems. *Hear Res* 207:1–9.

Witt, RM, Galligan, MM, Despinoy, JR, & Segal, R (2009). Olfactory behavioral testing in the adult mouse. *J Vis Exp*, 949.

Wong, EWP, Mruk, DD, & Cheng, CY (2008). Biology and regulation of ectoplasmic specialization, an atypical adherens junction type, in the testis. *Biochim Biophys Acta* 1778:692–708.

World Health Organisation (2008). *International statistical classification of disease.* Geneva, Switzerland.

Worthey, EA, Raca, G, Laffin, JJ, Wilk, BM, Harris, JM, Jakielski, KJ, Dimmock, DP, Strand, Ea, & Shriberg, LD (2013). Whole-exome sequencing supports genetic heterogeneity in childhood apraxia of speech. *J Neurodev Disord* 5:29.

Xia, J, Zhang, X, Staudinger, J, & Huganir, RL (1999). Clustering of AMPA receptors by the synaptic PDZ domain-containing protein PICK1. *Neuron* 22:179–87.

Xiao, N, Kam, C, Shen, C, Jin, W, Wang, J, Lee, KM, et al. (2009). PICK1 deficiency causes male infertility in mice by disrupting acrosome formation. *J Clin Invest* 119:802–812.

Xu, J, Kam, C, Luo, Jh, & Xia, J (2014). PICK1 Mediates Synaptic Recruitment of AMPA Receptors at Neurexin-Induced Postsynaptic Sites. *J Neurosci* 34:15415–15424.

Xu, X, Toselli, PA, Russell, LD, & Seldin, DC (1999). Globozoospermia in mice lacking the casein kinase II alpha' catalytic subunit. *Nat Genet* 23:118–21.

Al-Yagon, M & Mikulincer, M (2004). Socioemotional and Academic Adjustment Among Children with Learning Disorders: The Mediational Role of Attachment-Based Factors. *J Spec Educ* 38:111–123.

Yan, HHN, Mruk, DD, Lee, WM, & Cheng, CY (2007). Ectoplasmic specialization: a friend or a foe of spermatogenesis? *Bioessays* 29:36–48.

Yanagimachi, R (1994). "Mammalian fertilization". In: *Physiol Reprod*. Ed. by E Knobil & JD Neill. New York: Raven Press. 189–317.

Yao, R, Ito, C, Natsume, Y, Sugitani, Y, Yamanaka, H, Kuretake, S, Yanagida, K, Sato, A, Toshimori, K, & Noda, T (2002). Lack of acrosome formation in mice lacking a Golgi protein, GOPC. *Proc Natl Acad Sci* 99:11211–6.

Yildiz, Y, Matern, H, Thompson, B, Allegood, JC, Warren, RL, Ramirez, DMO, Hammer, RE, Hamra, FK, Matern, S, & Russell, DW (2006). Mutation of beta-glucosidase 2 causes glycolipid storage disease and impaired male fertility. *J Clin Invest* 116:2985–94.

Ylisaukko-oja, T, Peyrard-Janvid, M, Lindgren, CM, Rehnström, K, Vanhala, R, Peltonen, L, Järvelä, I, & Kere, J (2004). Family-based association study of DYX1C1 variants in autism. *Eur J Hum Genet Publ online 06 Oct 2004; | doi101038/sjejhg5201272* 13:127.

Yuan, W, Zhou, L, Chen, JH, Wu, JY, Rao, Y, & Ornitz, DM (1999). The mouse SLIT family: secreted ligands for ROBO expressed in patterns that suggest a role in morphogenesis and axon guidance. *Dev Biol* 212:290–306.

Zeisel, A, Muñoz-Manchado, AB, Codeluppi, S, Lönnerberg, P, La Manno, G, Juréus, A, Marques, S, Munguba, H, He, L, Betsholtz, C, Rolny, C, Castelo-Branco, G, Hjerling-Leffler, J, & Linnarsson, S (2015). Cell types in the mouse cortex and hippocampus revealed by single-cell RNA-seq. *Science* 347.

Zhang, C, Zhang, J, Yin, R, Zhou, J, & Chang, S (1996). Experimental research on the reading disability of Chinese students. *Psychol Sci*, 222–256.

Zhang, J (2012). Genetic redundancies and their evolutionary maintenance. *Adv Exp Med Biol* 751:279–300.

Zhang, Y, Li, J, Song, S, Tardif, T, Burmeister, M, Villafuerte, SM, Su, M, McBride, C, & Shu, H (2016). Association of DCDC2 Polymorphisms with Normal Variations in Reading Abilities in a Chinese Population. *PLoS One* 11. Ed. by K Paterson:e0153603.

Zhao, H, Chen, Y, Zhang, BP, & Zuo, PX (2016). KIAA0319 gene polymorphisms are associated with developmental dyslexia in Chinese Uyghur children. *J Hum Genet*.

Zhong, R, Yang, B, Tang, H, Zou, L, Song, R, Zhu, LQ, & Miao, X (2013). Meta-analysis of the Association Between DCDC2 Polymorphisms and Risk of Dyslexia. *Mol Neurobiol* 47:435–442.

Zhu, F, Gong, F, Lin, G, & Lu, G (2013). DPY19L2 gene mutations are a major cause of globozoospermia: identification of three novel point mutations. *Mol Hum Reprod* 19:395–404.

Zhu, Gd, Salazar, G, Zlatic, SA, Fiza, B, Doucette, MM, Heilman, CJ, Levey, AI, Faundez, V, & L'hernault, SW (2009). SPE-39 family proteins interact with the HOPS complex and function in lysosomal delivery. *Mol Biol Cell* 20:1223–40.

Ziegler, JC & Goswami, U (2005). Reading acquisition, developmental dyslexia, and skilled reading across languages: a psycholinguistic grain size theory. *Psychol Bull* 131:3–29.

Zou, L, Chen, W, Shao, S, Sun, Z, Zhong, R, Shi, J, Miao, X, & Song, R (2012). Genetic variant in KIAA0319, but not in DYX1C1, is associated with risk of dyslexia: an integrated meta-analysis. *Am J Med Genet B Neuropsychiatr Genet* 159B:970–6.

Zuo, Px, Wu, Hr, Li, Zc, Cao, Xd, Pang, Lj, Yang, L, Liu, F, & Zhao, F (2012). Association of polymorphisms in the DCDC2 gene with developmental dyslexia in the Han Chinese. *Chin Med J (Engl)* 125:622–5.